U.PORTO
INSTITUTO DE CIÊNCIAS BIOMÉDICAS ABEL SALAZAR
UNIVERSIDADE DO PORTO

Intracellular trafficking of AIP56, a bacterial AB toxin targeting NF-κB

LILIANA MARISA GONÇALVES PEREIRA
TESE DE DOUTORAMENTO APRESENTADA
AO INSTITUTO DE CIÊNCIAS BIOMÉDICAS ABEL SALAZAR
DA UNIVERSIDADE DO PORTO EM
CIÊNCIAS BIOMÉDICAS

2014

Liliana M. G. Pereira

Intracellular trafficking of AIP56, a bacterial AB toxin targeting NF-κB

Tese de Candidatura ao grau de Doutor em Ciências Biomédicas submetida ao Instituto de Ciências Biomédicas Abel Salazar da Universidade do Porto.

Orientador – Doutor Nuno Miguel Simões dos Santos

Categoria – Investigador auxiliar

Afiliação – Instituto de Biologia Molecular e Celular

Co-orientador - Doutora Ana Maria Silva do Vale

Categoria – Investigadora auxiliar

Afiliação – Instituto de Biologia Molecular e Celular

De acordo com o disposto no Decreto-Lei nº 74/2006 de 24 de Março, esclarece-se serem da nossa responsabilidade a execução das experiências que estiveram na origem dos resultados apresentados, assim como a sua interpretação, discussão e redação.
Trabalho desenvolvido durante este doutoramento resultou na publicação de dois artigos científicos e uma patente:

Pereira LM, Pinto RD, Silva DS, Moreira AR, Beitzinger C, Oliveira P, Sampaio P, Benz R, Azevedo JE, dos Santos NM, do Vale A (2014) Intracellular trafficking of AIP56, an NF-κB cleaving toxin from *Photobacterium damselae piscicida*. *[accepted for publication in Infection and Immunity]*

Silva DS, **Pereira LM**, Moreira AR, Ferreira-da-Silva F, Brito RM, Faria TQ, Zornetta I, Montecucco C, Oliveira P, Azevedo JE, Pereira PJ, Macedo-Ribeiro S, do Vale A, dos Santos NM (2013) The apoptogenic toxin AIP56 is a metalloprotease A-B toxin that cleaves NF-kappab p65. *PLoS Pathog* **9:** e1003128

dos Santos NM, do Vale A, **Pereira LM**, Silva DS, Azevedo JE , Pereira PJ, Macedo-Ribeiro S (2014) UK Intellectual Property Office patent WO2014109658A2 (peptides; use of AIP56 for targeting NF-κB and as a delivery system)

Durante este longo caminho contei com a ajuda e apoio de muitos, aos quais estou eternamente grata. O meu sincero Obrigada, a todos os que contribuíram para a realização deste trabalho. Obrigada por nunca deixarem de acreditar em mim e por me fazerem acreditar que "Sabemos muito mais do que julgamos, podemos muito mais do que imaginamos" (José Saramago).

Liliana Marisa

Funding

The author was supported by national funds through a grant from Fundação para a Ciência e a Tecnologia (SFRH/BD/43501/2008).

The work was funded by FEDER through Programa Operacional Factores de Competitividade – COMPETE, and by national funds through Fundação para a Ciência e a Tecnologia - FCT under the projects FCOMP-01-0124-FEDER-009501 (PTDC/CVT/099544/2008) and FCOMP-01-0124-FEDER-009036 (PTDC/BIA-PRO/101111/2008).

Governo da República Portuguesa

FEDER
Fundo Europeu de Desenvolvimento Regional

UNIÃO EUROPEIA

TABLE OF CONTENTS

LIST OF ABBREVIATIONS

ADP	adenosine diphosphate
AIP56	apoptosis inducing protein of 56 kDa
ANTXR1	anthrax toxin receptor 1
ANTXR2	anthrax toxin receptor 2
APCs	antigen presenting cells
AP2	clathrin adaptor protein 2
Arf	ADP-ribosylation factor
ATP	adenosine triphosphate
BoNT	botulinum neurotoxins
cAMP	cyclic adenosine monophosphate
CDCs	cholesterol dependent cytolysins
CGTs	clostridial glucosylating toxins
COPI	coat protein complex I
CT	cholera toxin
DT	diphtheria toxin
EF	edema factor
EF-2	elongation factor 2
ER	endoplasmic reticulum
ERAD	ER-associated protein degradation
GTP	guanosine-5'-triphosphate
GDP	guanosine 5′-diphosphate
HB-EGF	heparin-binding epidermal growth factor
Hsp90	heat-shock protein 90
Hsc70	heat shock cognate 71 kDa protein
IKK	IκB kinase
IκBs	inhibitors of NF-κB

JNK	c-Jun N-terminal kinase
LBPA	lysophosphatidic acid
LF	lethal factor
LPS	lypopolysaccharide
LRP6	lipoprotein-receptor-related protein 6
LT	heat-labile enterotoxins
MAPK	mitogen activated protein kinase
mBMDM	mouse bone marrow derived macrophages
MG132	Z-Leu-Leu-Leu-CHO
MHC-II	major histocompatibility complex class II
NF-κB	nuclear factor-κappa B
PA	protective antigen
PAMPs	pathogen-associated molecular patterns
PCR	polymerase chain reaction
PDI	protein disulphide isomerase
PE	*Pseudomonas* exotoxin A
PFTs	pore-forming toxins
Phdp	*Photobacterium damselae piscicida*
PK	protein kinase
PMSF	phenylmethylsulfonyl fluoride
PRRs	pattern-recognition receptors
PT	pertussis toxin
Rab	rabenosyn
RHD	Rel homology domain
RIPs	receptor interacting proteins
ROS	reactive oxygen species
SAgs	Superantigen toxins
sbPBS	sea bass phosphate saline buffer

sbPL	sea bass peritoneal leukocytes
SNARE	soluble N-ethylmaleimide-sensitive factor activating protein receptor
STs	heat-stable toxins
Stx	Shiga toxin
TCR	T-cell receptor
TeNT	tetanus neurotoxin
TLRs	toll-like receptors
TNF	tumour necrosis factor
TNFRs	TNF-receptors
TRAF	TNF-receptor associated factor
TRAIL	TNF-related apoptosis-inducing ligand
V-ATPase	vacuolar adenosine triphosphatase pump

ABSTRACT

Bacterial toxins comprise a large and diverse family of molecules recognized as primary virulence factor(s) of a variety of pathogenic bacteria. Studies on bacterial AB toxins contributed not only to clarify their role in infection but revealed also their potential as tools to study cellular processes and also as therapeutic agents.

The AIP56 (**A**poptosis **I**nducing **P**rotein of **56** kDa) toxin is a major virulence factor of *Photobacterium damselae piscicida* (*Phdp*), a Gram-negative bacterium that infects economically important fish species and is considered one of the most relevant pathogens in mariculture. In infected fish, AIP56 spreads systemically triggering apoptosis of macrophages and neutrophils, leading to the impairment of the host phagocytic defense and favoring *Phdp* survival and dissemination. This process of apoptosis culminates in post-apoptotic secondary necrosis with the release of the phagocyte's cytotoxic contents, contributing to the genesis of the infection-associated necrotic lesions. Structurally, AIP56 is an AB-type toxin composed by two domains linked by a disulphide bridge, with the A domain displaying the catalytic activity and the B domain responsible for the binding/translocation of the toxin. Recently, we have reported that AIP56 is a metalloprotease that cleaves NF-κB p65 at the Rel homology domain. NF-κB is an evolutionarily conserved transcription factor that regulates the expression of inflammatory and anti-apoptotic genes and plays a key role in host responses to microbial pathogen invasion. The proteolytic activity of AIP56 against NF-κB results in the removal of crucial residues involved in DNA interaction, compromising the NF-κB transcriptional activity.

Despite the knowledge about the toxic effects of AIP56, its structure and intracellular target, nothing was known about the susceptibility of different types of cells to AIP56 neither about the mechanisms involved in toxin uptake and intracellular trafficking. The studies included in this thesis aimed at clarifying the details of the interaction of AIP56 with target cells and at identifying the intracellular pathways followed by the toxin during intoxication.

Bacterial AB toxins, such as AIP56, have cytoplasmic targets and therefore must cross biological membranes to reach the intracellular milieu. To enter the cells, they act as opportunistic ligands, exploiting existing receptors and diverse mechanisms of endocytosis and intracellular trafficking. After receptor-mediated endocytosis some toxins, like diphtheria or anthrax toxin, can take the short journey/endosomal pathway and translocate from the endosomes through a pH-dependent mechanism while others, like Shiga or cholera toxins, can follow the long journey/retrograde pathway and travel to the endoplasmic reticulum from where the translocation occurs.

In the work herein presented, we show that, although *Phdp* is not able to infect mammals, AIP56 is able to enter and cleave p65 in different mammalian cell lines. We also show that, similarly to what was previously reported for sea bass leukocytes, mouse bone marrow derived macrophages undergo NF-κB p65 depletion and apoptosis in response to AIP56. Using both sea bass peritoneal leukocytes and mouse bone marrow derived macrophages, we disclosed key steps involved in the entry and intracellular trafficking of AIP56. Fluorescence microscopy and western-blotting analysis showed that AIP56 is rapidly endocytosed and competition assays revealed that, similarly to what was reported for sea bass peritoneal leukocytes, intoxication of mouse bone marrow derived macrophages involves interaction of AIP56 C-terminal region with cell surface components, suggesting the existence of a conserved receptor. Pharmacological inhibition of clathrin-dependent endocytosis regulators revealed that, as in the case of diphtheria toxin, AIP56 endocytosis occurs mainly through a clathrin-dependent process not requiring functional actin dynamics.

Data obtained in this study indicate that, alongside with diphtheria, anthrax and clostridial neurotoxins, AIP56 is a “short-trip” toxin that reaches the cytosol after translocation from endosomes using an acidic-pH dependent mechanism. Indeed, we found that pharmacological inhibitors that prevent endosome acidification inhibited AIP56-mediated p65 cleavage and that an acidic pulse was sufficient to trigger translocation of cell-surface bound AIP56 across the cytoplasmic membrane into the cytosol. In agreement with these findings, AIP56 became more hydrophobic at pH ≤ 5.5 and was able to interact with artificial lipid bilayer membranes only at acidic pH.

Usually, for “short-trip” AB toxins, a minor pool reaches the cytosol by translocating from endosomes whereas the rest is routed to lysosomes for degradation. In this work, using biochemical approaches and confocal microscopy we found that part of endocytosed AIP56 follows the endocytic recycling route and is recycled into the extracellular medium by a mechanism requiring PI3K activity but independent on endosome acidification.

The here reported results show that AIP56 cleaves NF-κB not only in fish but also in mammalian cells and disclose important aspects of AIP56 trafficking, revealing that these are conserved between fish and mammalian cells. Since there are several (so far uncharacterized) AIP56 full-length homologues in different bacterial species, expanding the knowledge on AIP56 intoxication mechanism, not only adds to the understanding of *Phdp* pathogenesis but may also shed light on the pathogenesis of other bacteria producing AIP56-like toxins. Apart from its intrinsic biologic interest, the evidences supporting that a significant pool of endocytosed AIP56 follows the recycling pathway and is released into the extracellular medium suggest a novel intracellular route amongst the

ones already established for bacterial AB toxins. This makes AIP56 an attractive tool for studying a poorly understood intracellular route. Moreover, it is well known that uncontrolled activation of NF-κB is associated with several human pathologies, including inflammatory diseases and cancers, and thus the observation that AIP56 acts on mammalian cells confers considerable biotechnological potential to the toxin. Altogether, the data presented in this thesis not only contribute to a better understanding of AIP56-associated pathogenicity but also open doors to the use of AIP56 as a biotechnological/therapeutic tool specifically targeting NF-κB.

RESUMO

As toxinas bacterianas constituem uma família ampla e diversificada de moléculas que inclui elementos considerados factores de virulência chave de várias bactérias patogénicas. Os estudos das toxinas bacterianas demonstraram a sua elevada importância não só como factores cruciais para o estabelecimento de várias infeções, mas também como ferramentas para o estudo de processos celulares eucarióticos e como agentes terapêuticos.

A AIP56 (***A**poptosis **I**nducing **P**rotein of **56** kDa*) é uma toxina que desempenha um papel central na virulência da *Photobacterium damselae piscicida* (*Phdp*), uma bactéria Gram-negativa que infecta várias espécies de peixes marinhos, sendo considerado um dos patogéneos mais relevantes em maricultura. Nos peixes infectados, a AIP56 dissemina-se de forma sistémica e induz apoptose de macrófagos e neutrófilos, comprometendo a defesa fagocítica do hospedeiro e contribuindo para a sobrevivência e disseminação da bactéria. O processo de apoptose culmina em necrose secundária, com libertação de moléculas citotóxicas que contribuem para a génese das lesões necróticas características da infeção por *Phdp*. Estruturalmente, AIP56 é uma toxina do tipo AB, composta por dois domínios unidos entre si por uma ponte dissulfureto, em que o domínio A é responsável pela actividade catalítica e o domínio B pela ligação/translocação da toxina. Recentemente, mostramos que a AIP56 é uma metaloprotease que corta a subunidade p65 do NF-κB no domínio Rel. O NF-κB é um factor de transcrição conservado evolutivamente que controla a expressão de genes pró-inflamatórios e anti-apoptóticos e desempenha um papel importante nas respostas dos hospedeiros à invasão por agentes patogénicos microbianos. A proteólise do p65 levada a cabo pela AIP56 remove resíduos cruciais envolvidos na interacção do NF-κB com o DNA, comprometendo a sua actividade transcricional.

Embora sejam já conhecidos alguns detalhes da estrutura da AIP56 e tenha sido identificado um alvo intracelular da toxina, os detalhes da interação da AIP56 com diferentes tipos celulares e os mecanismos envolvidos na entrada e tráfico no interior das células permanecem por esclarecer. Com este estudo, pretendeu-se clarificar mecanismos envolvidos na interação da AIP56 com diferentes células e identificar as vias intracelulares seguidas durante a intoxicação.

As toxinas do tipo AB, como a AIP56, actuam em alvos intracelulares e, por conseguinte, precisam de atravessar a membrana celular para alcançar o citosol. Para entrar nas células, estas toxinas agem como ligantes oportunistas explorando receptores e diversos mecanismos de endocitose e tráfego intracelular existentes na célula alvo.

Após endocitose mediada por receptor, algumas toxinas, como a da difteria ou antrax, seguem a via endosomal e translocam a partir dos endossomas por meio de um mecanismo dependente do pH, enquanto outras, como a toxina Shiga ou a toxina da cólera, seguem a via retrógrada até ao ER, de onde ocorre a translocação.

Embora a *Phdp* não seja capaz de infectar células de mamífero, trabalhos desenvolvidos no âmbito desta dissertação permitiram identificar vários tipos celulares de mamíferos susceptíveis à AIP56, mostrando que a toxina tem a capacidade de entrar e cortar o p65 em diferentes linhas celulares. No entanto, apenas em macrófagos de ratinho derivados da medula óssea (mBMDM) ocorreu depleção do p65 e apoptose em resposta à intoxicação, efeitos anteriormente descritos apenas em leucócitos peritoneais de robalo (sbPL), um hospedeiro natural da *Phdp*. Usando sbPL e mBMDM, clarificamos mecanismos importantes envolvidos na entrada e tráfico intracelular da AIP56. Usando microscopia de fluorescência e análise por western-blotting verificamos que a toxina é rapidamente endocitada. Ensaios de competição sugerem a existência de um receptor conservado para a AIP56 porque, tal como em sbPL, a entrada da AIP56 em mBMDM envolve a interacção da região C-terminal da toxina com elementos localizados à superfície da célula alvo. A inibição farmacológica de reguladores da endocitose dependente da clatrina revelou que, tal como no caso da toxina da difteria, AIP56 é endocitada maioritariamente por uma via dependente da clatrina mas independente da actina.

Em estudos que visaram esclarecer os mecanismos de translocação da AIP56, verificámos que compostos que impedem a acidificação endossomal inibem a chegada da toxina ao citosol. Verificámos ainda que um choque acídico é suficiente para desencadear a translocação da toxina que se encontra ligada à superfície da membrana celular das células alvo directamente para o citoplasma. Em consonância com estas observações, mostrámos que a pH ≤ 5.5 a hidrofobicidade da toxina aumenta e esta torna-se capaz de interagir com membranas bi-lipídicas artificiais. Em conjunto, os dados obtidos no âmbito desta dissertação indicam que a AIP56 é uma toxina do tipo "*short-trip"* que chega ao citosol atravessando a membrana dos endossomas primários por um mecanismo dependente do pH.

No caso das toxinas "*short-trip"*, está descrito que apenas um pequeno número de moléculas internalizadas atinge o citosol, sendo a grande maioria encaminhada para degradação nos lisossomas. No caso da AIP56, estudos de microscopia confocal e ensaios bioquímicos, mostraram que uma proporção significativa da toxina internalizada é reciclada e libertada novamente no compartimento extracelular, através de um mecanismo dependente da actividade da enzima fosfatidilinositol-3-cinase (PI3K) mas independente da acidificação dos endossomas.

Os dados aqui reportados mostram que a AIP56 corta a subunidade p65 do NF-κB não só em células de peixe mas também em células de mamífero e revelam aspectos importantes do tráfico da AIP56, mostrando que estes são conservados entre células de peixe e de mamífero. Uma vez que existem várias proteínas homólogas à AIP56 (até agora não caracterizadas) em diferentes bactérias, o reforço do conhecimento sobre os mecanismos de intoxicação da AIP56 não só contribuirá para aumentar a compreensão sobre o papel desta toxina no contexto da infecção pela *Phdp* mas poderá também esclarecer a patogénese de outras bactérias que produzem toxinas idênticas à AIP56. Para além do interesse biológico intrínseco, os resultados que mostram que a AIP56 segue a via endocítica de reciclagem revelam uma nova via de tráfico intracelular para toxinas AB. Isto faz com que a toxina possa ser uma potencial ferramenta para estudo de uma via intracelular pouco caracterizada. Para além disso, é sabido que a activação descontrolada do NF-κB está associada a diversas patologias humanas, incluindo as doenças inflamatórias e cancros e, portanto, a observação de que AIP56 actua em células de mamíferos confere considerável potencial biotecnológico à toxina. Em conjunto, os dados apresentados nesta tese não só contribuem para uma melhor compreensão da patogenicidade associada à AIP56, como também abrem portas ao uso da AIP56 como uma ferramenta biotecnológica/terapêutica tendo como alvo o NF-κB.

CHAPTER I

INTRODUCTION

A. Bacterial protein toxins

1. Overview

The term “bacterial toxin” was used for the first time in 1888 at Pasteur Institute when Roux and Yersin discovered diphtheria toxin in sterile filtrates of *Corynebacterium diphtheriae* (Roux & Yersin, 1888). Two years later, Knud Faber, in Denmark, and Tizzonni and Cattani, in Italy, found the tetanus toxin, secreted by *Clostridium tetani* (Alouf & Popoff, 2006). In 1896 Van Ermengem identified botulinum toxin as a toxin secreted by the bacterium *Clostridium botulinum* (Alouf & Popoff, 2006). Since then, many studies allowed the identification of several bacterial toxins with different structures and modes of action, revealing that together they constitute a large family with very diverse members (Lemichez & Barbieri, 2013).

Nowadays, more than hundred years later, the interest in studying toxins remains high for a number of reasons. First, because they are recognized as the primary virulence factor of a variety of pathogenic bacteria and have the capacity to induce many of the symptoms characteristic of the pathology. And second, because studies on bacterial protein toxins have provided remarkable insight not only into fundamental aspects of host/pathogen interactions but also into the basic biology of eukaryotic cells and have revealed the potential biomedical applications of bacterial toxins.

2. Main types of bacterial protein toxins

Bacterial toxins are often classified into several functional groups based on their structures and modes of action. They can be delivered into host cells by injection, using an injection apparatus build up by the bacteria (e.g. type III secretion system), or they can be secreted by the bacterium into the surrounding milieu (e.g. exotoxins). In this case, they may intoxicate host cells on the neighborhood or distantly from the bacterial pathogen, either by acting directly on host cells plasma membrane or by delivering toxic enzymatic components into the cytosol after entering by receptor-mediated endocytosis.

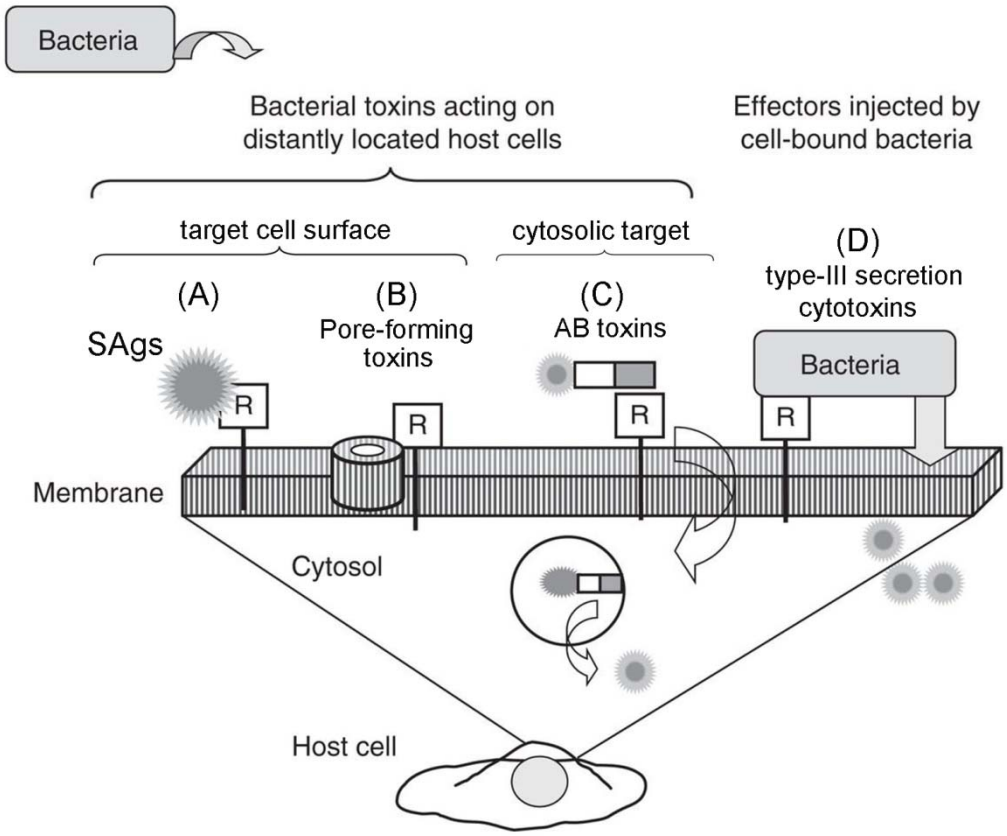

Figure 1.1. The four major classes of bacterial protein toxins. Bacterial toxins can: **(A) and (B)** act on the target cell surface to irreparable damage the cell membrane or alter normal cellular signal transduction; **(C)** exhibit enzymatic activity once the molecule has gained access to the cytoplasm of the sensitive cell by endocytosis; **(D)** inject the catalytic domain into the host cell using an injection apparatus of the bacterial pathogen. Whereas in classe (D) the bacterial pathogen needs to be in contact with host cell in order to exert toxicity, in the classe (A) (B) and (C) the toxins often act distantly from the bacterial pathogen. (From Lemichez & Barbieri, 2013)

2.1. Effectors delivered through injection

Whereas a high variety of bacterial toxins act distantly from the bacterial pathogen, a group of toxins are synthesized within the bacterium and are delivered directly into the host cell by an injection apparatus of the producing microorganism. Included in this group are the type III secreted cytotoxins/effectors widespread among Gram-negative bacteria which are injected directly into the cytoplasm of eukaryotic cells by type III secretion systems (T3SS) (Cornelis, 2006; Galan & Wolf-Watz, 2006; Hayes et al, 2010; Izore et al, 2011; Marlovits & Stebbins, 2010; Worrall et al, 2011). These are needle-like, membrane-anchored, multi-component complexes present in pathogenic bacteria, characterized by affecting the physiology of the host cell by delivering of a large amount of molecules in a short period of time (Lemichez & Barbieri, 2013). The structure of the T3SS apparatus (Figure 1.2) itself can display notable similarities amongst different bacterial species, although the nature of translocated effectors is widely different (Blocker et al, 2003a;

Galan & Wolf-Watz, 2006). Some authors considered these injected effectors distinct from bacterial toxins because while bacterial toxins usually have a single biochemical activity and target specific components of the host cell, effector proteins exert their specific function in concert with the activities of multiple other bacterial effectors delivered by the same machine (Galán, 2009).

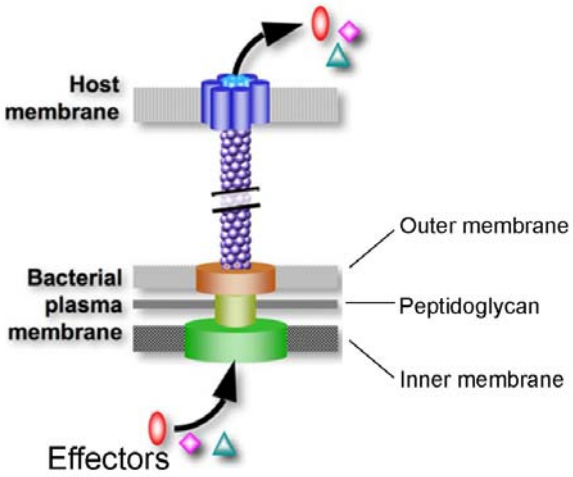

Figure 1.2. Type III secretion system. Schematic representation of a type III secretion system (T3SS). The T3SS apparatus has a part anchored in the bacterial membrane, formed by several ring structures that span the inner and outer membranes, and an extracellular part that is the needle (purple protrusion). The needle is thought to engage a bacterial pore-forming complex in the host cell membrane that allows the arrival of the bacterial effectors into the host cell cytosol. (From http://carbon.bio.ku.edu/research.html)

2.2. Exotoxins

2.2.1. Exotoxins acting at cell surface

Exotoxins acting at cell surface can display its toxicity by interfering with signal transduction pathways, by displaying enzymatic activities towards membrane compounds or by forming pores (Popoff, 2005).

Superatigens (SAgs) produced by a variety of bacteria, including *Sthapylococcus aureus*, *Streptococcus* sp., *Mycoplasma arthritidis* and *Yersinia pseudotuberculosis* are examples of bacterial toxins acting at cell surface by corrupting signal transduction pathways (McCormick et al, 2001; Yoshino et al, 1994). SAgs stimulate the interaction of peptide-independent MHC II with T cell receptor at the surface of antigen-presenting cells (Figure 1.3A). These hijacks T-cell antigen recognition (Henkel et al, 2010) leading to a non-specific activation of the immune response that culminates in a powerful inflammatory response (Fraser & Proft, 2008; Muller-Alouf et al, 2001).

Also as examples of toxins that can display their toxic program at the cell membrane are bacterial hyaluronidases, collagenases, and phospholipases that enzymatically alter

the extracellular matrix or the plasma membrane of eukaryotic cells. These include the α-toxin of *Clostridium perfringens*, which has phospholipase C activity (Songer, 1997); *Streptococcus pyogenes* streptokinase, which can hydrolyze plasminogen to plasmin and dissolve clots (Lottenberg et al, 1994); and the clostridial collagenases, which can degrade collagen (Harrington, 1996).

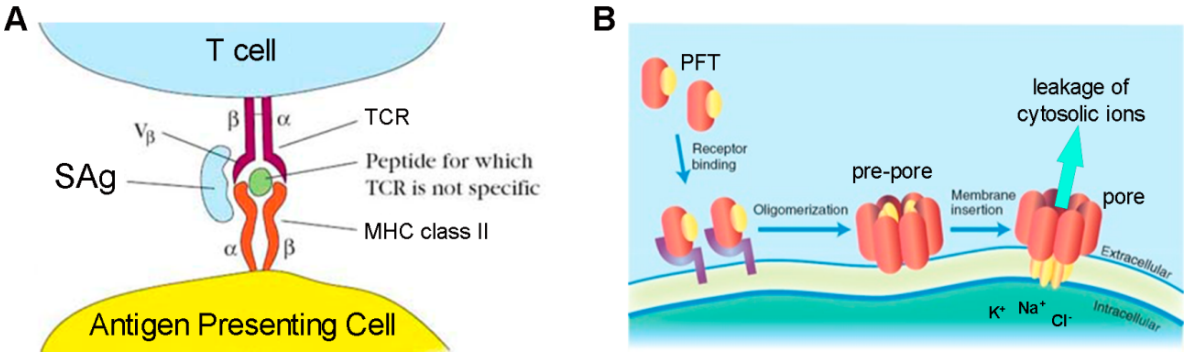

Figure 1.3. Exotoxins acting at the cell surface. (A) Schematic representation of T-cell activation by SAg. Sags stimulate T cells by cross-linking major histocompatibility complex (MHC) class II antigens and T-cell receptors (TCR). (Adapted from http://biosiva.50webs.org/antigens.htm). **(B)** Pore-forming toxins. Schematic representation of pore formation induced by an exotoxin. PFT: pore forming toxin. (Adapted from http://vdg.epfl.ch/PoreFormingToxins).

Pore forming toxins (PFTs) are characterized by forming pores of different size and molecular selectivity in the membranes of bacteria, plants and mammals that result in loss of membrane integrity corrupting cell signaling, and changes in the concentration of ions in the target cell cytosol that leads to ion imbalance (Bischofberger et al, 2009; Bischofberger et al, 2012; Iacovache et al, 2008). While pathogenic bacteria produce PFTs to affect their hosts in order to promote colonization and spread (Aboulaich et al, 2004) some bacteria can produce PFTs to kill other bacteria. As example, some *Escherichia coli* species produce pore-forming colicins to kill related bacteria (Lakey et al, 1994). PFTs are secreted as monomeric proteins that, after binding to the cell surface via specific receptors, assemble into oligomeric structures which undergo a conformational change that generates hydrophobic patches. This allows spontaneous insertion into the lipid bilayer that culminates in membrane permeabilization and release of cytosolic ions (Figure 1.3B) (Bischofberger et al, 2012). Based on the multimeric structure involved in membrane insertion, PFTs are classified in α-PFTs or β-PFTs (Henkel et al, 2010). α-PFTs, such as colicins, insert into the membrane as an α-helix while β-PFTs like the cholesterol-dependent cytolisins, primarily produced by Gram-positive bacteria (Park et al, 2004; Rosado et al, 2008; Rossjohn et al, 2007) insert into the membrane as β-sheets.

2.2.2. Exotoxins with cytosolic targets

To be successful, intracellular acting toxins must access their substrates inside target cells. Usually, these toxins are internalized by receptor-mediated endocytosis before reaching the cytosol from intracellular compartments (Lauvrak et al, 2004; Montecucco & Papini, 1995).

Toxins that are internalized by receptor-mediated endocytosis and act at the cytosol of host cells are called AB toxins (Lemichez & Barbieri, 2013) and will be discussed in detail below (Section 3). According to the nature of the target and the type of modification, these toxins cause a dramatic alteration of cellular functions such as protein synthesis, cell homeostasis, cell cycle progression, vesicular traffic, actin cytoskeletal rearrangements, and signaling pathways (Table 1) (Henkel et al, 2010; Lemichez & Barbieri, 2013; Popoff, 2005).

Table 1. Examples of bacterial AB toxins that enzymatically modify cytosolic targets

Toxin	Enzymatic activity	Cellular target	Effect	Reference
Toxins targeting actin cytoskeleton components				
Clostridium botulinum C2 toxin	ADP-ribosyl transferase	Actin	Depolymerization	(Aktories et al, 1986)
Clostridum perfringens iota toxin	ADP-ribosyl transferase	Actin	Depolymerization	(Aktories, 2011)
Photorhabdus luminescens Tc (TccC3-subunit)	ADP-ribosyl transferase	Actin	Actin clustering	(Lang et al, 2010)
Clostridium difficile toxins A and B	Glucosyltransferase	Rho proteins	Actin depolymerization	(Just et al, 1995)
Escherichia coli CNF1	Deamidase	Rac1, RhoA, Cdc42 (Q61 or Q63)	Actin polymerization	(Lemonnier et al, 2007)
Toxins targeting SNARE machinery				
Clostridium tetani TeNT	Zinc metalloprotease	VAMP / synaptobrevin	Neurotransmission inhibition	(Hill et al, 2007)
Clostridium botulinum, BoNT A, E	Zinc metalloprotease	SNAP25	Neurotransmission inhibition	(Hill et al, 2007)
Clostridium botulinum, BoNT B, D, F, G	Zinc metalloprotease	VAMP / synaptobrevin	Neurotransmission inhibition	(Hill et al, 2007)
Clostridium botulinum, BoNT C	Zinc metalloprotease	SNAP25, syntaxin	Neurotransmission inhibition	(Hill et al, 2007)

Table 1. Continued

Toxin	Enzymatic activity	Cellular target	Effect	Reference
Toxins targeting cell translational machinery				
Corynebacterium Diphtheriae DT	ADP- ribosyl transferase	EF2 (diphthamide-715)	Translation inhibition	(Murphy, 2011)
Pseudomonas aeruginosa exotoxin A	ADP- ribosyl transferase	EF2 (diphthamide-715)	Translation inhibition	(Murphy, 2011)
Shigella dysenteriae Stx	N-glycosylase	28S ribosomal RNA	Translation inhibition	(Johannes & Romer, 2010)
Toxins targeting cAMP, MAP kinase and NF-κB signaling components				
Vibrio cholera CT	ADP- ribosyl transferase	Heterotrimeric G-protein ($G\alpha_s$)	cAMP induction	(Aktories, 2011)
Bordetella pertussis Ptx	ADP- ribosyl transferase	Heterotrimeric G-protein ($G\alpha_s$)	cAMP induction	(Aktories, 2011)
Bacillus anthracis ET	Adenylate cyclase	cAMP modulated proteins	cAMP production	(Leppla, 1982)
Bacillus anthracis LT	Zinc metalloprotease	MAP kinase kinases (except MEK5)	MAP Kinase signaling	(Collier & Young, 2003)
Photobacterium damselae piscicida, AIP56	Zinc metalloprotease	NF-κB p65	NF-κB p65 depletion	(Silva et al, 2013)

CNF, cytotoxic necrotizing factor; DT, diphtheria toxin; Stx, Shiga toxin; TeNT, tetanus toxin; BoNT, botulinum neurotoxin; CT, cholera toxin; Ptx, pertussis toxin; ET, edema toxin; LT, lethal toxin. (Adapted from Lemichez & Barbieri, 2013).

3. AB toxins

3.1. Overview

AB toxins can be single proteins or oligomeric proteins complexes organized into distinct domains and are characterized by an overall similar structural and functional architecture (Figure 1.4). Nevertheless, concerning the molecular organization, the AB toxin family includes members with different structural arrangements (Figure 1.4), adapted to the specific requirements of the intoxication pathway (Montecucco & Papini, 1995).

Usually, AB toxins are synthesized and secreted by the pathogen as inactive molecules that are activated through proteolytic cleavage performed by either a host (e.g. cholera toxin, ricin, clostridial neurotoxins) or a pathogen protease (e.g. Shiga toxin and *Pseudomonas* exotoxin A) at a region between two cysteine residues. In the case of diphtheria toxin, it can result from the action of bacterial proteases or occur at the host cell surface mediated by a furin or furin-like protease (Gill & Dinius, 1971; Tsuneoka et al, 1993).

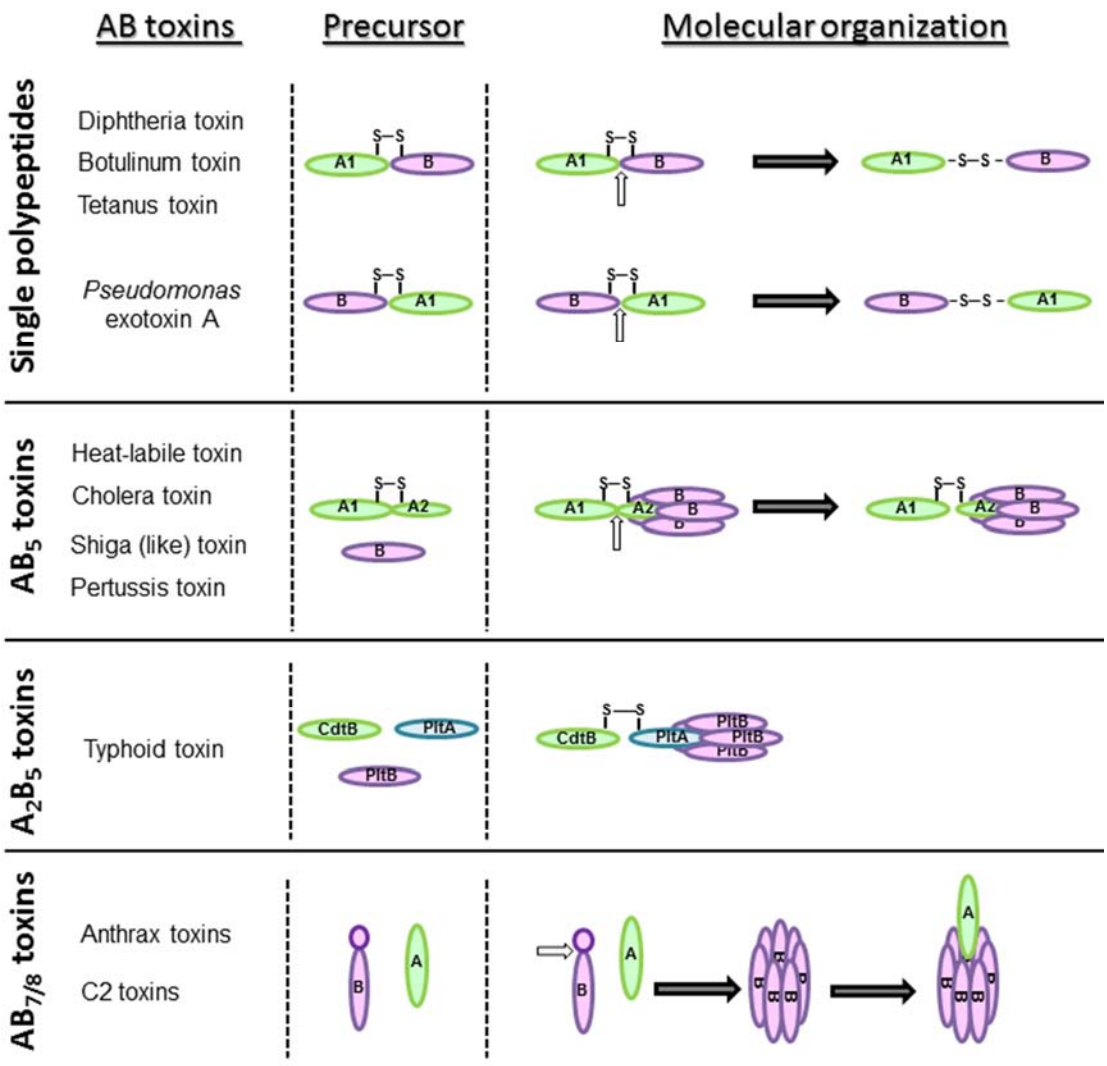

Figure 1.4. Structural organization of AB toxins. AB toxins are composed by two domains, the A domain (A) responsible for the catalytic activity and the B domain (B) responsible for binding and delivery of the A domain into cytosol, usually linked by a disulfide bond (S-S). In general, proteolytic cleavage (open arrows) of the toxin is required for activity. Such cleavage can occurs in the region between the A and B domains, in the A domain or in the B domain (open arrows).

3.2. Molecular organization

3.2.1. Single polypeptide

In single polypeptide AB toxins, including diphtheria toxin, *Pseudomonas aeruginosa* exotoxin A, tetanus neurotoxin (TeNT) and botulinum neurotoxins (BoNT/A-G), the A and B domains are contiguous (Collier, 2001; Turton et al, 2002; Weldon & Pastan, 2011; Wolf & Elsasser-Beile, 2009), until proteolytic cleavage. The cleavage results in a di-chain toxin molecule with the A moiety and the B moiety linked by a disulfide bond (Ahnert-Hilger et

al, 1990; Chaudhary et al, 1990; Collier, 2001; Corboy & Draper, 1997; DasGupta, 1971; Fryling et al, 1992; Gill & Dinius, 1971; Krieglstein et al, 1991; Tsuneoka et al, 1993; Weller et al, 1989). Upon encountering reducing conditions the catalytic domain is released. Whereas most AB toxins secreted as single polypeptides are cleaved by proteases of the eukaryotic cell (e.g. furin) or secreted by the pathogen, some have the capacity of auto-proteolytic processing (Aktories, 2007; Shen, 2010). These toxins, in addition to the characteristic domains of AB toxins, have an autocatalytic/self-cutting cysteine protease domain in the N-terminal region responsible for toxin processing. Accordingly, it has been proposed that in these toxins the AB model could be extended to an ABCD model whereas A represents the biological activity, B the binding, C the cutting and D the delivery domain (Jank & Aktories, 2008). Among the ABCD toxins are the *Clostridium dificille* toxin A and B, the hemorrhagic and lethal toxins from *Clostridium sordelli* and the α-toxin from *Clostridium novyi* (Aktories, 2007; Shen, 2010).

3.2.2. Oligomeric complexes (AB_5, A_2B_5 and $AB_{7/8}$)

Cholera toxin (Ctx), the closely related heat labile enterotoxins (LT), pertussis toxin (Ptx) and Shiga toxin (Stx) are examples of AB_5 toxins (Merritt & Hol, 1995). In the case of AB_5 toxins, discrete genes encode the A and B fragments that assemble as non-covalent complexes in which the A fragment (the catalytic domain) rests upon a donut-shaped pentamer of B fragments (the receptor-binding domain) (Beddoe et al, 2010). The proteolytic cleavage occurs in the A moiety resulting in two fragments, A1 and A2, linked by a disulfide bond (Booth et al, 1984; Garred et al, 1995b; Grant et al, 1994; Krueger et al, 1991). The A2 domain consists of an α-helix that penetrates into the central pore of the pentameric B-domain, tethering the A- and B-domains together through non-covalent interactions (Fraser et al, 1994; Sixma et al, 1993a; van den Akker et al, 1996) while the A1 domain contains the enzymatic activity and is translocated into cytosol after reduction of the disulfide linkage.

Recently, an unprecedented chimeric A_2B_5 toxin secreted by *Salmonella enterica* serovar Typhi (*S.* Typhi) has been described and proposed to constitute the founding member of the A_2B_5 organization (Song et al, 2013). This toxin was named typhoid toxin and is organized by two covalently linked A domains non-covalently associated to a pentameric B domain (Figure 1.4). The A domains, CdtB and PltA, are homologues of the A domain of cytolethal distending toxin and pertussis, respectively, and its single B domain, PltB, is homologous to one of the components of the hetero-pentameric B domain of pertussis toxin. Crystal structure of the chimeric A_2B_5 toxin showed that, similarly to the

B domains of AB_5 toxins, the PltB oligomer is arranged as a pentamer but, in contrast to AB_5 toxins instead of one A domain has two domains (CdtB and PltA). The disulphide bound linking the two A domains seems to be essential for the integrity of the holotoxin. Furthermore, this ensures that CdtB and PltA are delivered simultaneously to the same target cell and upon reduction of the disulphide bond (most likely by reductases of the endoplasmic reticulum) PltA and CdtB would be freed from one another allowing them to translocate into the cytosol and reach their place of action (Song et al, 2013).

For $AB_{7/8}$ toxins, including anthrax toxin (Collier & Young, 2003; Young & Collier, 2007) and C2 toxin (Aktories & Barth, 2004a; Aktories & Barth, 2004b), different genes encode the A and B domains, which are released as separate polypeptides that interact at the surface of the host cell. $AB_{7/8}$ toxins are so termed because its B domain (the receptor-binding domain) is composed by seven or eight subunits that form a ring-shaped heptamer or octamer (Barth et al, 2004). The B domain is activated at cell surface by proteolytic cleavage (serum proteases or furin proteases) and assembles into a heptameric/octameric complex that recruits the A domain (Blank, 2006; Sun, 2012a). Usually the B domain oligomerizes to form a pore that binds with high affinity host cell receptors and the enzymatic A subunit, allowing endocytosis of the complex and delivering of the A subunit into the cytosol (e.g. C2 toxin (Aktories & Barth, 2004a)) or into the lumen of the intraluminal vesicles of endosomal carrier vesicles (e.g. anthrax toxin (Abrami et al, 2013; Abrami et al, 2004)).

3.3. Application of bacterial AB toxins

In agreement with the key role of bacterial toxins in the establishment and development of the infections induced by several bacterial pathogens, inactivated toxin-based vaccines have been successfully used to protect from toxin-induced diseases. Accordingly, vaccines based on inactivated bacterial toxins (toxoid vaccines) are routinely used to promote antitoxin immunity for the treatment and prevention of bacterial infections (Holmgren et al, 2005; Holmgren et al, 1977; Hu et al, 2013; Karczewski et al, 2014; Kitchin, 2011; Mortimer, 1978), including vaccines against tetanus, diphtheria and pertussis that integrate the obligatory Portuguese immunization program.

Bacterial protein toxins have provided remarkable insight not only into fundamental aspects of host/pathogen interactions but also into basic mechanisms of eukaryotic cells such as: receptor endocytosis, vesicular trafficking, translocation through intracellular membranes, and regulation and function of cellular targets (Table 2).

Moreover, AB toxins have diverse characteristics that make them promising tools for diagnosis and treatment of different diseases, including cancer and inflammatory diseases (Lemichez & Barbieri, 2013; Odumosu et al, 2010; Sandvig et al, 2010): (i) they can interact with the cell machinery of diverse cell types and thus, are useful to treat different diseases; (ii) they have very high toxicity, i.e. small amounts are sufficient to intoxicate the target cells (Yamaizumi et al, 1978); (iii) they are very stable enzymes, with few inhibitors, and can survive temperature extremes and proteolytic degradation, allowing them to remain active long enough to display toxicity; (iv) and they are easily produced in *E. coli* (Fitzgerald, 1996; Johannes & Decaudin, 2005). Another important feature is their modular structure and corresponding mechanisms of action that make them suitable to modifications that can redirect their potent cytotoxicity from disease to a therapeutic function.

Table 2. Mechanisms of basic biology revealed by studies of protein toxins. Adapted from Sandvig & van Deurs, 2005.

Date	Mechanism revealed
1979	Demonstration of the recycling of endocytosed material through studies with plant toxin ricin (Sandvig & Olsnes, 1979).
1980	Studies with diphtheria toxin revealed the direct penetration of a protein across the eukaryotic cell membrane in response to low pH (Draper & Simon, 1980; Sandvig & Olsnes, 1980).
1985-1987	Evidence for clathrin-independent endocytosis through studies with plant toxin ricin (Moya et al, 1985; Sandvig et al, 1987).
1986	Studies with ricin showed that conjugates of a particular ligand (e.g. ricin) with different probes can influence the intracellular destiny of the ligand (van Deurs et al, 1986).
1992	Studies with Shiga toxin revealed a retrograde transport all the way from the cell surface to the Golgi apparatus, the ER and the nuclear envelope (Sandvig et al, 1992).
1999	Studies using a GPI-anchored diphtheria toxin receptor demonstrated that GPI-anchored proteins could be endocytosed by clathrin- and caveolin-independent endocytosis (Skretting et al, 1999).

In some circumstances, the toxins are used in their native form. Successful examples of the use of holotoxins is the use of the powerful botulinum neurotoxin type A (BoNT/A) in disorders related to muscle hyperactivity, including eye movement abnormalities, cervical and laryngeal dystonia, writer's cramp, hemifacial spasm, tremors, and tics (Averbuch-Heller & Leigh, 1997; Kessler & Benecke, 1997; Wheeler, 1997), and also in cosmetic treatments to reduce deep wrinkles caused by the contraction of facial muscles (Carter & Seiff, 1997). Another example is Shiga toxin. Shiga toxin binds to the cell surface glycosphingolipid Gb3, which is overexpressed in various cancer cells (Distler et al, 2009; Johannes & Decaudin, 2005; Kovbasnjuk et al, 2005) leading to the suggestion that the toxin could be used in its native form for diagnosis of cancer cells (LaCasse et al, 1999; LaCasse et al, 1996; Lingwood et al, 1998; Murray et al, 1985; Taga et al, 1995).

However, due to the possible toxicity of the holotoxins, in most instances, toxins need to be modified for therapeutic proposes. A good example is the use of the catalytic domain of toxins, like *Pseudomonas* exotoxin A (PE) and diphtheria toxin (DT) (Doherty et al, 2006; Duvic & Talpur, 2008; Pastan et al, 2006; Pastan et al, 2007; Potala et al, 2008; Shapira & Benhar, 2010; Weldon & Pastan, 2011; Wolf & Elsasser-Beile, 2009; Wong et al, 2007) as the cell-killing component of immunotoxins (Li et al, 2013). Immunotoxins (IT; Figure 1.5) are proteins constructed by replacing the toxin's natural binding domain by an antibody or malignant cell-binding ligand that redirects cell killing activity to malignant cells (Brinkmann, 1996; Li et al, 2013). After binding of the antibody to a target cell antigen, the IT is internalized, processed and delivered into the cytosol, where it induces cell death (FitzGerald et al, 2004; Kreitman, 1999; Kreitman, 2009; Pastan et al, 2007). Immunotoxins have been used in treatment of hematologic malignancies and solid tumors and have demonstrated potent clinical efficacy (FitzGerald et al, 2004; Johannes & Decaudin, 2005; Kreitman, 1999; Kreitman, 2009; Li et al, 2013; Pastan et al, 2007; Sandvig et al, 2010; Sandvig & van Deurs, 2000).

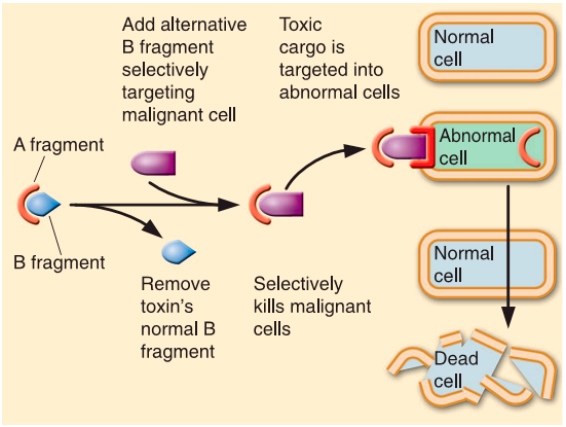

Figure 1.5. Application of bacterial toxins in therapeutics. Immunotoxins (IT) therapy using the catalytic domain of an AB toxin. IT are composed by a cell recognition (binding) domain that selectively targets malignant cells, which concentrates the toxin on the surface of the target cell, usually linked by a disulphide bridge, to the enzyme active and translocating domains of a bacterial AB toxin (B domain). The translocation domain enables the toxin to cross a membrane to reach the cytosol and the catalytic domain is responsible for cell death. (From Blank, 2006).

Despite their use in immunotoxins, toxins can also be used as tools to induce an immune response. In this case, the domain responsible for binding and internalizing of the toxin, the B domain, is used as a vector to deliver desired cargos into cell. Indeed, the B subunit of Shiga toxin (Haicheur et al, 2003; Haicheur et al, 2000; Lee et al, 1998; Sandvig et al, 2010; Sandvig & van Deurs, 2000; Smith et al, 2002), cholera toxin (Czerkinsky et al, 1996; Eriksson & Holmgren, 2002; Porgador et al, 1998; Sun et al,

1994; Sun et al, 2000), *E.coli* heat-labile toxin (Loregian et al, 1999; Marcello et al, 1994) and *Pseudomonas* exotoxin A (Donnelly et al, 1993) have been used as vectors to deliver antigen epitopes for presentation to MHC I, triggering an immune response (Haicheur et al, 2003; Haicheur et al, 2000; Lee et al, 1998; Smith et al, 2002).

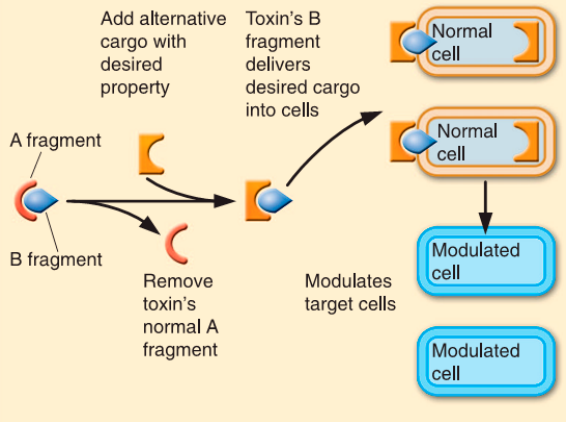

Figure 1.6. Application of bacterial toxins in therapeutics. The binding domain of an AB toxin (B domain) used as vector. The toxin B domains are used to deliver heterologous cargo into target cells. Method used to treat human cancers, infectious diseases and autoimmune diseases. (From Blank, 2006).

B. Intoxication pathways of bacterial AB toxins

1. General concepts on endocytosis

The plasma membrane of a cell is not just a simple physical barrier that separates the cytoplasm from the outer world but constitutes one of the most complex components of the cell that can defend it against the invasion of microbial pathogens (Sun, 2012a).

Endocytosis, the internalization of plasma membrane components, extracellular ligands and soluble molecules, is a key process in all eukaryotic cells. It has a fundamental role in a diversity of cellular processes, ranging from nutrient uptake to maintenance of cellular homeostasis, generation of cell polarity, synaptic vesicle recycling, regulation of cell-surface expression of signaling receptors, remodeling of the plasma membrane, antigen presentation and cell migration (Doherty & McMahon, 2009). To efficiently coordinate such processes, endocytic pathways must possess a high variability in terms of regulation, specificity for different cargoes, and ultimate destination within cells. Indeed it is now evident that there are several mechanisms of endocytosis differentially regulated but that may operate in parallel (Doherty & McMahon, 2009; Kumari et al, 2010). Despite the variety of endocytosis pathways these can be classically divided into

clathrin-dependent endocytosis or clathrin-independent endocytosis (Doherty & McMahon, 2009).

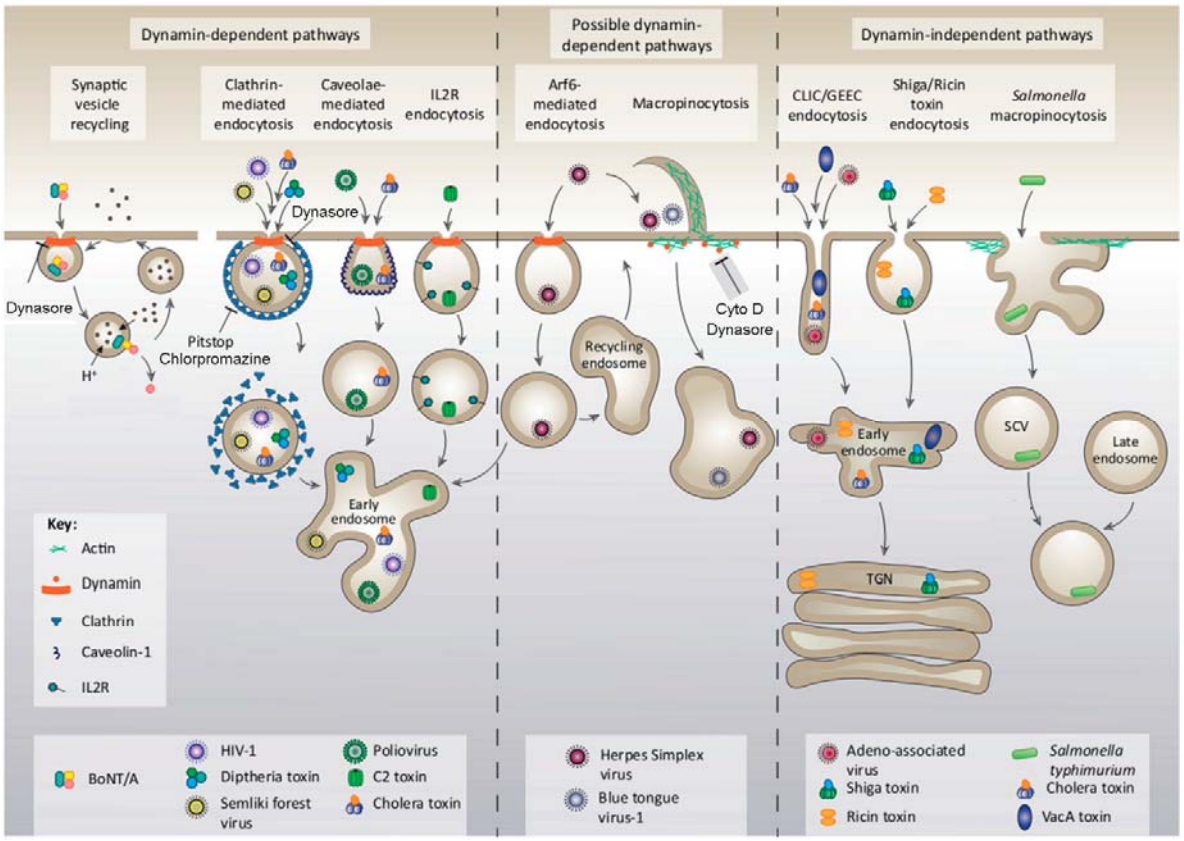

Figure 1.7. Different endocytic pathways and small molecules that can inhibit these pathways. Endocytic pathways dependent on dynamin can be inhibit by a potent cell-permeable inhibitor of dynamin (dynasore) (Kirchhausen et al, 2008; Macia et al, 2006); clathrin-mediated endocytosis can be inhibit by preventing the uncoating of clathrin (Pitstop) (Harper et al, 2013) or by altering the distribution of clathrin and AP-2 preventing formation of clathrin-coated pits at the plasma membrane (chlorpromazine) (Wang et al, 1993). Actin filaments are involved in formation of plasma membrane ruffles important for macropinocytosis, therefore macropinocytosis can be inhibited by break-down of actin filaments (cytochalasin D – cyto D) (Ohmori & Toyama, 1992; Sampath & Pollard, 1991). (From Harper et al, 2013).

1.1. Clathrin-dependent endocytosis

The most well-characterized endocytic pathway is the clathrin-mediated endocytosis. Because, in many cell types, it is the major pathway for receptor-dependent endocytosis it was incorrectly used for several years as synonymous of receptor-mediated endocytosis. This mechanism of endocytosis is dependent on adaptor proteins and proceeds through a series of well-defined morphological alterations and intermediates (McMahon & Boucrot, 2011). It involves cargo recognition by a specific receptor at the plasma membrane and coat assembly, followed by concentration in clathrin-coated pits that undergo progressive invagination and after scission form clathrin-coated vesicles (Roth & Porter, 1964; Schmid & McMahon, 2007). During this process, soluble clathrin is recruited from the cytoplasm to

the plasma membrane and the clathrin triskelia assemble into a polygonal lattice at the plasma membrane to form coated pits (Bonifacino & Lippincott-Schwartz, 2003; Kirchhausen, 2000). Clathrin interacts in a coordinated fashion with a diversity of adaptor and accessory proteins that coordinate clathrin polymerization into curved lattices stabilizing the deformation of the attached membrane (Doherty & McMahon, 2009; Ehrlich et al, 2004; Kirchhausen, 1999; Schmid et al, 2006). Clathrin-coat nucleation at plasma membrane and stabilization of the clathrin-coated pit requires cargo acquisition via subunits of adaptor protein 2 (AP2) and of various AP2-binding partners (Edeling et al, 2006; Kelly et al, 2008). The process of invagination is promoted by BAR (Bin Amphiphysin Rvs) domain-containing proteins, such as endophilin and amphiphysin, and is further facilitated by epsin (e.g. Eps15) (Abrami et al, 2003) and inherent curvature properties of assembled clathrin structures (Doherty & McMahon, 2009). Finally, the pinching off of the endocytic vesicles from the plasma membrane, that irreversibly releases the clathrin-coated vesicle into the interior of the cell, is promoted by the large GTPase dynamin (Baba et al, 1995; Bashkirov et al, 2008; Damke et al, 1994; Praefcke & McMahon, 2004; Pucadyil & Schmid, 2008; Roux & Antonny, 2008; Schmid et al, 1998; Sever et al, 2000). After released into cell, clathrin-coated vesicles are uncoated and fuse with early endosomes.

1.2. Clathrin-independent endocytosis

Clathrin-independent endocytosis is less characterized but equally important. During several years it has been thought that clathrin-dependent endocytosis was the only existing endocytic mechanism. Interestingly the first description on the existence of non-clathrin dependent endocytosis was through pioneering studies on cellular uptake of AB toxins (Moya et al, 1985; Sandvig & Moskaug, 1987; Sandvig et al, 2008; Sandvig & van Deurs, 1990). Nowadays it is clear that a cell can have several endocytic mechanisms that are independent on clathrin. In contrast to clathrin-dependent endocytosis, these mechanisms of endocytosis do not use known coat complexes for cargo recruitment and budding of transport intermediates. Instead they might exploit the constituents of the plasma membrane to their own benefit (Hansen & Nichols, 2009; Le Roy & Wrana, 2005; Mayor & Pagano, 2007; Nichols & Lippincott-Schwartz, 2001; Sandvig et al, 2011; Sandvig et al, 2008).

Clathrin-independent endocytic pathways are responsible for internalization of either large particles or small solutes and includes phagocytosis, caveolae-mediated uptake, macropinocytosis and constitutive non-clathrin uptake. Phagocytosis, usually restricted to phagocytes, is the process involved in uptake of large particles that typically occurs after a

phagocytic stimulus (Flannagan et al, 2012). The non-clathrin pathways underlying the uptake of smaller cargoes include caveolae, macropinosomes or a little-understood constitutive process of plasma membrane internalization such as CLIC/GEEC-type (clathrin-independent carriers/GPI-enriched early endosomal compartments) endocytosis (Kirkham & Parton, 2005; Mayor & Pagano, 2007), the putative flotillin-associated endocytic structures (Frick et al, 2007), circular dorsal ruffles (Orth & McNiven, 2006), and entosis (Overholtzer et al, 2007). It is known that a diverse array of molecular machinery is involved in these pathways, including dynamin and actin (Damke et al, 1994; Lamaze et al, 2001; Pelkmans et al, 2002; Tse et al, 2003), however questions about the organization of markers for non-clathrin pathways within the plasma membrane and how interactions with ligands and the cellular matrix can modulate these endocytic pathways are still not clear.

So far, the most commonly reported and understood non clathrin-coated plasma membrane buds are known as caveolae (for “little caves”) (Doherty & McMahon, 2009). Caveolae are small invaginated plasma membrane domains, with a defined and characteristic flask-shaped morphology (Stan, 2002), enriched in cholesterol and glycosphingolypids (Hailstones et al, 1998; Parton et al, 1994; Parton & Simons, 2007; Pelkmans et al, 2001; Rodal et al, 1999; Rothberg et al, 1990), exclusively taking place at microdomains of the plasma membrane denoted as lipid rafts (Nabi & Le, 2003). They are characterized by the abundant presence of the integral membrane protein caveolin 1 responsible for caveolar biogenesis (Rothberg et al, 1992). Cargoes internalized by caveolae are delivered to neutral pH caveosomes (Nichols, 2003; Pelkmans & Helenius, 2002).

2. Endocytosis of AB toxins

The first barrier encountered by bacterial AB toxins on host cells is the plasma membrane and to overcome this barrier they exploit mechanisms of endocytosis as portals of entry into host cells. The cells have not developed specific receptors for toxins and therefore these act as opportunistic ligands by using existing receptors, which can be proteins, glycoproteins, glycolipids or another compound, but in a lipid environment (Blank, 2006; Geny & Popoff, 2006). In the entry process of an AB toxin, the B domain recognizes one or more plasma membrane receptors and assists the movement of the A domain across the membrane. Cells lacking specific receptors are generally resistant to intoxication (Blank, 2006) highlighting the relevance of toxin-receptor complexes in the

intoxication process. If, or how, different receptors/endocytosis regulate sorting of the toxins into defined intracellular pathways is still not clear.

Bacterial AB toxins can exploit different endocytotic mechanisms and can use exclusively one or more than one endocytic pathway to enter the cells. While diphtheria toxin, clostridial glucosylating toxins (CGTs) and anthrax toxin are thought to predominantly use clathrin-dependent endocytosis mechanisms, other toxins, including Shiga, cholera and tetanus toxins enter cells by one of several alternative clathrin-independent endocytic pathways. In the case of Shiga and cholera toxins it seems that endocytosis can occur either through clathrin-dependent or independent pathways.

Diphtheria toxin binds to a transmembrane protein that serves as precursor for heparin-binding epidermal growth factor (HB-EGF) (Collier, 2001; Naglich et al, 1992) and is internalized, in different cell types, via clathrin-mediated endocytosis (Lemichez et al, 1997; Skretting et al, 1999) dependent on clathrin adaptor protein 2 (AP2) but independent on actin (Abrami et al, 2010). Accordingly, treatments that remove the clathrin-coated pits (Moya et al, 1985) and pharmacological inhibition of dynamin (Papatheodorou et al, 2010) or expression of a dominant-negative mutant dynamin K44A, protect against diphtheria toxin (Simpson et al, 1998). CGTs are internalized by receptor mediated endocytosis, although far less is known about the specific binding structures for most clostridial glucosyltransferases. Nevertheless, it is known that this toxin family is internalized by a dynamin dependent mechanism governed by clathrin (Kushnaryov & Sedmak, 1989; Papatheodorou et al, 2010).

In the case of anthrax toxin the process of endocytosis is more complex. Anthrax toxin is a tripartite toxin composed by two enzymatic subunits, the calmodulin-dependent adenylate cyclase edema factor (EF), and the zinc-dependent metalloprotease lethal factor (LF), which require the third subunit, the protective antigen (PA), to interact with cells. PA is an 83 kDa protein, organized into four domains, essentially composed of hydrophilic β-strands, that binds to cells via one of two receptors: tumor endothelial marker 8 (TEM8, also called ANTXR1) and capillary morphogenesis 2 (CMG2, also called ANTXR2) (Abrami et al, 2005; Scobie & Young, 2005; van der Goot & Young, 2009; Young & Collier, 2007). A coreceptor, the cell surface protein lipoprotein-receptor-related protein 6 (LRP6), seems to be also involved in PA-binding as well as toxin internalization (Wei et al, 2006; Young & Collier, 2007). After binding to its receptor (Figure 1.8), PA is proteolytically activated (Singh et al, 1989) by members of the furin family of transmembrane proteases, which cleave the 20kDa N-terminal domain of PA83 (Collier & Young, 2003; Klimpel et al, 1992). The resulting PA monomers (63 kDa, PA63) self-associates into a heptameric (PA^{7mer}) ring-like structure and form a pre-pore structure

(Abrami et al, 2000; Lacy et al, 2004; Nassi et al, 2002; Petosa et al, 1997) capable of binding a combination of three molecules of EF and/or LF (Mogridge et al, 2002; Pimental et al, 2004), via homologous N-terminal domains (Bragg & Robertson, 1989; Quinn et al, 1991). The heptamerization of PA is promoted by its concentration in lipid rafts domains at cell membrane and is accelerated by the presence of EF and/or LF (Abrami et al, 2005; Wigelsworth et al, 2004). Following lipid-raft association (a pre-requisite for efficient endocytosis) (Abrami et al, 2003; van der Goot & Young, 2009), endocytosis of the anthrax toxin-receptor complexes occurs through a mechanism that requires clathrin and the large GTPase dynamin (Abrami et al, 2003; Boll et al, 2004), but not the caveolar proteins caveolin-1 (Abrami et al, 2003). Nevertheless, anthrax endocytosis occurs via a non-canonical clathrin-dependent route that depends on β-arrestins and the heterotetrameric adaptor complex AP-1 but not on the more conventional adaptor complex AP-2. In contrast to diphtheria toxin, anthrax endocytosis is strongly actin dependent (Abrami et al, 2010).

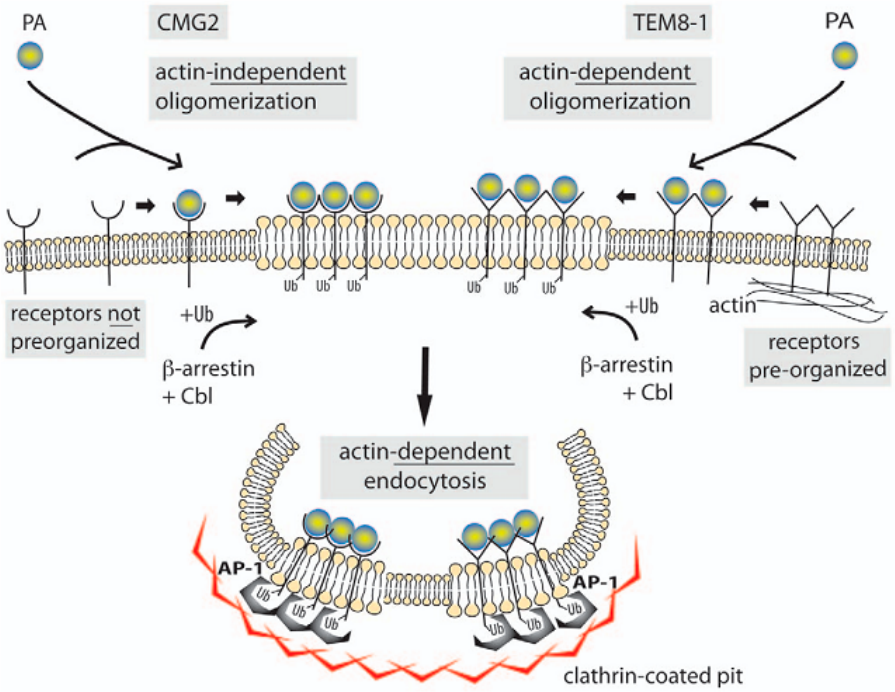

Figure 1.8. Schematic representation of anthrax toxin endocytosis. As represented in the figure, TEM8-1 is pre-organized at the cell surface by the cortical actin cytoskeleton while CMG2 is not. After binding to cell surface receptor, PA83 is cleaved by furin originating PA63. PA63 heptamerizes forming a pre-pore complex that can bind LF and/or EF and trigger raft association of the toxin–receptor complex which facilitates the interaction with partner proteins. Within rafts, β-arrestin mediates the recruitment of cellular E3 ligase Cbl that ubiquitinates a conserved receptor lysine residue (Lys352 in TEM8-1 and Lys350 in CMG2) (Abrami et al, 2006; Young & Collier, 2007), modifies the cytoplasmic tails of the receptor, thus allowing the interaction with proteins of the endocytic machinery harboring Ub-interacting domains. The clathrin-

dependent endocytic machinery is thus recruited, the heterotetrameric adaptor AP-1 and finally clathrin, and the toxin–receptor complex is internalized in clathrin-coated pits (CCP). The pinch off of the CCP-containing toxin requires both actin and dynamin. (From Abrami et al, 2010).

Shiga toxin binds to the neutral glycosphingolipid Gb3 by a quite complex mechanism (Sandvig et al, 2009; Windschiegl et al, 2009) and can be then endocytosed by different pathways (Khine & Lingwood, 1994; Lingwood, 1999; Nichols & Lippincott-Schwartz, 2001; Sandvig et al, 2009; Sandvig et al, 2002; Sandvig & van Deurs, 2000). The composition of the Shiga receptor, the Gb3 species, are thought to be essential for sorting of the toxin (Bergan et al, 2012; Lingwood et al, 2010; Sandvig et al, 2013). Different evidences point to a clathrin-dependent endocytosis: shortly after incubation at 37ºC the toxin-receptor complex has been found in clathrin-coated pits (Sandvig et al, 1989) and conditions that interfere with clathrin-dependent endocytosis (Sandvig et al, 2002; Sandvig & van Deurs, 1996; Nichols et al, 2001; Lauvrak et al, 2004) have been shown to inhibit Shiga toxicity and uptake. However, there is a large variability in the sensitivity of cells to Shiga toxin that corroborates the hypothesis that a certain fraction might be endocytosed by other pathways as well. According to this, when clathrin expression was down-modulated the toxin still entered cells efficiently (Lauvrak et al, 2004; Saint-Pol et al, 2004). Also, Shiga toxin has the ability to induce tubular structures at the plasma membrane, originated from caveolae and dependent on plasma membrane cholesterol, actin and dynamin for pinching off, that can contribute for a minor part of the toxin that is endocytosed (Hansen et al, 2009; Romer et al, 2007).

Cholera toxin B domain binds to the glycosphingolipid GM1 receptor found in membrane microdomains on the plasma membrane, named lipid rafts (Fujinaga et al, 2003). Each B domain monomer has a binding site for GM1, making it able to bind up to five GM1 molecules at once. After receptor binding, the toxin can enter the cell by several endocytic mechanisms including clathrin-dependent and independent pathways. Amongst the clathrin-independent pathways cholera toxin can take advantage of lipid raft/caveolae mediated endocytic pathway, ADP-ribosylation factor 6 (Arf6)-associated endocytic pathway, as well as caveolae and dynamin-independent pathways (Bharati & Ganguly, 2011; Hansen et al, 2005; Massol et al, 2004; Orlandi & Fishman, 1998; Torgersen et al, 2001; Wernick et al, 2010). However, it is not clear whether all the different types of uptake mediate Golgi transport and cholera toxicity.

As discussed above, bacterial toxins can take advantage of several existing receptors and endocytic mechanisms to be internalized and arrive to their target to exert toxicity.

3. Intracellular intoxication pathways

Independently on how bacterial toxins are endocytosed, they generally first end up in early endosomes (Gould & Lippincott-Schwartz, 2009; Jovic et al, 2010), a complex compartment composed by a mosaic of proteins and lipid domains and with tubular and multivesicular elements (Huotari & Helenius, 2011).

Usually, upon endocytosis bacterial AB toxins follow one of the two classical intracellular trafficking pathways (Figure 1.9) for traveling to translocation portals where they cross the membrane barrier into cytosol. With exception of *Pseudomonas* exotoxin A, which can take advantage of the two intracellular routes to arrive into cytosol (Box 1), AB toxins can either translocate from endosomes in response to low pH or take the long way round and traffic all the way to the Golgi apparatus and the endoplasmic reticulum (ER) from where translocation into cytosol occurs (Blank, 2006; Sandvig & van Deurs, 2005; Watson & Spooner, 2006).

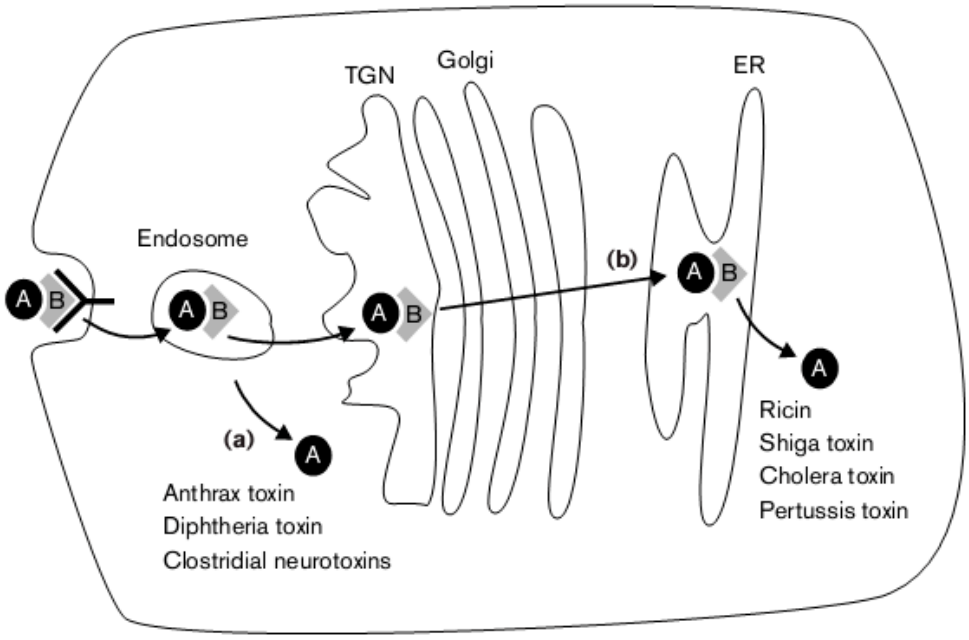

Figure 1.9. Classical intracellular trafficking routes of AB toxins. AB toxins bind to host cell receptors through their B domains and are endocytosed. The A domain can be translocated from endosomes to cytosol in response to low pH (a) or can travel retrogradely to the ER before reaching the cytosol (b). (From Falnes & Sandvig, 2000).

3.1. Endosomal pathway (short journey)

Several toxins, including diphtheria toxin (Moskaug et al, 1988; Olsnes et al, 1990), clostridial neurotoxins (Turton et al, 2002), the large clostridial toxins (Jank & Aktories, 2008; Pruitt & Lacy, 2012), anthrax toxin (Young & Collier, 2007) and C2 toxin (Barth, 2004; Barth et al, 2000; Blocker et al, 2003b) take the endosomal pathway, also referred as short journey, taking advantage of the acidic endosomal pH (resulting from the activity

of the vacuolar ATPase proton pump) to translocate the A domain into the cytosol. Because they take the short journey to arrive into their target are commonly named “short-trip” toxins.

Basically, after receptor mediated endocytosis, “short-trip” toxins are embedded in endocytic vesicles that fuse with endosomes from where translocation of the A domain takes place through a pH dependent mechanism. In the case of diphtheria toxin (Montecucco et al, 1985; Sandvig & Olsnes, 1980; Sandvig & Olsnes, 1981), anthrax toxin (Milne & Collier, 1993), CNF1 (Falnes & Sandvig, 2000), *Costridium difficile* toxin B (Qa'Dan et al, 2000) and clostridial neurotoxins (Blocker et al, 2003b; Puhar et al, 2004), among others, acidic endosomal pH triggers a proteolytic processing and/or conformational change that results on partial unfolding of the protein with exposure of hydrophobic areas. Then, the translocation region of the B domain interacts with the endosomal membrane, forms a cation-selective pore and mediates the translocation of the A domain into cytosol. Consistent with this, most of the toxins that translocate from endosomes share the property of forming ion channels in lipid bilayers at low pH (Bachmeyer et al, 2001; Bann, 2012; Blaustein et al, 1987; Blocker et al, 2003b; Chenal et al, 2002; Galloux et al, 2008; Genisyuerek et al, 2011; Giesemann et al, 2006; Hoch et al, 1985; Qa'Dan et al, 2000; Shone et al, 1987; Silverman et al, 1994b), both in artificial membranes (Barth et al, 2001; Donovan et al, 1981; Finkelstein, 1994; Kagan et al, 1981; Lang et al, 2008; Schmid et al, 1994) and living cells (Barth et al, 2001; Blocker et al, 2003b; Li & Shi, 2006; Madshus et al, 1994; Milne & Collier, 1993; Olsnes et al, 1990; Papini et al, 1988; Sandvig & Olsnes, 1988). Another characteristic of toxins that translocate from endosomes in response to low pH, is that surface-bound toxin can directly translocate from the plasma membrane by exposing cells to low pH, mimicking what occurs at endosomes (Draper & Simon, 1980; Sandvig & Olsnes, 1980; Sandvig & van Deurs, 2005). Consistent with this, inhibitors that interfere with endosome acidification (Figure 1.10) can inhibit translocation of several “short-trip” toxins (Friedlander, 1986; Kaiser et al, 2011; Kim & Groman, 1965; Leppla et al, 1980; Menard et al, 1996; Sandvig & Olsnes, 1980; Sandvig et al, 1984; Umata et al, 1990; Williamson & Neale, 1994). During the translocation process or after reaching the cytosol, the disulfide bond linking the A and B domain is reduced (Papini et al, 1993) and the A domain is released into the cytosol leaving the B subunit behind. Once in the cytosol, usually with participation of cytosolic factors, the A domain refolds and renatures into a catalytically active enzyme.

The translocation of “short-trip” toxins into cytosol can occur either from early or late endosomes. To illustrate this variety, an example of a toxin that translocates from

early endosomes, diphtheria toxin, and of a toxin that translocates from late endosomes, anthrax toxin, is detailed below.

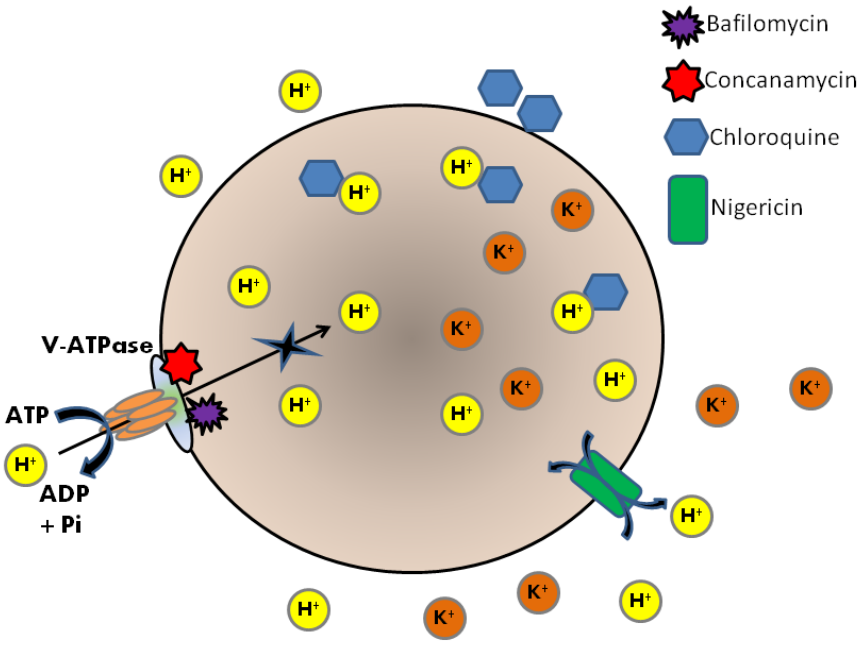

Figure 1.10. Compounds that inhibit endosome acidification. Bafilomycin A1 and concanamycin A are highly specific V-ATPases inhibitors which bind to the c-subunit of the membrane V0 complex, blocking proton pump (Drose et al, 1993; Huotari & Helenius, 2011; Huss & Wieczorek, 2009; Toei et al, 2010); chloroquine is a weak base that in its unprotonated form is permeable, but after accumulation in acidic organelles it traps protons and becomes membrane impermeable resulting in a subsequent increase of the pH (Ohkuma & Poole, 1978); nigericin and monensin are acidic ionophores that exchange protons for potassium ions (Ohkuma & Poole, 1978).

3.1.1. Diphtheria toxin

Diphtheria toxin (DT) is the best characterized example of a “short-trip” toxin that translocates from early endosomes. As described earlier, DT is composed by three functional and structural regions: an N-terminal enzymatic domain, corresponding to the A domain; a transmembrane/translocation domain in the middle, involved in translocation of the catalytic domain into cytosol, and a C-terminal receptor-binding domain, both comprising the B domain. The A and B domain are linked by a disulfide bridge with a furin-sensitive loop which nicking and reducing is a prerequisite for toxicity (Collier, 1975; Collier, 2001; Papini et al, 1993).

After binding to the cell surface receptor by its C-terminal domain, DT is endocytosed by a clathrin dependent mechanism and transported to early endosomes where the translocation of the catalytic domain into the cytosol occurs (Lemichez et al, 1997). Toxin that does not translocate follows the degradative pathway to lysosomes where degradation takes place (Geny & Popoff, 2006; Lemichez et al, 1997) (Figure 1.11). The endosomal acidic pH plays a crucial role in DT toxicity. Indeed, under endosomal

acidic conditions DT undergoes a dynamic unfolding (Boquet et al, 1976; Ladokhin, 2013; Leka et al, 2014; Murphy, 2011) that leads to insertion of the B domain into the membrane and formation of a transmembrane ion channel (Donovan et al, 1981; Falnes & Sandvig, 2000; Kagan et al, 1981; Olsnes et al, 1990; Papini et al, 1988; Sandvig & Olsnes, 1988; Silverman et al, 1994a), which is an essential prerequisite step for the translocation of DT catalytic domain (Murphy, 2011). The use of v-ATPase inhibitors confirmed that pore forming activity was associated with the action of the v-ATPase pump in the endosomal vesicle membrane (Bowman et al, 1988; Murphy, 2011).

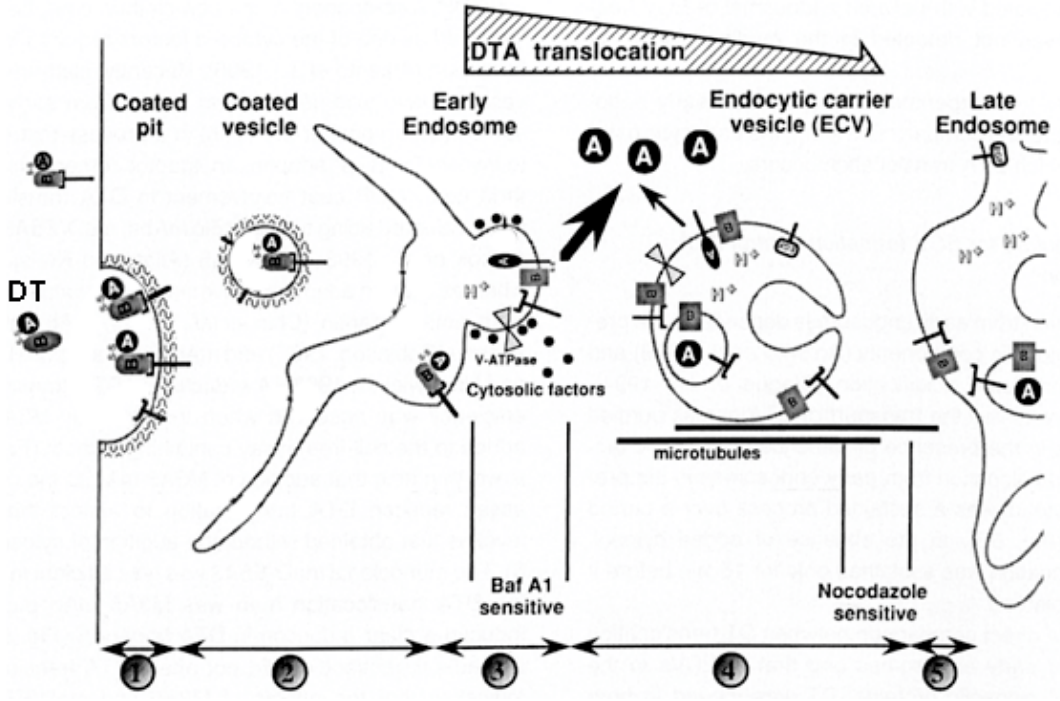

Figure 1.11. Intracellular trafficking of diphtheria toxin (DT). After receptor-mediated endocytosis in clathrin coated-vesicles (1), DT reaches early endosomes (2), from where the catalytic A domain (DTA) is translocated through a pH-dependent mechanism. Translocation can be inhibited by the V-ATPase proton pump inhibitor bafilomycin A1 (Baf A1) (3). The remaining protein follows the degradative pathway to lysosomes, where degradation of the toxin occurs, in a microtubule dependent way that can be inhibited by nocodazole (a compound that disrupts microtubules) (4) (5). During the course to the degradative destination some DTA can also be translocated from intermediates between early and late endosomes, the ECV (4). (From Lemichez et al, 1997).

In what concerns the translocation process, two different hypotheses came out. In vitro studies, using artificial lipid membranes in the absence of other proteins (Hayashibara & London, 2005; Murphy, 2011; Oh et al, 1999; Ren et al, 1999), led to a model in which delivery of the A-domain is achieved through the chaperone-like activity of the translocation domain (T-domain) where it would act as a transmembrane chaperone that forms a pore and binds to the hydrophobic A chain surface maintaining it

in an unfolded state during translocation (Chenal et al, 2002; Hammond et al, 2002; Ladokhin et al, 2004; Ren et al, 1999). Later, the crystal structure of DT (Choe et al, 1992) allowed analyzing in more detail the functional activity of each DT domain and the re-interpretation of earlier findings. Among other evidences, studies based in the translocation domain have shown that while pore formed by the two strongly hydrophobic TH8-TH9 α-helices is important for the catalytic domain delivery into cytosol, it is not in itself sufficient (Cabiaux et al, 1993; Cabiaux et al, 1994; Hu et al, 1998; Mindell et al, 1994; O'Keefe et al, 1992; Silverman et al, 1994b; vanderSpek et al, 1994). Later on, it was demonstrated that transmembrane helix 1 (TH1) of the T-domain possesses a potential entry motif, designated T1 (Murphy, 2011; Ratts et al, 2005), and that KXKXX COPI complex binding motifs in TH1 are essential for catalytic domain delivery to the cytosol (Madshus, 1994; Ratts et al, 2005; Trujillo et al, 2010). Additionally, some host cell factors (Lemichez et al, 1997; Ratts et al, 2003), like β-COP from the COPI complex (Cabiaux et al, 1993) along with ATP (Sandvig & Olsnes, 1982) have been suggested to be involved in the translocation process.

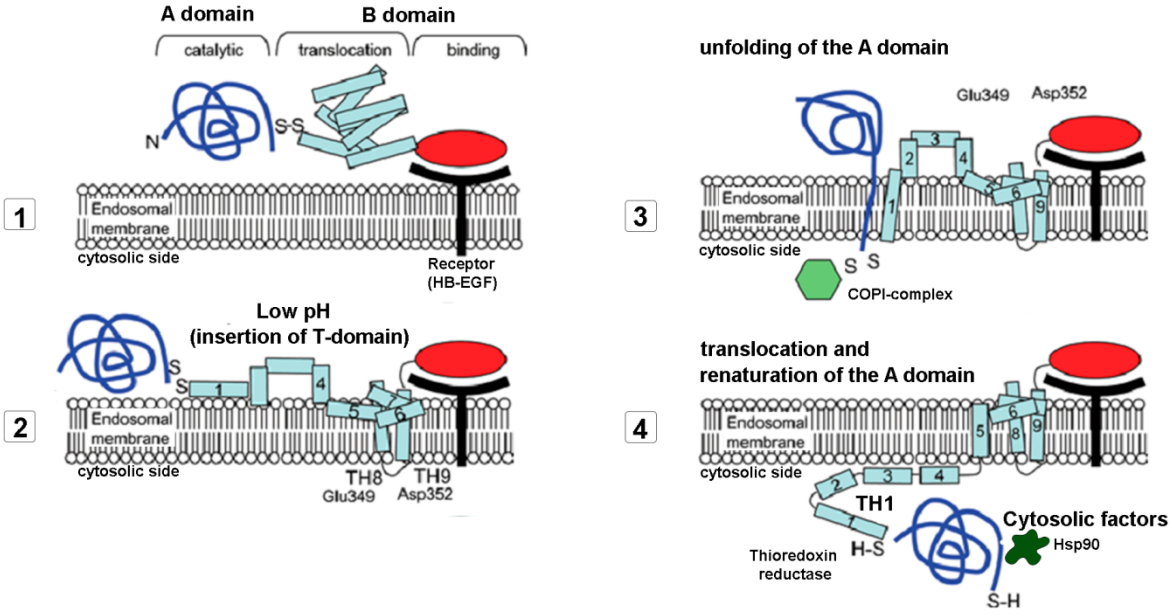

Figure 1.12. Translocation mechanism of diphtheria toxin (DT). (Adapted from Geny & Popoff, 2006).

It is now evident that the mechanism of DT translocation into cell cytosol is facilitated by target cell proteins, all acting in a systematic and ordered fashion in the delivery process. So a current accepted hypothesis for DT catalytic A domain (DTA) translocation (Figure 1.12) proposes that: once in the early endosome, DT undergoes pH-induced conformational changes that result in the exposure of buried hydrophobic regions

that will facilitate the interaction with the hydrophobic membrane. The transmembrane α–helices, TH8-TH9 and TH5-TH7, from the translocation domain, insert into the endosomal vesicle membrane resulting in the formation of a transmembrane pore. Membrane lipids seem to play a role in the T-domain structural change that allow the insertion of such helices into the membrane (Ladokhin, 2013). KXKXX motifs of TH1 emerge on the cytosolic side of the vesicle membrane, COPI complex binds to these sequences and facilitate the translocation of the unfolded catalytic A domain. During the translocation process, the interchain disulfide bridge is reduced, possibly by cytoplasmic thioredoxin reductase, and the catalytic A domain is released in the cytosol. At neutral cytosolic pH with the help of the cytoplasmic chaperone heat-shock protein 90 (Hsp90) (and possibly Hsc70) the catalytic A domain refolds generating its ADP-ribosyltransferase active form. Finally the catalytic A domain catalyzes the NAD^+-dependent ADP-ribosylation of elongation factor 2 (EF2) and inhibits cellular protein synthesis (Collier, 1967) that culminates in cell death by apoptosis (Kochi & Collier, 1993; Murphy, 2011).

3.1.2. Anthrax toxin

The entry of anthrax toxin into the cell cytosol is a little bit more complex than that of DT. As previously mentioned (Section 2), anthrax toxin is a tripartite toxin composed by two enzymatic subunits, the calmodulin-dependent adenylate cyclase edema factor (EF), and the zinc-dependent metalloprotease lethal factor (LF), which require the third subunit, the protective antigen (PA), to interact with cells. The receptor-anthrax toxin complex is endocytosed within a lipid raft environment into clathrin-coated vesicles (Abrami et al, 2010; Abrami et al, 2006; Abrami et al, 2003; Boll et al, 2004), migrates to the intraluminal vesicles and from there to late endosomes. As occurs with DT, several evidences indicate that low endosomal pH plays a crucial role in the translocation process of anthrax toxin (Abrami et al, 2005; Kochi et al, 1994; Puhar & Montecucco, 2007; Wang et al, 1996; Wang et al, 1997; Wigelsworth et al, 2004; Young & Collier, 2007): at low pH, PA dissociates from the receptor and pre-pore suffers conformational changes leading to its insertion into the membrane and formation of a functional pore; acidic pH, also triggers conformational changes on EF and LF that result in partial unfolding of these subunits with exposure of hydrophobic regions that allow their translocation through the PA pore; compounds that inhibit endosome acidification also inhibit EF and LF translocation (Friedlander, 1986; Guidi-Rontani et al, 2000). In what concerns the compartment from where translocation occurs, available data are contradictory. While some evidences point to the hypothesis that part of the toxin can translocate from early endosomes (Dal Molin et

al, 2006), many evidences corroborate the hypothesis that translocation of EF and LF occurs from late endosomes (Abrami et al, 2004; Abrami et al, 2005). It seems that the two enzymatic domains of anthrax toxin can exit from endosomal compartments at various stages of the endocytic route, depending on the specific receptor to which PA is bound (Rainey et al, 2005), more likely and preferentially from late endosomes after multivesicular bodies (MVB) back-fusion (Abrami et al, 2004; Abrami et al, 2005; Puhar & Montecucco, 2007; Thoren & Krantz, 2011). Consistent with this, toxin delivery is inhibited by: (i) disruption of late endosomes function through expression of a dominant-negative form of Rab5; (ii) a lysophosphatidic acid (LBPA)-specific antibody that inhibit formation of late endosomes; (iii) knocking-down ALIX, a protein involved in multivesicular body biogenesis; (iv) the microtubule depolymerizing drug nocodazole (Abrami et al, 2004; Young & Collier, 2007). Based on these data, Abrami and colleagues (Abrami et al, 2004; Abrami et al, 2005) proposed a model for anthrax catalytic domains translocation (Figure 1.13) where they defend that although the pore formation occurs preferentially in the intraluminal vesicles, the translocation of EF and LF occurs mainly from late endosomes. According to this model, upon endocytosis, the toxin-receptor complex is delivered to early endosomes. Once in the early endosomes, the low pH triggers the membrane insertion of PA and the partial unfolding of EF and LF. PA inserts into the membrane of intraluminal vesicles rather than the limiting membrane of early endosomes forming a pore through a mechanism possibly regulated by the toxin-receptor complex and that helps to maintain the membrane integrity of endosomes. Instead of translocation into cytosol, in this case EF and/or LF translocate into the lumen of the intraluminal vesicles (topological equivalent to the cytoplasm (Gruenberg & Stenmark, 2004; Murk et al, 2003; van der Goot & Gruenberg, 2006)) where refolding takes place (Abrami et al, 2004). Translocation through the PA pore is driven by a proton gradient (Krantz et al, 2006) with PA pore playing a crucial role by blocking protons passage, and thus maintaining the pH gradient that drives translocation (Collier, 2009; Krantz et al, 2005). Additionally, cofactors from the host cell seem to also play a role in the translocation process. Similarly to DT, LF has T1-like motifs with multiple coatomer I complex binding motifs that require COPI complex for efficient translocation (Tamayo et al, 2008). Furthermore, the cytoplasmic chaperone heat-shock protein 90 and cyclophilin have been shown to play a role in the cytosolic delivery of the anthrax related fusion protein LFnDTA (Dmochewitz et al, 2010). After translocation, EF and/or LF are packaged into endosomal carrier vesicles (ECV) and transported to late endosomes. Finally, intraluminal vesicles undergo back-fusion with the limiting membrane of late endosomes and EF and LF translocate into the cytosol. While LF is fully translocated to the cytosol in the perinuclear region, EF translocation is only

partial once it remains bound to a membrane fraction of the endosome (Guidi-Rontani et al, 2000; Zornetta et al, 2010). EF is biologically active in its membrane-bound form (Dal Molin et al, 2006; Guidi-Rontani et al, 2000), only requiring the exposure of its ATP and calmodulin binding domains to the cytosol (Labruyere et al, 1990; Ladant et al, 1989).

It is noteworthy that by being isolated in the lumen of intraluminal vesicles, EF and LF are protected from proteases and degradation in contrast to PA that is degraded. Recently, Abrami and colleagues (Abrami et al, 2013) showed that a major advantage of this delivery route is the protection/preservation of the toxin for a long time (up to a week) allowing it to be exocytosed and infect naïve cells.

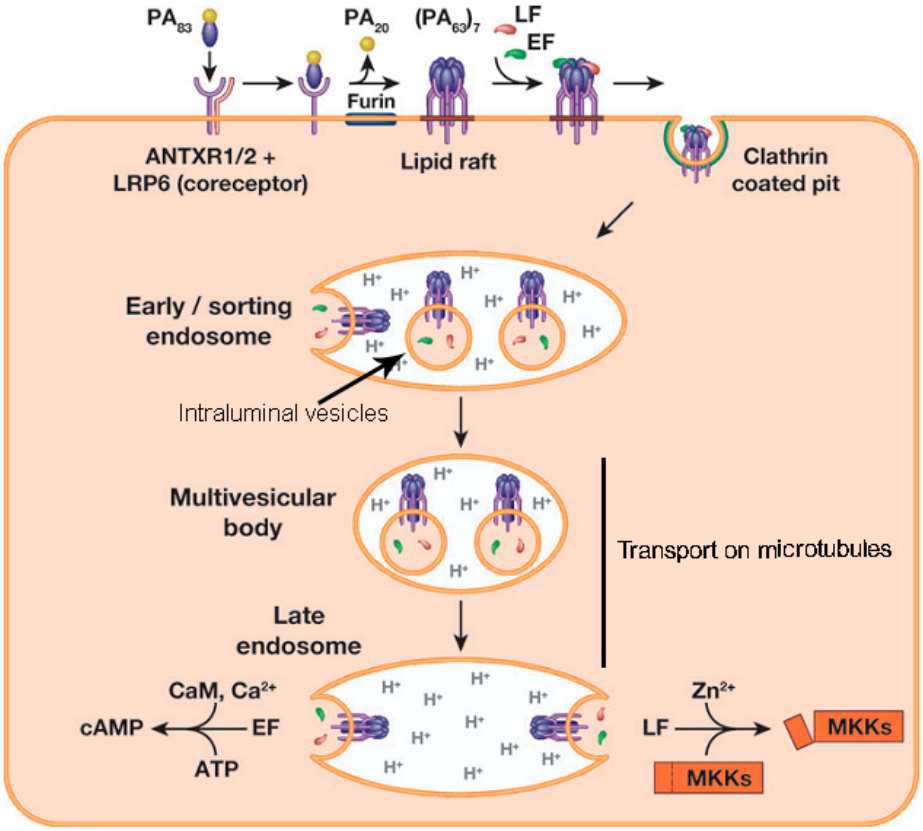

Figure 1.13. Intracellular trafficking of anthrax toxin. (Adapted from Young & Collier, 2007).

3.2. Retrograde pathway (the long journey)

After endocytosis, endosomes are an obligatory through station for AB toxins. However, while toxins like diphtheria toxin, anthrax, clostridial neurotoxins, among others, translocate from endosomes in a pH-dependent manner, others, such as Shiga and cholera toxins do not depend on endosomal acidic pH for intoxication of cells. Rather, after endocytosis, they escape the lysosomal degradative pathway by being transported,

either from early or recycling endosomes, to the trans-Golgi network (TGN) and from the Golgi retrogradely to the endoplasmic reticulum (ER). In the ER the catalytic A domain is liberated from the holotoxin by reduction of the disulfide bond and translocated to the cytosol (Geny & Popoff, 2006; Sandvig et al, 2013; Sandvig & van Deurs, 2005).

The ER is where folding and assembly of secretory and transmembrane proteins occur assisted by numerous molecular chaperones, principally calnexin/calreticulin and BiP/Grp94 (Gregers et al, 2013). To maintain ER homeostasis, misfolded proteins have to be degraded. This is achieved by retro-translocation through the Sec61 translocon to the cytosol for ubiquitinylation and degradation by the proteasome – the ER associated degradation (ERAD). It is believed that protein toxins that follow the retrograde pathway disguise themselves as misfolded proteins and take advantage of this cellular system to arrive into the cytosol (Bergan et al, 2012; Bharati & Ganguly, 2011; Blank, 2006; Cho et al, 2012; Gregers et al, 2013; Hazes & Read, 1997; Sandvig et al, 2009; Sandvig et al, 1993; Sandvig et al, 2002; Sandvig et al, 2013; Sandvig et al, 2004; Sandvig et al, 2010; Sandvig & van Deurs, 2005; Sokolowska et al, 2011; Spooner & Lord, 2012). Once in the cytosol, in contrast to ER substrates destined for proteasomal destruction, these toxins escape degradation, undergo folding to a catalytic conformation and inactivate their cytosolic targets (Johannes & Romer, 2010). Most of them inhibit protein synthesis in an enzymatic manner (May et al, 2013) with the exception of cholera toxin which increases the level of cAMP by ADP-ribosylation of adenylate cyclase (Spangler, 1992).

Similarly to the toxins that translocate from endosomes, some of the bacterial toxins retrogradely transported need to be proteolytically cleaved and activated by furin (Garred et al, 1995b; Sandvig et al, 2013). Because furin is expressed in most cells and tissues (Halban & Irminger, 1994) and seems to be localized primarily in the *trans*-Golgi network (TGN) (Bosshart et al, 1994; Molloy et al, 1994) but cycles between TGN, endosomes and cell surface (Bosshart et al, 1994; Klimpel et al, 1992; Tsuneoka et al, 1993), furin-cleavage can occur either at the plasma membrane, in the endosomes or in the Golgi apparatus (Bonifacino & Rojas, 2006; Mallet & Maxfield, 1999).

The translocation from ER is common to all retro-translocated toxins but the exact mechanism of arriving into ER and translocation seems to be cell-type and toxin dependent. In fact, retrograde transport of toxins through the Golgi to the ER can occur by more than one mechanism. To illustrate this variability, a detailed description of cholera and Shiga toxin retrograde pathway is provided below.

3.2.1. Cholera toxin

Cholera toxin (CT) is an example of a bacterial toxin that travels retrogradely (Sandvig et al, 1996) and translocates from ER into the cytosol. CT binds to the ganglioside GM1 at the plasma membrane via its B-domain, is endocytosed and travels from early or recycling endosomes through the *trans*-Golgi network (TGN) into the ER (Cho et al, 2012; Lencer & Saslowsky, 2005; Wernick et al, 2010), in a pathway regulated by a combination of cellular lipid (Chinnapen et al, 2012; Glebov et al, 2006; Wolf et al, 2002) and protein components (Badizadegan et al, 2004; Geiger et al, 2013; Saslowsky et al, 2010). An alternative pathway where CT could be directly sorted from early endosomes to ER without intersecting the TGN has also been described (Saslowsky et al, 2010).

The Golgi complex has a central position in the secretory pathway playing a crucial role in the regulation of cargo transport from the ER to the Golgi complex (anterograde pathway) and also from the Golgi into the ER (retrograde pathway) (Cancino et al, 2013; Cancino & Luini, 2013). A key player in this Golgi control system is the KDEL receptor. Usually, cargos carry components that can be then sensed by the KDEL receptor (KDELR) in the Golgi complex that results in the activation of this receptor and initiates signalling pathways that can activate anterograde and retrograde trafficking (Cancino et al, 2013). The presence of the retrograde targeting signal KDEL sequence in the catalytic domain of CT (Sixma et al, 1993b) leads to the suggestion that this toxin would exploit the coat protein I (COPI; responsible for retrograde transport of KDEL receptors) and KDEL receptor-dependent pathway to go from the Golgi complex to the ER. Surprisingly it was found that mutation or removal of the KDEL motif from the catalytic domain of CT does not inhibit the access of the toxin to the ER (Lencer et al, 1995; Fujinaga et al, 2003). Furthermore, the B domain of CT, which does not possess a KDEL motif, is able to traffic retrogradely to ER (Bharati & Ganguly, 2011; Fujinaga et al, 2003). These observations indicated that a KDEL signal was not mandatory for CT retrograde transport (Bharati & Ganguly, 2011; Feng et al, 2004; Lencer et al, 1995), suggesting that COPI-mediated retrograde traffic from Golgi to ER was not required (Lencer et al, 1995). Nevertheless, mutation in the KDEL motif of CT results in a delay in intoxication leading to the hypothesis that the KDEL motif present in the catalytic domain of CT may be used to enhance toxicity (Lencer et al, 1995).

During the intracellular route to ER (Figure 1.14), the catalytic domain of CT is proteolytically activated by a host cell protease (Lencer et al, 1997) originating two A domain peptides, CTA1 and CTA2, linked by a disulfide bridge. Once in the ER the disulfide bridge is reduced by oxidoreductases and the enzymatically active portion of the A domain, CTA1, is dissociated from the remaining toxin followed by unfolding assisted by ER lumenal chaperones, protein disulfide isomerase (PDI) and flavoenzyme Ero1p (Cho

et al, 2012; Tsai & Rapoport, 2002; Tsai et al, 2001). Unfolded CTA1 is stabilized in a competent state for retro-translocation by the ER luminal chaperone Hsp40 and ERdj3/HEDJ complex (Massey et al, 2011) along with the Hsp70 chaperone Bip

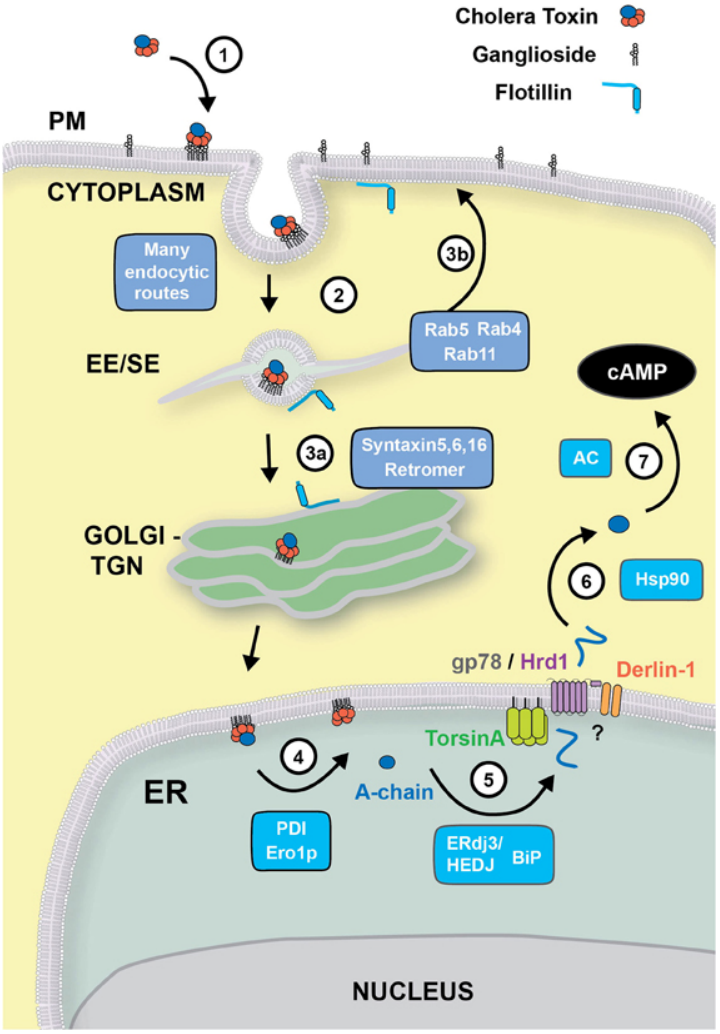

Figure 1.14. Intracellular trafficking of cholera toxin. (1) After binding to the ganglioside GM1, cholera tocin (CT) is endocytosed by various endocytic routes. (2) All the endocytic pathways end up in the early/sorting endosomes (EE/SE) from where sorting occurs to the TGN (3a), to the recycling endosomes (3b) or to late endosomes (not shown). (4) From the Golgi, the toxin is transported to the ER where the dissociation of the A domain from the B domain occurs with the aid of PDI and Erop1p. (5) The A-chain is then unfolded by the ERdj3/HEDJ complex along with BiP, where it is translocated across the ER membrane into the cytosol with the aid of TorsinA, gp78/Hrd1 and Derlin-1. (6) Once in the cytosol, the A-chain rapidly refolds in an Hsp90-dependent manner where its catalytic activity stimulates adenylate cyclase (AC) resulting in an intracellular increase of cAMP (7). (From Cho et al, 2012).

(Nishikawa et al, 2005; Shen & Hendershot, 2005; Winkeler et al, 2003). Further, CTA1 is target to the ER membrane for retro-translocation into cytosol through a still unknow protein-conducting channel. Some evidences point to retro-translocation through the Sec61 translocon (Schmitz et al, 2000), involved in the ERAD pathway (responsible for

transfer of degradation substrates from the ER to proteasome (Pilon et al, 1997; Wiertz et al, 1996)), but other translocation channels could be involved, with greatest evidence for the protein complex centered on the E3 ubiquitin ligases HRD1 and gp78 (Bernardi et al, 2010). It is known that many ERAD substrates are pulled from the ER membrane by the cytosolic AAA-ATPase p97 (Jarosch et al, 2002; Ye et al, 2001). However, in the case of CT it seems that another ER luminal AAA-ATPase, Torsin A (Kothe et al, 2005; Nery et al, 2011) may be involved. Unlike retro-translocated ERAD substrates that once in the cytosol are destined for the proteasome to degradation, CTA1 rapidly refolds in its catalytic active form and evades the degradative fate (Rodighiero et al, 2002). Refolding of CTA1 is mediated in part by the small GTPase ADP-ribosylation factor 6 (Arf6) (Ampapathi et al, 2008; Cho et al, 2012; Teter et al, 2006), the cytosolic chaperone Hsp90 and Hsc70 (Spooner et al, 2008; Taylor et al, 2010). Finally, the refolded catalytic active CTA1 activates adenylate cyclase by ADP-ribosylation of the heterotrimeric protein G-protein, with increase of the intracellular cAMP that causes an excessive secretion of fluid and electrolytes culminating in the massive diarrhea that typifies cholera disease (Spangler, 1992; Wernick et al, 2010).

3.2.2. Shiga toxin

Shiga toxin (Stx) is another example of a toxin that follows the retrograde pathway to gain access to cytosol (Sandvig et al, 1992). After binding strictly to the neutral glycosphingolipid Gb3 through its pentameric B domain, Stx is endocytosed either by clathrin-dependent or independent mechanisms (Sandvig et al, 2013). The toxin then travels from early or recycling endosomes (Lieu & Gleeson, 2010; Mallard et al, 1998; McKenzie et al, 2012) to the TGN network (McKenzie et al, 2009) in a dynamin (Lauvrak et al, 2004) and cholesterol (Falguieres et al, 2001) dependent way, and from the Golgi to the ER from where it translocates to the cytosol (Figure 1.15). Interestingly, Stx is able to stimulate its own transport into Golgi (Lauvrak et al, 2006) by: (i) recruiting clathrin at the cell surface (Utskarpen et al, 2010; Walchli et al, 2009); (ii) increasing microtubules assembly (Hehnly et al, 2006), necessary for the retrograde transport to the Golgi complex (Chen et al, 2005; Itin et al, 1999; Murshid & Presley, 2004; Yoshino et al, 2005); (iii) activation of Protein kinase C delta isoenzyme (Torgersen et al, 2007) and Mitogen-activated protein kinase p38 (Walchli et al, 2008); (iv) releasing cytoplasmic phospholipase A2 from an Annexin A1 complex (Tcatchoff et al, 2012).

It is currently accepted that the endosomal acidic pH is not a prerequisite for translocation of toxins that follow the retrograde pathway. Accordingly, although a recent study showed that different compounds that increase endosomal pH protect against Stx

(Dyve Lingelem et al, 2012) the effect was not due to the endosomal pH as such, but to other factors that play a role in interfering with the transport of Stx, with the proton pump activity playing a role in the efficient endosome to Golgi transport (Dyve Lingelem et al, 2012).

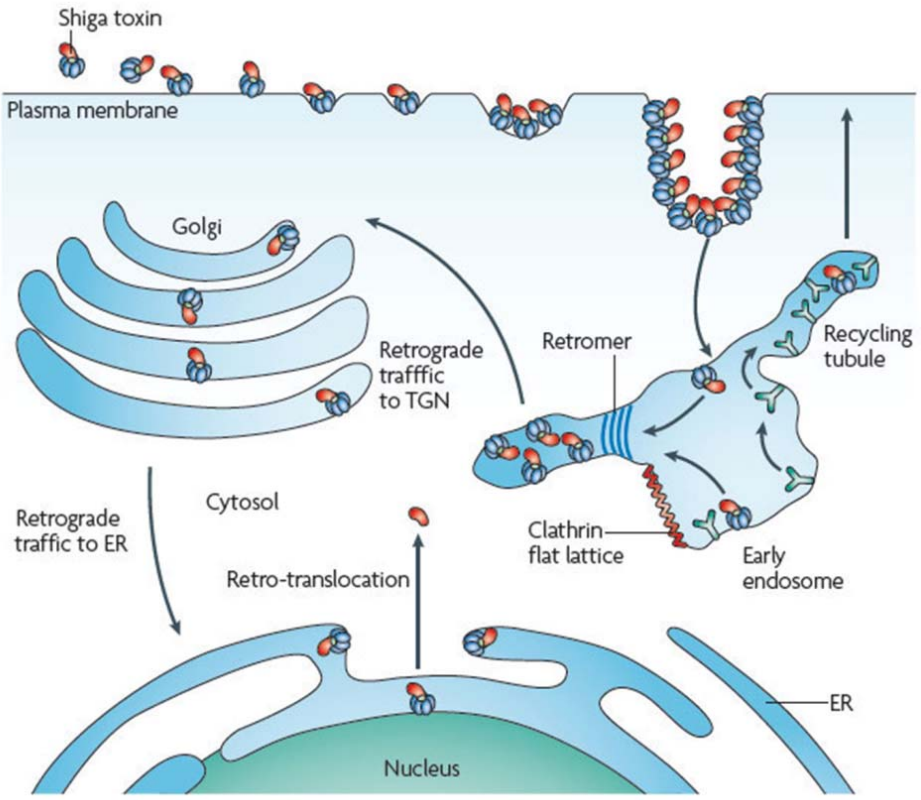

Figure 1.15. Intracellular trafficking of Shiga toxin. Upon endocytosis, Shiga toxin reaches early endosomes. Here the toxin undergoes retrograde sorting to *trans*-Golgi network (TGN) bypassing the late endosomes/lysosomes in a retromer-dependent manner. Finally, the toxin reaches the endoplasmic reticulum (ER) from where it takes advantage of the ERAD machinery to translocate into cytosol. Y-shapes correspond to the transferrin receptor protein (TfR) that concentrates in recycling tubules in the early endosome and recycles back to the plasma membrane. (From Johannes & Romer, 2010).

Contrarily to cholera toxin, Stx does not have a KDEL sequence and, not surprisingly, is sorted from Golgi to ER in a COPI-independent way through a Rab6- (Bassik et al, 2013; Girod et al, 1999; Jackson et al, 1999; White et al, 1999) and ARF1-dependent route (Moreau et al, 2011). Intriguingly, Bassik *et al.* (Bassik et al, 2013) showed recently that knockdown of COPI protect cells against Stx. Nevertheless, it is not clear if the knockdown of COPI interferes only with the complex or if it results in secondary changes of the Golgi apparatus (Sandvig et al, 2013). Similarly to cholera, during the endocytic route to ER, Stx is activated by furin cleavage. Furin cleaves the A domain of the toxin resulting in two A fragments, A1- (containing catalytic activity) and A2-fragments, linked by a disulfide bridge (Garred et al, 1995a; Garred et al, 1995b). After arrival in the

ER, two processing steps required for an efficient translocation of A1-fragment into cytosol take place: the A1-fragment is released from A2-fragment plus B domain by reduction of the disulfide bridge (Garred et al, 1995b; Lee et al, 2010; Sandvig et al, 2013) and the A1-fragment unfolds by a chaperone-mediated mechanism. The dissociation mechanism seems to be similar to the one described for cholera toxin with the ER lumenal chaperone protein disulfide isomerase (PDI) playing an important role (Cho et al, 2012; Fagerquist & Sultan, 2010; Lord et al, 2003; Spooner et al, 2004). Also similar to cholera toxin, ERdj3/HEDJ and BiP have been shown to be involved in stabilizing the unfolded A1-fragment and later targeting it to the retro-translocation channels (Cho et al, 2012; Falguieres & Johannes, 2006; Yu & Haslam, 2005). The unfolded A1-fragment is probably targeted to the ER membrane, where retro-translocation occurs, presumably through the protein-conducting channel Sec61p (Cho et al, 2012; Sandvig & van Deurs, 2002a; Sandvig & van Deurs, 2002b; Yu & Haslam, 2005). Although the involved molecular details remain to be explored (Spooner & Lord, 2012). Finally in the cytosol, A1-fragment inhibits protein synthesis by removing one single adenine from the 28S RNA of the 60S subunit of the ribosome (Bergan et al, 2012), and may induce signaling leading to apoptosis (Cherla et al, 2003; Lee et al, 2008; Tesh, 2010).

Box 1. Cytotoxic pathways of *Pseudomonas* exotoxin A

Exotoxin A from *Pseudomonas aeruginosa* is produced as a single polypeptide chain composed of domain I, domain II and domain III, responsible for receptor binding, translocation and catalytic activity, respectively (Allured et al, 1986; Pastan et al, 1992). The first essential step in the cytotoxic pathway of *Pseudomonas* exotoxin A (PE) is the binding of PE domain I to the CD91 receptor, also called alpha2-macroglobulin receptor/low density lipoprotein receptor related protein (α2MR/LRP) on the host cell membrane. Then, PE enters the cells (Kounnas et al, 1992) and after endocytosis, exposure to low endosomal pH leads to receptor dissociation and conformational changes within PE structure (Idziorek et al, 1990; Ogata et al, 1992; Sandvig & Moskaug, 1987; Wolf & Elsasser-Beile, 2009). From here two different situations have been documented (Morlon-Guyot et al, 2009) for arrival of PE into cytosol:

(I) On the one side, the pH induced conformational changes mediates insertion of domain II (translocation domain) into the endosome membrane and the entire toxin translocate from endosomes into cytosol (Morlon-Guyot et al, 2009). Different data involved acidic pH in the PE translocation: (i) drugs that inhibit endosome acidification, as the weak bases ammonium chloride, methylamine and chloroquine and the inhibitor of the vacuolar proton-pump ATPase bafilomycin A1 protect cells from PE cytotoxicity (Beaumelle et al, 1993; Beaumelle et al, 1992; Clague et al, 1994; Morris & Saelinger, 1986; Olsnes & Sandvig, 1988; Pastan et al, 1992; Taupiac et al, 1996); (ii) cells unable to show endosomal acidification are resistant to PE (Robbins et al, 1984); (iii) acidic pH promotes PE insertion into model membranes (Jiang & London, 1990). Interestingly, contrarily to what has been described for toxins that translocate from endosomes through endosome-cytosol pH gradient, like in the case of diphtheria toxin, PE is not able to translocate directly from the plasma membrane when exposed to an acidic media (Olsnes & Sandvig, 1988; Taupiac et al, 1996). In the case of PE, the acidic endosomal pH is only a prerequisite for translocation (Jiang & London, 1990; Mere et al, 2005) but the energy for translocation of the full-length PE is directly driven by ATP hydrolysis (Taupiac et al, 1996).

(II) On the other side, after reaching the endosomal compartment, PE can travel retrogadely to the ER through two different pathways (Smith et al, 2006; Wolf & Elsasser-Beile, 2009). Most of the PE is internalized by clathrin-coated pits but, alternatively, it can bind to CD91 receptor and associate with detergent-resistant microdomains (DRM) to be endocytosed via caveosomes. Once in the acidic endosomal compartment, the toxin undergoes conformational changes and can be proteolytically processed by furin within an exposed loop of the translocation domain (Ogata et al, 1992). This results in a N-terminal fragment of 28 kDa and a 37 kDa C-terminal fragment (most of domain II and the entire enzymatic domain III) (Ogata et al, 1990; Wedekind et al, 2001). After reduction of the disulfide bridge, possibly by protein disulfide isomerases (PDI) or PDI-like enzyme (McKee & FitzGerald, 1999), the 37 kDa C-terminal fragment is released and travels via late endosomes and a Rab9-dependent route to the trans-Golgi network (TGN) (PE endocytosed via clathrin) or can pass directly from the EE to the TGN in a pathway independent of the small GTPase Rab9 (PE endocytosed via caveosomes). The 37 kDa C-terminal fragment is then transported to the ER via its C-terminal KDEL-like sequence REDL (PE endocytosed via clathrin) (Jackson et al, 1999; Kreitman & Pastan, 1995) or in a lipid-dependent sorting pathway, controlled by Rab6 (PE endocytosed via caveosomes) (Smith et al, 2006; White et al, 1999). Despite the retrograde pathway used, the PE fragments in the ER translocate into cytosol using sequences of the translocation domain II (Ogata et al, 1990; Theuer et al, 1993) and via the translocon Sec61p (Hazes & Read, 1997; Koopmann et al, 2000; Wolf & Elsasser-Beile, 2009).

There is a lack of correlation between the described pathways and PE efficiency and toxicity. However, different lines of evidence support the relevance of the retrograde transportation to ER for translocation and toxicity. PE has a carboxyl-terminal sequence (REDLK) in the C-terminal domain that is similar to ER retrieval motif KDEL and is required for toxicity (Chaudhary et al, 1990). Moreover, replacing this carboxyl-terminal sequence (REDLK) by KDEL enhances toxicity (Seetharam et al, 1991) and overexpression of lysozyme-KDEL that inhibits KDEL-mediated ER system reduced PE toxicity (Jackson et al, 1999). Also, in highly sensitive cells, PE needs to be proteolytically cleaved to express full toxicity (Pastan et al, 1992; Taupiac et al, 1996). So far, it seems that, depending on the cell type, PE may enter cells directly from endosomes or can be processed and transported retrogradely to the ER before it reaches the cytosol. Nevertheless, further studies are needed in order to disclose the intriguingly mechanisms of PE intoxication.

C. AIP56

1. Role in *Photobacterium damselae piscicida* virulence

AIP56 (**A**poptosis **I**nducing **P**rotein of **56** kDa) is a bacterial exotoxin identified by do Vale and colleagues (do Vale et al, 2005) as the major virulence factor of *Photobacterium damselae piscicida* (*Phdp)*.

Phdp (Trůper & De'clari, 1997) is the causative agent of a bacterial septicaemia (known as pseudotuberculosis, photobacteriosis or pasteurellosis, the latter due to the previous classification of *Phdp* in the genus *Pasteurella*), an important bacterial disease affecting different marine fish species worldwide, including sea bass, sole, yellow-tail, gilt-head seabream and turbot both in wild and in culture (Romalde, 2002; Thune et al, 1993). Because of its wide host range, massive mortality, ubiquitous geographical distribution, widespread antibiotic resistance and lack of efficient vaccines, *Phdp* infection is recognized as one of the most threatening bacterial diseases in mariculture (Andreoni & Magnani, 2014). This disease, in its acute form, has a septicaemic nature with a short course and very high mortality (Hawke et al, 1987; Romalde, 2002; Thune et al, 1993).

Phdp is highly pathogenic, with characteristics of an extracellular pathogen (Lopez-Doriga et al, 2000; Magariños et al, 1996a; Magariños et al, 1996b; Magariños et al, 1992b; Noya & Lamas, 1997; Noya et al, 1995b). After entering the host, *Phdp* proliferates and spreads to several organs, including spleen, liver and kidney (Barnes et al, 2005; Magariños et al, 1996c; Toranzo et al, 1991). In advanced disease, apoptosing macrophages and neutrophils are present in spleen, head kidney, blood and gut lamina propria that present exuberant cytopathology (do Vale et al, 2007). It is of note that fish head kidney is equivalent to mammalian bone marrow in terms of haematopoietic activity and that cells of the fish immune system are mostly located in the head kidney, spleen, gut and thymus (Rombout et al, 2005; Scapigliati et al, 2002). Diseased fish often present whitish nodules (granulomatous lesions) in several internal organs, including kidney, spleen and liver, consisting of bacterial accumulation and apoptotic and necrotic cell debris (Figure 1.16). Consequently, the disease has been named to as pseudotuberculosis. Despite the severity of the pathology in marine fish species, the range of growth temperatures (15-30ºC) and the strict salt requirement (Magariños et al, 1992a) render *Phdp* unable to infect fresh water fish and mammals.

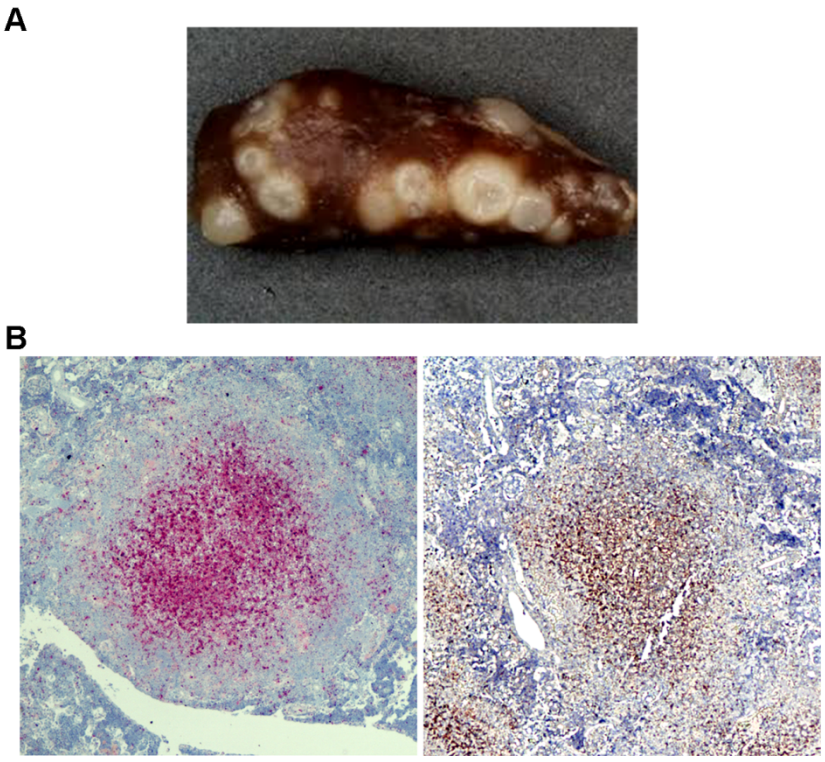

Figure 1.16. Phathological changes in organs of *Phdp* infected fish. (A) Macroscopic view of a spleen from a *Phdp* infected sea bass, showing the presence of whitish nodules consisting of bacterial accumulation and apoptotic and necrotic cell debris that named the pathology as pseudotuberculosis. **(B)** Histophatological analysis of head kidney from *Phdp* infected sole showing that the whitish nodules correspond to areas of cell destruction. In these areas numerous apoptotic cells, positive for TUNEL (left panel; red area) and for active caspase-3 (right panel; brownish area), are observed. Objective 5x. (From do Vale et al, 2007).

It has been shown that *Phdp*-induced apoptotic death of macrophages and neutrophils (do Vale et al, 2003) results from the activity of AIP56 (do Vale et al, 2005). Indeed, it has been shown that in infected fish, the toxin is systemically distributed (Figure 1.17) and depletes macrophages and neutrophils by post-apoptotic secondary necrosis (do Vale et al, 2007). The death of the phagocytes, which involves both extrinsic and intrinsic apoptotic pathways with activation of caspases -8, -9, and -3 and loss of mitochondrial membrane potential, translocation of cytochrome C to the cytosol and over-production of reactive oxygen species (ROS) (Costa-Ramos et al, 2011), inevitably leads to a severe depletion in the number of these cells. This results not only in the impairment of host phagocytic defense (do Vale et al, 2007; do Vale et al, 2003; do Vale et al, 2005) but also affects cytokine production (Nascimento et al, 2007a; Nascimento et al, 2007b), further impairing the host immune response. The depletion of the host phagocytes together with the dramatic weakening of the host immune responses contributes to the establishment of a septicaemia and bacteraemia infection by allowing the rapid spread of the bacteria throughout the infected host, with massive extracellular multiplication

occurring mainly in spleen and head kidney (do Vale et al, 2007; do Vale et al, 2003). Furthermore, the occurrence of a secondary necrotic process in which the apoptosing phagocytes lyse and release their cytotoxic contents contributes to the genesis of the infection-associated necrotic lesions (do Vale et al, 2007; Silva et al, 2008).

These observations, together with the fact that (i) AIP56 gene is present in all *Phdp* virulent strains and absent in the non-virulent isolates tested, (ii) AIP56 is the most abundant protein of mid-exponential phase virulent *Phdp* culture supernatants; (iii) passive immunization of sea bass with anti-AIP56 antibodies provides significant protection against *Phdp* challenge and, (iv) intraperitoneal injection of AIP56 reproduces the pathology of the disease and leads to a dose-dependent lethality (do Vale et al, 2007; do Vale et al, 2005), established AIP56 as a key player in the etiopathogenesis of *Phdp.*

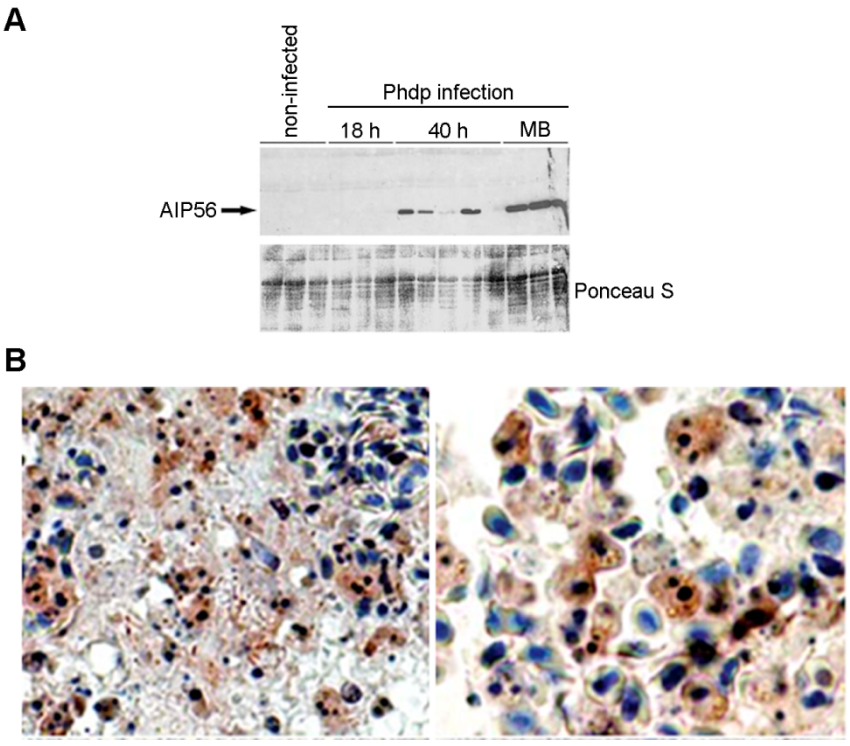

Figure 1.17. During *Phdp* infection AIP56 is systemically distributed. **(A)** AIP56 exotoxin is present in the plasma of sea bass with advanced *Phdp* infection. Western blotting analysis using an anti-AIP56 rabbit serum (upper panel) showing the presence of AIP56 in the plasma of infected sea bass (each lane corresponds to one animal; MB: moribund fish). Non-infected fish were used as control. Protein loading was controlled by staining with Ponceau S (lower panel). **(B)** AIP56 is present in apoptosing cells and apoptotic bodies in advanced disease. Spleen from an infected sea bass immunolabeled for AIP56 (brownish red). Left panel: magnification of an area of cell destruction; right panel: magnification of blood in a vessel of spleen. (Adapted from do Vale et al, 2007).

2. AIP56, an AB toxin that cleaves NF-κB p65

AIP56 is an exotoxin encoded in a high-copy plasmid (pPHDP10 plasmid) present in virulent *Phdp* strains from diverse geographical origins (do Vale et al, 2005). The location of the AIP56 gene in a high-copy plasmid is probably the reason why *Phdp* virulent strains are capable of producing large amounts of toxin (Figure 1.16B).

Protein and nucleotide sequence together with heterologous expression of AIP56 in *E. coli* cells helped to characterize the primary structure of the toxin. AIP56 was first annotated as a 513 amino acid precursor protein, including an N-terminal cleavable signal peptide of 16 amino acid residues (GeneBank Accession number DQ066884) (do Vale et al, 2005). However, an alternative GTG start codon exists, 21 nucleotides ahead of the previously annotated ATG start codon, extending the signal peptide to 23 amino acids and the full length protein to 520 amino acids (Silva, 2010). AIP56 has only two cysteine residues (C^{262} and C^{298}) and a zinc-binding region signature HEXXH, typical of most zinc metallopeptidases (Jongeneel et al, 1989).

Limited proteolysis experiments revealed that AIP56 is composed by two domains linked by a disulfide bridge established between its two unique cysteine residues (C^{262} and C^{298}) (Silva et al, 2013). Using constructs corresponding to the N- and C-terminal domains of the toxin ($AIP56^{1-285}$ and $AIP56^{286-497}$, respectively) and chimeric proteins consisting of the *Bacillus anthracis* lethal factor N-terminal region fused to AIP56 N-terminal (LF^{11-363}.$AIP56^{1-261}$) and C-terminal (LF^{11-363}.$AIP56^{299-497}$) it was confirmed that AIP56 is an AB-type toxin, possessing a catalytic A domain at its N-terminal, and a B domain involved in binding/internalization into target cells at its C-terminal region (Silva et al, 2013).

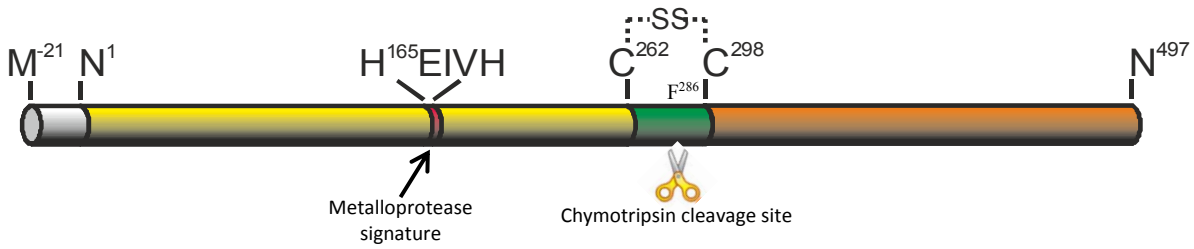

Figure 1.18. Schematic representation of AIP56. AIP56 is structurally composed by two different domains, the catalytic A domain and the binding B domain, linked by a disulfide bridge (SS) between the two unique cysteines residues (C^{262} and C^{298}). After proteolytic cleavage between Phe285 and Phe286 (F286) and under reducing conditions two independent domains were originated, with the metalloprotease signature within the catalytic A domain.

It is now recognized that AIP56 is the founding member of a continuously growing family of bacterial proteins. Indeed, since it was first described (do Vale et al, 2005),

several open reading frames coding for AIP56 full-length homologues were identified in different organisms, mainly in marine *Vibrio* species but also in *Arsenophonus nasoniae*. Interestingly, AIP56 seems to have originated from a fusion of two components: one related to NleC, which is a type III secreted effector present in several enteric pathogenic bacteria (Baruch et al, 2010) associated with human illness and death worldwide (Clarke, 2001); and another related with a protein of unknown function from *Acrythosiphon pisum* bacteriophage APSE-2 (Degnan et al, 2009).

Recently, it has been demonstrated that during intoxication of sea bass peritoneal leukocytes, the catalytic activity of AIP56 results in the depletion of NF-κB p65 (Silva et al, 2013). Considering that NF-κB is an evolutionarily conserved transcription factor that regulates the expression of inflammatory and anti-apoptotic genes, playing a key role in host responses to microbial pathogen invasion (Box 2) (Gilmore & Wolenski, 2012), AIP56-induced NF-κB p65 depletion likely explains the disseminated apoptosis observed during *Phdp* infection. Interestingly, similar to what was described for NleC (Baruch et al, 2010), the cleavage occurs in the Rel-homology domain at the Cys^{39}-Glu^{40} peptide bound (Silva et al, 2013), key residues of p65 involved in DNA interaction (Chen et al, 1998; Garcia-Pineres et al, 2001). Further studies with a mutated version of the toxin ($AIP56^{AAIVAA}$) containing a disrupted putative zinc-binding motif showed that disruption of the zinc metalloprotease signature does not induce major structural changes in the toxin but abolishes AIP56 apoptogenic activity and p65 cleavage, confirming AIP56 as a zinc dependent metalloprotease (Silva et al, 2013).

It is now known that AIP56 (i) is the major virulence factor of *Photobacterium damselae piscicida* with pathological consequences well studied and documented, (ii) is an AB toxin, with an A domain displaying the metalloprotease activity linked by a single disulfide bridge to a B domain responsible for the binding/internalization of the toxin and (iii) cleaves the cytosolic target NF-κB p65 at the Cys^{39}-Glu^{40} peptide bound. Despite that, the interaction of AIP56 with different cell types, the endocytosis mechanisms and the intracellular route that the toxin exploits to arrive to its cytosolic target(s) have not been explored.

Box 2. Nuclear factor-κB (NF-κB)

The transcription factor NF-κB, first described in 1986 (Sen & Baltimore, 1986), comprises a family of evolutionarily conserved transcription factors, , master regulators of immune, inflammatory and antiapoptotic responses (Gilmore & Wolenski, 2012; Wolenski et al, 2013). In mammals, the NF-κB family is composed by five elements: RelA/p65, RelB, c-Rel, p50 (NF-κB1), and p52 (NF-κB2) (see Figure). Each member contains an N-terminal conserved region known as the Rel homology domain (RHD) (Ghosh et al, 1998), which makes contact with DNA and supports subunit dimerization (Hayden & Ghosh, 2012). This domain can be divided into three structural regions: (i) the N-terminal domain that contains sequences required for dimerization and nuclear localization, (ii) the dimerization domain that mediates the association of NF-κB subunits to form combinatorial dimmers, and (iii) the nuclear localization signal (Ghosh et al, 2012; Huang et al, 2010; Zheng et al, 2011). The C-terminal transactivation domains (TADs) that confer the ability to initiate transcription are only present in p65, c-Rel, and RelB (Hayden & Ghosh, 2012). The p52 and p50 are synthesized as large precursors (p100 and p105, respectively) that undergo proteolytic processing (Blank et al, 1991; Fan & Maniatis, 1991; Mellits et al, 1993; Mercurio et al, 1993) and, instead of a C-terminal TAD, contain a glycine-rich region (GRR), multiple ankyrin repeats (ANK) and a death domain (DD) (Ghosh et al, 2012). The five different proteins of NF-κB family form different combinations of homo- or hetero-dimers contributing to the transcriptional selectivity of the NF-κB response (Oeckinghaus & Ghosh, 2009; Smale, 2012). In most unstimulated cells, NF-κB is retained inactive in the cytoplasm by forming a complex with inhibitors of NF-κB (IκBs). These IκBs are characterized by presence of multiple ankyrin repeats (ANK) that interact with the Rel-homology domain, preventing the translocation of NF-κB to the nucleus (Ghosh et al, 2012; Hinz et al, 2012; Oeckinghaus & Ghosh, 2009). Curiously, the NF-κB precursor's p105 and p100 contain at their C-terminal multiple ankyrin repeats and they can also display an IκB-like function (Ghosh et al, 2012). There are two NF-κB signaling pathways, classical (or canonical) and alternative (or non-canonical), which lead to its activation and translocation to the nucleus. In the canonical pathway (characteristic of p65/p50 dimmer) the activation of NF-κB occurs mainly by inflammatory stimuli including activation of TNF receptor-1 (TNFR1), IL-1 receptor and Toll-like receptors (TLRs). Upon stimulation, the IKK (IκB kinase) complex (consisting of two catalytically active kinases, IKKα and IKKβ and a regulatory subunit IKKγ or NEMO) is activated, which results in phosphorylation of IκBα (bound to NF-κB dimers) leading to its polyubiquitination, subsequent proteosomal degradation and nuclear translocation of liberated NF-κB dimers (Xiao, 2004). Once at the nucleus, the NF-κB dimers bind specific DNA sequences (κB sites), and promote transcription of target genes (Le Negrate, 2012; Vallabhapurapu & Karin, 2009). By contrast with the classical NF-κB pathway the non-canonical pathway strictly depends on IKKα phosphorylation and activation but is independent of IKKβ and IKKγ. The stimuli is restricted to specific members of the TNF cytokine family including B-cell activating factor (BAFF), CD40 ligand, lymphotoxin-β, TNFR2 ligands, among others (Sun, 2012b). This pathway leads to activation of p52/RelB dimer through the activation of the NF-κB-inducing kinase (NIK) and is based on processing of the p52 precursor protein, p100. The processing of p100 is a signal-induced and posttranslational event (Xiao et al, 2001) and, because p100 preferentially interacts with RelB (Solan et al, 2002), the processing of p100 not only generates p52 but also causes p52/RelB nuclear translocation (Sun, 2011). Due to NF-κB important roles in the regulation of apoptosis and inflammation as well as innate and adaptive immunity, abnormal activation contributes to the pathophysiology of a variety of diseases, from inflammatory and autoimmune diseases to cancer (DiDonato et al, 2012; Li & Verma, 2002; Wong & Tergaonkar, 2009). Furthermore, as a consequence of the crucial role of NF-κB in immune response, many successful pathogens have evolved a variety of mechanisms to subvert NF-κB signaling pathway.

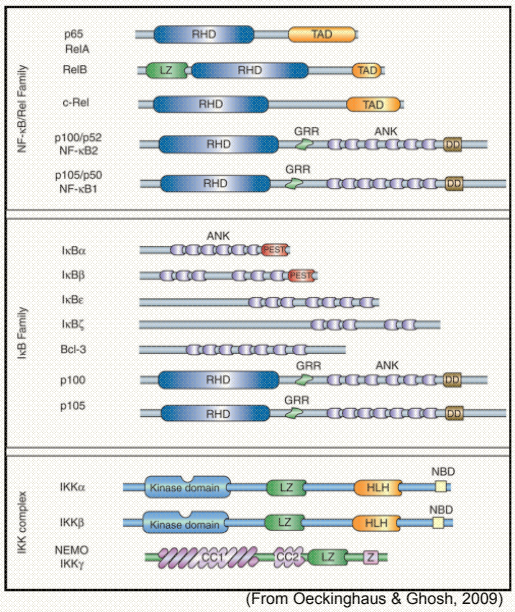

(From Oeckinghaus & Ghosh, 2009)

CHAPTER II

AIMS OF THE STUDY

Previous studies on AIP56 were focused on the elucidation of its toxic effects and their contribution to the pathology caused by *Photobacterium damselae piscicida* (*Phdp).* AIP56 was identified as an exotoxin secreted by virulent strains of *Phdp*, which acts by triggering apoptosis of macrophages and neutrophils, resulting in lysis of these cells by post-apoptotic secondary necrosis. It has been demonstrated that this leads not only to the impairment of host immune defences allowing establishment of a septicemic infection, but also to the release of the cytotoxic contents of the phagocytes, causing tissue damage. More recently, it has been shown that AIP56 is a zinc-metalloprotease that cleaves NF-κB p65, compromising the NF-κB transcriptional activity. In terms of structural organization, it has been reported that AIP56 is an AB toxin, having an N-terminal/A domain responsible for the metalloprotease activity connected by a disulfide bridge to a C-terminal/B domain involved in binding and internalization of the toxin into cells.

Although it is well established that AIP56 is a key virulence factor of *Phdp* and despite the available knowledge on its structural organization, no information is available concerning the trafficking of AIP56 in intoxicated cells. Moreover, the activity of AIP56 has been only tested in fish cells and nothing was known about the susceptibility of other cells to AIP56.

In this thesis, we aimed at extending the characterization of AIP56 by:

1. Analysing the susceptibility of mammalian cells to AIP56
2. Investigating the mechanism involved in AIP56 endocytosis
3. Identifying the intracellular trafficking routes followed by AIP56 during intoxication

CHAPTER III

MATERIAL AND METHODS

1. Experimental animals and cells

1.1. Ethics statement

This study was carried out in accordance with European and Portuguese legislation for the use of animals for scientific purposes (Directive 2010/63/EU; Decreto-Lei 113/2013). The work was approved by Direcção-Geral de Alimentação e Veterinária (DGAV), the Portuguese authority for animal protection (ref. 004933, 2011-02-22).

1.2. Experimental animals

1.2.1. Experimental fish

Sea bass (*Dicentrarchus labrax*) were purchased from a commercial fish farm and housed in a recirculating ozone-treated salt-water (25-30‰) system at 20 ± 2ºC, with a 12 h light/dark cycle and fed at a ratio of 2% body weight per day with a commercial pelleted diet. Fish were euthanized with 2-phenoxyethanol (Panreac; 5 ml/10 L). Water quality was maintained with mechanical and biological filtration and ozone-disinfection.

1.2.2. Experimental mice

The C57BL/6 wild-type and TNF-α deficient mice were purchased from Charles River (Madrid, Spain) and bred and housed at the Instituto de Biologia Molecular e Celular (IBMC) animal facility. The mice were fed sterilized food and water *ad libitum*. TLR4 deficient mice were a kindly gift from University of Minho. For the experimental treatments, 4- to 12-week-old males were used. Mice were euthanized by isofluorane anesthesia followed by cervical dislocation.

1.3. Cells

1.3.1. Sea bass peritoneal leucocytes (sbPL)

Sea bass peritoneal leucocytes were obtained as described (Costa-Ramos et al, 2011) from fish weighting between 100 to 200 g. Briefly, 12 to 20 days after stimulation with Incomplete Freund's Adjuvant, the peritoneal cells were collected in L-15 medium adjusted to 322 mOsm and supplemented with 10% inactivated FBS, 1% penicillin/streptomycin and 20 U ml^{-1} heparin (Braun) (supplemented L-15). The peritoneal population of cells consist of approximately 70% macrophages and 20% neutrophils with the presence of small numbers of eosinophilic granular cells, lymphocytes and erythrocytes (Costa-Ramos et al, 2011). Unless otherwise stated, cells were used at a concentration of 2×10^6 cells ml^{-1} in L-15 supplemented medium.

1.3.2. Mouse bone marrow derived macrophages (mBMDM)

Macrophages were derived from femurs of 4- to 12-week-old C57BL/6 male mice, following a previously established protocol (Gomes et al, 2008). Briefly, femurs were removed and flushed with 5 mL of Hanks' balanced salt solution (HBSS). The resulting cell suspension was centrifuged and the cells resuspended in supplemented DMEM (DMEM with 10 mM glutamine, 10 mM HEPES, 1 mM sodium pyruvate, 10% heat inactivated FBS, 1% penicillin/streptomycin and 10% of L929 cell conditioned medium (LCCM) as a source of Macrophage Colony Stimulating Factor (M-CSF)). In order to remove fibroblasts, the cells were cultured overnight, at 37°C in a humidified chamber in a 7% CO_2 atmosphere, on a cell culture dish. The non-adherent cells were collected, centrifuged, resuspended in supplemented DMEM at a concentration of 4×10^5 cells ml^{-1} (or 5×10^5 cells ml^{-1} for the recycling experiments), plated in different cell culture plates according to the experiment they will be used (Table 1) and incubated again at 37°C in a humidified chamber in a 7% CO_2 atmosphere. Three days later, 10% LCCM/well was added and on the 7th day of culture, the medium was renewed. Cells were used at day 10, when they were fully differentiated into macrophages.

Table 1. mBMDM culture conditions

Experiment	Culture plate	Cell dilution	Volume/well
Western blotting	24 well	4×10^5 cells ml^{-1}	1 ml
Caspase-3	24 well	4×10^5 cells ml^{-1}	1 ml
Resazurin	96 well	4×10^5 cells ml^{-1}	200 µl
Fluorescence microscopy	24 well (containing LPS-free 12-mm coverslips)	4×10^5 cells ml^{-1}	1 ml
Recycling	24 well	5×10^5 cells ml^{-1}	1 ml

1.3.3. Cell lines

Cells were propagated and maintained in tissue culture flasks in the respective medium (Table 2) at 37°C in a humidified chamber in a 7% CO_2 atmosphere. Twenty four hours before the experiment cells were seeded in 24-well plates for p65 cleavage and morphology analysis or in 96-well plates for viability assays (conversion of resazurin to resorufin assay).

To differentiate THP-1 monocytes in macrophages, THP-1 monocytes were seeded in 24-well plates at 4 x 10^5 cells ml^{-1} and stimulated for 16-18 hours with 0.1 µg ml^{-1} phorbol 12-myristate 13-acetate (PMA, Sigma-Aldrich). Cells were washed with PBS and then

incubated in fresh medium without PMA for more 24 hours at 37°C in a humidified chamber in a 7% CO_2 atmosphere before being used.

Table 2. Cell lines culture conditions

Cell line designation	Culture medium	Culture plate	Cell dilution	Volume/well
J774A.1 Reticulum cell sarcoma monocyte/macrophage BALB/C mice cell line	DMEM + 10%FBS	24 well	$2x10^5$ cells ml^{-1}	1 ml
		96 well		100 µl
Raw 264.7 Abelson murine leukemia virus induced tumor monocyte/macrophage BALB/C mice cell line	DMEM + 10%FBS	24 well	$2x10^5$ cells ml^{-1}	1 ml
		96 well		100 µl
THP-1 Acute monocytic leukemia peripheral blood human monocyte	RPMI+10%FBS +1%HEPES+0.5%NEAA +0.5%EAA+ 0.1% 2-mercaptoethanol	24 well	$4x10^5$ cells ml^{-1}	1 ml
		96 well		100 µl
HeLa Cervix adenocarcinoma human epithelial cell line	DMEM + 10%FBS	24 well	$1x10^5$cells ml^{-1}	1 ml
		96 well		100 µl
Vero Kidney epithelial cells extracted from an African green monkey	DMEM + 10%FBS	24 well	$1x10^5$ cells ml^{-1}	1 ml
		96 well		100 µl
CHO Epithelial cells extracted from Chinese Hamster Ovary	DMEM + 10%FBS	24 well	$1.2x10^5$ cells ml^{-1}	1 ml
		96 well		100 µl

2. Recombinant proteins

The different proteins used to perform this work are represented in table 3. AIP56 proteins and chimeric proteins were expressed in *E. coli* while sbp65Rel was synthesized *in vitro* as ^{35}S-labeled proteins using rabbit reticulocyte lysates. Protective antigen (PA), the receptor binding for anthrax lethal factor (LF) (Collier, 2009), was obtained as previously described (Tonello et al, 2004) and was kindly provided by Cesare Montecucco (University of Padova, Italy).

Table 3. Recombinant proteins used in this study

Name	Description	Expression system
AIP56	Wild type, full length his-tagged AIP56 toxin	*E. coli*
AIP56^{AAIVAA}	His-tagged AIP56 metalloprotease mutant corresponding to a full-length version of the toxin in which key residues for zinc ion coordination and water molecule activation (His^{165}, Glu^{166}, His^{169} and His^{170}) were substituted by alanines	*E. coli*
AIP56$^{1-285C262S}$	His-tagged AIP56 N-terminal truncate (AIP56$^{1-285}$) with cysteine 262 mutated to serine	*E. coli*
AIP56$^{286-497C298S}$	His-tagged AIP56 C-terminal truncate (AIP56$^{286-497}$) with cysteine 298 mutated to serine	*E. coli*
LF$^{11-263}$·AIP56$^{1-261}$	LF·AIP56 chimeric protein consisting of the amino-terminus of anthrax lethal factor (LF$^{11-263}$) fused to AIP56 N-terminal region (AIP56$^{1-261}$)	*E. coli*
LF$^{11-263}$·AIP56$^{299-497}$	LF·AIP56 chimeric protein consisting of the amino-terminus of anthrax lethal factor (LF$^{11-263}$) fused to AIP56 C-terminal region (AIP56$^{299-497}$)	*E. coli*
sbp65Rel	Sea bass NF-κB p65 Rel homology domain (Met^{1}-Arg^{188})	Rabbit reticulocyte

2.1. Production and purification of recombinant proteins expressed in *E. coli*

Recombinant AIP56, AIP56^{AAIVAA}, AIP56$^{1-285C262S}$, AIP56$^{286-497C298S}$, LF$^{11-263}$·AIP56$^{1-261}$ and LF$^{11-263}$·AIP56$^{299-497}$ were produced and purified as previously described (Silva et al, 2013). Briefly, AIP56, AIP56$^{286-497C298S}$, LF$^{11-263}$·AIP56$^{1-261}$ and LF$^{11-263}$·AIP56$^{299-497}$ were purified from the soluble fraction of induced *E. coli* cells by metal-affinity chromatography. This was followed by an anion exchange chromatography in the case of AIP56 or a size exclusion chromatography in the case of AIP56$^{286-497C298S}$. AIP56^{AAIVAA} and AIP56$^{1-285C262S}$ were purified from inclusion bodies by metal-affinity chromatography under denaturing conditions, refolded, and subjected to size exclusion chromatography. To obtain AIP56Myc and AIP56V5, pET28aAIP56H+ plasmid (do Vale et al, 2005) was amplified using the forward primer AIP56NdeFw1 together with AIP56MycXhoRv1 or AIP56V5XhoRv1. The PCR products were subcloned into pGEM-T Easy vector (Promega) and cloned into the pET28a(+) plasmid (Promega), yielding the plasmids pET28aAIP56MycH+ and pET28aAIP56V5H+. AIP56Myc and AIP56V5 were expressed in *E. coli* BL21(DE3) and purified following the same protocol used for AIP56 (Silva et al, 2013).

2.2. Cell-free expression of ^{35}S-labeled sbp65Rel

The coding region (Met^{1}-Arg^{188}) of sea bass p65 Rel domain (sbp65Rel) was amplified by PCR from cDNA obtained as described in (Pinto et al, 2012) using primers DLp65Fw1NcoI and DLp65Rv4XhoI. For production of ^{35}S-labeled sbp65Rel the reverse primer

DLp65Rv2XhoI, that introduces a stop codon before the 6xHis-tag of the pET-28a(+)vector, was used instead of DLp65Rv4XhoI, with the purpose of producing a protein without a 6xHis-tag. PCR products were cloned in pET-28a(+). Untagged sbp65Rel was produced as ^{35}S-labeled proteins in rabbit reticulocyte lysates by *in vitro* translation using the TNT T7 Quick Coupled transcription/Translation kit (Promega), in the presence of Redivue™ L-[^{35}S] methionine (specific activity of N1000 Ci/mmol) following the manufacturer's instructions.

Table 4. Primers used in this study.

Primer designation	Nucleotide sequence 5′→3′
AIP56NdeFw1	CGCCATATGGCATAACCTTCAATGATGGT
AIP56MycXhoRv1	CGCCTCGAGAAGATCTTCTTCAGAAATAAGTTTCTGTTCATTAATGAATTGTGGCGCGTGGGGAT
AIP56V5XhoRv1	CGCCTCGAGCGTAGAATCGAGACCGAGGAGAGGGTTAGGGATAGGCTTACCATTAATGAATTGTG GCGCGTGGGGAT
DLp65Fw1NcoI	CGCCCATGGAAGGTGTGTATGGATGGAGCCTG
DLp65Rv2XhoI	GCGCTCGAGTCACCTGTTGTCATAGATGGGCTGCG
DLp65Rv4XhoI	GCGCTCGAGCCTGTTGTCATAGATGGGCTGCG

2.3. Protein quantification

Recombinant proteins were quantified by measuring absorbance at 280 nm and using the extinction coefficient calculated by the ProtParam tool (http://www.expasy.org/tools/protparam.html), using the Edelhoch method (Edelhoch, 1967), but with the extinction coefficients for Trp and Tyr determined by Pace et al (Pace et al, 1995).

3. Fluorescent labelling of AIP56

AIP56 labelled with Alexa Fluor 488 (Alexa 488-AIP56) was prepared using the Alexa Fluor Protein Labelling Kit (A-10235) from Molecular Probes following the manufacturer's instructions. AIP56 labelled with FITC (FITC-AIP56) was prepared using the Fluoreporter FITC Protein Labelling Kit (F6434) from Molecular Probes following the manufacturer's instructions.

4. *In vitro* analysis of AIP56 catalytic activity

To prove that the inhibitors used in this study do not interfere with AIP56 activity, cleavage of AIP56 cytosolic substrate was evaluated *in vitro,* using *in vitro* translated ^{35}S-labeled sbp65Rel synthesized as previously described on section 2.2. ^{35}S-labeled sbp65Rel was incubated for 2 h at 22ºC with 100 nM (5.7 µg ml^{-1}) of recombinant AIP56 in the presence of the inhibitors at the concentration described on table 5 (also used for the *ex vivo*

assays) in a final volume of 20 µl adjusted with 10 mM Tris-HCl pH 8.0, 150 mM NaCl. The reaction was stopped by adding SDS-PAGE sample buffer and p65 cleavage assessed by autoradiography.

Table 5. Inhibitors used in this study.

Inhibitor	Supplier	Reference	Concentration	Pre-incubation
Ammonium Chloride	Merck	1011450500	30 mM	1 h
Bafilomycin A1	Sigma	B1793	10 nM	
Chloroquine diphosphate salt		C6628	100 µM	
Chlorpromazine		C8138	30 µM	
Concanamycin A		C9705	10 nM	
Cytochalasin D		C8273	4 µM	
Dynasore		D7693	80 µM	
Monensin sodium salt		M5273	5 µM	
Nigericin sodium salt		N7143	50 nM	
MG132	Calbiochem	CAS 133407-82-6	20 µM	
LY294002	Cell Signaling	9901	10 µM	
Colcemid	Gibco	15210-040	0.27 µM	3 h
Nocodazole		M1404	30 µM	
Taxol	Sigma	T1912	20 µM	

5. *In vitro* analysis of AIP56 pH induced conformational changes

5.1. Tryptophan and TNS fluorescence

Tryptophan and TNS fluorescence at different pH values was analyzed in a PerkinElmer LS45 Luminescence Spectrometer with excitation of 270 nm and an emission scan of 310 nm to 450 nm or excitation of 366 nm and an emission scan of 380 to 500 nm, respectively. The following buffers were used: for pH 4.0, 4.5, 5.0, and 5.5, 150 mM NaCl, 100 mM ammonium acetate; for pH 6.0 and 6.5, 150 mM NaCl, 100 mM morpholineethanesulfonic acid (MOPS); for pH 7.0 and 7.5, 150 mM NaCl, 100 mM HEPES (Qa'Dan et al, 2000). TNS was added to each buffer at a final concentration of 150 µM. AIP56Myc was added to a final concentration of 1.5 µM (8.7 µg ml^{-1}) in a final volume of 300 µL. Fluorescence measurements were done after 15 min incubation at RT. For the pH shift experiments, the toxin was incubated with TNS at pH 4.0 for 15 min at RT and the fluorescence recorded. The pH was then adjusted to 7.5 by gradual addition of 1 N NaOH and the fluorescence recorded again. Since the pH 7.5 was not within the buffering range of ammonium acetate, the pH of the sample was checked following the analysis to confirm that the desired pH value was maintained. Experiments were repeated at least three times and in each experiment, fluorescence intensities were determined by averaging two readings.

6. Black lipid bilayer experiments

The methods used for black lipid bilayer experiments have been previously described in detail (Benz et al, 1978). The instrumentation consisted of a Teflon chamber with two aqueous compartments connected by a small circular hole, with a surface area of about 0.4 mm^2. Membranes were formed across the hole by painting on a 1% (w/v) solution of diphytanoyl phosphatidylcholine (Avanti Polar Lipids, Alabaster, AL) in n-decane. The aqueous salt solution (150 mM KCl) was buffered with 2 mM CaCl2 and 10 mM of either HEPES (pH 7.4 or pH 7.0), MES (pH 6.5 or pH 6.0) or CH3COOK (pH 5.5, pH 5.0 or pH 4.5) added to the cis compartment of the chamber. Reducing conditions were established by addition of 1 mM DTT after the membrane had turned black. Approximately 10 µg of protein were used for each measurement; purified protein samples mixed 1:1 with cholesterol suspension in water were added to the cis compartment of the chamber after the membrane had turned black. The membrane current was measured with a pair of Ag/AgCl electrodes with salt bridges switched in series with a voltage source and a highly sensitive current amplifier (Keithley 427). The amplified signal was recorded by a strip chart recorder. The applied membrane potential was 50 mV. All measurements were performed at RT and each experiment was repeated at least twice.

7. pH-induced translocation across the cell membrane

To address if an acidic pulse can drive translocation of cell-bound AIP56 across the cell membrane we followed the protocol first described for diphtheria toxin (Barth et al, 2000; Draper & Simon, 1980; Sandvig & Olsnes, 1980). Different pH values were obtained by adding sufficient H_3PO_4 to a buffer containing 0.5 mM MgCl2, 0.9 mM CaCl2, 2.7 mM KCl, 1.5 mM KH_2PO_4, 3.2 mM Na_2HPO_4, and 184 mM NaCl for sbPL or 137 mM NaCl for mBMDM. In all experiments, concanamycin A (10 nM final concentration) was maintained during the entire assay, including washes, to inhibit normal toxin uptake.

sbPL were incubated in supplemented L-15 medium (pH 7.4) with 10 µg ml^{-1} of AIP56 in the presence or absence of 10 nM concanamycin A for 30 min on ice, washed twice in phosphate buffers at pH 7.0, pH 5.5 or pH 5.0, resuspended and incubated in the different buffers for 10 min at RT. Cells were collected by centrifugation, resuspended in supplemented L-15 and incubated at 22ºC for 2 h with or without concanamycin A. mBMDM monolayers were incubated in supplemented DMEM with 5 µg ml^{-1} of AIP56 in the presence or absence of 10 nM concanamycin A for 30 min on ice. Supernatant was removed and cells were incubated at the different pH for 1 h at 37ºC in a humidified chamber in the presence of 7% CO_2. After 1 h incubation, supernatants were removed, fresh supplemented DMEM was

added and cells were incubated for further 2 h at 37ºC with or without concanamycin A. Mock-treated cells and cells treated only with toxin were used as controls and NF-κB p65 cleavage was analyzed by western blotting and used as a read-out.

8. Intoxication assays: NF-κB p65 cleavage read-out

sbPL: cells obtained as described in section 1 were pulsed with 10 μg ml^{-1} of AIP56, FITC-AIP56 or Alexa 488-AIP56 for 30 min on ice, washed 3 x with ice-cold sbPBS (PBS with osmotic strength adjusted to 322 mOsm) by centrifugation at 500 g for 5 min at 4ºC and then transferred to 22ºC. Mock-treated cells were used as control. At the indicated times, cells were collected by centrifugation (500 g, 5 min, 4ºC), washed once with sbPBS and lysed by addition of SDS-PAGE sample buffer. Cleavage of NF-κB p65 was evaluated by western blotting, as described in section 18.

Mammalian cells: cells were incubated with AIP56 or with $AIP56^{AAIVAA}$ at the indicated concentration for 30 min on ice, washed twice with PBS to remove unbound toxin, resuspended in complete medium without toxin and then transferred to 37ºC for the indicated time-intervals. In experiments using chimeric proteins, mBMDM were continuously incubated with 0.5 μg ml^{-1} (8.75 nM) AIP56 or 10 nM of anthrax protective antigen (PA) together with 20 nM of LF^{1-254}·$AIP56^{1-261}$ or LF^{1-254}·$AIP56^{299-497}$. In all experiments, mock treated cells were included as controls. At the indicated times cells were washed once with PBS and resuspended in SDS-PAGE sample buffer to further analyze NF-κB p65 cleavage by western blotting as described in section 18.

9. Analysis of cellular morphology

sbPL: cellular morphology was assessed by light microscopy morphological analysis of cytospin preparations, fixed in 10% formalin in ethanol followed by neutrophils' peroxidase detection using the Antonow's technique (Afonso et al, 1997; do Vale et al, 2002) and staining with hemacolor (Merck). A set of morphological alterations such as occurrence of cell rounding and shrinkage, nuclear fragmentation and/or chromatin condensation, cell blebbing and formation of apoptotic bodies (Hacker, 2000) was considered. Experiments were performed using cells collected from at least 3 individual fish. The percentage of apoptotic cells was determined in a blind fashion by scoring a minimum of 350 cells per slide. Cytospins preparations were analysed under an Olympus microscope equipped with an X-cite lamp source (series 120PC) and an Olympus DP72 microscope digital camera. Images were acquired using cellSens Dimension software.

Mammalian cells: cellular morphology was assessed by morphological evaluation of the cell monolayers by phase-contrast microscopy (Olympus CKX41). Morphological alterations such as shrinkage and rounding up of the cells, membrane blebbing and detachment of the cells were considered. Images were captured using an Olympus sc30 camera and the "analySIS getIT" Olympus software.

10. Viability assay: conversion of resazurin to resorufin

The indicator dye resazurin can be used to measure the metabolic capacity of the cells - indicator of cell viability. Viable cells retain the ability to reduce resazurin into highly fluorescent resorufin while nonviable cells rapidly lose metabolic capacity, do not reduce the indicator dye, and thus do not generate a fluorescent signal (Magnani & Bettini, 2000; Springer et al, 1998; White et al, 1996).

Mammalian cells were left untreated or incubated with the appropriated recombinant protein. At the indicated times 20 µl of resazurin at 1.25 mM (diluted in water) was added *per* well (final concentration 0.125 mM). Cells were again incubated at 37°C to allow them to convert resazurin to resorufin, and after 3 h the fluorescent signal was measured on a Spectra Max Gemini XS fluorimeter (Molecular Devices) at an excitation wavelength of 560 nm and an emission wavelength of 590 nm.

11. Detection of apoptosis

11.1. Caspase-3 assay

The activity of caspase-3 in total cell lysates was determined using a commercial fluorimetric assay (EnzChek Caspase-3 Assay Kit, Molecular Probes), following the manufacturer´s instructions. Briefly, soluble extracts prepared from AIP56 or AIP56^{AAIVAA} treated cells were allowed to react with 100 µM Z-DEVD–AMC in 1x reaction buffer for 3 h at RT and in the dark. Fluorescence was measured on a Spectra Max Gemini XS fluorimeter (Molecular Devices) at an excitation wavelength of 360 nm and an emission wavelength of 460 nm. In sbPL experiments the results are expressed as relative fluorescent units (RFU). In mBMDM, to normalize the results, the protein concentration in each sample was determined using the Bio-Rad Protein Assay (Bio-Rad 1-800-424-6723) following the recommended procedure for microtiter plates. In some experiments, the results, in relative fluorescence units per nanogram of protein (RFU/ng) were converted to fold increase by comparing to the values obtained in extracts from mock-treated cells.

11.2. TUNEL assay

The internucleosomal DNA fragmentation was detected by TUNEL staining of DNA strand breaks with the In Situ Cell Death Detection Kit, POD (Roche Diganostics) following the manufacturer's instructions. Propidium iodide (PI) at 1 μg ml^{-1} was used as a nuclei counterstain.

12. Competition assay

$AIP56^{286\text{-}497C298S}$ was tested, in competition experiments, for its ability to inhibit AIP56-mediated p65 cleavage. The competition assays were performed as previously described (Silva et al, 2013). Briefly, cells were pre-incubated for 15 min on ice with 7 μM A domain ($AIP56^{286\text{-}497C298S}$) or with 7 μM B domain ($AIP56^{286\text{-}497C298S}$) followed by incubation for further 15 min on ice with an 800-fold lower concentration of AIP56 (8.75 nM (0.5 μg ml^{-1}) of AIP56) in the presence of the competitors. Cells were washed once with ice cold supplemented DMEM and incubated at 37ºC for 2 h. Mock-treated cells and cells only treated with each of the proteins were used as control. NF-κB p65 cleavage was assessed by western blotting as described on section 18.

13. Detection of the intracellular AIP56

13.1. Western blotting

Cells were intoxicated with the appropriated recombinant protein as described in intoxication assays section 8. When specified, cells were pre-treated and incubated in the presence of MG132, concanamycin A, bafilomycin A1, dynasore, chlorpromazine, cytochalasin D or nocodazole at the concentration and pre-incubation time described in table 5. At different time-points, aliquots were collected and cells were washed twice with ice-cold PBS and incubated for 10 min on ice with 500 μg ml^{-1} (in PBS) of pronase E from *Streptomyces griseus* (P5147, Sigma Aldrich) to digest the extracellular cell-associated toxin. Cells treated with the toxin, washed and incubated in PBS without protease were used as control. Protease was inactivated with phenylmethylsulfonyl fluoride (PMSF) at a final concentration of 250 μg ml^{-1}. Cells were washed in PBS, resuspended in SDS-PAGE sample buffer and analyzed by western blotting for detection of AIP56 as described on section 18.

13.2. Fluorescence microscopy

To monitor AIP56 entry and intracellular behavior by fluorescence microscopy cells were incubated with 10 μg ml^{-1} of Alexa 488-AIP56 or FITC-AIP56 for 30 min on ice, then the medium was replaced by supplemented medium without toxin and cells were switched to

37ºC for mBMDM or to 22ºC for sbPL. At different time-points, cells were washed three times with PBS and fixed with ice-cold 4% paraformaldehyde (w/v in PBS) for 10 min at RT. To counterstain the cell limits, cells were permeabilized for 10 min at RT with 0.1% Triton X-100 in PBS, washed and incubated with blocking buffer (10% FBS in 0.1% Tween in PBS) for 30 min prior to incubation for 1 h with the F-actin probe Alexa Fluor 594-Phalloidin 5 U ml^{-1} also diluted in blocking buffer. Nuclei were counterstained with 0.2 µg ml^{-1} DAPI (4', 6-diamidino-2-phenylindole) and coverslips were mounted on a glass-slide with Vectashield (Vector laboratories) and sealed with polish nail. Samples were 3D analyzed on a laser scanning confocal microscope (Leica TCS SP5 II running LAS AF 2.6 software - Leica Microsystems, Germany) using a 60x/1.40 N.A. oil immersion objective, with a pixel size of 60 nm and a z step size of 210 nm. The 3D image stacks were deconvolved with Huygens Professional software (SVI, Netherlands) applying the Maximum Likelihood Estimation restoration algorithm. Restored images were processed and maximum intensity projected with Fiji software (Schindelin et al, 2012).

14. Recycling assay

mBMDM were incubated for 30 min on ice in serum-free medium containing 10 µg ml^{-1} AIP56V5, transferred to 37ºC for 5 min to allow AIP56 to be endocytosed (pulse) and switched to ice again. Cells were washed 3x with ice-cold PBS and the third wash was collected and precipitated with trichloroacetic acid (TCA). After washing, cells were incubated for 10 min on ice with 125 µg ml^{-1} pronase E (pronE) in PBS, to remove extracellular toxin. Then cells were washed twice with PBS, treated with 250 µg ml^{-1} PMSF/PBS (1 ml/well) to inhibit protease activity and washed 3x with ice-cold PBS followed by washing with 250 µl/well serum-free medium containing 10 µg ml^{-1} $AIP56^{286\text{-}497C298S}$ .The medium from the last wash was collected and precipitated with TCA. Then cells were incubated at 37ºC in a humidified chamber with 7% CO_2 in serum-free medium containing 10 µg ml^{-1} $AIP56^{286\text{-}497C298S}$ (to prevent re-entry of recycled full-length AIP56). At different time-intervals, supernatant was collected and precipitated with TCA and the corresponding cell monolayer was washed twice with PBS and lysed with SDS-PAGE sample buffer. TCA precipitates were resuspended in SDS-PAGE sample buffer and the equivalent to 12 wells for supernatant and washes and 4 wells for monolayer (pellet) was analyzed by western blotting for detection of AIP56V5 using an anti-V5 antibody. Membranes were reprobed with an anti-GAPDH antibody (used as cytosolic marker).

In some experiments, cells were incubated with 10 µM LY294002 or 10 nM of concanamycin A for 1 h at 37ºC before pulse with AIP56V5. In this case, the inhibitor was maintained during the entire chase.

15. Inhibition of endocytosis and trafficking

15.1. Inhibitors

Before the intoxication assay (see section 8) with the appropriated recombinant toxin, cells were pre-treated with the inhibitor for 1 h or 3 h (see Table 5) at the appropriated temperature. Cells treated with dynasore were incubated in culture medium lacking FBS. AIP56 was added to a final concentration of 5 μg ml^{-1} for mBMDM or 10 μg ml^{-1} for sbPL and cells were switched to 37ºC or 22ºC respectively and incubated for a maximum of 2 h while maintaining the inhibitory conditions. Analysis of NF-κB p65 cleavage by western-blotting was used as a read-out. In sbPL experiments the inhibitory effect of the inhibitors was also evaluated by AIP56-induced apoptotic morphological alterations (as described in section 9).

15.2. Lag-time experiments

Cells were intoxicated with AIP56 as described in section 8 and at the indicated time-points concanamycin A, at a final concentration of 10 nM, was added to the cells. Internalization of the toxin was assessed by evaluating the cleavage of NF-κB p65 by western blotting as described on section 18.

16. Phagocytosis assay

Listeria monocytogenes EGD (wild-type NCTC 7973, kindly provided by Didier Cabanes, Group of Molecular Microbiology, Instituto de Biologia Molecular e Celular, Universidade do Porto, Porto, Portugal) was grown in brain-heart infusion (BHI; Difco) to an optical density at 600 nm of 0.8, pelleted by centrifugation, washed 3x and resuspended in warm complete DMEM without FBS and antibiotic. mBMDM were incubated with 4 μM cytochalasin D, 80 μM dynasore or 30 μM chlorpromazine for 1 h at 37ºC or left untreated prior to phagocytosis assay. Bacteria were added to untreated or treated mBMDM (5 x 10^5 cells/well, 24 well-plates) at a multiplicity of infection of 10 bacteria per cell and incubated for 30 min at 37ºC. Monolayers were washed 3x with warm complete DMEM without antibiotic, extracellular bacteria were killed with 20 μg ml^{-1} gentamicin (Lonza) for 1 h at 37ºC, cells washed again 3x, lysed with 0.1% Triton X-100 and serial dilutions plated in BHI agar. Colony forming units (CFU) were determined after 24 h incubation at 37ºC and normalized to CFU in cells treated with bacteria in the absence of the inhibitors. Assays were performed in triplicate.

17. Fluorescence microscopy

17.1. Immunofluorescence

For fluorescence microscopy studies, mBMDM cultured on LPS-free 12-mm glass coverslips were incubated in supplemented DMEM with 10 μg ml^{-1} FITC-AIP56 or Alexa 488-

AIP56 for 30 min on ice. The supernatant was removed, replaced by supplemented medium without toxin and cells switched to 37ºC for a maximum of 60 min. At different time-points, cells were washed once with PBS and processed for immunofluorescence. mBMDM monolayers were either fixed with ice-cold 4% paraformaldehyde (w/v in PBS) for 10 min at RT and permeabilized with 0.1% Triton X-100 in PBS for 10 min at RT (for immunodetection of EEA, LAMP-1 and GM130) or fixed with ice-cold methanol for 10 min at RT (for detecting GRP78 Bip). Cells were incubated with blocking buffer (10% FBS in 0.1% Tween in PBS (PBS-T)) for 30 min prior to the addition of primary antibodies. The primary antibodies were diluted in blocking buffer as described in table 6 and incubated overnight at 4ºC in a humidified chamber. After several washes, the secondary antibodies, diluted in blocking buffer, were incubated with the cells for 1 h at RT in a humidified chamber. Nuclei were counterstained with 0.2 µg ml^{-1} DAPI and preparations were mounted with Vectashield. Samples were 3D analysed on a laser scanning confocal microscope (Leica TCS SP5 II running LAS AF 2.6 software - Leica Microsystems, Germany) using a 60x/1.40 N.A. oil immersion objective, with a pixel size of 60 nm and a z step size of 210 nm. Each fluorochrome was imaged by sequential acquisition in order to avoid crosstalk between channels. The 3D image stacks were deconvolved with Huygens Professional software (SVI, Netherlands) applying the Maximum Likelihood Estimation restoration algorithm. Restored images were processed and maximum intensity projected with Fiji software (Schindelin et al, 2012).

To control the effect of microtubule destabilizing agents (nocodazole, colcemid and taxol) and the effect of cytochalasin D on actin filaments, cells were incubated with the inhibitors at 22ºC (sbPL) or at 37ºC (mBMDM) for 3h in the case of microtubules inhibitors or 1 h for cytochalasin D. Cells were washed, fixed with ice-cold 4% paraformaldehyde (w/v in PBS) for 10 min at RT, washed 3x with PBS, permeabilized with 0.1% Triton-X100 for 10 min at RT, washed 3x as above and blocked for 15 min (10% FBS, 0.01% Tween 20 in PBS). Cells treated with microtubules destabilizing agents were incubated for 1 h with the primary antibody mouse monoclonal anti-α-Tubulin washed as described above and incubated with the fluorescence-conjugated secondary antibody Alexa Fluor 488 goat anti-mouse IgG (H+L), both diluted in blocking buffer. In the case of cytochalasin D, cells were incubated for 1 h with the F-actin probe Alexa Fluor 594-Phalloidin also diluted in blocking buffer. Nuclei were counterstained with 0.2 µg ml^{-1} DAPI and preparations were mounted with Vectashield. Slides were analysed under an Olympus microscope equipped with an X-cite lamp source (series 120PC) and an Olympus DP72 microscope digital camera. Images were acquired using cellSens Dimension software, processed and maximum intensity projected with Fiji software (Schindelin et al, 2012).

Table 6. Antibodies and fluorescent probes used in this study

	Supplier	Reference	Application	Dilution
Primary antibody				
NF-κB p65 C-terminal domain (c-20) rabbit polyclonal	Santa Cruz Biotechnology	sc-372	Western blot	1:3000
GAPDH (6C5) mouse monoclonal		sc-32233		1:20000
c-Myc (9E10) mouse monoclonal		sc-40		1:7500
V5 mouse monoclonal	Invitrogen	R960-25		1:5000
Anti-AIP56 rabbit serum	(do Vale et al, 2005)			1:5000
Sea bass NF-κB p65 rabbit serum	produced using the peptide SIFNSGNPARFVS located at the C-terminal region of sea bass p65 antigen as described (Silva et al, 2013)			1:1500
Early Endosomal Antigen 1 (EEA1) (C-terminal) rabbit polyclonal	Sigma	E3906	Immunofluorescence	1:500
Lysosomal membrane glycoprotein LAMP-1 mouse monoclonal	Abcam	ab13523		1:75
GRP78 Bip rabbit polyclonal		ab32618		1:50
GM130 mouse monoclonal	BD Biosciences	610822		1:500
Mouse anti-α-tubullin	Invitrogen	32-2500		1:2500
Secondary antibody				
Sheep anti-mouse HRP-conjugated	The Binding Site	AP271	Western blot	1:20000
Sheep anti-rabbit HRP-conjugated		AP311		1:20000
Goat anti-rabbit alkaline phosphatase conjugated	Sigma Aldrich	A9919		1:30000
Goat anti-mouse alkaline phosphatase conjugated		A2429		1:10000
Alexa Fluor 568 goat anti-rabbit IgG (H+L)	Molecular Probes	A-11011	Immunofluorescence	1:1000 for GRP78 Bip
Alexa Fluor 568 goat anti-mouse IgG (H+L)		A-11004		1:500 for LAMP-1 1:1000 for GM130
Alexa Fluor 594 donkey anti-rabbit IgG (H+L)		A-11012		1:10000 for EEA1
Fluorescent probes				
Alexa Fluor 647-Transferrin conjugated	Invitrogen	T23366	Fluorescence microscopy	500 ug ml^{-1}
Alexa Fluor 594 Phalloidin		A12381		5 U ml^{-1}

17.2. Transferrin experiments

For transferrin experiments, mBMDM were incubated in supplemented DMEM without FBS with 10 µg ml^{-1} Alexa 488-AIP56 for 20 min on ice, the supernatant was removed and replaced by ice-cold supplemented DMEM with 500 µg ml^{-1} Alexa 647-Transferrin conjugated and incubated for more 10 min on ice. Then cells were switched to 37ºC and incubated for a maximum of 60 min. At the time-intervals indicated cells were washed twice with PBS and fixed with ice-cold 4% paraformaldehyde (w/v in PBS) for 10 min at RT. Cell were washed 3x with PBS and nuclei were counterstained with 0.2 µg ml^{-1} DAPI and preparations mounted with Vectashield. Samples were 3D analysed on a laser scanning confocal microscope (Leica TCS SP5 II running LAS AF 2.6 software - Leica Microsystems, Germany) as described on step 17.1.

17.3. Acridine Orange

The efficacy of concanamycin A in inhibiting the endosomal vacuolar ATPase pump was confirmed through acridine orange staining. Cells were incubated for 1 h in the presence of 10 nM concanamycin A or DMSO (vehicle of concanamycin A) and then 0.5 µg ml^{-1} of acridine orange (AO) were added and the cells incubated for further 15 min at 22ºC (sbPL) or 37ºC (mBMDM). Cells were washed twice with PBS and fixed with ice-cold 4% paraformaldehyde (w/v in PBS) for 10 min at RT. Nuclei were counterstained with 0.2 µg ml^{-1} DAPI and coverslips were mounted with Vectashield prior to visualization of endosomal acidification by AO fluorescence.

18. SDS-PAGE and Western blotting

SDS-PAGE was performed using the Laemmli discontinuous buffer system (Laemmli, 1970). Prior to loading, the samples were boiled for 5 min in SDS-PAGE sample buffer (50 mM Tris-HCl (pH 8.8), 2% SDS, 0.05% bromofenol blue, 10% glycerol, 2 mM EDTA and 100 mM DTT). For western blotting analysis, the proteins were transferred onto nitrocellulose membranes. The efficiency of transfer was controlled by staining with Ponceau S. The membranes were blocked for 1 h at RT with 5% skimmed milk in tris-buffered saline (TBS) containing 0.1% Tween 20 (TBS-T) followed by incubation for 1 h at RT with the primary antibodies diluted in blocking buffer (see table 6). Immunoreactive bands were detected using horseradish peroxidase-linked secondary antibodies (table 6; sheep anti-rabbit HRP-conjugated or sheep anti-mouse HRP-conjugated) and ECL West Dura Chemiluminescence substrate (Pierce biotechnology) or alkaline phosphatase conjugated secondary antibodies (table 6; goat anti-rabbit alkaline phosphatase conjugated or goat anti-mouse alkaline phosphatase conjugated) and NBT/BCIP (50 µg ml^{-1} / 50 µg ml^{-1}) (Promega).

Blots shown correspond to representative results of at least 3 independent experiments. The quantification of the blots was performed by densitometry analysis using Fiji software. Loading correction was achieved by dividing the density of AIP56, p65 or cl-p65 band by the respective density of Ponceau S. In the case of the recycling assays, the densities of the GAPDH bands were used instead of Ponceau S.

19. Statistical analysis

Statistical analysis of results presented in Figures 4.2, 4.7, 4.8, 4.9, 4.13B, 4.13C, 4.16 and 4.19 involved performing one-way or two-way ANOVA. Normality of the data was tested by the Kolmogorov-Smirnov test; homogeneity of variances was assessed using the Levene test; p-values for individual comparisons were calculated using Tukey's Honest Significant Difference (HSD) multiple comparisons test. Figures 4.3, 4.6, 4.11B, 4.12B and 4.13A present several regression models where the dependent variable is modeled as a function of time. In order to obtain these curves, several models were studied (linear, quadratic, inverse and logarithmic) and the selected models were based on the quality of the adjustment, in particular, the residuals distribution as well as the coefficient of determination R^2. The analysis of the residuals included the verification of normality as well as the study of extreme values. Analyses were performed using the SPSS software and significance was set at $p<0.05$.

CHAPTER IV

RESULTS

1. Interaction of AIP56 with mammalian cells

We have previously shown that AIP56 is a metalloprotease AB toxin that cleaves NF-κB p65 at an evolutionary conserved peptide bond, formed by the Cys^{39}-Glu^{40} residues, located at the N-terminal region of the Rel homology domain. We also showed that incubation of sea bass peritoneal leukocytes (sbPL) with the toxin *ex vivo* results in NF-κB p65 depletion (Silva et al, 2013). However nothing was known about the interaction of AIP56 with different cell types. Furthermore, there was a lack of appropriate and established tools (e.g. antibodies, protocols, etc.) available to study AIP56 trafficking in fish cells. These led us to search for an alternative model. Although mammals are not susceptible to infection by *Phdp*, likely due to temperature and osmolarity restrictions (Magariños et al, 1992), we decided to evaluate the susceptibility of different mammalian cells to AIP56. Thus, we tested macrophage (J774A.1, Raw264.7, THP-1) and epithelial (HeLa, CHO, Vero) cell lines as well as primary macrophages (mouse bone marrow derived macrophages, mBMDM).

1.1. AIP56 cleaves NF-κB p65 in different cell lines but does not induce apoptosis

To investigate the susceptibility of different mammalian cell lines to AIP56, cells were left untreated or incubated with the toxin and, at different time-points, samples were collected for assessment of NF-κB p65 cleavage and for morphological and viability analysis. Mock-treated cells were used as control and the metalloprotease mutant $AIP56^{AAIVAA}$ was included in some experiments, to assess the involvement of the metalloprotease activity in AIP56 intoxication. As shown in Figure 4.1A, AIP56 was able to enter and cleave NF-κB p65 in J774A.1, Raw264.7 and HeLa cells. However, contrarily to what was previously reported for sea bass peritoneal leukocytes (Silva et al, 2013), the decrease in p65 levels was transient and after 24 h incubation the normal levels of p65 were fully recovered (Figure 4.1B). Accordingly, phase-contrast microscopy revealed no morphological alterations, even after 24 h incubation (Figure 4.1C). In agreement with the absence of morphological alterations, no differences in the viability (metabolic capacity) of cells treated with AIP56 was observed when compared to cells untreated or treated with the catalytically inactive mutant $AIP56^{AAIVAA}$ (Figure 4.1D). The susceptibility to AIP56 was found to be cell-type dependent, since no p65 cleavage was observed in THP-1, CHO or Vero cell lines (Figure 4.1A).

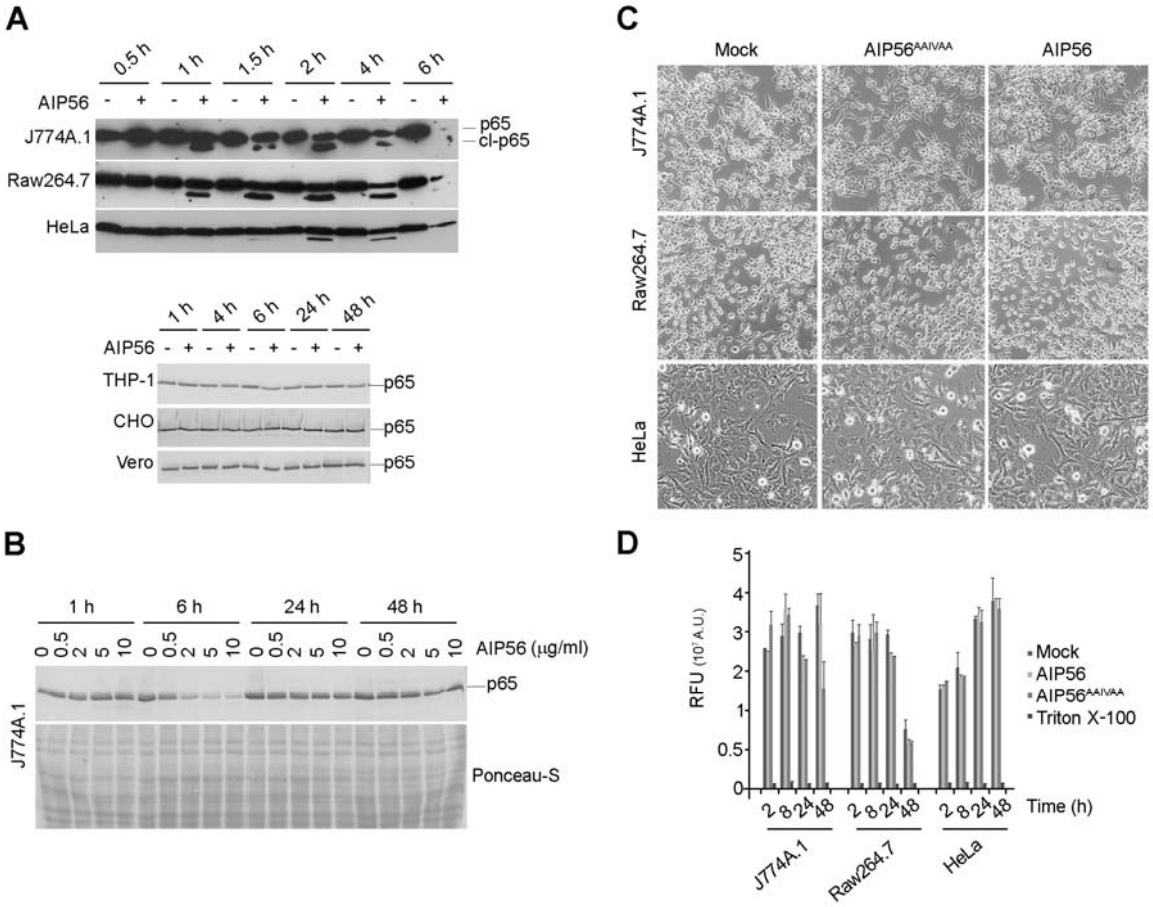

Figure 4.1. AIP56 cleaves NF-κB p65 in mammalian cell lines but does not induce apoptosis. (A) Cell lines were left untreated or incubated with 10 μg ml^{-1} AIP56, washed to remove unbound toxin and chased at 37ºC for the indicated time-points. Cleavage of NF-κB p65 was analyzed by western blotting (ECL detection: J774A.1, Raw264.7 and HeLa; chromogenic detection: THP-1, CHO and Vero; cl-p65: p65 cleavage fragment). **(B)** Kinetic analysis of AIP56-induced NF-κB p65 cleavage in J774A.1 cells. Cells were treated as described in A with the indicated concentrations of AIP56. Cleavage of NF-κB p65 was analyzed by western blotting (chromogenic detection). To control the protein loading, the membrane was stained with Ponceau S (bottom panel). The blots shown in A and B are representative of four independent experiments. **(C)** Incubation of different cell lines with AIP56 does not result in morphological alterations. Phase contrast microscopy of macrophage (J774A.1 and Raw264.7 cells) and epithelial (HeLa) cell lines incubated with 10 μg ml^{-1} AIP56 or the catalytically inactive mutant $AIP56^{AAIVAA}$ for 24 hours at 37ºC. Images shown are derived from one out of four independent experiments. **(D)** Mammalian cell lines incubated with AIP56 have no alterations in metabolic capacity. Cells were incubated with 10 μg ml^{-1} of AIP56 or $AIP56^{AAIVAA}$ and at the indicated time-points the indicator dye resazurin was added. Cells were incubated for more 3 h at 37ºC, and the conversion of resazurin in resorufin measured at an excitation wavelength of 560 nm and an emission wavelength of 590 nm. Results are expressed as relative fluorescence units (RFU) (mean ± SD, *n*=4).

1.2. AIP56 induces depletion of NF-κB p65 and apoptosis in mBMDM

To access the susceptibility of mBMDM to AIP56, cells were incubated with the toxin for a maximum of 24 h and analyzed by phase contrast microscopy for detection of morphological alterations and by western blotting for accessing the occurrence of NF-κB

p65 cleavage. When mBMDM were treated with AIP56, morphological alterations were evident from 6-24 h incubation (Figure 4.2A). These alterations were dependent on the metalloprotease activity of the toxin, since they did not occur after incubation with the AIP56 metalloprotease mutant AIP56^{AAIVAA} (Figure 4.2A). The cellular alterations included shrinkage and rounding up of the cells and membrane blebbing, and resulted in the detachment of almost all cells after 24 h incubation (Figure 4.2A), suggesting the occurrence of an apoptotic death process. Assessment of nuclear DNA fragmentation by TdT-mediated dUTP Nick-End Labeling (TUNEL) and fluorimetric measurement of caspase-3 activity confirmed that mBMDM exposed to AIP56 were undergoing apoptosis (Figure 4.2B and 4.2C). As expected, cells treated with AIP56^{AAIVAA} revealed no signs of apoptosis (Figure 4.2B and 4.2C). Western blotting analysis revealed that intoxication of mBMDM by recombinant AIP56 resulted in time- and dose-dependent decrease of NF-κB p65 protein levels leading to a complete depletion at longer incubation times (Figure 4.2D). Altogether, these results indicate that, similarly to what has been reported in sbPL, intoxication of mBMDM by AIP56 results in p65 depletion and apoptosis.

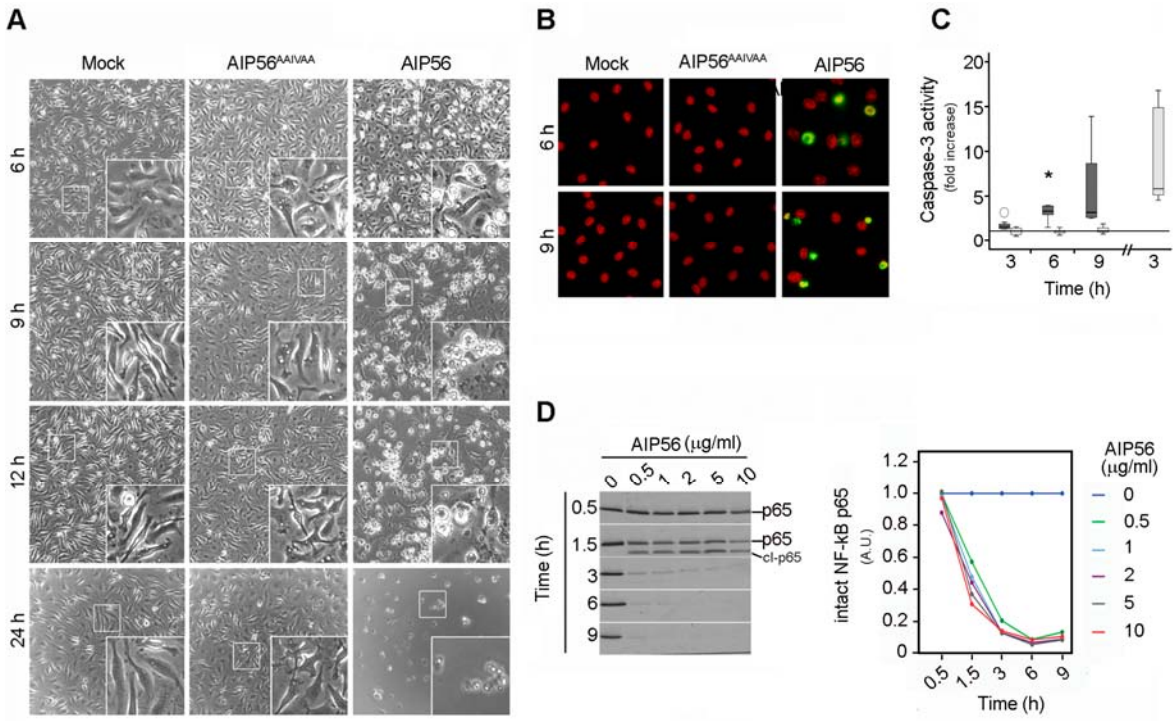

Figure 4.2. Intoxication of mBMDM with AIP56 leads to NF-κB p65 depletion and apoptosis. (A) Incubation of mBMDM with AIP56 results in apoptotic morphological alterations and cell loss. Phase contrast microscopy of mBMDM incubated with 5 μg ml^{-1} of recombinant AIP56 or AIP56^{AAIVAA} for the indicated time-points. Images shown are derived from one out of three independent experiments. **(B)** Incubation of mBMDM with AIP56 results in the appearance of TUNEL-positive and condensed nuclei. Cells were incubated with 5 μg ml^{-1} of recombinant AIP56 or catalytic inactive AIP56^{AAIVAA} for the indicated time-points and processed for the detection of DNA fragmentation by TUNEL (green). Nuclei were counterstained with propidium iodide (red). Images shown are derived from one out of three independent experiments. **(C)** Incubation of

mBMDM with AIP56 results in caspase-3 activation. Cells were incubated with 5 µg ml^{-1} recombinant AIP56 or $AIP56^{AAIVAA}$ for the indicated time-points and caspase-3 activity determined by fluorimetry using the substrate Z-DEVD-AMC. The results, in relative fluorescence units per nanogram of protein were converted to fold increase by comparing to values obtained in extracts from mock-treated cells (*n*=7; the middle bar corresponds to the median and the lower and upper side of the boxes, the first and third quartiles; circle and asterisk signal extreme observations). The fold increase in caspase-3 activity following treatment with $AIP56^{AAIVAA}$ (white bars) is not statistically different from 1 whereas it is significantly different from 1 at all time-points following treatment with recombinant AIP56 (dark grey bars) (p-values for 3, 6 and 9 h: 0.018, 0.008, 0.033, respectively). Statistical analysis involved performing one sample t-test for the hypothesis that the fold increase is equal to 1. Extracts from staurosporine-treated cells (light grey bar) were used as a positive control (*n*=5). **(D)** Incubation of mBMDM with AIP56 results in NF-κB p65 depletion. Cells were left untreated or incubated with the indicated doses of recombinant AIP56 for 30 min on ice, washed and chased at 37ºC for the indicated times. Cleavage of NF-κB p65 was analyzed by western blotting (chromogenic detection). The graph shows quantification of the blots. Loading correction was achieved by dividing the density of p65 band by the respective density of Ponceau S. The results were divided by the same constant in order to set to 1 the mean of the control (cells not exposed to recombinant AIP56). Plotted values correspond to the estimated means of three independent experiments. Dose and time dependence on intact p65 levels were tested by two-way ANOVA (dose main effect p<0.001, time main effect p<0.001 and interaction dose with time p<0.001; there was a significant difference of the group "no toxin (dose 0)" with respect to the other groups, Tukey´s HSD p<0.001).

The presence of the p65 cleavage fragment (cl-p65) is time-dependent, since it was detected in cells up to 1.5 h after intoxication but not in cells subjected to longer incubation times (Figure 4.2 D). Similarly, in sbPL, the p65 cleavage fragment was detected up to 4 h but was no longer visible after intoxication for 6 h (Figure 4.3). Using the proteosomal inhibitor MG132, we found that degradation of the p65-cleavage fragment originated by AIP56 depends on proteosomal activity, in agreement to what has been reported for the p65 cleavage fragment resulting from the activity of the type III effector NleC (Yen et al, 2010). It is possible that the faster degradation of the cleavage fragment observed in mBMDM results from an increased activity of the proteasomal machinery in mBMDM than in sbPL.

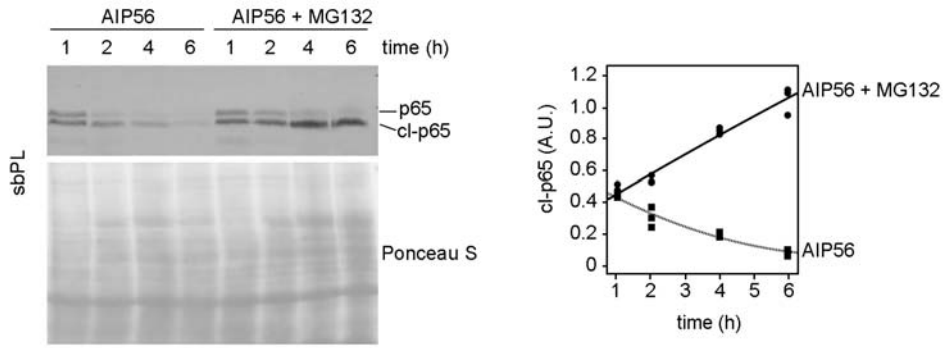

Figure 4.3. Degradation of the AIP56-generated NF-κB p65 cleavage fragment (cl-p65) is dependent on the activity of the proteasome. sbPL were left untreated or incubated with 20 µM of the proteosomal inhibitor MG132 for 1 h, pulsed with 10 µg ml^{-1} of recombinant AIP56 for 30 min on ice, washed to remove unbound toxin, shifted to 22ºC and chased for the indicated time-points. Cleavage of NF-κB p65 was analyzed by western blotting (chromogenic detection). To control the

protein loading, the membrane was stained with Ponceau S (bottom panel). The graph shows the results of the quantification of the blots from three independent experiments. Values correspond to density of cl-p65 relative to density of Ponceau S of the respective lane. The quadratic regression model represents cl-p65 as a function of time (AIP56 R^2=0.941, AIP56+MG132 R^2=0.958).

1.3. Apoptosis of mBMDM induced by AIP56 occurs in the absence of TNF-α or TLR4 signaling

Depending on the cell type, down-regulation of NF-κB p65 *per se* may not be sufficient to induce apoptosis. However it is also known that cells with depletion of NF-κB p65 are more susceptible to start an apoptotic process in response to different stimuli, including TNF-α and TLRs ligands (Beg & Baltimore, 1996; Hsu et al, 2004; Wang et al, 1996).

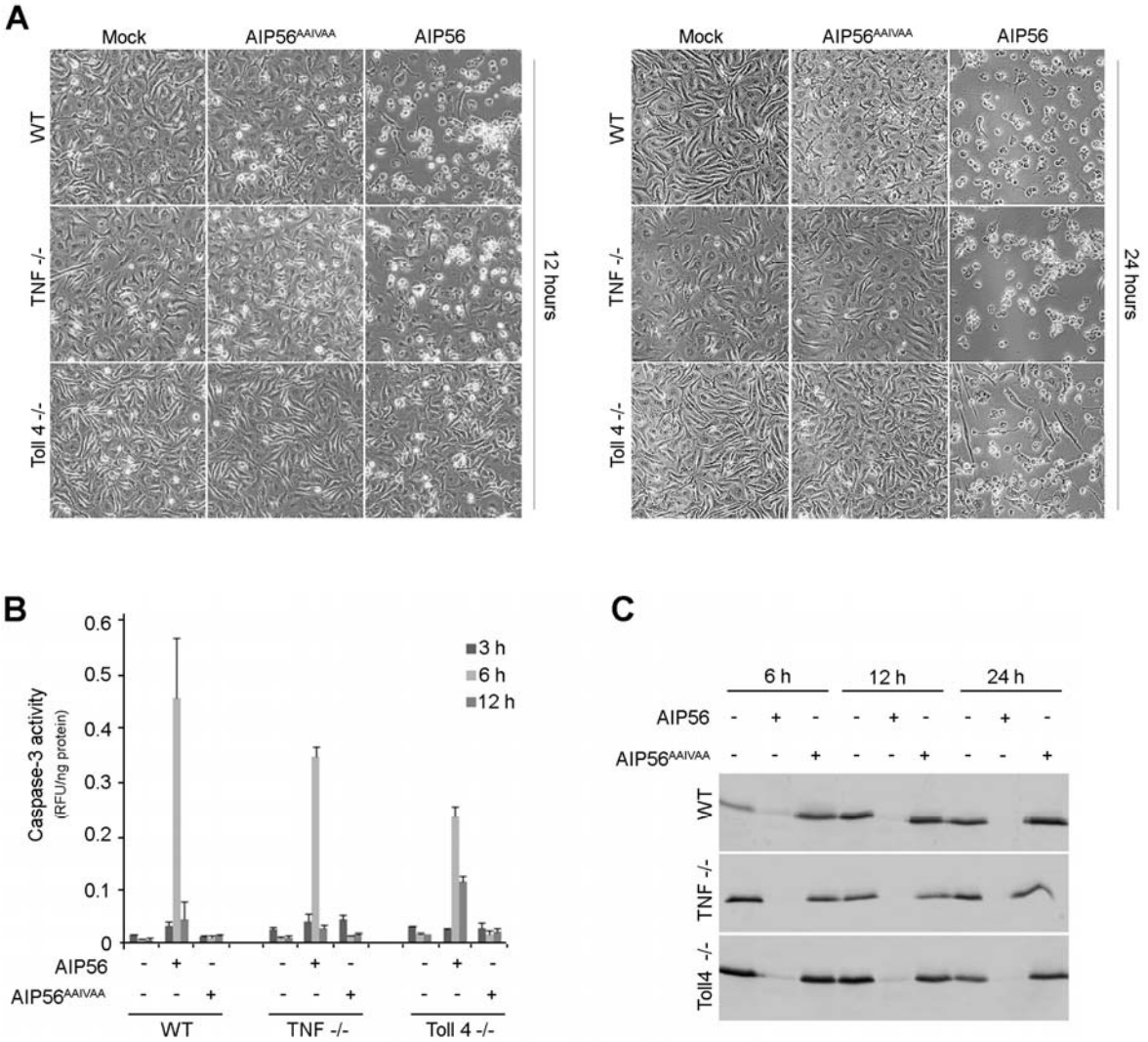

Figure 4.4. AIP56-induced apoptosis in mBMDM occurs in the absence of TNF-α or TLR4 signaling. (A) Phase contrast microscopy of mBMDM incubated with 5 μg ml^{-1} AIP56 or the catalytically inactive mutant $AIP56^{AAIVAA}$ for the indicated time-points. Images shown are derived from one out of two independent experiments. **(B)** Incubation of TNF-$\alpha^{-/-}$ or

TLR-4$^{-/-}$ mBMDM with AIP56 results in the activation of the effector caspase-3. Cells were incubated with 5 μg ml^{-1} recombinant AIP56 or the catalytically inactive mutant AIP56^{AAIVAA} for the indicated time-points and caspase-3 activity determined by fluorimetry using the substrate Z-DEVD-AMC. The results are presented as relative fluorescence units (RFU) per nanogram (ng) of protein. The bar graph shows the results of two independent experiments (mean ± SD, *n*=2). **(C)** Incubation of TNF-α$^{-/-}$ or TLR-4$^{-/-}$ mBMDM with AIP56 results in NF-κB p65 depletion. Cells were left untreated or incubated with 5 μg ml^{-1} AIP56 or AIP56^{AAIVAA} for 30 min on ice, washed to remove unbound toxin and chased at 37ºC for the indicated time-points. Wild-type (WT) mBMDM were used as control. Cleavage of NF-κB p65 was analyzed by western blotting (chromogenic detection). The blot shown is representative of two independent experiments.

To determine if TNF-α or TLR-4 signaling were involved in AIP56-induced toxicity, we performed the intoxication assays in mBMDM from TNF-α and TLR-4 knockout mice. As shown in Figure 4.4A, similarly to what was observed in wild type cells, morphological alterations typical of an apoptotic death process were observed in TNF-α$^{-/-}$ and TLR-4$^{-/-}$ macrophages treated with AIP56. The detection of DNA fragmentation by TUNEL (not shown) and the detection of caspase-3 activity (Figure 4.4B) confirmed that AIP56 induces apoptosis in TNF-α$^{-/-}$ and TLR-4$^{-/-}$ cells. In agreement with this observation, intoxication of TNF-α$^{-/-}$ or TLR-4$^{-/-}$ macrophages resulted in complete depletion of NF-κB p65 (Figure 4.4C). However, a slight delay in toxicity was observed in TLR-4$^{-/-}$ macrophages when compared to WT or TNF-α$^{-/-}$ cells (Figure 4.4A). While in WT macrophages after 12 h incubation the cellular apoptotic morphology is evident, with some cells detached, in TLR-4$^{-/-}$ macrophages cellular morphological alterations were only slightly evident (Figure 4.4A). Accordingly, in TLR-4$^{-/-}$ cells, the levels of caspase-3 activity were found to be lower at 6 h and prolonged to 12 h after infection with AIP56 (Figure 4.4B). These results indicate that TNF-α or TLR4 signaling are not mandatory for intoxication of mBMDM in response to AIP56 but suggest that TLR4 signaling may potentiate toxicity.

2. AIP56 endocytic uptake

2.1. AIP56 is rapidly endocytosed in vesicle-like structures

The observation that AIP56 cleaves NF-κB indicates that the toxin is able to reach the cytosol of target cells. To investigate the entry mechanisms used by the toxin we used fluorescence microscopy and biochemical approaches.

In order to perform the fluorescence microscopy studies we labeled AIP56 with fluorescein isothiocyanate (FITC) or Alexa Fluor 488. Alexa Fluor 488 dye is spectrally similar to fluorescein but more photostable (Panchuk-Voloshina et al, 1999). Furthermore, unlike fluorescein, the fluorescence of the Alexa Fluor 488 dye is insensitive to pH changes (in the range between pH 4 and 10) (Panchuk-Voloshina et al, 1999). The use of

a pH insensitive fluorescent dye is particularly relevant in cellular trafficking experiments, since different intracellular compartments have different pH. Although fluorescent labeled AIP56 was not as active as unlabeled toxin, it retained the ability to cleave NF-κB p65 and to induce apoptosis upon addition to cells (Figure 4.5A and B) and, therefore, was used to study AIP56 intracellular trafficking. Since similar results were obtained using FITC- or Alexa Fluor 488-labeled AIP56 (Figure 4.5C) both proteins were used to perform different experiments.

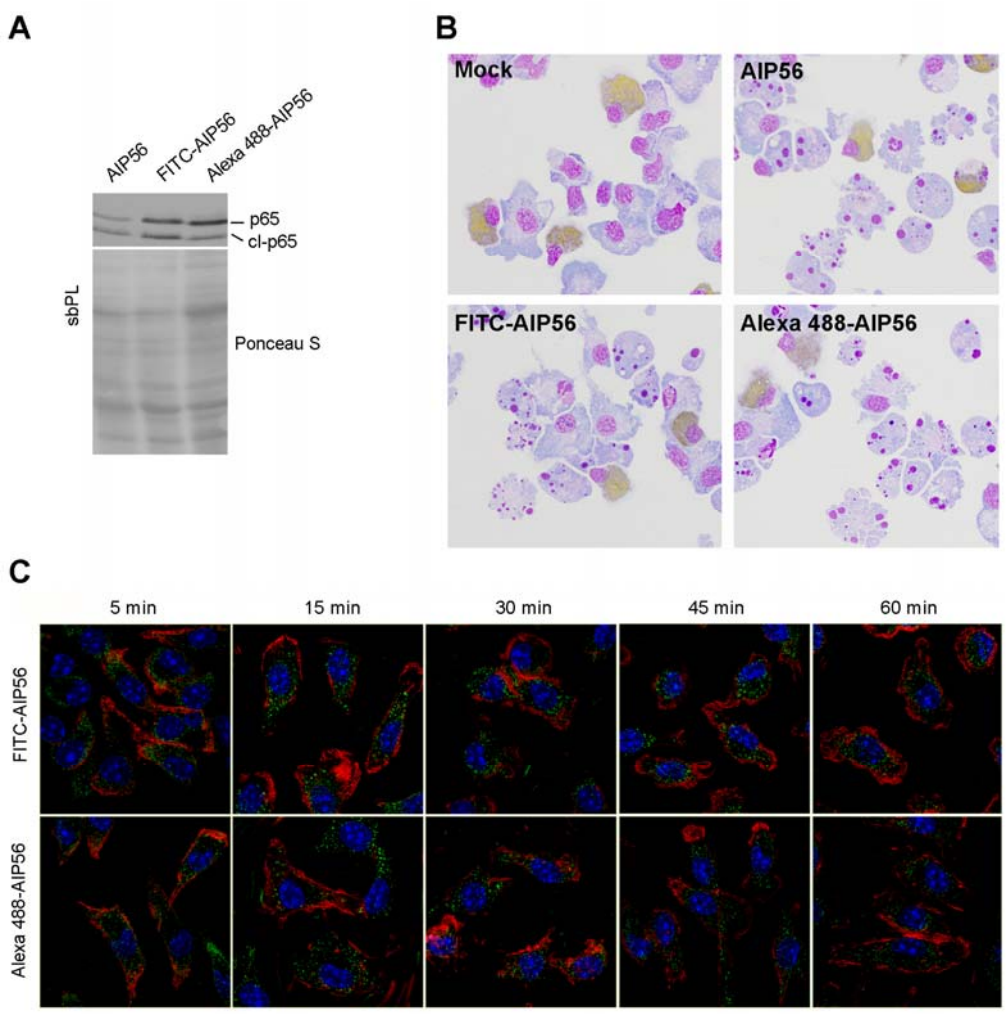

Figure 4.5. Fluorescent labeled AIP56 retained toxicity. (A) sbPL were incubated with 10 μg ml^{-1} of the indicated proteins for 30 min on ice, washed to remove unbound toxin and chased for 2 h at 22ºC. Cleavage of NF-κB p65 was analyzed by western blotting (chromogenic detection). **(B)** sbPL were incubated with 10 μg ml^{-1} AIP56, FITC-AIP56 or Alexa 488-AIP56, for 4 h at 22ºC. Mock-treated cells were used as control. Images shown are representative cytospin preparations stained with Antonow´s (Afonso et al, 1998; do Vale et al, 2002) for labelling neutrophils (brown) followed by hemacolor. Note the presence of several apoptotic cells in samples incubated with AIP56, FITC-AIP56 or Alexa 488-AIP56 and their absence in mock-treated cells. **(C)** Confocal microscopy of mBMDM incubated with FITC-AIP56 or Alexa 488-AIP56 resulted in similar observations. Representative confocal images of mBMDM pulsed with FITC-AIP56 or Alexa 488-AIP56 (green) for 30 min on ice, washed and chased at 37ºC. At the indicated times, cells were fixed, actin was labeled with Alexa Fluor 594-Phalloidin (red) and nuclei were counterstained with DAPI (blue). A merge of the different channels is shown.

To analyze AIP56 internalization, fluorescent labeled toxin was incubated with cells for 30 min on ice, unbound toxin was washed out and cells were then transferred and incubated for different time intervals at 22ºC or 37ºC for sbPL or mBMDM, respectively. Incubation of fluorescent labeled AIP56 with sbPL or mBMDM resulted in similar observations (Figure 4.6A). After 5 min incubation with sbPL or mBMDM, AIP56 was observed in vesicle-like structures (Figure 4.6A), suggesting that binding of the toxin to the

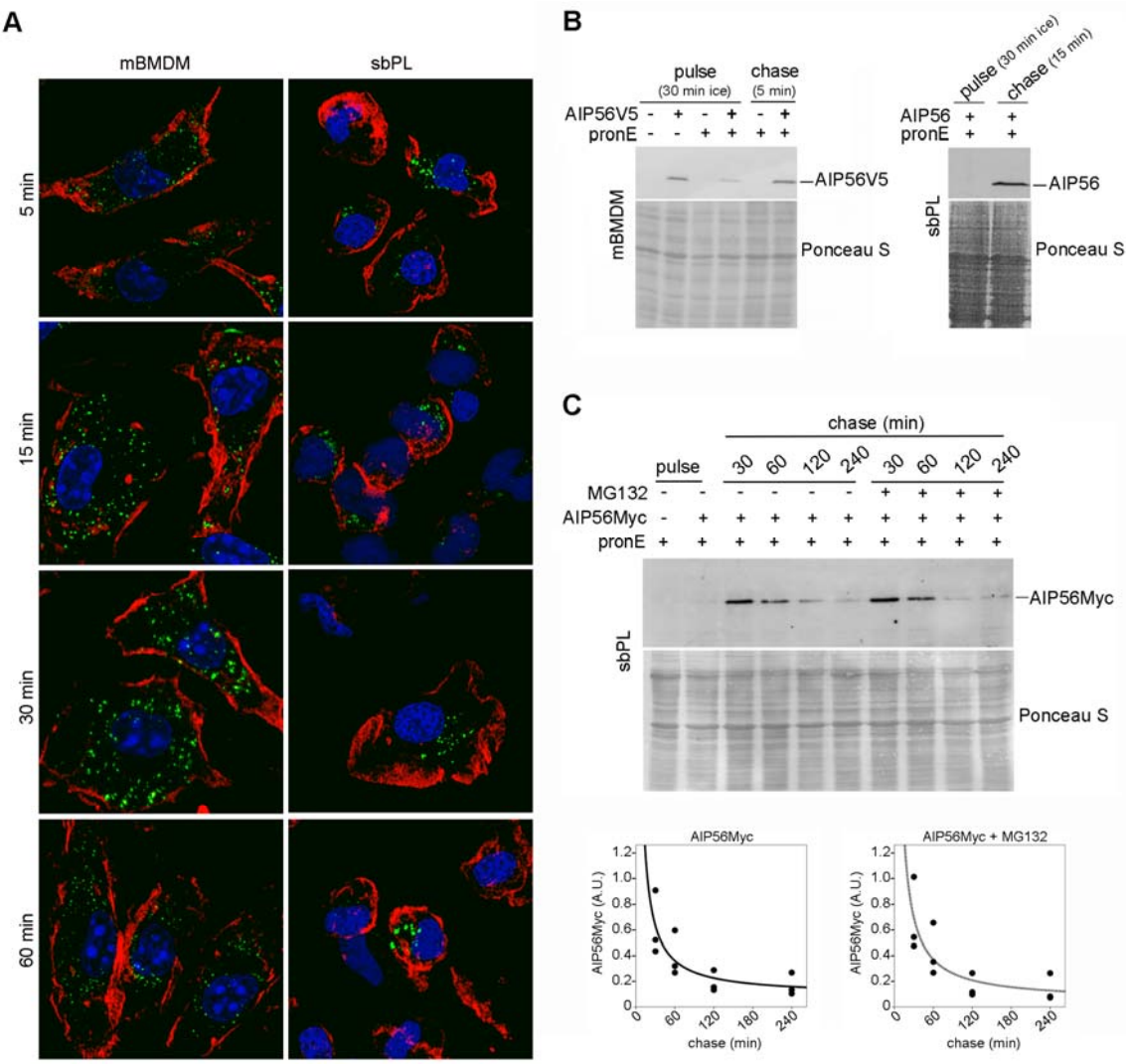

Figure 4.6. AIP56 is rapidly endocytosed into vesicle-like structures (A) Representative confocal images of mBMDM and sbPL pulsed with 10 µg ml^{-1} Alexa 488-AIP56 (green) for 30 min on ice, washed and chased at the appropriate temperature for the indicated time-points. After fixation, F-actin was stained with Alexa 594-Phalloidin (red) and nuclei with DAPI (blue). A merge of the different channels is shown. Images shown are derived from one out of three independent experiments. **(B)** Shortly after incubation with mBMDM or sbPL, AIP56 localizes in a protease protected compartment. mBMDM or sbPL were pulsed with 5 µg ml^{-1} AIP56V5 or 10 µg ml^{-1} AIP56, respectively, washed to remove unbound toxin and shifted to 37ºC (mBMDM) or 22ºC (sbPL). At the indicated time-points, to remove extracellular toxin, cells were treated with pronase E (pronE) and the intracellular pool detected by western blotting (mBMDM: anti-V5 antibody, chromogenic detection; sbPL: anti-AIP56 rabbit serum, ECL detection). The blots shown are representative of three independent experiments. **(C)** Intracellular AIP56 decreases at longer chasing times in a proteosomal-independent way. sbPL were

incubated with 20 μM of the proteosomal inhibitor MG132 for 1 h before incubation with 10 μg ml^{-1} AIP56Myc as described in (B). Intracellular AIP56 was detected by western blotting using an anti-c-Myc antibody (ECL detection). The activity of MG132 was confirmed by looking at its inhibitory effect upon the degradation of the AIP56-generated NF-κB p65 cleavage fragment (These experiments were done in parallel with those shown in Figure 4.3). The graphs show quantification of the blots (three independent experiments). Loading correction was achieved by dividing the density of AIP56Myc band by the respective density of Ponceau S. The inverse regression models represent AIP56Myc as a function of time (AIP56Myc R^2=0.635 and AIP56Myc+MG132 R^2=0.643).

cell surface was followed by endocytosis. Over time, the AIP56-positive vesicles increased in size and were found to concentrate in a more perinuclear area, and from 30 minutes onwards the AIP56-associated fluorescence gradually decreased (Figure 4.6A). Western blotting analysis confirmed the internalization of the toxin (Figure 4.6B). This analysis showed that in mBMDM, after a 30 min pulse on ice followed by a 5 min incubation at 37ºC, a significant proportion of the toxin had been internalized (Figure 4.6B). Similar results were obtained in sbPL (Figure 4.6B), but in this case, the shorter time that we were able to analyze was 15 min, because in these cells endocytosis cannot be blocked by cooling as in mammalian cells (not shown) and they needed to be centrifuged for washing. A kinetic analysis of the entry in sbPL revealed a marked decrease of intracellular toxin after 60 min incubation (Figure 4.6C), not prevented by the proteosomal inhibitor MG132 (Figure 4.6C), suggesting that did not result from proteosomal degradation of the toxin.

2.2. AIP56 intoxication in mBMDM involves interaction of the C-terminal region of the toxin with cell surface components

Previous studies with sbPL showed that the entry of the toxin involves specific interaction of its C-terminal region with cell surface components (Silva et al, 2013). To investigate if the C-terminal region of AIP56 is also playing a role in the entry of the toxin in mBMDM, we performed a competition assay testing the ability of the C-terminal truncate $AIP56^{286\text{-}497C298S}$ (corresponding to the toxin's B domain) (Silva et al, 2013) to inhibit the arrival of the toxin into the cytosol. The N-terminal truncate $AIP56^{1\text{-}285C262S}$ corresponding to the toxin's A domain (Silva et al, 2013) was used as a control. The competitors were allowed to incubate with cells for 15 min on ice to block the receptors at cell surface before the addition of AIP56. The cleavage of p65 was assessed after 2 h incubation and was used as a read-out for the presence of the toxin in the cytosolic compartment. Pre-incubation of the cells with the C-terminal truncate inhibited p65 cleavage whereas no inhibition was observed when the N-terminal truncate was used as a competitor (Figure 4.7A), indicating that in mBMDM the C-terminal domain of AIP56 was

able to block the internalization of the full-length toxin. This suggests that, similarly to what has been reported for sbPL, the entry of AIP56 in mBMDM involves interaction of its C-terminal domain with cell surface receptors.

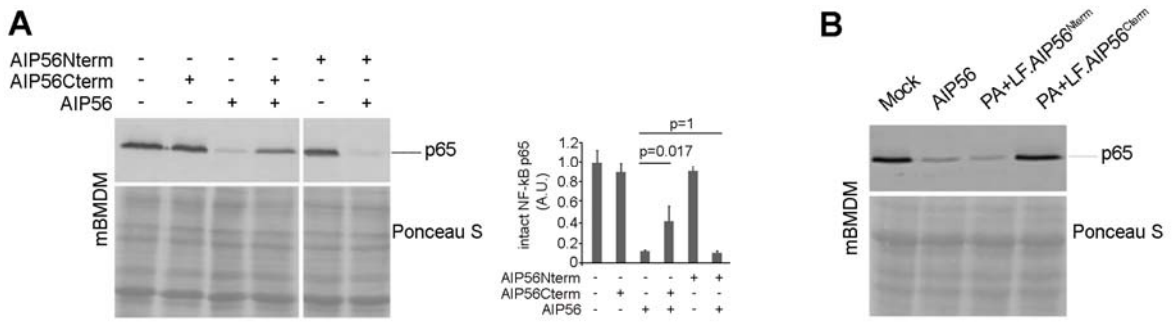

Figure 4.7. AIP56 C-terminal domain is involved in binding/entry into mBMDM and the N-terminal domain plays the catalytic role. (A) Intoxication of mBMDM by AIP56 is inhibited by the toxin's B domain AIP56$^{286\text{-}497C298S}$. Cells were incubated with 7 μM of AIP56$^{1\text{-}285C262S}$ (AIP56Nterm) or AIP56$^{286\text{-}497C298S}$ (AIP56Cterm) for 15 min on ice, followed by further 15 min incubation with an 800-fold lower concentration of recombinant AIP56 in the presence of the competitor. Cells were washed and incubated at 37ºC for 2 h. Cleavage of NF-κB p65 was assessed by western blotting (chromogenic detection). The bar graph shows the quantification of the blots and combines the results of three independent experiments (mean ± SD). Loading correction was achieved by dividing the density of p65 by the respective density of Ponceau S. The results were divided by the same constant in order to set to 1 the mean of the control (mock-treated cells). The significance of differences was tested by one-way ANOVA. p-values for individual comparisons were calculated using Tukey's HSD multiple comparisons test and are indicated in the graph. **(B)** Delivery of AIP56 N-terminal domain into the cell's cytosol reproduces the activity of the full length toxin. mBMDM were incubated for 2 h at 37ºC with 20 nM of LF$^{11\text{-}263}$·AIP56$^{1\text{-}261}$ (LF·AIP56^{Nterm}) or LF$^{11\text{-}263}$·AIP56$^{299\text{-}497}$ (LF·AIP56^{Cterm}) in the presence of 10 nM of PA and cleavage of NF-κB p65 detected by western blotting (chromogenic detection). Mock treated cells and cells incubated with 0.5 μg ml^{-1} (8.75 nM) of AIP56 were used as control. The blot shown is representative of three independent experiments.

For finding out whether in mBMDM the N-terminal domain does not need the C-terminal domain to exert its catalytic effect, a strategy to deliver the AIP56 N-terminal portion into the cell cytosol was delineated based on the *Bacillus anthracis* protective antigen (PA)/lethal factor (LF) delivering system, as already performed with great success in sbPL (Silva et al, 2013) and in the delivering of the catalytic domain of different toxins like diphtheria toxin, shiga toxin and Pseudomonas exotoxin into the cytosol (Arora & Leppla, 1993; Arora & Leppla, 1994; Milne et al, 1995). Because the first 263 N-terminal residues of LF were found to be sufficient for recognition and binding to the protective antigen (PA), the receptor binding subunit of LF (Collier, 2009), and able to cause cellular uptake of fused polypeptides (Arora & Leppla, 1993), chimeric proteins consisting of LF N-terminal region (LF$^{11\text{-}263}$) fused to AIP56's N-terminal (LF$^{11\text{-}263}$·AIP56$^{1\text{-}261}$) or C-terminal (LF$^{11\text{-}263}$·AIP56$^{299\text{-}497}$) domain were produced. LF$^{11\text{-}263}$·AIP56$^{299\text{-}497}$ was used as control. ·mBMDM were intoxicated with 20 nM of the chimeric proteins in the presence of 10 nM

PA. By western blotting analysis a significant decrease in p65 levels was observed in cells incubated with LF^{11-263}.$AIP56^{1-261}$, reproducing the effect of AIP56 holotoxin, while no differences in p65 levels was observed in cells incubated with LF^{11-263}.$AIP56^{299-497}$ (Figure 4.7B). This confirms that, like occurs in sbPL, in mBMDM AIP56 N-terminal domain plays the catalytic role and the C-terminal domain is involved in binding/entry into mBMDM.

2.3. AIP56 endocytosis and toxicity require dynamin and clathrin

To enter host cells, bacterial toxins are known to use clathrin-dependent and/or clathrin-independent endocytic mechanisms. Dynamin is a GTPase involved in endocytic membrane fission that is known to be involved in clathrin-dependent endocytosis, although it may also participate in clathrin-independent endocytosis pathways (Ferguson & De Camilli, 2012). To investigate if AIP56 endocytosis is dependent on clathrin and/or dynamin, we inhibited their functions using the specific cell-permeable inhibitors chlorpromazine (Wang et al, 1993) and dynasore (Kirchhausen et al, 2008), respectively.

In vitro tests, using *in vitro* translated ^{35}S-labeled sbp65Rel as substrate, confirmed that chlorpromazine and dynasore did not affect AIP56 metalloprotease activity (Figure 4.8A). Phagocytosis assays confirmed that they were acting specifically (Figure 4.8B). Phagocytic uptake was not affected by dynasore or chlorpromazine, confirming that these inhibitors are not having a broad inhibitory effect upon all endocytic pathways. In contrast, phagocytosis was strongly inhibited by cytochalasin D, confirming disruption of actin function by the inhibitor.

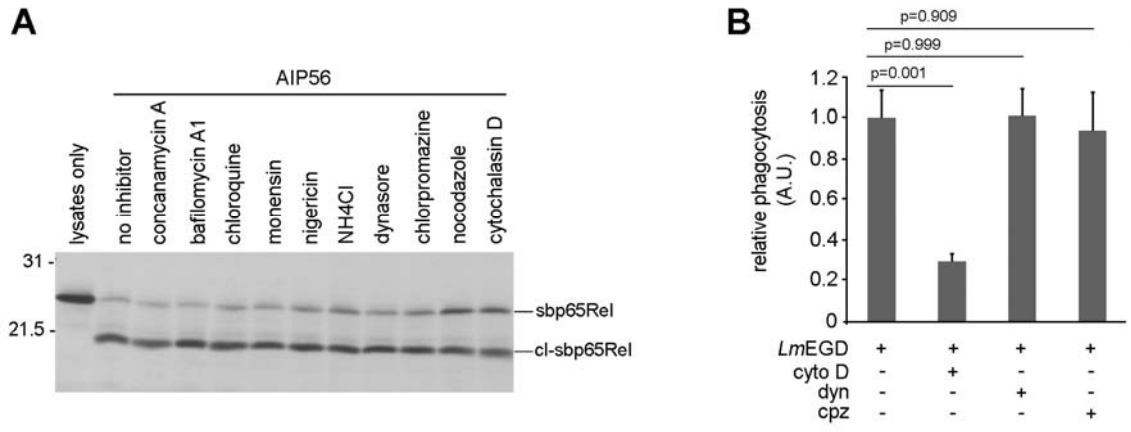

Figure 4.8. AIP56 metalloprotease activity is not abolished by inhibitors of the intracellular trafficking and endocytic pathway. (A) The inhibitors of intracellular trafficking and endocytosis used in this work do not inhibit AIP56 activity *in vitro. In vitro* translated ^{35}S-labeled sbp65Rel was incubated for 2 h at 22ºC with 100 nM (5.7 µg ml^{-1}) AIP56 in the presence of the inhibitors at the concentration used for the *ex vivo* assays (see table 5 in Chapter III) in a final volume of 20 µl. ^{35}S-labeled sbp65Rel incubated with AIP56 in the absence of the inhibitors was used as control. The reaction was stopped by adding SDS-PAGE sample buffer and p65 cleavage assessed by autoradiography. The result shown is representative of two independent experiments. **(B)** Phagocytic uptake was strongly inhibited by cytochalasin D but was not

affected by dynasore or chlorpromazine. mBMDM were incubated with cytochalasin D (cyto D), dynasore (dyn) or chlorpromazine (cpz) for 1 h at 37ºC or left untreated prior to phagocytosis assay. *Listeria monocytogenes* EGD (*Lm*EGD) was added to the cells and incubated for 30 min at 37ºC. Extracellular bacteria were killed with gentamicin for 1 h at 37ºC, cells were washed, lysed and serial dilutions plated in BHI agar. Colony forming units (CFU) were determined after 24 h incubation and normalized to CFU in cells treated with bacteria in the absence of the inhibitors. Assays were performed in triplicate. The obtained values were divided by the same constant in order to set to 1 the mean of the control (*Lm*EGD with no inhibitor) and are presented as means ± SD of four independent experiments. The significance of differences was tested by one-way ANOVA. p-values for the comparisons to *Lm*EGD with no inhibitor were calculated using Tukey's HSD multiple comparisons test and are indicated in the graph.

To test the effect of chlorpromazine and dynasore in AIP56 endocytosis, we treated mBMDM with the inhibitors or left the cells untreated before pulsing with recombinant toxin for 30 min on ice. Cells were washed, transferred to 37ºC and after 2 min chase, extracellular toxin was removed with pronase E. As shown in Figure 4.9A, endocytosed AIP56 was detected in control cells but not in cells pre-treated with chlorpromazine and dynasore. The inhibitory effect of the inhibitors upon AIP56 endocytosis together with the observation that the AIP56-dependent cleavage of p65 was strongly inhibited by pre-treatment with chlorpromazine and was prevented by pre-treatment with dynasore (Figure 4.9B) suggests that a significant pool of AIP56 is endocytosed through a clathrin- and dynamin-dependent pathway.

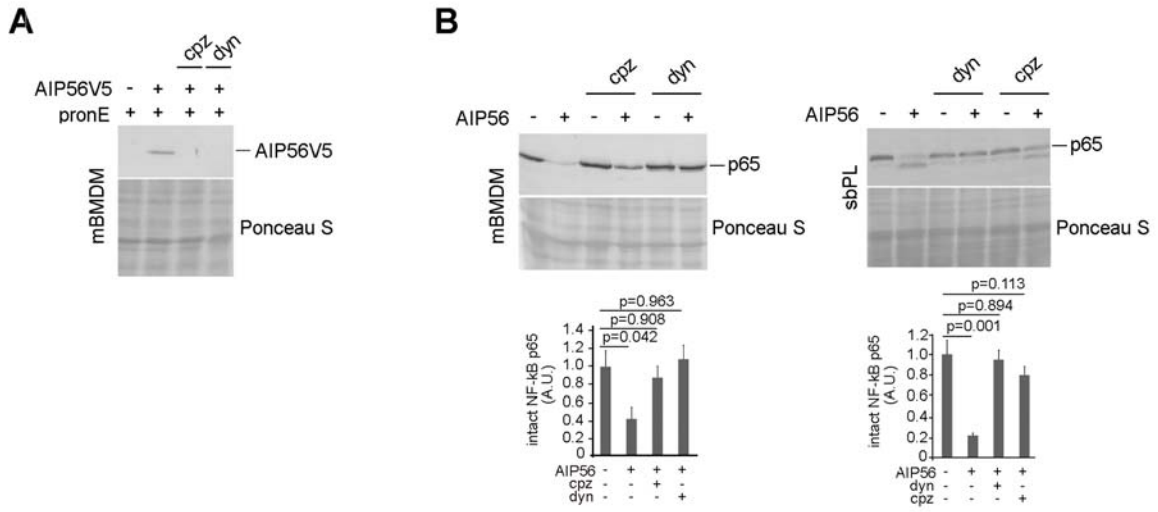

Figure 4.9. AIP56 endocytosis and toxicity require clathrin and dynamin. (A) AIP56 endocytosis is prevented by chlorpromazine and dynasore. mBMDM were pre-treated with chlorpromazine (cpz) or dynasore (dyn), pulsed with AIP56V5 in the presence of the inhibitors for 30 min on ice, washed and incubated at 37ºC in culture medium with the inhibitor. After 2 min, surface-exposed toxin was removed with pronase E (pronE) and the intracellular pool was detected by western blotting (chromogenic detection). The result shown is representative of three independent experiments. **(B)** AIP56-mediated cleavage of NF-κB p65 is inhibited by chlorpromazine and dynasore. mBMDM or sbPL were treated with chlorpromazine or dynasore, pulsed with AIP56 for 30 min on ice, washed and shifted to 37ºC (mBMDM) or 22ºC (sbPL) for 2 h, while maintaining the inhibitory conditions. Cleavage of NF-κB p65 was assessed by western blotting (chromogenic detection).

The graphs show the quantification of the blots. Loading correction was achieved by dividing the density of p65 by the respective density of Ponceau S. The results used for each graph were divided by the same constant in order to set to 1 the mean of the control (mock-treated cells). Each graph combines the results of three independent experiments (mean ± SD). The significance of differences was tested by one-way ANOVA. p-values for individual comparisons were calculated using Tukey's HSD multiple comparisons test and are indicated in the graphs.

2.4. Microtubules and actin dynamics are dispensable for intoxication by AIP56

Functional actin dynamics are required for several endocytic processes, from clathrin-dependent to clathrin-independent endocytosis (Doherty & McMahon, 2009). To determine if internalization of AIP56 depends on actin, we disrupted actin filaments with cytochalasin D and assessed whether the disruption inhibited endocytosis of the toxin and arrival of the toxin into the cytosol (assessed using AIP56-mediated p65 cleavage as a read-out). The efficacy of cytochalasin D treatment was confirmed by phagocytosis assays (Figure 4.8B) and by staining actin filaments with the F-actin probe Alexa Fluor-594 Phalloidin (Figure 4.10A). Treatment with cytochalasin D did not inhibit AIP56 endocytosis (Figure 4.10B) and did not significantly affect AIP56-dependent p65 cleavage (Figure 4.10C), indicating that AIP56 intoxication does not require functional actin dynamics.

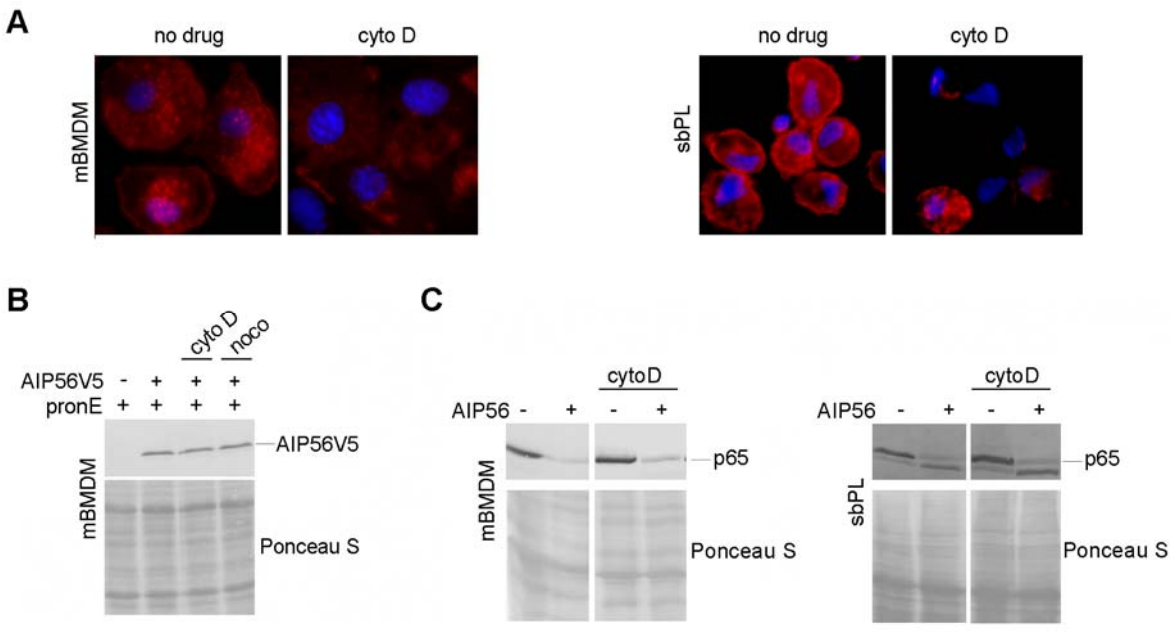

Figure 4.10. AIP56 intoxication is independent on actin filaments and microtubules. **(A)** Effect of cytochalasin D treatment on actin filaments. Cells were pre-treated with cytochalasin D (cyto D) and then processed for fluorescence microscopy to detect actin filaments using the F-actin probe Alexa Fluor-594 Phalloidin (red). Nuclei were counterstained with DAPI (blue). A merge of the different channels is shown. Images shown are derived from one out of three experiments. **(B)** AIP56 endocytosis is not inhibited by cytochalasin D or nocodazole. mBMDM were treated with cytochalasin D or

nocodazole (noco) before incubation with 5 μg ml^{-1} AIP56 in the presence of the inhibitors for 30 min on ice, washed and incubated at 37ºC in culture medium containing the inhibitors. After 5 min, surface-exposed cell-associated toxin was removed with pronase E (pronE) and the intracellular pool was detected by western blotting using an anti-V5 antibody (chromogenic detection). **(C)** The arrival of AIP56 into the cytosol is not prevented by cytochalasin D. sbPL or mBMDM were treated with cytochalasin D at the appropriate temperature prior to incubation with AIP56 for 30 min on ice in the presence of the inhibitor. Cells were washed and shifted to 22ºC (sbPL) or 37ºC (mBMDM) for 2 h while maintaining the inhibitory conditions. Cleavage of NF-κB p65 was assessed by western blotting (chromogenic detection). The blots shown are representative of three independent experiments.

The involvement of microtubules in AIP56 uptake was investigated using the microtubule depolymerizing agents nocodazole (Vasquez et al, 1997) and colcemid (Yang et al, 2010) and also the microtubule stabilizing agent taxol (Schiff et al, 1979). The effect of these compounds on microtubules was confirmed by immunofluorescence using an anti-α-tubulin antibody. As shown in Figure 4.11A, in cells treated with PBS microtubules radiate from the cell center to the cell periphery while in cells treated with nocodazole or colcemid a dramatic decrease in the number of microtubules per cell was noticed. In cells treated with taxol, an increase in tubulin polymerization was observed (Figure 4.11A). The effect of nocodazole was also confirmed by testing its effect in the delivery of the AIP56 catalytic domain using the PA+LF delivery system. It is known that cytoplasmic release of anthrax lethal factor (LF) occurs preferentially from late endosomes in a microtubule-dependent way and that depolymerization of microtubules with nocodazole delays LF toxicity (Abrami et al, 2004). It is also known that AIP56 catalytic domain can be delivered into the cytosol using the PA+LF system (Silva et al, 2013). Therefore, to confirm functional disruption of microtubules by nocodazole in mBMDM, we tested the effect of the inhibitor upon delivery of AIP56 catalytic domain by PA+LF. This was used as a control in AIP56-intoxication assays performed in the presence of nocodazole. As shown in Figure 4.11B, disruption of microtubules with nocodazole delayed the delivery of the AIP56 catalytic domain using the PA+LF delivery system (LF^{11-263}.$AIP56^{1-261}$) but did not affect AIP56-dependent p65 cleavage. Accordingly, when mBMDM or sbPL were pre-treated with colcemid or taxol, which also interfere with microtubules dynamics, no differences in AIP56-dependent p65 cleavage was observed when compared to cells only treated with the toxin (Figure 4.11C). These results, together with the fact that nocodazole does not inhibit AIP56 endocytosis (Figure 4.10B), strongly suggest that AIP56 exploits a microtubule-independent intoxication pathway.

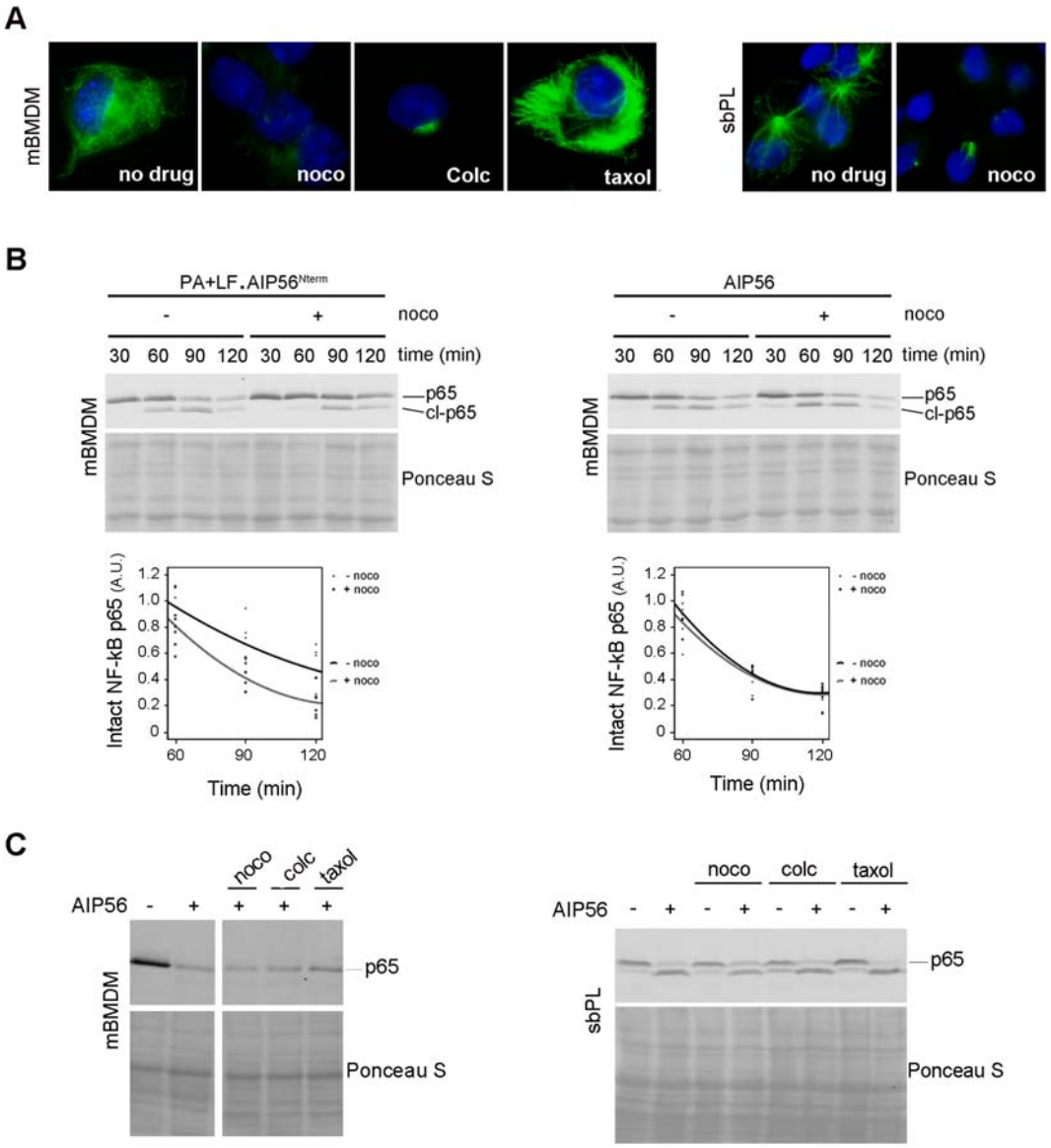

Figure 4.11. AIP56 intoxication is independent on microtubules. **(A)** Effect of nocodazole, colcemid and taxol on microtubules. Cells were treated with nocodazole (noco), colcemid (colc) or taxol and microtubules were visualized after staining with an anti-α-tubulin antibody (green). Untreated cells were used as control. Nuclei were counterstained with DAPI (blue). Images shown are derived from one out of three experiments. **(B)** Nocodazole does not affect AIP56 intoxication but delays the delivery of the AIP56 catalytic domain into the cytosol through the PA+LF delivery system. mBMDM were left untreated or treated with nocodazole before incubation with 5 μg ml^{-1} (89 nM) AIP56 or 10 nM PA + 20 nM LF^{11-263}·$AIP56^{1-261}$ (PA+LF·$AIP56^{Nterm}$) for 30 min on ice, washed and incubated in culture medium with or without the inhibitor. At the indicated time-points, cells were washed and processed for western blotting (chromogenic detection) for assessing NF-κB p65 cleavage. The experiment was repeated six times. Quadratic regression models were estimated of intact p65 as function of time. In the case of PA+LF·AIP56, R^2 for the two models (-noco and +noco) was, respectively, 0.786 and 0.638; for AIP56, R^2 for the two regression models (-noco and +noco) was, respectively, 0.863 and 0.874. **(C)** The arrival of AIP56 into the cytosol is not prevented by compounds that interfere with microtubules dynamics. sbPL or mBMDM were treated with nocodazole, colcemid or taxol at the appropriate temperature prior to incubation with AIP56 for 30 min on ice in the presence of the inhibitor. Cells were washed, shifted to 22ºC (sbPL) or 37ºC (mBMDM) and incubated for 2 h in culture medium while maintaining the inhibitory conditions. Cleavage of NF-κB p65 was assessed by western blotting (chromogenic detection). The blots shown are representative of three independent experiments.

3. AIP56 intracellular pathway

3.1. Upon endocytosis, AIP56 localizes in early endosomes and then is routed to the recycling endocytic compartment

To further characterize the intracellular trafficking of AIP56, cells were pulsed with Alexa 488-AIP56 for 30 min on ice, washed to remove unbound toxin and transferred to 37ºC. At different chase times, cells were processed for immunofluorescence to assess the co-localization of the toxin with established markers of intracellular compartments (Figure 4.12). Co-localization experiments are only reported for mBMDM, because most of the commercially available antibodies and probes are not validated or do not work on fish cells. After 2 min chase, Alexa 488-AIP56 was observed in peripheral endocytic vesicles negative for all the markers tested, but shortly after (5 min chase), part of the toxin-containing vesicles were positive for the early endosome marker EEA-1 (Figure 4.12). The co-localization with EEA-1 reached a maximum at 15/20 min and afterwards markedly decreased, being minimal at 60 min (Figure 4.12). These results indicate that after endocytosis, AIP56 localizes in early endosomes, where it remains for 20-30 min. In a more detailed analysis of cells immunostained for EEA-1 (Figure 4.12B), we can observe that AIP56 starts by appearing in the lumen of EEA1 positive vesicles to then, after 15 to 20 min, appear co-localizing with EEA1 in the cytosolic endosomal membrane, in vesicles “donuts-like”. To define the compartment where AIP56 was being delivered after leaving early endosomes, we looked for co-localization of the toxin with the late endosome/lysosome marker LAMP-1, the Golgi apparatus marker GM130 or the endoplasmic reticulum marker GRP78 Bip. Alexa 647-Transferrin was used as a marker of the recycling route (Figure 4.12 A). It is of note that, in macrophages (Casbon et al, 2009; Cox et al, 2000; Halaas et al, 2010; Marcil et al, 2008; Stanley et al, 2014; Wainszelbaum et al, 2006) similarly to what occurs in other cells (Maxfield & McGraw, 2004), transferrin is recycled back to the cell surface using two kinetically distinguishable mechanisms of recycling: fast and slow recycling. This supports the use of transferrin as a marker for the recycling pathway in macrophages and, in particular, in mBMDM. Co-localization of Alexa 488-AIP56 with Alexa 647-Transferrin was evident at 5 min and was maintained during the remaining chase (Figure 4.12), suggesting that after leaving early endosomes, the toxin was delivered to the recycling endocytic compartment. In agreement with this hypothesis, Alexa 488-AIP56 was never observed to co-localize with LAMP-1 (Figure 4.12A) or markers of Golgi apparatus and endoplasmic reticulum (Fig. 4.12A).

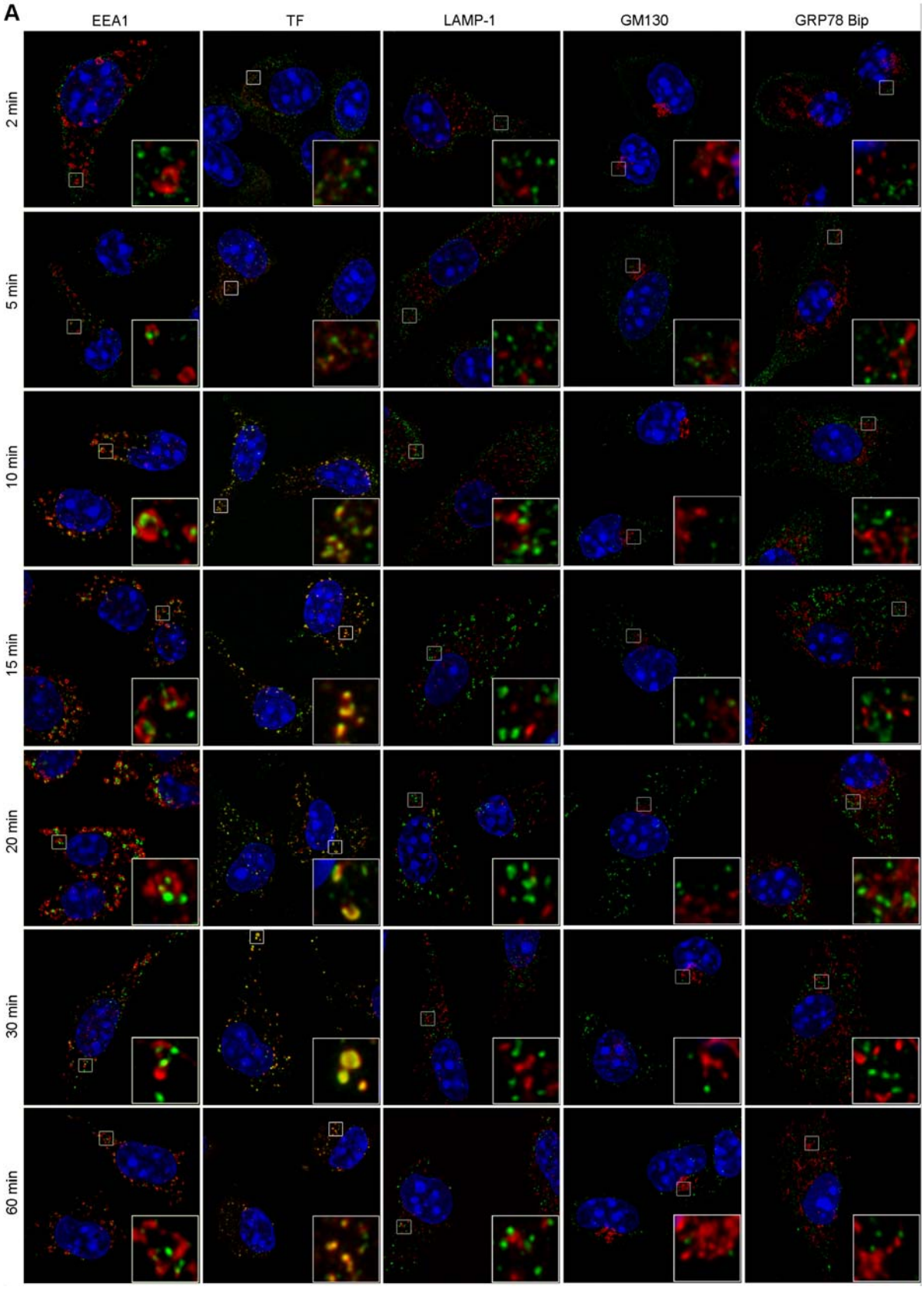
A
EEA1
TF
LAMP-1
GM130
GRP78 Bip
2 min
5 min
10 min
15 min
20 min
30 min
60 min

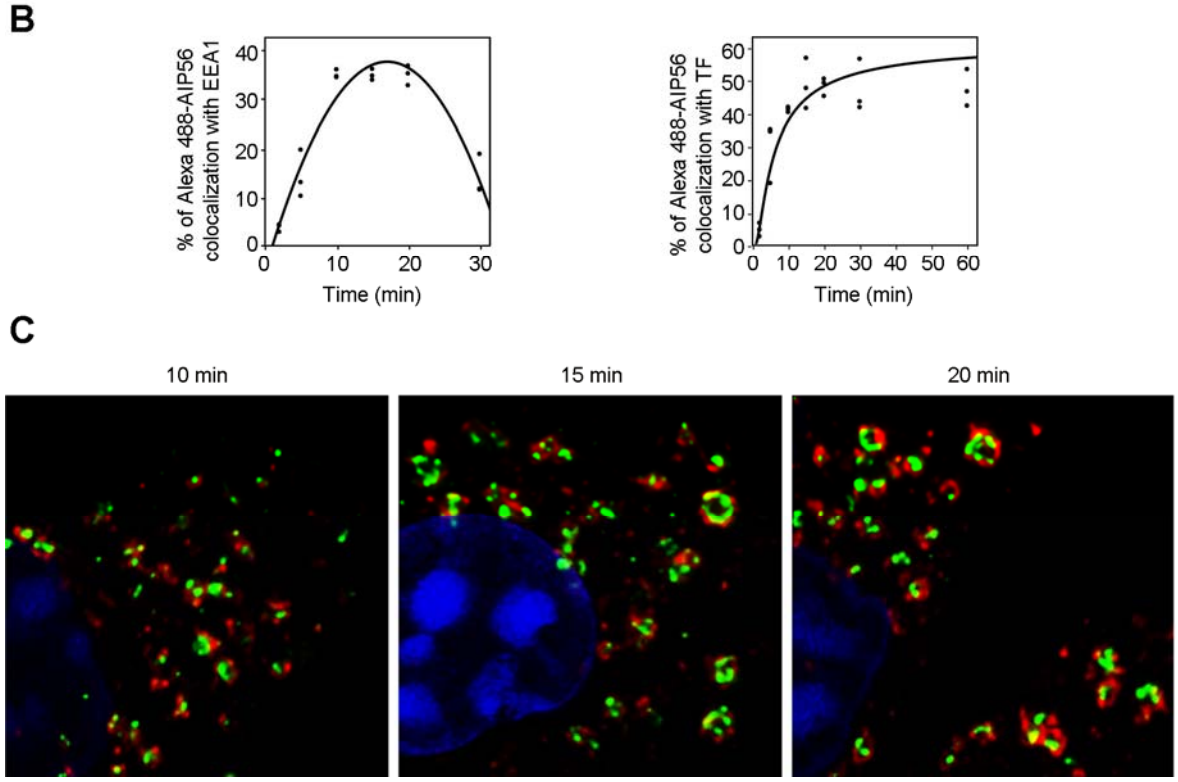

Figure 4.12. Shortly after endocytosis AIP56 localizes in early endosomes and then is routed to the recycling compartment. (A) Representative confocal images of mBMDM pulsed with Alexa 488-AIP56 (green) for 30 min on ice, washed and chased at 37ºC. At the times shown, the cells were fixed and processed for immunofluorescence. Early endosomes were stained with an anti-EEA1 antibody, LE/lysosomes were labelled with anti-LAMP-1, Golgi apparatus with anti-GM130, the endoplasmic reticulum with anti-GRP78 Bip and the entire recycling pathway with a continuous incubation with Alexa 647-Transferrin (TF). Nuclei (blue) were counterstained with DAPI. A merge of the different channels is shown. Insets are magnified views of boxed areas. **(B)** Quantification of Alexa 488-AIP56 colocalization with EEA1 and TF. For each marker, the percentage of colocalization was determined for several cells ($n \geq 15$) obtained from at least three independent experiments. Each point in the plot corresponds to the average of an independent experiment. Linear regression models were developed for each of the marker. In the case of TF the model represents TF concentration as a function of the logarithm of time (R^2=0.71) whereas for EEA1 represents the logarithm of EEA1 as a function of the logarithm of time (R^2=0.91). For the remaining components the observed colocalization and its variation with time was negligible so that the best linear model was an almost horizontal line (not shown). **(C)** Details of confocal images from cells immunostained for EEA-1. mBMDM were treated with FITC-AIP56 (green) as described in (A) and immunostained for EEA1 (red). Nuclei (blue) were counterstained with DAPI. A merge of the different channels is shown.

3.2. Shortly after endocytosis a pool of AIP56 is recycled back to the extracellular medium through a mechanism requiring PI3K activity but independent on endosome acidification.

The observation that AIP56 was delivered to the recycling endocytic compartment following endocytosis, suggested that the toxin was being recycled back to the extracellular medium. To investigate this hypothesis, we allowed mBMDM to bind AIP56

and internalize it for 5 min (pulse), removed the extracellular and surface-exposed cell-associated toxin with pronase E, chased the cells at 37ºC and analyzed the presence of the toxin inside cells and in the extracellular medium at different chasing times. The absence of AIP56 in the last wash after pronase E treatment (Figure 4.13A, lane 5) confirmed that the extracellular AIP56 was effectively removed before chasing. After 2 min chase, AIP56 was detected in the extracellular medium (Figure 4.13A, lane 7). The amount of extracellular AIP56 increased along the kinetic (Figure 4.13A, lanes 7-10) and was paralleled by a decrease in the amount of cell-associated toxin (Figure 4.13A, lanes 12-15), indicating that during chase, intracellular AIP56 was being recycled to the extracellular medium. The cytosolic enzyme GAPDH was only detected in cell lysates (Figure 4.13), confirming that the AIP56 detected in the supernatant did not result from cell lysis and consequent leakage of intracellular proteins.

Since phosphoinositide 3-kinase (PI3K), an evolutionarily conserved enzyme complex which phosphorylates phosphatidylinositol lipid substrates into 3-phosphoinositides (Foster et al, 2003; Vanhaesebroeck et al, 2010), has been shown to play a key role in regulating the recycling pathway (Carpentier et al, 2013; Hunyady et al, 2002; Lindmo & Stenmark, 2006; Naughtin et al, 2010; Raiborg et al, 2013) we analyzed the involvement of PI3K in AIP56 recycling. For this, we performed recycling assays in the presence of LY294002, a reversible pan-inhibitor of PI3K activity (Knight et al, 2004; Vlahos et al, 1994). The effect of LY294002 upon PI3K activity was controlled by confirming LY294002-induced inhibition of the phosphorylation of Akt, a downstream target of PI3K (Laird et al, 2009) (Figure 4.14A). As shown in Figure 4.13B, in the presence of LY294002 recycling of AIP56 was strongly inhibited (compare lanes 6 and 7 with lanes 10 and 11, respectively) and an increase in cell-associated toxin was observed (compare lanes 12 and 13 with lanes 14 and 15, respectively), suggesting that recycling of AIP56 is dependent on PI3K activity. Because PI3K is involved in a wide range of cellular processes (Foster et al, 2003) including regulation of the endocytic pathway we also analyzed the effect of this inhibitor in AIP56 toxicity. As shown in Figure 4.13B, no differences in AIP56-dependent p65 cleavage was observed in cells treated with LY294002 when compared to those incubated with the toxin in the absence of the inhibitor, indicating that the AIP56 intoxication pathway is independent of PI3K activity.

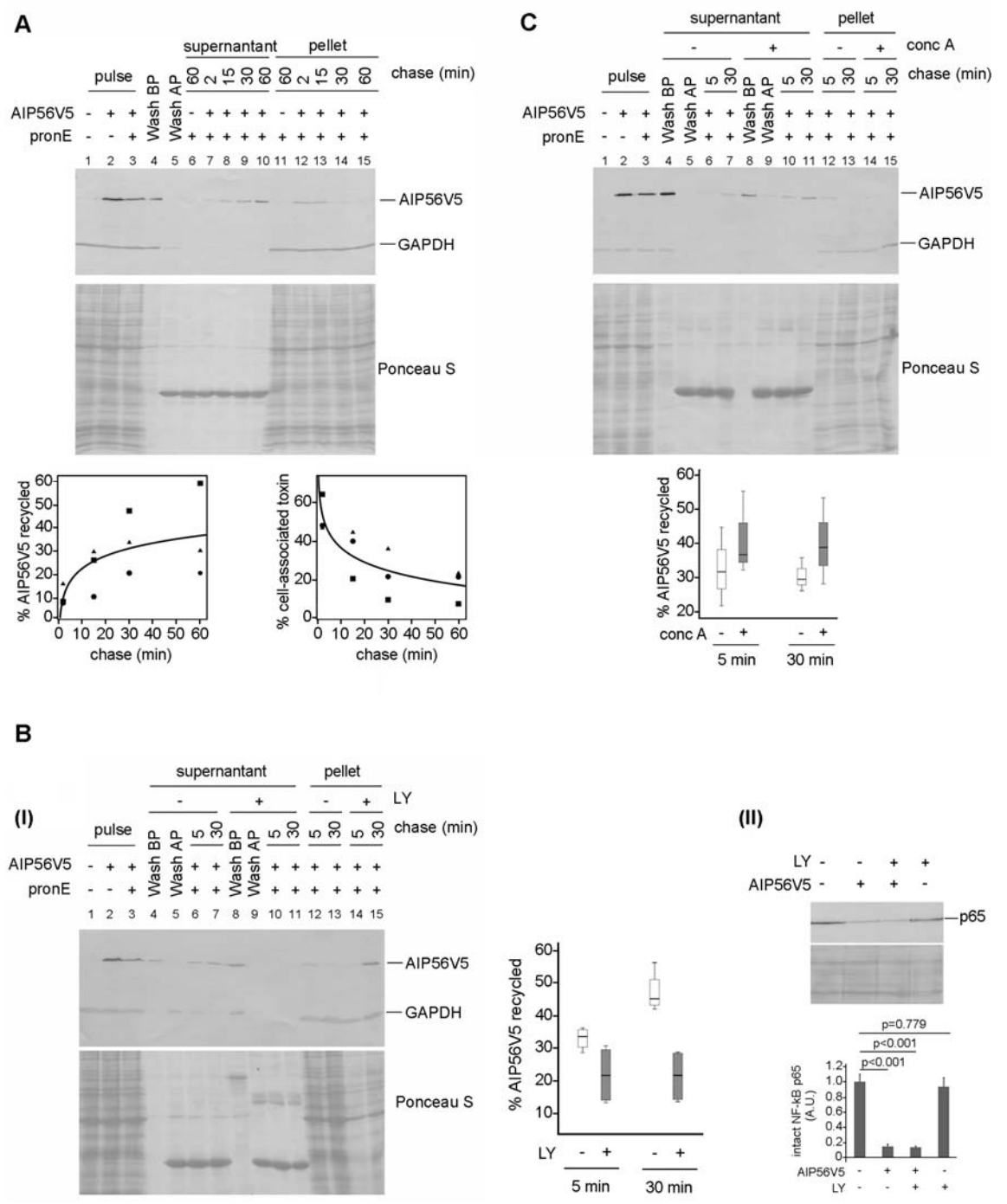

Figure 4.13. After endocytosis AIP56 is recycled back to the extracellular medium by a mechanism requiring PI3K activity but independent on endosomal acidification. (A) mBMDM were left untreated or incubated with 10 μg ml^{-1} AIP56V5 on ice for 30 min followed by 5 min incubation at 37ºC (pulse). Cells were washed, extracellular toxin was removed with pronase E (pronE), and cells were washed again and chased at 37ºC for different time intervals. Cell-associated (pellet) and recycled (supernatant) AIP56V5 was detected by western blotting (anti-V5 antibody; chromogenic detection). To control the efficacy of pronase E treatment, we analyzed the presence of the toxin in the last wash before pronase E treatment (wash BP) and in the last wash after pronase E treatment (wash AP). Samples (washes, supernatants and pellets) from 12 wells were pooled and the equivalents to 12 wells for washes/supernatants or 4 wells for pellets were loaded in the gels. GAPDH was used as a cytosolic marker. The graphs show the quantification of the recycled or cell associated AIP56V5 relative to the total internalized protein (lane 3) and combines results from three independent experiments (represented by

different symbols). The logarithmic regression model represents the percentage of recycled or cell associated AIP56V5 as a function of time (recycled R^2=0.451, cell-associated R^2=0.679). **(B)** LY294002 inhibits the recycling of AIP56 into the extracellular medium but not it´s toxicity. (I) mBMDM were left untreated or treated with LY294002 (LY) before performing the recycling or toxicity assays in the presence of the inhibitor. The recycling protocol was the same as described in (A). The graph shows the quantification of the blots and combines results from four independent experiments (the middle line in each box corresponds to the median and the lower and upper side of the boxes to the first and third quartiles; whiskers represent the smallest and largest observed values). Values correspond to percentage of recycled AIP56V5 relative to the total internalized protein (lane 3). Statistical analysis involved performing two-way ANOVA (main effect of inhibitor $p<0.001$, main effect of time $p=0.073$, inhibitor and time interaction $p=0.059$). (II) Toxicity (cleavage of NF-kB) was assessed and quantified as described in Figure 4.9B. The significance of differences was tested by one-way ANOVA (three independent experiments; mean ± SD). p-values for individual comparisons were calculated using Tukey's HSD multiple comparisons test and are indicated in the graph. **(C)** Recycling of AIP56 into the extracellular medium is not inhibited by concanamycin A. mBMDM were treated with concanamycin A (conc A) or left untreated before performing the recycling assay as described in A, but in the presence of concanamycin A. The graph shows the quantification of the blots and combines results from three independent experiments (the middle line in each box corresponds to the median and the lower and upper side of the boxes to the first and third quartiles; whiskers represent the smallest and largest observed values). Values correspond to percentage of recycled AIP56V5 relative to the total internalized protein (lane 3). Statistical analysis involved performing two-way ANOVA (main effect of inhibitor $p=0.180$, main effect of time $p=0.784$, inhibitor and time interaction $p=0.942$).

We also investigated if recycling of AIP56 was dependent on endosome acidification because it is reported that the exposure of ligand-receptor complexes internalized by receptor-mediated endocytosis to low endosomal pH is required for the efficient sorting of several cargos and recycling of receptors (Hunyady et al, 2002; Jovic et al, 2010). The recycling experiment was repeated in the presence of concanamycin A, an inhibitor of the endosomal vacuolar ATPase pump responsible for endosome acidification (Huss & Wieczorek, 2009). The efficacy of concanamycin A in inhibiting the vacuolar ATPase pump was confirmed using the fluorophore acridine orange. Acridine orange is a weak base that becomes protonated and accumulates in acidic endosomes exhibiting a concentration-dependent shift from green (low concentration) to red (high concentration) fluorescence (Zelenin, 1993). Cells were visualized by fluorescence microscopy and as shown in Figure 4.14B in the absence of concanamycin A, acidic vesicles appeared orange because acridine orange was trapped within the endosomes and its concentration increased, while in the presence of the inhibitor no red/orange staining was detected, confirming the inhibitory effect of concanamycin A. As shown in Figure 4.13C, recycling of AIP56V5 was not inhibited by concanamycin A (compare lanes 6 and 7 with lanes 10 and 11, respectively), suggesting that it does not require low endosomal pH for efficient sorting.

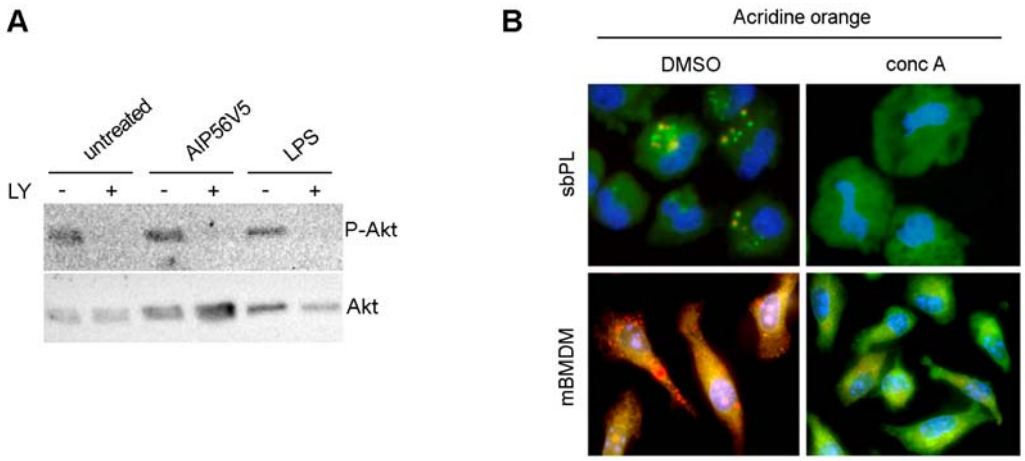

Figure 4.14. Control of the activity of LY294002 and concanamycin A. **(A)** LY294002 inhibits PI3K activity in mBMDM. Cells were treated for 1 h at 37ºC with 10 μM LY294002 or left untreated before incubation with 100 ng/ml bacterial LPS (known to stimulate the phosphorylation of Akt, a downstream target of PI3K (Laird et al, 2009)) or with 5 ug ml^{-1} AIP56V5 (used also as a stimulus). After incubation for 10 min at 37ºC, cells were washed and total and phosporylated Akt (P-Akt) analyzed by western-blotting (chromogenic detection). Note that in the presence of LY294002 no P-Akt is observed, confirming that LY294002 is inhibiting PI3K activity. The blot shown is representative of three independent experiments. **(B)** Concanamycin A inhibits the vacuolar ATPase pump in sbPL and mBMDM. Cells were incubated with 10 nM concanamycin A (concA) or vehicle (DMSO) before incubation for 15 min at 22ºC (sbPL) or 37ºC (mBMDM) with 0.5 μg ml^{-1} acridine orange (AO) in the presence of the inhibitor. Cells were washed and processed for fluorescence microscopy. Nuclei were counterstained with DAPI. Images shown correspond to the overlay of the green and red channels and are representative of two independent experiments.

4. Translocation of AIP56 into the cytosol

4.1. Endosome acidification is required for arrival of AIP56 into the cytosol

The indication that following endocytosis, AIP56 entered early endosomes and that after 20/30 min trafficked into the endocytic recycling compartment suggests that in order to reach its cytosolic target, this toxin translocates from early or recycling endosomes. AB toxins that translocate from endosomes (e.g., diphtheria, tetanus and botulinum toxins) are inhibited by agents that prevent acidification of endosomes/lysosomes (Falnes & Sandvig, 2000; Montecucco & Papini, 1995; Sandvig & van Deurs, 2005), because the trigger for translocation is the low endosomal pH. To clarify the mechanism involved in the translocation of AIP56 into the cytosol, several compounds known to inhibit endosome acidification were tested for their ability to inhibit AIP56 trafficking and toxicity. Those included ammonium chloride and chloroquine, known to diffuse into the endosomes/lysosomes and become protonated with a subsequent increase of the pH in the vesicles (Ohkuma & Poole, 1978); monensin and nigericin, acidic ionophores that have the same effect of ammonium chloride and chloroquine (Ohkuma & Poole, 1978) and also bafilomycin A1 and concanamycin A, potent inhibitors of the endosomal

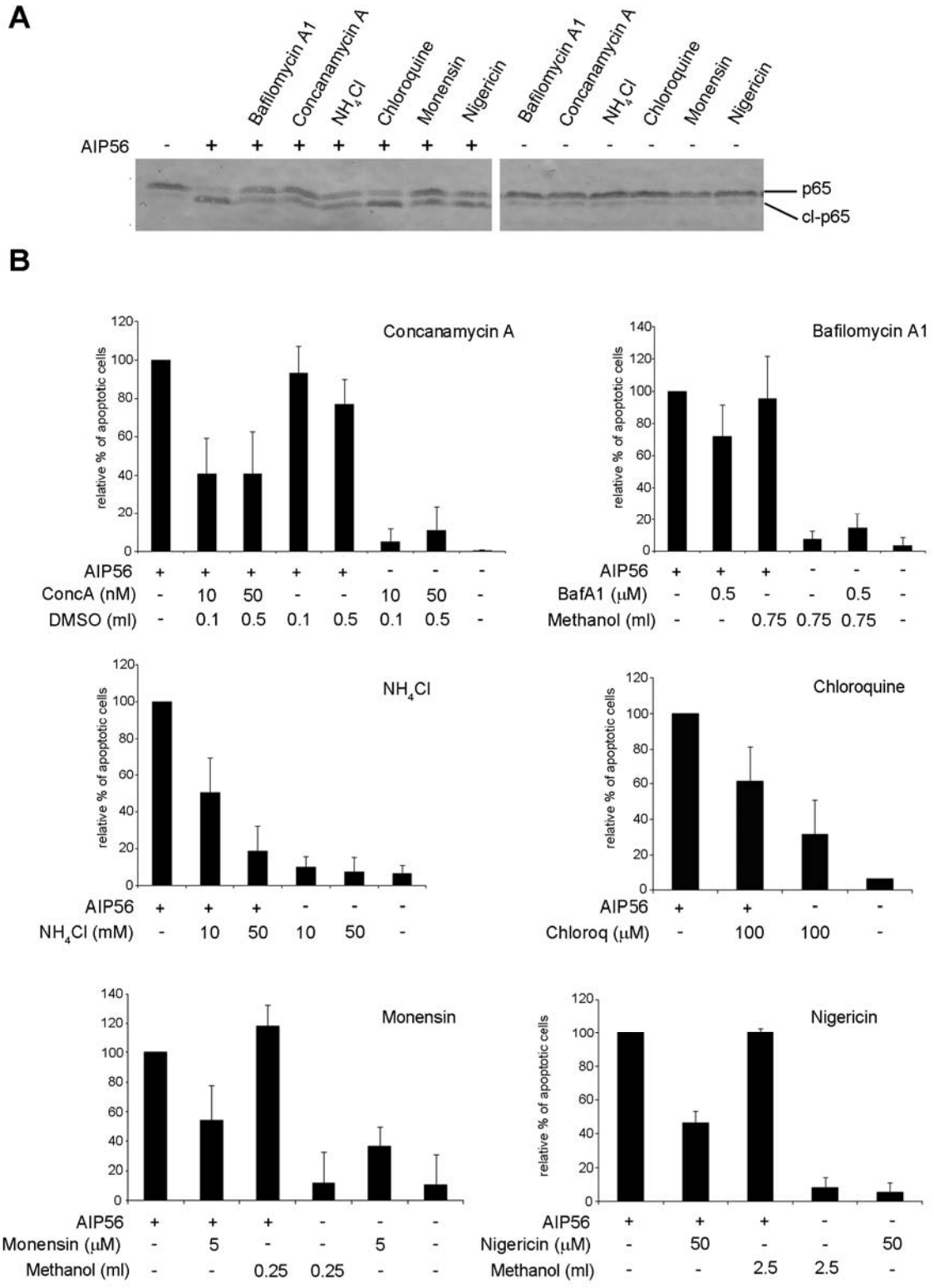

Figure 4.15. Endosome acidification is required for AIP56-dependent cleavage of p65 and AIP56-associated apoptosis. (A) Compounds that inhibit endosome acidification prevent AIP56-dependent cleavage of p65. sbPL were treated with the indicated inhibitor before incubation with 10 μg ml^{-1} AIP56 for 30 min on ice. Cells were washed, shifted to 22ºC and incubated for 2 h while maintaining the inhibitory conditions. Mock treated cells, cells treated with AIP56 in the absence of the inhibitor and cells treated only with the inhibitor were used as controls. Cleavage of p65 was assessed by

western blotting (chromogenic detection). To control the protein loading, the membrane was stained with Ponceau S (bottom panels). Numbers on the left indicate the position of the molecular weight markers, in kDa. The blot shown is representative of three independent experiments. **(B)** Compounds that inhibit endosome acidification inhibit AIP56-induced apoptosis. Cells were treated as described in A and the percentage of apoptotic cells determined after 4 h incubation by morphological analysis of cytospin preparations stained with hemacolor. Pictures were randomly taken and the percentage of cells with apoptotic morphology determined by counting a minimum of 300 cells in a blinded fashion. Results are expressed as the percentage of cells with apoptotic morphology (mean ± SD, *n*=4) relative to the percentage of apoptotic cells in samples treated only with AIP56.

vacuolar ATPase pump that block the acidification of early and late endosomes as well as lysosomes (Huss & Wieczorek, 2009). These compounds did not affect the *in vitro* catalytic activity of AIP56 (Figure 4.8A), and had almost no effect on cell viability at the doses and incubation times employed (not shown). When sbPL were treated with each inhibitor before incubation with AIP56, the cleavage of p65 (Figure 4.15A) and the AIP56-associated apoptosis (Figure 4.15B) were inhibited.

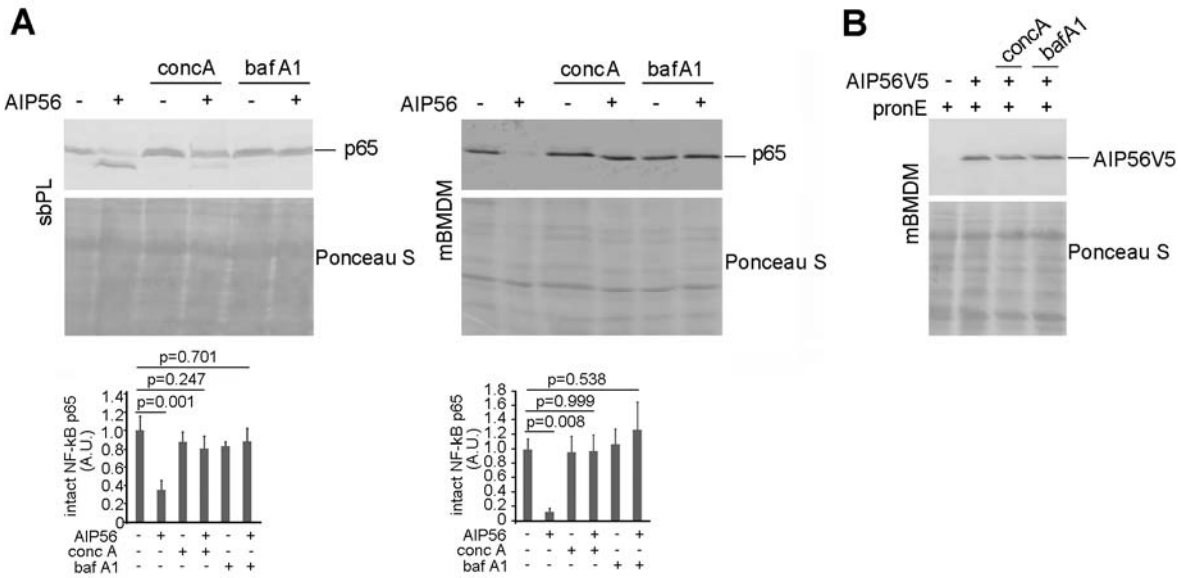

Figure 4.16. AIP56 translocation into the cytosol is dependent on endosome acidification. Concanamycin A (concA) and bafilomycin A1 (bafA1) prevent the AIP56-dependent cleavage of p65 but do not inhibit AIP56 endocytosis. **(A)** sbPL or mBMDM were treated with the indicated inhibitor before incubation with 10 μg ml^{-1} (sbPL) or 5 μg ml^{-1} (mBMDM) AIP56 in the presence of the inhibitor for 30 min on ice. Cells were washed, shifted to 22ºC (sbPL) or 37ºC (mBMDM) and incubated for 2 h while maintaining the inhibitory conditions. Mock treated cells, cells treated with AIP56 in the absence of the inhibitor and cells treated only with the inhibitor were used as control. Cleavage of p65 was assessed by western blotting (chromogenic detection). The graphs show quantification of the blots and combine the results of three independent experiments (mean ± SD). Loading correction was achieved by dividing the density of p65 by the respective density of Ponceau S. The results used for each graph were divided by the same constant in order to set to 1 the mean of the control (mock-treated cells). The significance of differences was tested by one-way ANOVA. p-values for individual comparisons were calculated using the Tukeys´s HSD multiple comparisons and are indicated in the graphs. **(B)** mBMDM were left untreated or treated with concanamycin A or bafilomycin A1 at 37ºC before incubation with 5 μg ml^{-1} AIP56V5 in the presence of the inhibitors for 30 min on ice (pulse), washed and incubated at 37ºC in culture medium containing the

inhibitor. After 5 min, surface-exposed cell-associated toxin was removed with pronase E (pronE) and the endocytosed pool detected by western blotting using an anti-V5 antibody (chromogenic detection). To control the protein loading, the membrane was stained with Ponceau S (bottom panels). The blot shown is representative of three independent experiments.

The protective effect of concanamycin A and bafilomycin A1, the two most potent inhibitors of endosome acidification, were also tested in mBMDM. By western blotting analysis, we confirmed that, similarly to what was observed in sbPL, concanamycin A and bafilomycin A1 inhibited AIP56-dependent p65 cleavage in mBMDM (Figure 4.16A). Pharmacological inhibitors can act at the cell membrane or at different steps of the intracellular trafficking pathways. To exclude that concanamycin A and bafilomycin A1 were blocking AIP56 toxicity by interfering with the initial steps of AIP56 uptake at the cell membrane, mBMDM were treated with the inhibitors or left untreated (control) before pulsing for 30 min on ice with AIP56V5. The cells were washed and after 5 min chase at 37ºC, surface-exposed toxin was removed with pronase E and the intracellular pool of AIP56 detected by western blotting. As shown in Figure 4.16B neither inhibitor affected AIP56 endocytosis, confirming that they are blocking an intracellular step of AIP56 trafficking.

4.2. Time-course of AIP56 translocation

To analyze the time of AIP56 arrival to its cytosolic substrate we performed kinetic studies of the p65 cleavage. Cells were incubated with AIP56 and at the times indicated (Figure 4.17A) samples were collected for western blotting analysis. After 60 min incubation with AIP56, cleavage of NF-κB p65 (cl-p65) was detected, confirming that by that time, AIP56 had arrived into the cytosol (Figure 4.17A).

To complement the kinetic experiments and to gain insight into the time-course of AIP56 translocation, we took advantage of the inhibitory effect of concanamycin A on AIP56 toxicity. Cells were incubated with AIP56 for 30 min on ice, washed to remove unbound toxin and transferred to 37ºC (mBMDM) or 22ºC (sbPL). At the times indicated (Figure 4.17B) concanamycin A was added and after 2 h incubation p65 cleavage was analyzed to assess the arrival of AIP56 into the cytosol. As shown in Figure 4.17B concanamycin A markedly inhibited AIP56-dependent p65 cleavage when added up to 15 min following AIP56 treatment. However, addition of the inhibitor 30 min after toxin treatment resulted only in partial inhibition of p65 cleavage and afterwards, the addition of concanamycin A had no effect on p65 degradation. These results were further supported

by quantifying AIP56-associated apoptosis in sbPL (Figure 4.17C). Addition of concanamycin A up to 15 min following AIP56 treatment resulted in a significant decrease in the percentage of cells with apoptotic morphology (Figure 4.17C), while addition of the inhibitor 30 min after incubation with AIP56 had only a minimal inhibitory effect on the AIP56-induced apoptosis (Figure 4.17C). When concanamycin A was added 45 min after treatment with the toxin, no protective effect was observed (Figure 4.17C). Altogether, these results indicate that after 15-30 min incubation some AIP56 is no longer susceptible to the effect of concanamycin A, suggesting that it was already translocated into the cytosol to exert its toxic effect. Since by confocal microscopy of intoxicated mBMDM, AIP56 was found to be localized in EEA-1 positive vesicles up to 20/30 min incubation, these observations are consistent with the hypothesis that the toxin reaches the cytosol by translocating from early endosomes.

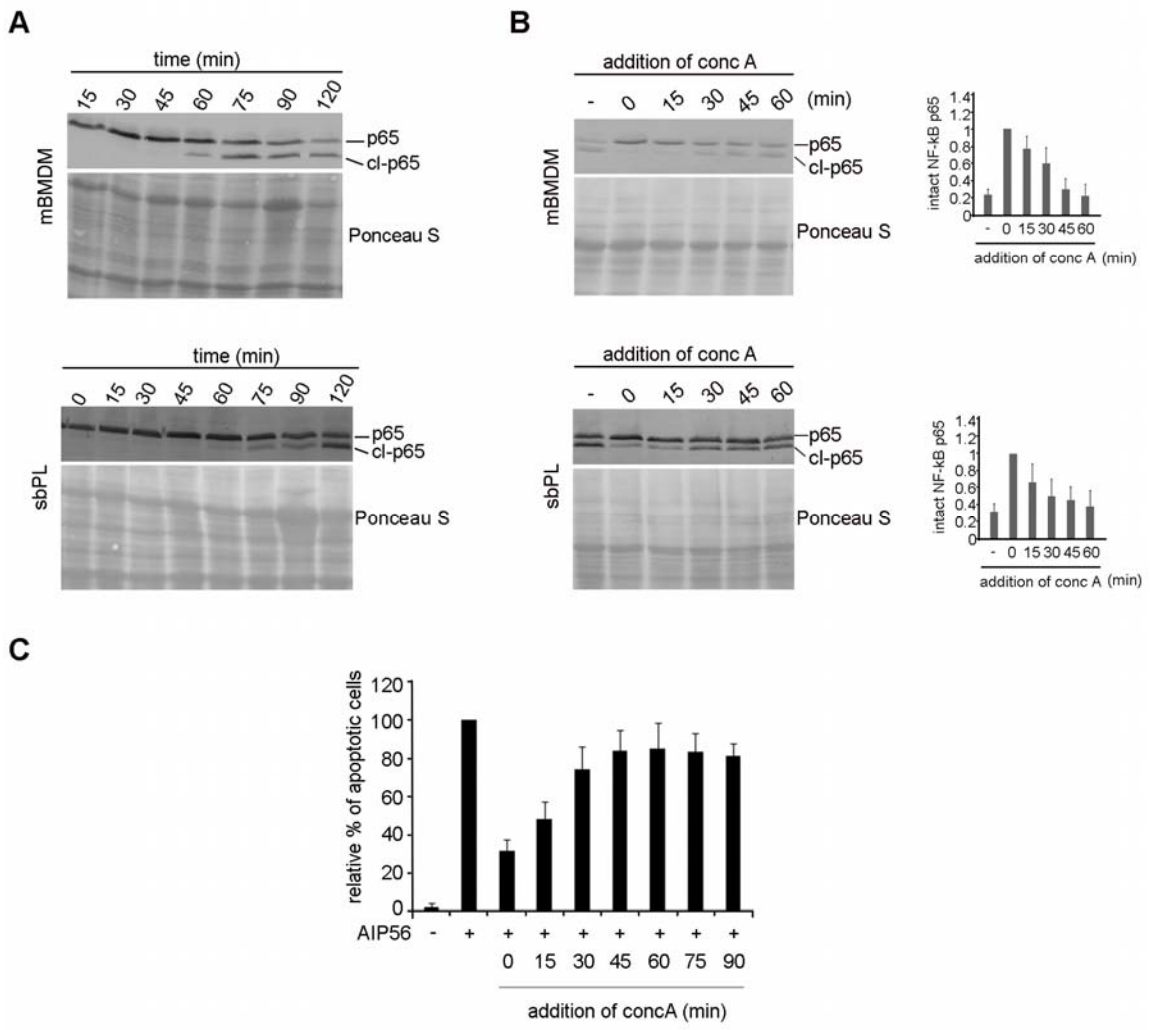

Figure 4.17. Time-course of AIP56 translocation. (A) Kinetic analysis of AIP56-induced NF-κB p65 cleavage. mBMDM or sbPL were left untreated or incubated with 5 or 10 µg ml^{-1} AIP56, respectively, for 30 min on ice, washed and transferred to

37ºC (mBMDM) or 22ºC (sbPL). At the indicated time-points, cells were washed and cleavage of p65 analysed by western blotting (chromogenic detection). The blots shown are representative of three independent experiments. **(B)** mBMDM or sbPL were left untreated or incubated with 5 or 10 µg ml^{-1} AIP56, respectively, for 30 min on ice, washed and transferred to 37ºC (mBMDM) or 22ºC (sbPL) . Concanamycin A (concA) was added at the indicated times and after 2 h, cleavage of p65 was assessed by western blotting (chromogenic detection). The bar graphs show the results of the quantification of the blots (intact NF-kB p65 relative to cells treated with concA at time 0, mean ± SD, *n*=3). **(C)** sbPL were incubated as described in B and the percentage of apoptotic cells determined after 4 h incubation by morphological analysis of cytospin preparations stained with hemacolor. Pictures were randomly taken and the percentage of cells with apoptotic morphology determined by counting a minimum of 300 cells in a blinded fashion. Results are expressed as the percentage of cells with apoptotic morphology (mean ± SD, four independent experiments) relative to the percentage of apoptotic cells in samples treated only with AIP56.

4.3. At acidic pH, AIP56 undergoes reversible conformational changes and interacts with artificial lipid bilayer membranes

Considering that toxins that translocate from endosomes undergo conformational rearrangements at endosomal pH (Qa'Dan et al, 2000), pH-induced structural changes in AIP56 were monitored analyzing TNS fluorescence. TNS is a commercial probe that is non-fluorescent in water and becomes fluorescent when bound to hydrophobic regions of a protein (Sachdev et al, 1973). Recombinant toxin was incubated with TNS at different pH values for 15 min and fluorescence analyzed. As shown in Figure 4.18A, while TNS fluorescence at pH 6.0 and above was not higher than background levels, at pH 5.5 fluorescence markedly increased. The increase continued at pH 5.0, 4.5 and 4.0 and was found to be reversible, since returning the toxin that had been incubated at pH 4.0 to pH 7.0 resulted in a strong decrease in fluorescence intensity (Figure 4.18B). These results indicate that AIP56 exhibits a reversible increase in hydrophobicity when exposed to an acidic (pH 5.5-4.0) environment. Because TNS is an “external” probe of protein hydrophobicity, the intrinsic fluorescence of tryptophan residues was also analyzed. Changes in tryptophan fluorescence can be used to detect protein conformational alterations because the fluorescence is quenched in presence of an aqueous solvent. As shown in Figure 4.18C, tryptophan fluorescence from AIP56 decreases as pH declines, suggesting that under acidic conditions tryptophan-containing domains move into more aqueous environments or that hydrophobic pockets move away from tryptophans.

Following the observation that AIP56 undergoes pH-induced conformational changes, we used black lipid bilayers (Benz et al, 1978) to determine whether the toxin is able to interact with lipid membranes and if the observed pH-induced conformational changes play a role in the interaction. When tested at neutral pH values (pH 7.0-7.4) recombinant AIP56 failed to exhibit membrane activity in black lipid membranes. However, acidification of the aqueous phase at the side of the cis-compartment triggered membrane activity

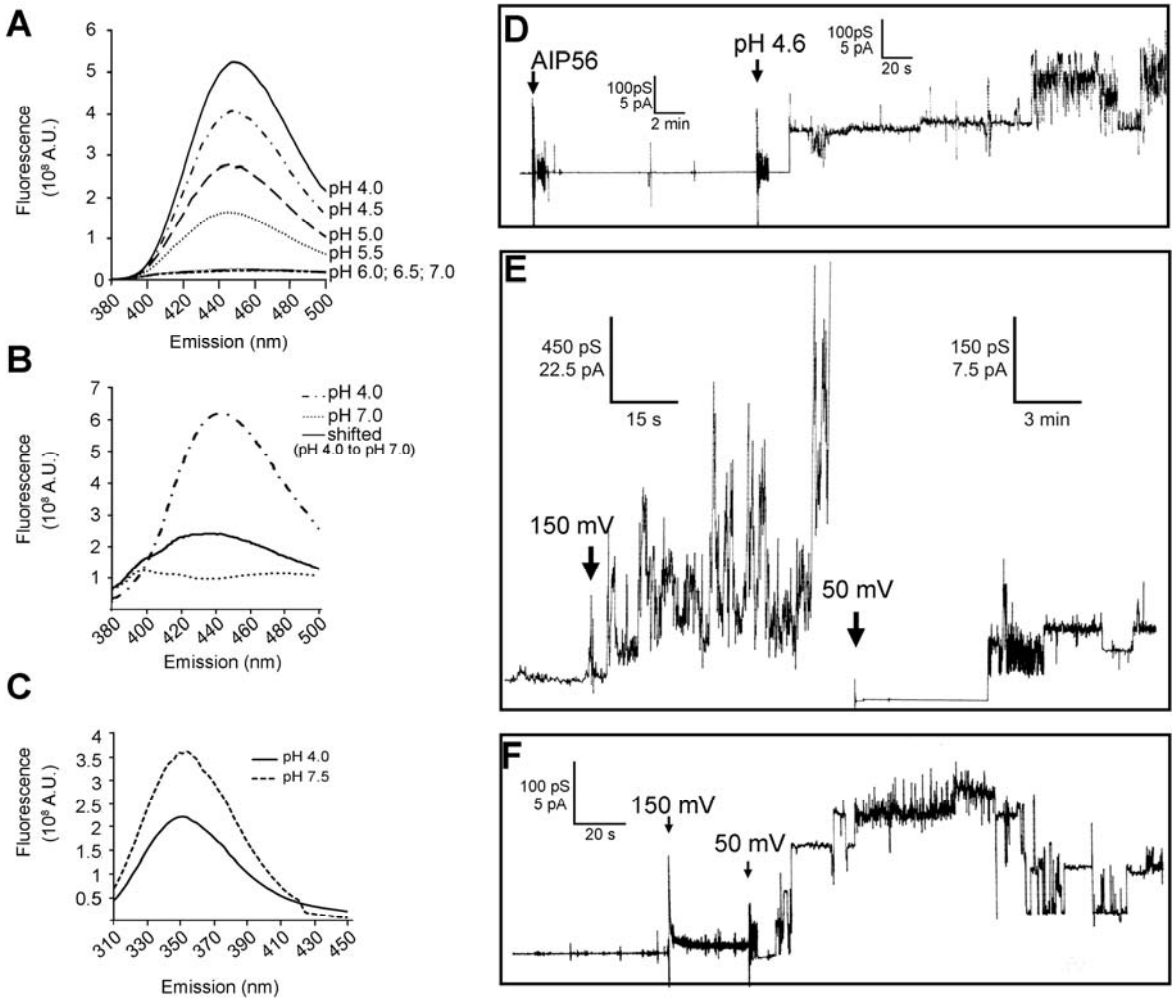

Figure 4.18. Under acidic conditions AIP56 undergoes reversible conformational changes and interacts with lipid bilayer membranes. (A) TNS analysis of pH-induced hydrophobic transitions in AIP56Myc. The toxin was incubated with TNS at the indicated pH values, and fluorescence analyzed. **(B)** TNS fluorescence analysis following a pH shift. AIP56Myc was incubated with TNS at pH 4.0, and fluorescence analyzed as described in (A); the pH was then adjusted to 7.0 and the TNS emission spectrum was recorded again. **(C)** Intrinsic tryptophan fluorescence of AIP56Myc incubated at pH 7.5 or pH 4.0. In experiments A, B and C, fluorescence intensities were determined by averaging two readings and background fluorescence (TNS + buffer alone for TNS analysis or buffer alone for tryptophan) subtracted to the fluorescence of each experimental sample. Each spectrum represents the average of four independent experiments. **(D)** Current recording of a diphytanoyl phosphatidylcholine/n-decane membrane in the presence of recombinant AIP56. The applied membrane potential was 50 mV. Initial experimental conditions consisted of 150 mM KCl, 2 mM $CaCl_2$, 1 mM DTT, 10 mM HEPES pH 7.4. Addition of recombinant AIP56 mixed 1:1 with cholesterol suspension in water to the cis compartment of the chamber (left-side arrow) had no effect on membrane conductivity. Acidification of the aqueous at the cis-compartment by addition of 10 mM CH_3COOK pH 4.6 (right-side arrow) triggered membrane activity. The experiment was repeated three times. **(E)** Membranes activity could also be triggered by a 150 mV voltage-pulse. Current recording of a diphytanoyl phosphatidylcholine/n-decane membrane in the presence of recombinant AIP56 mixed 1:1 with cholesterol suspension in water. Measurements were performed in 150 mM KCl, 2 mM $CaCl_2$, 10 mM MES pH 6.0 and under these conditions, membrane activity was triggered by a 150mV pulse (left-side of panel E, arrow), which finally resulted in membrane rupture. A very stable signal could be observed when only 50 mV were applied to a diphytanoyl phosphatidylcholine/n-decane membrane in the presence of recombinant AIP56 mixed 1:1 with cholesterol suspension in water (right-side of panel E). The experiment was repeated three times. **(F)** Mutations in the metalloprotease signature do not impair the interaction of AIP56

with lipid bilayer membranes. Current recording of a diphytanoyl phosphatidylcholine/n-decane membrane in the presence of AIP56^{AAIVAA} mixed 1:1 with cholesterol suspension in water. Measurements were performed in 150 mM KCl, 2 mM $CaCl_2$, 10 mM MES pH 6.0. Membrane activity was triggered under these conditions by a 150 mV pulse (left-side arrow) and stabilized by lowering the applied voltage to 50 mV (right-side arrow). The experiment was repeated twice.

(Figure 4.18D). Accordingly, when recombinant AIP56 was added to the cis chamber at acidic pH (6.5 to 4.5) membrane activity was also triggered after a 150 mV voltage-pulse (Figure 4.18E) leading to an undefined but step-wise increase in membrane-conductivity (left side of Figure 4.18E), which was followed by membrane rupture. A very stable signal was observed when voltage was kept to 50 mV (right side of Figure 4.18E). The catalytic mutant AIP56^{AAIVAA} behaved similar to AIP56 (Figure 4.18F), indicating that mutations in the metalloprotease signature did not impair AIP56's membrane activity. The observed current fluctuations were irregular and inhomogeneous, indicating that interaction of AIP56 with bilayer membranes does not lead to the formation of regular channels comparable to the ones formed by other AB toxins such as anthrax toxins (Finkelstein, 1994; Schmid et al, 1994) or *Clostridium botulinum* C2 (Finkelstein, 1994; Schmid et al, 1994). The current fluctuations induced by AIP56 are similar to the ones reported to occur with the *C. botulinum* and *C. limosum* C3 toxins (Fahrer et al, 2009) as well as with the *C. difficile* TcdB and TcdA toxins (Barth et al, 2000; Giesemann et al, 2006), and may result from formation of transient channels.

4.4. Extracellular acidification triggers translocation of cell surface-bound AIP56 into the cytosol

The observation that inhibitors which prevent endosome acidification inhibited AIP56 toxicity, that AIP56 undergoes pH-induced conformational changes and is able to interact with black lipid bilayers at low pH prompted us to test if a low-pH pulse could drive the translocation of plasma membrane-bound AIP56 into the cytosol, similarly to what has been reported for several other bacterial toxins that translocate from endosomes through a pH-dependent mechanism (Draper & Simon, 1980; Sandvig & Olsnes, 1980). Concanamycin A was used to block endosomal toxin translocation and the cleavage of p65 used as a read-out for the arrival of AIP56 into the cytosol. mBMDM were incubated with recombinant AIP56 for 30 min on ice to allow toxin binding and then subjected to a pulse at pH 5.5 or 5.0 (pH 7.0 as control) at 37ºC. Afterwards, cells were incubated in supplemented culture medium at pH 7.4 for 2 h at 37ºC, washed and analyzed by western blotting for detection of p65 cleavage. In the absence of an acidic-pulse, concanamycin A inhibited AIP56 endosomal translocation and the concomitant cleavage of p65 (Figure

4.19). However, the inhibitory effect of concanamycin A on AIP56 toxicity was abolished when mBMDM with surface-bound toxin were exposed to pH 5.0 or 5.5 (Figure 4.19), indicating that an acidic pulse is sufficient to induce AIP56 translocation across the plasma membrane of targeted cells. Similar results were obtained when sbPL were used (not shown).

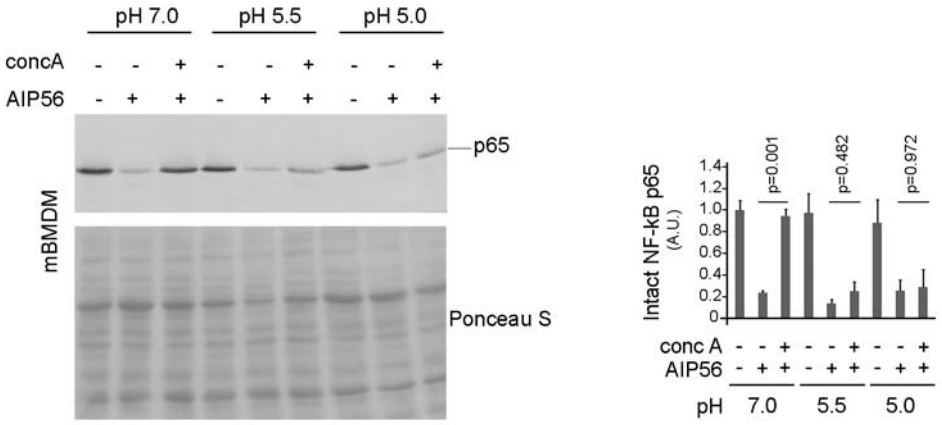

Figure 4.19. An acidic pulse can drive translocation of AIP56 across the cell membrane. mBMDM treated with concanamycin A (concA) (that was maintained during the entire assay to inhibit endosomal toxin translocation) or left untreated were incubated on ice with recombinant AIP56. After 30 min, medium was removed and cells incubated for 1 h at 37ºC with buffers at the indicated pH values followed by incubation in culture medium at pH 7.4 for 2 h. Cleavage of p65 was assessed by western blotting (chromogenic detection). The graph shows the quantification of the blots (mean ± SD; three independent experiments). Loading correction was achieved by dividing the density of p65 band by the respective density of Ponceau S. The results were divided by the same constant in order to set to 1 the mean of the control (mock-treated cells, pH 7.0). For each pH, significance of differences was assessed by one-way ANOVA. p-values for the comparisons with cells treated only with toxin were calculated using Tukey's HSD multiple comparisons test and are indicated in the graph.

CHAPTER V

DISCUSSION

1. AIP56 cleaves NF-κB p65 and induces apoptosis in mBMDM

The nuclear factor-κB (NF-κB) comprises a family of transcription factors, master regulators of inflammatory and antiapoptotic responses (Gilmore & Wolenski, 2012; Wolenski et al, 2013). NF-κB is evolutionary conserved from simple organisms as the demosponge *Amphimedon queenslandica* (Gauthier & Degnan, 2008; Meyer et al, 2009; Shinzato et al, 2011; Wolenski et al, 2013) to the fly *Drosophila melanogaster* (Gilmore & Wolenski, 2012; Wang et al, 2006), fish species (Correa et al, 2004; Kong et al, 2011; Schlezinger et al, 2000; Tacchi et al, 2011; Wang et al, 2009), and humans (Gilmore & Wolenski, 2012; Wang et al, 2006), suggesting that the proteins involved and their mechanisms of action are also evolutionary conserved, highlighting their pivotal role in biological responses. In mammals, it has been shown that the NF-κB family is composed by five elements, RelA/p65, RelB, c-Rel, p50 (NF-κB1), and p52 (NF-κB2), that can form different combinations of homo- or hetero-dimers, contributing to the transcriptional selectivity of the NF-κB response (Oeckinghaus & Ghosh, 2009; Smale, 2012). The most abundant heterodimer of the NF-κB family is p50/p65, often used synonymously for NF-κB. Under normal physiological conditions, NF-κB is retained inactive in the cytoplasm by forming a complex with the inhibitors of kappa B (IκB) proteins. Different stimuli, including bacterial and viral products and cytokines acting via cellular receptors such as Toll-like receptors (TLRs), Interleukin-1 receptor (IL-1R) and TNF receptors (TNFRs), can trigger a signaling cascade that results in phosphorylation and degradation of the inhibitory IκB proteins and activation and transport of the NF-κB complexes to the nucleus, culminating in the up-regulation of inflammatory and anti-apoptotic genes (Rahman & McFadden, 2011).

To counteract the crucial role of NF-κB in immunity, many successful pathogens have evolved a variety of mechanisms to subvert NF-κB signaling (Rahman & McFadden, 2011). Indeed, it has been shown that several pathogenic bacteria interfere with NF-κB signaling by targeting different intermediates of the NF-κB activation cascade (Baruch et al, 2010; Bhattacharjee et al, 2006; Christian et al, 2010; Muhlen et al, 2011; Ruckdeschel et al, 2001; Yen et al, 2010; Zheng et al, 2011), usually by injecting protein effectors directly into the cell´s cytosol through type III or type IV secretion systems (see reviews by Bhavsar et al, 2007; Neish & Naumann, 2011; Rahman & McFadden, 2011). Interestingly, AIP56 is the only described AB-type toxin targeting NF-κB. Previous studies showed that AIP56 cleaves sea bass NF-κB p65 at an evolutionary conserved site, the Cys^{39}-Glu^{40} peptide bond (Silva et al, 2013). Interestingly, Cys^{38} of human p65 (corresponding to sea bass Cys^{39}) has been shown to play a key role in NF-κB binding to DNA (Kelleher et al,

2007) and in regulation of the anti-apoptotic actions of NF-κB (Sen et al, 2012). Moreover, it is known that abnormal activation of this transcription factor contributes to the pathophysiology of a variety of diseases, including inflammatory and autoimmune diseases and cancer (DiDonato et al, 2012; Li & Verma, 2002; Wong & Tergaonkar, 2009), and Cys^{38} of human p65 has been described to be the target of several NF-κB inhibitors with reported anti-inflammatory and/or anticancer properties (Garcia-Pineres et al, 2001; Ha et al, 2009; Han et al, 2005; Harikumar et al, 2009; Liang et al, 2006; Sandur et al, 2006; Watanabe et al, 2008).

The lack of appropriate and established tools for studying intracellular trafficking in fish cells prompted us to search for mammalian cells susceptible to AIP56. During this search, we have found that although mammals are not susceptible to infection by *Photobacterium damselae piscicida*, likely due to temperature and salt-restricting conditions, AIP56 is able to enter and cleave cytosolic NF-κB p65 in different mammalian cells. We also found that the extent of p65 depletion and the occurrence of death upon incubation with AIP56 depend on the cell type: while in the mammalian cell lines tested p65 was not depleted and the cells did not die upon exposure to AIP56, in mBMDM p65 depletion and apoptosis were observed following incubation with the toxin. The different cellular fates upon AIP56 intoxication may be related to the existence of different NF-κB regulatory mechanisms in different cell-types. Alternatively, and similarly to what has been described for diphtheria toxin, in resistant cells AIP56 may be internalized through a non-specific endocytic mechanism that does not allow efficient intoxication. Indeed, studies on diphtheria toxin (DT) demonstrated that sensitivity of the cells to DT-toxicity is related to the presence of DT-specific cell surface-expressed receptor (Almond & Eidels, 1995; Middlebrook et al, 1978; Morris & Saelinger, 1983). While in sensitive cells, DT enters by receptor-mediated endocytosis through a clathrin-dependent mechanism, in resistant cells the toxin is mainly endocytosed through non-clathrin-coated regions of the plasma membrane, independently of the receptor. This mechanism of endocytosis allows the internalization of the toxin but not its toxicity suggesting that receptor-mediated endocytosis is required for efficient intoxication. The identification of AIP56 cell membrane receptor and the understanding of the entry mechanisms in different cell-types could help clarifying the toxin specificity. The observation that, similarly to sea bass macrophages (Silva et al, 2013), mBMDM undergo p65 depletion and apoptosis in response to AIP56 supported the use of these cells as an alternative model to study several details of AIP56 intoxication that could not be properly addressed using sbPL.

It is well known that NF-κB, and in particular its p65 subunit, is responsible for preventing apoptosis (Beg & Baltimore, 1996; Beg et al, 1995; Sen et al, 2012). However, apoptosis of eukaryotic cells is an active and complex process of cell suicide (Fuchs & Steller, 2011; Hacker, 2000; Ren & Savill, 1998) and inactivation of NF-κB alone may not explain its occurrence (Baichwal & Baeuerle, 1997; Liu et al, 1996; Natoli et al, 1998; Wang et al, 1996). Nevertheless, it is well established that cells with inactivated NF-κB are more susceptible to apoptosis in response to different stimulus including the inflammatory cytokine Tumor Necrosis Factor Alpha (TNF-α) and Toll-Like Receptors (TLRs) ligands (Beg & Baltimore, 1996; Hsu et al, 2004; Wang et al, 1996). Until now, it is not clear whether AIP56-mediated p65 cleavage/depletion *per se* is responsible for inducing apoptosis, in resemblance to what has been suggested for the macrophage apoptosis induced by the *Vibrio parahaemolyticus* type III secreted effector VP1686 (Bhattacharjee et al, 2006), or if it requires an additional stimulus, similarly to what has been described for the macrophage apoptosis induced by *Yersinia* outer protein (Yop) P in *Yersinia enterocolitica*, or its homologue YopJ in *Yersinia pseudotuberculosis* and *Yersinia pestis* (Cornelis et al, 1998; Orth, 2002), which have been shown to require stimulation of TLR4 (Haase et al, 2003; Ruckdeschel et al, 2001; Zhang & Bliska, 2003). Our results suggest that TNF-α and TLR4 signaling are dispensable for AIP56 toxicity. However, similarly to what was observed in studies of *Yersinia* YopP (Haase et al, 2003; Ruckdeschel et al, 2001; Zhang & Bliska, 2003), the apoptotic response triggered by AIP56 is delayed in the absence of TLR4. This suggests that although AIP56 toxicity is independent of TLR4 signaling, the toxin can take advantage of LPS to potentiate its intoxication mechanism, i.e. TLR4 signaling critically accelerates the onset of AIP56-induced apoptosis that otherwise occurs with a delayed kinetic. This result, points to the existence of a secondary stimulus that synergizes with the NF-κB inhibitory action of AIP56 to speed up apoptosis. Curiously, although TLR4 is known as a key component of the innate immune response against Gram-negative bacteria it is not always beneficial to the host. It has been demonstrated that bacteria and toxins can subvert TLR4 for their own benefit: TLR4 can facilitate the translocation of uropathogenic *E. coli* across renal collecting duct cells (Chassin et al, 2008); pertussis toxin from *Bordetella pertussis* uses TLR4 as a receptor and is largely dependent on TLR4 to induce intracellular signaling events (Kerfoot et al, 2004); TLR4 facilitates the binding of Shiga toxin to its receptor Gb3 enhancing its cytotoxicity (Torgersen et al, 2010); absence of TLR4 protects against anthrax lethal toxin-induced cardiac contractile dysfunction (Kandadi et al, 2012); and *Yersinia* YopP exploits TLR4 signaling to trigger apoptosis in macrophages (Ruckdeschel et al, 2001).

2. AIP56 undergoes receptor mediated endocytosis in a clathrin-dependent mechanism

Similar to diphtheria toxin, CNF1, botulinum and tetanus neurotoxins (Collier, 2001; Tana et al, 2013; Turton et al, 2002), AIP56 is a single-chain AB toxin that reaches the cytosolic compartment to exert its activity (Silva et al, 2013). Although this implies that the toxin must be able to enter the cells and reach the cytosolic compartment, the entry mechanism and trafficking pathways used by AIP56 were never investigated. Here, using sea bass peritoneal leukocytes (sbPL) and mouse bone marrow derived macrophages (mBMDM), we show that shortly after incubation with cells, AIP56 localizes in intracellular vesicular compartments initially scattered near the cell membrane but that over time concentrate in the perinuclear area, suggesting that binding of AIP56 to still unidentified cell-surface receptor(s) is followed by endocytosis into a vesicular/endosomal compartment from where it must escape to reach the cytosol.

Different bacterial AB toxins have distinct mechanism of internalization, but are usually internalized by receptor-mediated endocytosis before translocation into the cytosol (Falnes & Sandvig, 2000; Sandvig & van Deurs, 1996; Sandvig & van Deurs, 1999; Sandvig & van Deurs, 2005; Watson & Spooner, 2006). In the case of AIP56, similarly to what has been recently reported in sbPL (Silva et al, 2013), the binding to mBMDM occurs by interaction of the C-terminal region (the B domain) of the toxin with the host cell surface, suggesting that the toxin recognizes a conserved receptor and is endocytosed by receptor mediated endocytosis.

After binding to the cell surface receptor, bacterial AB toxins can be endocytosed by different mechanisms and can use exclusively one or more endocytic pathways (Falnes & Sandvig, 2000; Sandvig et al, 1993). While diphtheria toxin (Lemichez et al, 1997; Skretting et al, 1999), clostridial glucosylating toxins (CGTs), and anthrax toxin (Abrami et al, 2010; Abrami et al, 2003) are thought to predominantly use clathrin-dependent endocytosis, several protein toxins like cholera (Torgersen et al, 2001) and Shiga toxins (Sandvig et al, 2009; Sandvig et al, 2002) can be internalized either by clathrin-dependent or independent mechanisms. Our results indicate that following receptor binding, AIP56 endocytosis mainly occurs through a clathrin-dependent mechanism, since inhibition of clathrin-coated pits formation blocked AIP56 internalization. In agreement with this, inhibition of the large GTPase dynamin, known to play an important role in clathrin-mediated endocytosis by participating in the constriction and subsequent budding of coated pits (Damke et al, 1994; Ferguson & De Camilli, 2012; Praefcke & McMahon, 2004; Schmid et al, 1998), also blocked AIP56 entry. Clathrin-dependent endocytosis includes several internalization pathways, all relying on the use of the coat protein clathrin,

but differing in what concerns the requirement for other proteins, including actin (McMahon & Boucrot, 2011). Findings of the present study indicate that the actin cytoskeleton is not involved in AIP56 endocytosis, since depolymerization of F-actin by cytochalasin D (Sampath & Pollard, 1991) did not affect entry nor p65 cleavage by the toxin. This is similar to what has been reported for transferrin, a classical marker of clathrin-mediated endocytosis, that in several cell types has been shown to enter through a pathway independent of actin (Fujimoto et al, 2000), and also for diphtheria toxin, known to enter cells via a clathrin-dependent mechanism that is actin-independent (Abrami et al, 2010; Moya et al, 1985).

Altogether, these data suggest that AIP56 is endocytosed by a dynamin-dependent process mainly governed by clathrin that, as in the case of transferrin (Fujimoto et al, 2000) and diphtheria toxin (Abrami et al, 2010; Moya et al, 1985), does not involve actin. Since pharmacological inhibitors are not absolutely specific (Dutta & Donaldson, 2012; Ivanov, 2008) it would be interesting to complement our results with approaches involving protein depletion or overexpression of dominant-negative mutants that impair clathrin-dependent endocytosis.

3. AIP56 is a “short-trip” toxin that follows the endocytic recycling route

After receptor-mediated endocytosis, AB toxins end up in early endosomes, the central sorting and routing station in cells, and, in what concerns the cytosolic entry, fall in two main groups: some enter from early/late endosomes in response to low pH, whereas others are transported all the way to the Golgi apparatus and from there to the endoplasmic reticulum (ER) from where they translocate into the cytosol.

It was classically thought that molecules internalized via clathrin-dependent endocytosis are either recycled back to the plasma membrane or degraded via the lysosomal pathway (McMahon & Boucrot, 2011). However, there are toxins like Shiga and cholera toxins that upon internalization via clathrin-coated pits traffic retrogradely to the Golgi apparatus (Sandvig et al, 2002). In this study, we used confocal microscopy to dissect the intracellular route followed by AIP56. We found that within 5 minutes after endocytosis, AIP56 localizes in early endosomes (positive for EEA-1 and Alexa 647-Transferrin), where it remains for 15-20 min and then is routed to the recycling endocytic compartment (identified by labeling with Alexa 647-Transferrin). Using a recycling assay in which we allowed cells to internalize AIP56, removed extracellular and surface-associated toxin and then monitored the appearance of recycled toxin in the extracellular medium, we were able to demonstrate that part of the endocytosed AIP56 is rapidly recycled back to

the extracellular compartment. Recycled toxin is already detected at 2 min chase (following a pulse of 30 min on ice + 5 min 37ºC) and its amount increases over time, while decreasing the amount of cell-associated toxin. The fact that the decrease in intracellular AIP56 is not inhibited by the proteasomal inhibitor MG132 and that no co-localization of AIP56 with LAMP-1 was ever detected, suggests that the decrease of cell-associated AIP56 during intoxication does not result from proteosomal or lysosomal degradation, but mainly from recycling of the endocytosed toxin back into the extracellular medium. Consistent with this interpretation is the observation that PI3K, which has been described to play a key role in the endocytic recycling of several molecules, including transferrin (Spiro et al, 1996; van Dam et al, 2002) and AT1 angiotensin receptor (Hunyady et al, 2002), is required for the appearance of recycled AIP56 in the extracellular compartment.

For several recycled proteins, including transferrin receptor, two alternative recycling pathways have been described: a fast direct route from early endosomes or earlier compartments to the plasma membrane and a slower route involving the transport of cargo proteins to the endocytic recycling compartment (ERC) before transport to the plasma membrane (Grant & Donaldson, 2009; Maxfield & McGraw, 2004). The detection of recycled AIP56 after 2 min chase suggests that part of the toxin follows the fast recycling route while the observed co-localization with Alexa 647-Transferrin in a perinuclear compartment suggests that a pool of the toxin is recycled from the ERC. Based on the observation that AIP56 recycling requires PI3K activity, we speculate that the fast recycling route is playing a major role, since it is known that PI3K is mainly involved in the fast recycling (Hunyady et al, 2002; Naughtin et al, 2010; van Dam et al, 2002) with very few evidences of its involvement in slow recycling (Gillooly et al, 2000).

The efficient sorting and recycling of several cargos/receptors internalized by receptor-mediated endocytosis, requires exposure of ligand-receptor complexes to low endosomal pH (Jovic et al, 2010; Mellman, 1996; Mukherjee et al, 1997). Frequently, this leads to the dissociation of the ligands from the receptors (Jovic et al, 2010). The membrane-bound components (e.g. the receptors) are recycled back to the plasma membrane while the released ligands concentrate in the vesicular parts of the early endosomes and are then routed through a microtubule-dependent maturation process to late endosomes/lysosomes (Maxfield & McGraw, 2004; Mellman, 1996; Mukherjee et al, 1997). Several ligands, including transferrin (TF), move between the plasma membrane and sorting/recycling endosomal compartments remaining bound to their receptor and thus avoiding transport to lysosomes (Gibson et al, 1998; Sonnichsen et al, 2000; van Dam & Stoorvogel, 2002; van Dam et al, 2002). Iron-loaded transferrin (holo-TF) binds to

the transferrin receptor at cell surface and is endocytosed by clathrin-dependent endocytosis into early endosomes where the acidic pH facilitates the dissociation of the two atoms of Fe^{3+} from TF. The iron-free TF (apotransferrin), remaining bound to the receptor, is recycled back to the plasma membrane where, at neutral pH, apotransferrin dissociates leaving the transferrin receptor free to bind more TF (Dautry-Varsat et al, 1983; Klausner et al, 1983a; Klausner et al, 1983b; Mayle et al, 2012; Rao et al, 1983). Due to the requirement of acidic endosomal pH for iron release from apotransferrin, inhibitors that raise the acidic pH to neutrality, like the V-ATPase inhibitors concanamycin A and bafilomycin A1, reduce the release of recycling transferrin (Baravalle et al, 2005; Johnson et al, 1993; van Weert et al, 1995). In the case of AIP56, our results suggest that endosomal acidification is dispensable for the recycling and release of the toxin, since the appearance of recycled toxin into the extracellular medium was not affected by inhibition of the vacuolar ATPase pump with concanamycin A.

Although the release of endocytosed toxins back into the extracellular medium has been previously described for the plant toxin ricin (McIntosh et al, 1990; McIntosh et al, 1984; Sandvig & Olsnes, 1979) and for anthrax toxin (Abrami et al, 2013), and is likely to contribute to toxicity, none of those toxins have been reported to follow the endocytic recycling route (Abrami et al, 2013; Moisenovich et al, 2004). The release of endocytosed ricin seems to occur through a mechanism involving exocytosis of multivesicular bodies (McIntosh et al, 1990) allowing intoxication of bystander cell populations (McIntosh et al, 1984). In the case of anthrax, it has been demonstrated that the toxin is delivered into the extracellular medium in exosomes, contributing to prolonged toxicity and to transmission of the toxin to distant cells (Abrami et al, 2013). During this work, several attempts were made to detect activity of recycled AIP56. These consisted in large-scale recycling assays in which we recovered 48 ml of extracellular medium containing recycled AIP56 from eight 24-well plates and tried to concentrate the recycled toxin either using centrifugal devices or an immunoprecipitation protocol. However, we were unable to detect recycled toxin activity. This was likely due to significant losses of toxin during the procedures, since western blotting analysis of the concentrates revealed that the amount of AIP56 recovered was much less than expected and insufficient to perform activity tests. Therefore, the relevance of the putative recycling pathway and of recycled AIP56 for pathogenesis remains to be investigated. Nevertheless, we hypothesize that this mechanism may be relevant *in vivo*, especially during initial steps of infection, when the concentration of circulating toxin is still low.

Although monitoring the intracellular localization of fluorescence labeled AIP56 by microscopy allowed imaging of some details of its intracellular trafficking, the low

sensitivity restrains its usefulness to detect translocation of the toxin into the cytosol. However, several biochemical findings indicate that endosome acidification and low pH-triggered conformational changes are involved in AIP56 translocation: (1) the arrival of AIP56 into the cytosol requires endosome acidification, since AIP56-dependent p65 cleavage was prevented by inhibitors of the vacuolar ATPase pump (Huss & Wieczorek, 2009); (2) at pH 5.5 or lower AIP56 becomes more hydrophobic and is able to interact with artificial lipid bilayer membranes; (3) a low pH pulse promotes translocation of cell surface-bound AIP56 across the cytoplasmic membrane into the cytosol, similarly to what has been reported for several toxins that translocate from endosomes through a pH-dependent mechanism (Barth et al, 2000; Draper & Simon, 1980; Sandvig & Olsnes, 1980). Following endocytosis, AIP56 reaches early endosomes and then follows the recycling route leading to the hypothesis that translocation into the cytosol would occur from early and/or recycling endosomes. Since early endosomes are the first acidic compartment encountered by the toxin upon endocytosis, it is likely that at least the beginning of the translocation process occurs in early endosomes. The fact that in less than 30 min, when most of the toxin is still located in EEA-1 positive vesicles, an amount of AIP56 sufficient to intoxicate the cells is already at the cytosolic compartment together with the fact that inhibition of PI3K activity does not inhibit AIP56 toxicity fully agrees with the hypothesis that early endosomes are the first organelle along the recycling route from where the toxin translocates into the cytosol. The observation that microtubules depolymerization did not affect AIP56-mediated p65 cleavage is compatible with this interpretation and confirms that late endosomes/lysosomes are not involved in AIP56 intoxication, as it is known that maturation of early endosomes into late endosomes is a microtubule dependent process (Huotari & Helenius, 2011).

Altogether, the results herein presented show that AIP56 is a “short-trip” toxin that translocates from endosomes into cytosol in a pH-dependent manner. Additional studies are needed to further dissect the molecular mechanism underlying the different steps of AIP56 intracellular trafficking.

4. Future perspectives

In this study, we report that mBMDM are susceptible to AIP56 intoxication and, using both sbPL and mBMDM, define key steps involved in the entry and intracellular trafficking of the toxin. This opens new questions concerning AIP56 intoxication mechanisms that must be addressed in the future.

Our data clearly show that the extent of p65 depletion and the occurrence of death upon incubation with AIP56 is cell-type specific although the reasons for this specificity remain to be disclosed. The identification of AIP56 cell membrane receptor together with a more complete screening of AIP56 toxicity in different cell-types may contribute to clarify this question.

One of the aspects that urges to clarify is whether AIP56 needs to be processed in order to exert toxicity, like occurs in most bacterial AB toxins secreted as single polypeptides, or if unprocessed toxin may be translocated into cytosol, as described for *Pseudomonas* exotoxin A (Alami et al, 1998; Morlon-Guyot et al, 2009). For several bacterial AB toxins secreted as single polypeptides, proteolytic nicking and integrity of the disulfide bond linking the two domains are essential for toxicity (Knust et al, 2009; Krieglstein et al, 1991; Papini et al, 1993; Pirazzini et al, 2011; Rupnik et al, 2005; Sandvig & Olsnes, 1981; Schiavo et al, 1990). In the case of AIP56, several evidences suggest that proteolytic nicking and integrity of the disulfide bridge are not mandatory for intoxication (Silva et al, 2013). Indeed, there is no evidence of proteolytically processed AIP56 in the *Phdp* culture supernatant or in the serum of infected fish (do Vale et al, 2005), and despite several attempts we were unable to detect proteolytic processing of the toxin upon its interaction with host cells (not shown). Moreover, AIP56 does not requires proteolytic activation or reduction to display enzymatic activity *in vitro*, and disruption of the disulfide bridge linking the two structural domains by alkylation (Silva et al, 2013) or mutation (not shown) does not inhibit AIP56 toxicity.

Another issue that must be clarified is whether eukaryotic co-factors are involved in AIP56 translocation. It is becoming clear that the translocation of several bacterial AB toxins into the cell cytosol is facilitated by specific interactions with common cellular components. Indeed, it has been demonstrated that COPI complex and the cytoplasmic chaperone Hsp90 are key regulators in the translocation and refolding of the catalytic domain of several bacterial toxins. COPI complex has been shown to play a crucial role in the translocation of the catalytic domain of diphtheria (Murphy, 2011) and anthrax (Tamayo et al, 2008) toxins. The Hsp90 has been shown to play a role in the translocation from endosomes and in the cytosolic refolding of diphtheria toxin (Murphy, 2011), the anthrax related fusion protein LFnDTA (Dmochewitz et al, 2010), the *Clostridium botulinum* C2 toxin (Barth, 2011; Haug et al, 2003), the family of binary actin-ADP-ribosylating toxins (Kaiser et al, 2011) and in the translocation of the A1 subunit of cholera toxin from the endoplasmic reticulum to the cytosol (Taylor et al, 2010). These evidences lead to the hypothesis that divergent toxins probably follow a common

mechanism in the initial steps of catalytic domain translocation and should be taken into account when exploring the molecular details of AIP56 translocation.

One of the most interesting findings reported in this thesis is the occurrence of AIP56 recycling. This contrasts to what has been reported for other “short-trip” AB toxins which, in the absence of translocation are degraded in lysosomes. AIP56 is, therefore, the first AB toxin reported to follow the endocytic recycling pathway, adding a novel route to the trafficking of AB toxins. Future studies are needed to define the importance of AIP56 recycling for *Phdp* pathogenesis as well as to disclose the molecular mechanisms involved in the recycling of the toxin. Our data suggest that fast recycling is playing a major role in the recycling of AIP56. This could be confirmed by investigating the involvement of molecules, rather than PI3K, specifically associated to fast or slow-recycling routes. For instance, it is well recognized that Rab4 and Rab11 play key roles in the regulation of the recycling pathway with Rab4 associated to the fast recycling route and Rab11 associated to the slow recycling (Grant & Donaldson, 2009; Maxfield & McGraw, 2004). It would be interesting to evaluate the involvement of such Rab GTPases in AIP56 recycling. Another question that remains to be investigated is how AIP56 is efficiently sorted and recycled back to the extracellular medium. For several cargos/receptors internalized by receptor-mediated endocytosis the efficiency of recycling is dependent on low endosomal pH. Usually, under acidic endosomal pH, the ligands dissociate from the receptors (Jovic et al, 2010; Mellman, 1996; Mukherjee et al, 1997) and the membrane-bound components (e.g. the receptors) are recycled back to the plasma membrane while the released ligands are routed to late endosomes/lysosomes (Maxfield & McGraw, 2004; Mellman, 1996; Mukherjee et al, 1997). In the case of transferrin, after receptor-mediated endocytosis the endosomal acidic pH facilitates the release of Fe^{3+} but the iron-free transferrin remains bound to the receptor to avoid lysosomal degradation and to be efficiently recycled back to the cell surface where the neutral pH leads to dissociation of transferrin receptor from TF. In contrast, the recycling of AIP56 is independent on endosomal acidification. The mechanism/molecules contributing for AIP56 recycling need to be further investigated. The identification of the eukaryotic cell surface receptor recognized by the toxin will likely contribute to disclose this issue.

CHAPTER VI

CONCLUDING REMARKS

AIP56 is a plasmid-encoded protein secreted by *Photobacterium damselae piscicida* (*Phdp*), a Gram-negative bacterium that causes septicemic infections in several warm water fish species worldwide. In *Phdp* infections, the toxin is systemically distributed and induces apoptosis of the host macrophages and neutrophils (do Vale et al, 2007a; do Vale et al, 2003; do Vale et al, 2005). The inefficient clearing of the apoptosing cells due to phagocyte depletion culminates in a post-apoptotic secondary necrotic process with lysis of the apoptosing cells. This leads to the impairment of host immune defenses and contributes to the formation of the necrotic lesions observed in the diseased animals (do Vale et al, 2007a; do Vale et al, 2007b). Recent data from our laboratory demonstrated that AIP56 is an AB-type toxin that depletes the NF-κB p65 of the host cells (Silva et al, 2013), an observation that likely explains the apoptogenic activity of the toxin.

Until the beginning of this work, very little was known about the interaction of AIP56 with different cells and about the cell entry and intracellular trafficking mechanisms used by the toxin to reach its target. With this study, we demonstrated that although *Phdp* is not able to infect mammals, AIP56 enters and cleaves NF-κB p65 not only in fish leukocytes but also in mammalian cells. Additionally, our results disclosed important aspects of AIP56 trafficking showing that these are conserved between fish and mammals.

The findings reported here revealed that AIP56 is a “short-trip” toxin that follows two intracellular pathways that are at least partially independent: the intoxication pathway (that requires acidification of the endosomes and involves conformational changes in the toxin molecule but is independent on PI3K activity) and the recycling pathway (independent on endosome acidification but requiring PI3K activity). The evidences supporting that a significant pool of endocytosed AIP56 follows the recycling pathway and is released into the extracellular medium suggest a novel intracellular route amongst the ones already established for bacterial AB toxins. Additional studies are required to define the relevance of the AIP56 recycling for *Phdp* pathogenesis, but we anticipate that it may be particularly important during initial phases of infection, when the amount of secreted toxin is still limited.

Studies of toxin trafficking contributed to reveal detailed mechanisms of fundamental transport steps in cells, adding to the basic knowledge in cell biology. Furthermore, learning how toxins invade cells may help to find steps in which we can interfere with to prevent disease, leading to advances in medicine and physiology. In this context, disclosing the details of the intoxication mechanism used by AIP56 may contribute to find alternative strategies to prevent or treat *Phdp* infections. Additionally, it may expand the knowledge on the biology of AIP56-like toxins. Indeed, since we first described AIP56, a growing number of AIP56 full-length homologues, likely possessing key pathological roles

during infection, have been reported (up to now mainly in marine *Vibrio* species, but also in *Arsenophonus nasoniae*). None of them has been characterized so far and, therefore, studies on AIP56 will not only add to the understanding of *Phdp* pathogenesis, but will also contribute to shed light on the pathogenesis of infections caused by bacteria producing AIP56-like toxins.

Apart from the intrinsic biologic interest of AIP56, the AB-type structure of the toxin makes it suitable to modifications that can redirect its potent cytotoxicity from disease to a therapeutic function. However, the use of a toxin as a therapeutic must be grounded on a solid knowledge of its intoxication mechanism. In this context, the data presented in this study may contribute to the use of AIP56 as a biotechnological/therapeutic tool in situations associated to uncontrolled activation of NF-κB, such as inflammatory diseases and cancers.

CHAPTER VII

REFERENCES

Aboulaich N, Vainonen JP, Stralfors P, Vener AV (2004) Vectorial proteomics reveal targeting, phosphorylation and specific fragmentation of polymerase I and transcript release factor (PTRF) at the surface of caveolae in human adipocytes. *Biochem J* **383:** 237-248

Abrami L, Bischofberger M, Kunz B, Groux R, van der Goot FG (2010) Endocytosis of the anthrax toxin is mediated by clathrin, actin and unconventional adaptors. *PLoS Pathog* **6:** e1000792

Abrami L, Brandi L, Moayeri M, Brown MJ, Krantz BA, Leppla SH, van der Goot FG (2013) Hijacking Multivesicular Bodies Enables Long-Term and Exosome-Mediated Long-Distance Action of Anthrax Toxin. *Cell Rep* **5:** 986-996

Abrami L, Fivaz M, van der Goot FG (2000) Adventures of a pore-forming toxin at the target cell surface. *Trends Microbiol* **8:** 168-172

Abrami L, Leppla SH, van der Goot FG (2006) Receptor palmitoylation and ubiquitination regulate anthrax toxin endocytosis. *J Cell Biol* **172:** 309-320

Abrami L, Lindsay M, Parton RG, Leppla SH, van der Goot FG (2004) Membrane insertion of anthrax protective antigen and cytoplasmic delivery of lethal factor occur at different stages of the endocytic pathway. *J Cell Biol* **166:** 645-651

Abrami L, Liu S, Cosson P, Leppla SH, van der Goot FG (2003) Anthrax toxin triggers endocytosis of its receptor via a lipid raft-mediated clathrin-dependent process. *J Cell Biol* **160:** 321-328

Abrami L, Reig N, van der Goot FG (2005) Anthrax toxin: the long and winding road that leads to the kill. *Trends Microbiol* **13:** 72-78

Afonso A, Lousada S, Silva J, Ellis AE, Silva MT (1998) Neutrophil and macrophage responses to inflammation in the peritoneal cavity of rainbow trout *Oncorhynchus mykiss*. A light and electron microscopic cytochemical study. *Dis Aquat Organ* **34:** 27-37

Afonso AN, Ellis AE, Silva MT (1997) The leucocyte population of the unstimulated peritoneal cavity of rainbow trout (*Oncorhynchus mykiss*). *Fish & Shellfish Immunology* **7:** 335-348

Ahnert-Hilger G, Dauzenroth ME, Habermann E, Henschen A, Krieglstein K, Mauler F, Weller U (1990) Chains and fragments of tetanus toxin, and their contribution to toxicity. *J Physiol (Paris)* **84:** 229-236

Aktories K (2007) Self-cutting to kill: new insights into the processing of *Clostridium difficile* toxins. *ACS Chem Biol* **2:** 228-230

Aktories K (2011) Bacterial protein toxins that modify host regulatory GTPases. *Nat Rev Microbiol* **9:** 487-498

Aktories K, Barmann M, Ohishi I, Tsuyama S, Jakobs KH, Habermann E (1986) Botulinum C2 toxin ADP-ribosylates actin. *Nature* **322:** 390-392

Aktories K, Barth H (2004a) The actin-ADP-ribosylating *Clostridium botulinum* C2 toxin. *Anaerobe* **10:** 101-105

Aktories K, Barth H (2004b) *Clostridium botulinum* C2 toxin--new insights into the cellular up-take of the actin-ADP-ribosylating toxin. *Int J Med Microbiol* **293:** 557-564

Alami M, Taupiac MP, Reggio H, Bienvenue A, Beaumelle B (1998) Involvement of ATP-dependent *Pseudomonas* exotoxin translocation from a late recycling compartment in lymphocyte intoxication procedure. *Mol Biol Cell* **9:** 387-402

Allured VS, Collier RJ, Carroll SF, McKay DB (1986) Structure of exotoxin A of *Pseudomonas aeruginosa* at 3.0-Angstrom resolution. *Proc Natl Acad Sci U S A* **83:** 1320-1324

Almond BD, Eidels L (1995) The effect of receptor rapid-internalization signals on diphtheria toxin endocytosis and cell sensitivity. *Mol Microbiol* **18:** 623-630

Alouf J, Popoff M (2006) *Chapter 1- A 116-year story of bacterial protein toxins (1888-2004): From "diphtheric poison" to molecular toxinology.*, 3rd ed. edn. London: Academic Press.

Ampapathi RS, Creath AL, Lou DI, Craft JW, Jr., Blanke SR, Legge GB (2008) Order-disorder-order transitions mediate the activation of cholera toxin. *J Mol Biol* **377:** 748-760

Andreoni F, Magnani M (2014) Photobacteriosis: Prevention and Diagnosis. *Journal of Immunology Research* **2014:** 7

Arora N, Leppla SH (1993) Residues 1-254 of anthrax toxin lethal factor are sufficient to cause cellular uptake of fused polypeptides. *J Biol Chem* **268:** 3334-3341

Averbuch-Heller L, Leigh RJ (1997) Medical treatments for abnormal eye movements: pharmacological, optical and immunological strategies. *Aust N Z J Ophthalmol* **25:** 7-13

Baba T, Damke H, Hinshaw JE, Ikeda K, Schmid SL, Warnock DE (1995) Role of dynamin in clathrin-coated vesicle formation. *Cold Spring Harb Symp Quant Biol* **60:** 235-242

Bachmeyer C, Benz R, Barth H, Aktories K, Gilbert M, Popoff MR (2001) Interaction of *Clostridium botulinum* C2 toxin with lipid bilayer membranes and Vero cells: inhibition of channel function by chloroquine and related compounds in vitro and intoxification in vivo. *FASEB J* **15:** 1658-1660

Badizadegan K, Wheeler HE, Fujinaga Y, Lencer WI (2004) Trafficking of cholera toxin-ganglioside GM1 complex into Golgi and induction of toxicity depend on actin cytoskeleton. *Am J Physiol Cell Physiol* **287:** C1453-1462

Baichwal VR, Baeuerle PA (1997) Activate NF-kappa B or die? *Curr Biol* **7:** R94-96

Bann JG (2012) Anthrax toxin protective antigen--insights into molecular switching from prepore to pore. *Protein Sci* **21:** 1-12

Baravalle G, Schober D, Huber M, Bayer N, Murphy RF, Fuchs R (2005) Transferrin recycling and dextran transport to lysosomes is differentially affected by bafilomycin, nocodazole, and low temperature. *Cell Tissue Res* **320:** 99-113

Barnes AC, dos Santos NM, Ellis AE (2005) Update on bacterial vaccines: *Photobacterium damselae* subsp. *piscicida*. *Dev Biol (Basel)* **121:** 75-84

Barth H (2004) Uptake of binary actin ADP-ribosylating toxins. *Rev Physiol Biochem Pharmacol* **152:** 165-182

Barth H (2011) Exploring the role of host cell chaperones/PPIases during cellular up-take of bacterial ADP-ribosylating toxins as basis for novel pharmacological strategies to protect mammalian cells against these virulence factors. *Naunyn Schmiedebergs Arch Pharmacol* **383:** 237-245

Barth H, Aktories K, Popoff MR, Stiles BG (2004) Binary bacterial toxins: biochemistry, biology, and applications of common *Clostridium* and *Bacillus* proteins. *Microbiol Mol Biol Rev* **68:** 373-402

Barth H, Blocker D, Behlke J, Bergsma-Schutter W, Brisson A, Benz R, Aktories K (2000) Cellular uptake of *Clostridium botulinum* C2 toxin requires oligomerization and acidification. *J Biol Chem* **275:** 18704-18711

Barth H, Pfeifer G, Hofmann F, Maier E, Benz R, Aktories K (2001) Low pH-induced formation of ion channels by *clostridium difficile* toxin B in target cells. *J Biol Chem* **276:** 10670-10676

Baruch K, Gur-Arie L, Nadler C, Koby S, Yerushalmi G, Ben-Neriah Y, Yogev O, Shaulian E, Guttman C, Zarivach R, Rosenshine I (2010) Metalloprotease type III effectors that specifically cleave JNK and NF-kappaB. *EMBO J* **30:** 221-231

Bashkirov PV, Akimov SA, Evseev AI, Schmid SL, Zimmerberg J, Frolov VA (2008) GTPase cycle of dynamin is coupled to membrane squeeze and release, leading to spontaneous fission. *Cell* **135:** 1276-1286

Bassik MC, Kampmann M, Lebbink RJ, Wang S, Hein MY, Poser I, Weibezahn J, Horlbeck MA, Chen S, Mann M, Hyman AA, Leproust EM, McManus MT, Weissman JS (2013) A systematic mammalian genetic interaction map reveals pathways underlying ricin susceptibility. *Cell* **152:** 909-922

Beaumelle B, Alami M, Hopkins CR (1993) ATP-dependent translocation of ricin across the membrane of purified endosomes. *J Biol Chem* **268:** 23661-23669

Beaumelle B, Bensammar L, Bienvenue A (1992) Selective translocation of the A chain of diphtheria toxin across the membrane of purified endosomes. *J Biol Chem* **267:** 11525-11531

Beddoe T, Paton AW, Le Nours J, Rossjohn J, Paton JC (2010) Structure, biological functions and applications of the AB5 toxins. *Trends Biochem Sci* **35:** 411-418
Beg AA, Baltimore D (1996) An essential role for NF-kappaB in preventing TNF-alpha-induced cell death. *Science* **274:** 782-784

Beg AA, Sha WC, Bronson RT, Ghosh S, Baltimore D (1995) Embryonic lethality and liver degeneration in mice lacking the RelA component of NF-kappa B. *Nature* **376:** 167-170

Ben-Neriah Y, Karin M (2011) Inflammation meets cancer, with NF-kappaB as the matchmaker. *Nature immunology* 12: 715-723

Benz R, Janko K, Boos W, Lauger P (1978) Formation of large, ion-permeable membrane channels by the matrix protein (porin) of *Escherichia coli*. *Biochim Biophys Acta* **511:** 305-319

Bergan J, Dyve Lingelem AB, Simm R, Skotland T, Sandvig K (2012) Shiga toxins. *Toxicon* **60:** 1085-1107

Bernardi KM, Williams JM, Kikkert M, van Voorden S, Wiertz EJ, Ye Y, Tsai B (2010) The E3 ubiquitin ligases Hrd1 and gp78 bind to and promote cholera toxin retro-translocation. *Mol Biol Cell* **21:** 140-151

Bharati K, Ganguly NK (2011) Cholera toxin: a paradigm of a multifunctional protein. *Indian J Med Res* **133:** 179-187

Bhattacharjee RN, Park KS, Kumagai Y, Okada K, Yamamoto M, Uematsu S, Matsui K, Kumar H, Kawai T, Iida T, Honda T, Takeuchi O, Akira S (2006) VP1686, a *Vibrio* type III secretion protein, induces toll-like receptor-independent apoptosis in macrophage through NF-kappaB inhibition. *J Biol Chem* **281:** 36897-36904

Bhavsar AP, Guttman JA, Finlay BB (2007) Manipulation of host-cell pathways by bacterial pathogens. *Nature* **449:** 827-834

Bischofberger M, Gonzalez MR, van der Goot FG (2009) Membrane injury by pore-forming proteins. *Curr Opin Cell Biol* **21:** 589-595

Bischofberger M, Iacovache I, van der Goot FG (2012) Pathogenic pore-forming proteins: function and host response. *Cell Host Microbe* **12:** 266-275

Blank SR (2006) Portals and Pathways: Principles of Bacterial Toxin Entry into Host Cells. *Microbe* **1:** 26-32

Blank V, Kourilsky P, Israel A (1991) Cytoplasmic retention, DNA binding and processing of the NF-kappa B p50 precursor are controlled by a small region in its C-terminus. *EMBO J* **10:** 4159-4167

Blaustein RO, Germann WJ, Finkelstein A, DasGupta BR (1987) The N-terminal half of the heavy chain of botulinum type A neurotoxin forms channels in planar phospholipid bilayers. *FEBS Lett* **226:** 115-120

Blocker A, Komoriya K, Aizawa S (2003a) Type III secretion systems and bacterial flagella: insights into their function from structural similarities. *Proc Natl Acad Sci U S A* **100:** 3027-3030

Blocker D, Pohlmann K, Haug G, Bachmeyer C, Benz R, Aktories K, Barth H (2003b) *Clostridium botulinum* C2 toxin: low pH-induced pore formation is required for translocation of the enzyme component C2I into the cytosol of host cells. *J Biol Chem* **278:** 37360-37367

Boll W, Ehrlich M, Collier RJ, Kirchhausen T (2004) Effects of dynamin inactivation on pathways of anthrax toxin uptake. *Eur J Cell Biol* **83:** 281-288

Bonifacino JS, Lippincott-Schwartz J (2003) Coat proteins: shaping membrane transport. *Nat Rev Mol Cell Biol* **4:** 409-414

Bonifacino JS, Rojas R (2006) Retrograde transport from endosomes to the trans-Golgi network. *Nat Rev Mol Cell Biol* **7:** 568-579

Booth BA, Boesman-Finkelstein M, Finkelstein RA (1984) *Vibrio cholerae* hemagglutinin/protease nicks cholera enterotoxin. *Infect Immun* **45:** 558-560

Boquet P, Silverman MS, Pappenheimer AM, Jr., Vernon WB (1976) Binding of triton X-100 to diphtheria toxin, crossreacting material 45, and their fragments. *Proc Natl Acad Sci U S A* **73:** 4449-4453

Bosshart H, Humphrey J, Deignan E, Davidson J, Drazba J, Yuan L, Oorschot V, Peters PJ, Bonifacino JS (1994) The cytoplasmic domain mediates localization of furin to the trans-Golgi network en route to the endosomal/lysosomal system. *J Cell Biol* **126:** 1157-1172

Bouwmeester T, Bauch A, Ruffner H, Angrand PO, Bergamini G, Croughton K, Cruciat C, Eberhard D, Gagneur J, Ghidelli S, Hopf C, Huhse B, Mangano R, Michon AM, Schirle M, Schlegl J, Schwab M, Stein MA, Bauer A, Casari G, Drewes G, Gavin AC, Jackson DB, Joberty G, Neubauer G, Rick J, Kuster B, Superti-Furga G (2004) A physical and functional map of the human TNF-alpha/NF-kappa B signal transduction pathway. *Nat Cell Biol* **6:** 97-105

Bowman EJ, Siebers A, Altendorf K (1988) Bafilomycins: a class of inhibitors of membrane ATPases from microorganisms, animal cells, and plant cells. *Proc Natl Acad Sci U S A* **85:** 7972-7976

Bradley JR (2008) TNF-mediated inflammatory disease. *The Journal of pathology* **214:** 149-160

Bragg TS, Robertson DL (1989) Nucleotide sequence and analysis of the lethal factor gene (lef) from *Bacillus anthracis*. *Gene* **81:** 45-54

Brinkmann U (1996) Recombinant immunotoxins: protein engineering for cancer therapy. *Mol Med Today* **2:** 439-446

Cabiaux V, Mindell J, Collier RJ (1993) Membrane translocation and channel-forming activities of diphtheria toxin are blocked by replacing isoleucine 364 with lysine. *Infect Immun* **61:** 2200-2202

Cabiaux V, Quertenmont P, Conrath K, Brasseur R, Capiau C, Ruysschaert JM (1994) Topology of diphtheria toxin B fragment inserted in lipid vesicles. *Mol Microbiol* **11:** 43-50

Cancino J, Jung JE, Luini A (2013) Regulation of Golgi signaling and trafficking by the KDEL receptor. *Histochem Cell Biol* **140:** 395-405

Cancino J, Luini A (2013) Signaling circuits on the Golgi complex. *Traffic* **14:** 121-134

Carpentier S, N'Kuli F, Grieco G, Van Der Smissen P, Janssens V, Emonard H, Bilanges B, Vanhaesebroeck B, Gaide Chevronnay HP, Pierreux CE, Tyteca D, Courtoy PJ (2013) Class III phosphoinositide 3-kinase/VPS34 and dynamin are critical for apical endocytic recycling. *Traffic* **14:** 933-948

Carter SR, Seiff SR (1997) Cosmetic botulinum toxin injections. *Int Ophthalmol Clin* **37:** 69-79

Casanova JL, Abel L, Quintana-Murci L (2011) Human TLRs and IL-1Rs in host defense: natural insights from evolutionary, epidemiological, and clinical genetics. *Annu Rev Immunol* **29:** 447-491

Casbon AJ, Allen LA, Dunn KW, Dinauer MC (2009) Macrophage NADPH oxidase flavocytochrome B localizes to the plasma membrane and Rab11-positive recycling endosomes. *J Immunol* **182:** 2325-2339

Chassin C, Vimont S, Cluzeaud F, Bens M, Goujon JM, Fernandez B, Hertig A, Rondeau E, Arlet G, Hornef MW, Vandewalle A (2008) TLR4 facilitates translocation of bacteria across renal collecting duct cells. *J Am Soc Nephrol* **19:** 2364-2374

Chaudhary VK, Jinno Y, FitzGerald D, Pastan I (1990) *Pseudomonas* exotoxin contains a specific sequence at the carboxyl terminus that is required for cytotoxicity. *Proc Natl Acad Sci U S A* **87:** 308-312

Chen FE, Huang DB, Chen YQ, Ghosh G (1998) Crystal structure of p50/p65 heterodimer of transcription factor NF-kappaB bound to DNA. *Nature* **391:** 410-413

Chen JL, Fucini RV, Lacomis L, Erdjument-Bromage H, Tempst P, Stamnes M (2005) Coatomer-bound Cdc42 regulates dynein recruitment to COPI vesicles. *J Cell Biol* **169:** 383-389

Chenal A, Savarin P, Nizard P, Guillain F, Gillet D, Forge V (2002) Membrane protein insertion regulated by bringing electrostatic and hydrophobic interactions into play. A case study with the translocation domain of diphtheria toxin. *J Biol Chem* **277:** 43425-43432

Cherla RP, Lee SY, Tesh VL (2003) Shiga toxins and apoptosis. *FEMS Microbiol Lett* **228:** 159-166

Chinnapen DJ, Hsieh WT, te Welscher YM, Saslowsky DE, Kaoutzani L, Brandsma E, D'Auria L, Park H, Wagner JS, Drake KR, Kang M, Benjamin T, Ullman MD, Costello CE, Kenworthy AK, Baumgart T, Massol RH, Lencer WI (2012) Lipid sorting by ceramide structure from plasma membrane to ER for the cholera toxin receptor ganglioside GM1. *Dev Cell* **23:** 573-586

Cho JA, Chinnapen DJ, Aamar E, te Welscher YM, Lencer WI, Massol R (2012) Insights on the trafficking and retro-translocation of glycosphingolipid-binding bacterial toxins. *Front Cell Infect Microbiol* **2:** 51

Choe S, Bennett MJ, Fujii G, Curmi PM, Kantardjieff KA, Collier RJ, Eisenberg D (1992) The crystal structure of diphtheria toxin. *Nature* **357:** 216-222

Christian J, Vier J, Paschen SA, Hacker G (2010) Cleavage of the NF-kappaB family protein p65/RelA by the chlamydial protease-like activity factor (CPAF) impairs

proinflammatory signaling in cells infected with Chlamydiae. *J Biol Chem* **285:** 41320-41327

Clague MJ, Urbe S, Aniento F, Gruenberg J (1994) Vacuolar ATPase activity is required for endosomal carrier vesicle formation. *J Biol Chem* **269:** 21-24

Clarke SC (2001) Diarrhoeagenic *Escherichia coli*--an emerging problem? *Diagn Microbiol Infect Dis* **41:** 93-98

Collier RJ (1967) Effect of diphtheria toxin on protein synthesis: inactivation of one of the transfer factors. *J Mol Biol* **25:** 83-98

Collier RJ (1975) Diphtheria toxin: mode of action and structure. *Bacteriol Rev* **39:** 54-85

Collier RJ (2001) Understanding the mode of action of diphtheria toxin: a perspective on progress during the 20th century. *Toxicon* **39:** 1793-1803

Collier RJ (2009) Membrane translocation by anthrax toxin. *Mol Aspects Med* **30:** 413-422

Collier RJ, Young JA (2003) Anthrax toxin. *Annu Rev Cell Dev Biol* **19:** 45-70

Corboy MJ, Draper RK (1997) Elevation of vacuolar pH inhibits the cytotoxic activity of furin-cleaved exotoxin A. *Infect Immun* **65:** 2240-2242

Cornelis GR (2006) The type III secretion injectisome. *Nat Rev Microbiol* **4:** 811-825

Cornelis GR, Boland A, Boyd AP, Geuijen C, Iriarte M, Neyt C, Sory MP, Stainier I (1998) The virulence plasmid of Yersinia, an antihost genome. *Microbiol Mol Biol Rev* **62:** 1315-1352

Correa RG, Tergaonkar V, Ng JK, Dubova I, Izpisua-Belmonte JC, Verma IM (2004) Characterization of NF-kappa B/I kappa B proteins in zebra fish and their involvement in notochord development. *Mol Cell Biol* **24:** 5257-5268

Costa-Ramos C, Vale A, Ludovico P, Dos Santos NM, Silva MT (2011) The bacterial exotoxin AIP56 induces fish macrophage and neutrophil apoptosis using mechanisms of the extrinsic and intrinsic pathways. *Fish Shellfish Immunol* **30:** 173-181

Cox D, Lee DJ, Dale BM, Calafat J, Greenberg S (2000) A Rab11-containing rapidly recycling compartment in macrophages that promotes phagocytosis. *Proc Natl Acad Sci U S A* **97:** 680-685

Czerkinsky C, Sun JB, Lebens M, Li BL, Rask C, Lindblad M, Holmgren J (1996) Cholera toxin B subunit as transmucosal carrier-delivery and immunomodulating system for induction of antiinfectious and antipathological immunity. *Ann N Y Acad Sci* **778:** 185-193

Dal Molin F, Tonello F, Ladant D, Zornetta I, Zamparo I, Di Benedetto G, Zaccolo M, Montecucco C (2006) Cell entry and cAMP imaging of anthrax edema toxin. *EMBO J* **25:** 5405-5413

Damke H, Baba T, Warnock DE, Schmid SL (1994) Induction of mutant dynamin specifically blocks endocytic coated vesicle formation. *J Cell Biol* **127:** 915-934

DasGupta BR (1971) Activation of *Clostridium botulinum* type B toxin by an endogenous enzyme. *J Bacteriol* **108:** 1051-1057

Dautry-Varsat A, Ciechanover A, Lodish HF (1983) pH and the recycling of transferrin during receptor-mediated endocytosis. *Proc Natl Acad Sci U S A* **80:** 2258-2262

Degnan PH, Yu Y, Sisneros N, Wing RA, Moran NA (2009) *Hamiltonella defensa*, genome evolution of protective bacterial endosymbiont from pathogenic ancestors. *Proc Natl Acad Sci U S A* **106:** 9063-9068

DiDonato JA, Mercurio F, Karin M (2012) NF-kappaB and the link between inflammation and cancer. *Immunol Rev* **246:** 379-400

Distler U, Souady J, Hulsewig M, Drmic-Hofman I, Haier J, Friedrich AW, Karch H, Senninger N, Dreisewerd K, Berkenkamp S, Schmidt MA, Peter-Katalinic J, Muthing J (2009) Shiga toxin receptor Gb3Cer/CD77: tumor-association and promising therapeutic target in pancreas and colon cancer. *PLoS One* **4:** e6813

Dmochewitz L, Lillich M, Kaiser E, Jennings LD, Lang AE, Buchner J, Fischer G, Aktories K, Collier RJ, Barth H (2010) Role of CypA and Hsp90 in membrane translocation mediated by anthrax protective antigen. *Cell Microbiol* **13:** 359-373

do Vale A, Afonso A, Silva MT (2002) The professional phagocytes of sea bass (*Dicentrarchus labrax* L.): cytochemical characterisation of neutrophils and macrophages in the normal and inflamed peritoneal cavity. *Fish Shellfish Immunol* **13:** 183-198

do Vale A, Costa-Ramos C, Silva A, Silva DS, Gartner F, dos Santos NM, Silva MT (2007a) Systemic macrophage and neutrophil destruction by secondary necrosis induced by a bacterial exotoxin in a Gram-negative septicaemia. *Cell Microbiol* **9:** 988-1003

do Vale A, Costa-Ramos C, Silva DS, Macedo PM, Fernandes R, Sampaio P, Dos Santos NM, Silva MT (2007b) Cytochemical and ultrastructural study of anoikis and secondary necrosis in enterocytes detached in vivo. *Apoptosis* **12:** 1069-1083

do Vale A, Marques F, Silva MT (2003) Apoptosis of sea bass (*Dicentrarchus labrax* L.) neutrophils and macrophages induced by experimental infection with Photobacterium damselae subsp. piscicida. *Fish Shellfish Immunol* **15:** 129-144

do Vale A, Silva MT, dos Santos NM, Nascimento DS, Reis-Rodrigues P, Costa-Ramos C, Ellis AE, Azevedo JE (2005) AIP56, a novel plasmid-encoded virulence factor of *Photobacterium damselae* subsp. *piscicida* with apoptogenic activity against sea bass macrophages and neutrophils. *Mol Microbiol* **58:** 1025-1038

Doherty GJ, McMahon HT (2009) Mechanisms of endocytosis. *Annu Rev Biochem* **78:** 857-902

Doherty SD, Prieto VG, George S, Hazarika P, Duvic M (2006) High flotillin-2 expression is associated with lymph node metastasis and Breslow depth in melanoma. *Melanoma Res* **16:** 461-463

Donnelly JJ, Ulmer JB, Hawe LA, Friedman A, Shi XP, Leander KR, Shiver JW, Oliff AI, Martinez D, Montgomery D, et al. (1993) Targeted delivery of peptide epitopes to class I

major histocompatibility molecules by a modified *Pseudomonas* exotoxin. *Proc Natl Acad Sci U S A* **90:** 3530-3534

Donovan JJ, Simon MI, Draper RK, Montal M (1981) Diphtheria toxin forms transmembrane channels in planar lipid bilayers. *Proc Natl Acad Sci U S A* **78:** 172-176

Draper RK, Simon MI (1980) The entry of diphtheria toxin into the mammalian cell cytoplasm: evidence for lysosomal involvement. *J Cell Biol* **87:** 849-854

Drose S, Bindseil KU, Bowman EJ, Siebers A, Zeeck A, Altendorf K (1993) Inhibitory effect of modified bafilomycins and concanamycins on P- and V-type adenosinetriphosphatases. *Biochemistry* **32:** 3902-3906

Dutta D, Donaldson JG (2012) Search for inhibitors of endocytosis: Intended specificity and unintended consequences. *Cell Logist* **2:** 203-208

Duvic M, Talpur R (2008) Optimizing denileukin diftitox (Ontak) therapy. *Future Oncol* **4:** 457-469

Dyve Lingelem AB, Bergan J, Sandvig K (2012) Inhibitors of Intravesicular Acidification Protect Against Shiga Toxin in a pH-Independent Manner. *Traffic*

Edelhoch H (1967) Spectroscopic determination of tryptophan and tyrosine in proteins. *Biochemistry* **6:** 1948-1954

Edeling MA, Smith C, Owen D (2006) Life of a clathrin coat: insights from clathrin and AP structures. *Nat Rev Mol Cell Biol* **7:** 32-44

Ehrlich M, Boll W, Van Oijen A, Hariharan R, Chandran K, Nibert ML, Kirchhausen T (2004) Endocytosis by random initiation and stabilization of clathrin-coated pits. *Cell* **118:** 591-605

Eriksson K, Holmgren J (2002) Recent advances in mucosal vaccines and adjuvants. *Curr Opin Immunol* **14:** 666-672

Fagerquist CK, Sultan O (2010) Top-down proteomic identification of furin-cleaved alpha-subunit of Shiga toxin 2 from *Escherichia coli* O157:H7 using MALDI-TOF-TOF-MS/MS. *J Biomed Biotechnol* **2010:** 123460

Fahrer J, Kuban J, Heine K, Rupps G, Kaiser E, Felder E, Benz R, Barth H (2009) Selective and specific internalization of clostridial C3 ADP-ribosyltransferases into macrophages and monocytes. *Cell Microbiol* **12:** 233-247

Falguieres T, Johannes L (2006) Shiga toxin B-subunit binds to the chaperone BiP and the nucleolar protein B23. *Biol Cell* **98:** 125-134

Falguieres T, Mallard F, Baron C, Hanau D, Lingwood C, Goud B, Salamero J, Johannes L (2001) Targeting of Shiga toxin B-subunit to retrograde transport route in association with detergent-resistant membranes. *Mol Biol Cell* **12:** 2453-2468

Falnes PO, Sandvig K (2000) Penetration of protein toxins into cells. *Curr Opin Cell Biol* **12:** 407-413

Fan CM, Maniatis T (1991) Generation of p50 subunit of NF-kappa B by processing of p105 through an ATP-dependent pathway. *Nature* **354:** 395-398

Feng Y, Jadhav AP, Rodighiero C, Fujinaga Y, Kirchhausen T, Lencer WI (2004) Retrograde transport of cholera toxin from the plasma membrane to the endoplasmic reticulum requires the trans-Golgi network but not the Golgi apparatus in Exo2-treated cells. *EMBO Rep* **5:** 596-601

Ferguson SM, De Camilli P (2012) Dynamin, a membrane-remodelling GTPase. *Nat Rev Mol Cell Biol* **13:** 75-88

Finkelstein A (1994) The channel formed in planar lipid bilayers by the protective antigen component of anthrax toxin. *Toxicology* **87:** 29-41

Fitzgerald D (1996) Why toxins! *Semin Cancer Biol* **7:** 87-95

FitzGerald DJ, Kreitman R, Wilson W, Squires D, Pastan I (2004) Recombinant immunotoxins for treating cancer. *Int J Med Microbiol* **293:** 577-582

FitzGerald DJ, Wayne AS, Kreitman RJ, Pastan I (2011) Treatment of hematologic malignancies with immunotoxins and antibody-drug conjugates. *Cancer Res* **71:** 6300-6309

Flannagan RS, Jaumouille V, Grinstein S (2012) The cell biology of phagocytosis. *Annual review of pathology* **7:** 61-98

Foster FM, Traer CJ, Abraham SM, Fry MJ (2003) The phosphoinositide (PI) 3-kinase family. *J Cell Sci* **116:** 3037-3040

Fraser JD, Proft T (2008) The bacterial superantigen and superantigen-like proteins. *Immunol Rev* **225:** 226-243

Fraser ME, Chernaia MM, Kozlov YV, James MN (1994) Crystal structure of the holotoxin from *Shigella dysenteriae* at 2.5 A resolution. *Nat Struct Biol* **1:** 59-64

Frick M, Bright NA, Riento K, Bray A, Merrified C, Nichols BJ (2007) Coassembly of flotillins induces formation of membrane microdomains, membrane curvature, and vesicle budding. *Curr Biol* **17:** 1151-1156

Friedlander AM (1986) Macrophages are sensitive to anthrax lethal toxin through an acid-dependent process. *J Biol Chem* **261:** 7123-7126

Fryling C, Ogata M, FitzGerald D (1992) Characterization of a cellular protease that cleaves *Pseudomonas* exotoxin. *Infect Immun* **60:** 497-502

Fuchs Y, Steller H (2011) Programmed cell death in animal development and disease. *Cell* **147:** 742-758

Fujimoto LM, Roth R, Heuser JE, Schmid SL (2000) Actin assembly plays a variable, but not obligatory role in receptor-mediated endocytosis in mammalian cells. *Traffic* **1:** 161-171

Fujinaga Y, Wolf AA, Rodighiero C, Wheeler H, Tsai B, Allen L, Jobling MG, Rapoport T, Holmes RK, Lencer WI (2003) Gangliosides that associate with lipid rafts mediate transport of cholera and related toxins from the plasma membrane to endoplasmic reticulm. *Mol Biol Cell* **14:** 4783-4793

Galán JE (2009) Common themes in the design and function of bacterial effectors. *Cell Host Microbe* **5:** 571-579

Galan JE, Wolf-Watz H (2006) Protein delivery into eukaryotic cells by type III secretion machines. *Nature* **444:** 567-573

Galloux M, Vitrac H, Montagner C, Raffestin S, Popoff MR, Chenal A, Forge V, Gillet D (2008) Membrane Interaction of botulinum neurotoxin A translocation (T) domain. The belt region is a regulatory loop for membrane interaction. *J Biol Chem* **283:** 27668-27676

Garcia-Pineres AJ, Castro V, Mora G, Schmidt TJ, Strunck E, Pahl HL, Merfort I (2001) Cysteine 38 in p65/NF-kappaB plays a crucial role in DNA binding inhibition by sesquiterpene lactones. *J Biol Chem* **276:** 39713-39720

Garred O, Dubinina E, Holm PK, Olsnes S, van Deurs B, Kozlov JV, Sandvig K (1995a) Role of processing and intracellular transport for optimal toxicity of Shiga toxin and toxin mutants. *Exp Cell Res* **218:** 39-49

Garred O, van Deurs B, Sandvig K (1995b) Furin-induced cleavage and activation of Shiga toxin. *J Biol Chem* **270:** 10817-10821

Gauthier M, Degnan BM (2008) The transcription factor NF-kappaB in the demosponge *Amphimedon queenslandica*: insights on the evolutionary origin of the Rel homology domain. *Dev Genes Evol* **218:** 23-32

Geiger R, Luisoni S, Johnsson K, Greber UF, Helenius A (2013) Investigating endocytic pathways to the endoplasmic reticulum and to the cytosol using SNAP-trap. *Traffic* **14:** 36-46

Genisyuerek S, Papatheodorou P, Guttenberg G, Schubert R, Benz R, Aktories K (2011) Structural determinants for membrane insertion, pore formation and translocation of *Clostridium difficile* toxin B. *Mol Microbiol* **79:** 1643-1654

Geny B, Popoff MR (2006) Bacterial protein toxins and lipids: pore formation or toxin entry into cells. *Biol Cell* **98:** 667-678

Ghosh G, Wang VY, Huang DB, Fusco A (2012) NF-kappaB regulation: lessons from structures. *Immunol Rev* **246:** 36-58

Ghosh S, May MJ, Kopp EB (1998) NF-kappa B and Rel proteins: evolutionarily conserved mediators of immune responses. *Annu Rev Immunol* **16:** 225-260

Gibson A, Futter CE, Maxwell S, Allchin EH, Shipman M, Kraehenbuhl JP, Domingo D, Odorizzi G, Trowbridge IS, Hopkins CR (1998) Sorting mechanisms regulating membrane protein traffic in the apical transcytotic pathway of polarized MDCK cells. *J Cell Biol* **143:** 81-94

Giesemann T, Jank T, Gerhard R, Maier E, Just I, Benz R, Aktories K (2006) Cholesterol-dependent pore formation of *Clostridium difficile* toxin A. *J Biol Chem* **281:** 10808-10815

Gill DM, Dinius LL (1971) Observations on the structure of diphtheria toxin. *J Biol Chem* **246:** 1485-1491

Gillooly DJ, Morrow IC, Lindsay M, Gould R, Bryant NJ, Gaullier JM, Parton RG, Stenmark H (2000) Localization of phosphatidylinositol 3-phosphate in yeast and mammalian cells. *EMBO J* **19:** 4577-4588

Gilmore TD, Wolenski FS (2012) NF-kappaB: where did it come from and why? *Immunol Rev* **246:** 14-35

Girod A, Storrie B, Simpson JC, Johannes L, Goud B, Roberts LM, Lord JM, Nilsson T, Pepperkok R (1999) Evidence for a COP-I-independent transport route from the Golgi complex to the endoplasmic reticulum. *Nat Cell Biol* **1:** 423-430

Glebov OO, Bright NA, Nichols BJ (2006) Flotillin-1 defines a clathrin-independent endocytic pathway in mammalian cells. *Nat Cell Biol* **8:** 46-54

Gomes MS, Sousa Fernandes S, Cordeiro JV, Silva Gomes S, Vieira A, Appelberg R (2008) Engagement of Toll-like receptor 2 in mouse macrophages infected with *Mycobacterium avium* induces non-oxidative and TNF-independent anti-mycobacterial activity. *Eur J Immunol* **38:** 2180-2189

Gordon VM, Leppla SH (1994) Proteolytic activation of bacterial toxins: role of bacterial and host cell proteases. *Infect Immun* **62:** 333-340

Gould GW, Lippincott-Schwartz J (2009) New roles for endosomes: from vesicular carriers to multi-purpose platforms. *Nat Rev Mol Cell Biol* **10:** 287-292

Grant BD, Donaldson JG (2009) Pathways and mechanisms of endocytic recycling. *Nat Rev Mol Cell Biol* **10:** 597-608

Grant CC, Messer RJ, Cieplak W, Jr. (1994) Role of trypsin-like cleavage at arginine 192 in the enzymatic and cytotonic activities of *Escherichia coli* heat-labile enterotoxin. *Infect Immun* **62:** 4270-4278

Gregers TF, Skanland SS, Walchli S, Bakke O, Sandvig K (2013) BiP negatively affects ricin transport. *Toxins (Basel)* **5:** 969-982

Gruenberg J, Stenmark H (2004) The biogenesis of multivesicular endosomes. *Nat Rev Mol Cell Biol* **5:** 317-323

Guidi-Rontani C, Weber-Levy M, Mock M, Cabiaux V (2000) Translocation of Bacillus anthracis lethal and oedema factors across endosome membranes. *Cell Microbiol* **2:** 259-264

Ha KH, Byun MS, Choi J, Jeong J, Lee KJ, Jue DM (2009) N-tosyl-L-phenylalanine chloromethyl ketone inhibits NF-kappaB activation by blocking specific cysteine residues of IkappaB kinase beta and p65/RelA. *Biochemistry* **48:** 7271-7278

Haase R, Kirschning CJ, Sing A, Schrottner P, Fukase K, Kusumoto S, Wagner H, Heesemann J, Ruckdeschel K (2003) A dominant role of Toll-like receptor 4 in the signaling of apoptosis in bacteria-faced macrophages. *J Immunol* **171:** 4294-4303

Hacker G (2000) The morphology of apoptosis. *Cell Tissue Res* **301:** 5-17

Haicheur N, Benchetrit F, Amessou M, Leclerc C, Falguieres T, Fayolle C, Bismuth E, Fridman WH, Johannes L, Tartour E (2003) The B subunit of Shiga toxin coupled to full-size antigenic protein elicits humoral and cell-mediated immune responses associated with a Th1-dominant polarization. *Int Immunol* **15:** 1161-1171

Haicheur N, Bismuth E, Bosset S, Adotevi O, Warnier G, Lacabanne V, Regnault A, Desaymard C, Amigorena S, Ricciardi-Castagnoli P, Goud B, Fridman WH, Johannes L, Tartour E (2000) The B subunit of Shiga toxin fused to a tumor antigen elicits CTL and targets dendritic cells to allow MHC class I-restricted presentation of peptides derived from exogenous antigens. *J Immunol* **165:** 3301-3308

Hailstones D, Sleer LS, Parton RG, Stanley KK (1998) Regulation of caveolin and caveolae by cholesterol in MDCK cells. *J Lipid Res* **39:** 369-379

Halaas O, Steigedal M, Haug M, Awuh JA, Ryan L, Brech A, Sato S, Husebye H, Cangelosi GA, Akira S, Strong RK, Espevik T, Flo TH (2010) Intracellular *Mycobacterium avium* intersect transferrin in the Rab11(+) recycling endocytic pathway and avoid lipocalin 2 trafficking to the lysosomal pathway. *J Infect Dis* **201:** 783-792

Halban PA, Irminger JC (1994) Sorting and processing of secretory proteins. *Biochem J* **299 (Pt 1):** 1-18

Hammond K, Caputo GA, London E (2002) Interaction of the membrane-inserted diphtheria toxin T domain with peptides and its possible implications for chaperone-like T domain behavior. *Biochemistry* **41:** 3243-3253

Han Y, Englert JA, Yang R, Delude RL, Fink MP (2005) Ethyl pyruvate inhibits nuclear factor-kappaB-dependent signaling by directly targeting p65. *J Pharmacol Exp Ther* **312:** 1097-1105

Hansen CG, Bright NA, Howard G, Nichols BJ (2009) SDPR induces membrane curvature and functions in the formation of caveolae. *Nat Cell Biol* **11:** 807-814

Hansen CG, Nichols BJ (2009) Molecular mechanisms of clathrin-independent endocytosis. *J Cell Sci* **122:** 1713-1721

Hansen GH, Dalskov SM, Rasmussen CR, Immerdal L, Niels-Christiansen LL, Danielsen EM (2005) Cholera toxin entry into pig enterocytes occurs via a lipid raft- and clathrin-dependent mechanism. *Biochemistry* **44:** 873-882

Harikumar KB, Kunnumakkara AB, Ahn KS, Anand P, Krishnan S, Guha S, Aggarwal BB (2009) Modification of the cysteine residues in IkappaBalpha kinase and NF-kappaB (p65) by xanthohumol leads to suppression of NF-kappaB-regulated gene products and potentiation of apoptosis in leukemia cells. *Blood* **113:** 2003-2013

Harper CB, Popoff MR, McCluskey A, Robinson PJ, Meunier FA (2013) Targeting membrane trafficking in infection prophylaxis: dynamin inhibitors. *Trends Cell Biol* **23:** 90-101

Harrington DJ (1996) Bacterial collagenases and collagen-degrading enzymes and their potential role in human disease. *Infect Immun* **64:** 1885-1891

Haug G, Leemhuis J, Tiemann D, Meyer DK, Aktories K, Barth H (2003) The host cell chaperone Hsp90 is essential for translocation of the binary *Clostridium botulinum* C2 toxin into the cytosol. *J Biol Chem* **278:** 32266-32274

Hawke JP, Plakas SM, Minton RV, McPhearson RM, Snider TG, Guarino AM (1987) Fish pasteurellosis of cultured striped bass (*Morone saxatilis*) in coastal Alabama. *Aquaculture* **65:** 193-204

Hayashibara M, London E (2005) Topography of diphtheria toxin A chain inserted into lipid vesicles. *Biochemistry* **44:** 2183-2196

Hayden MS, Ghosh S (2012) NF-kappaB, the first quarter-century: remarkable progress and outstanding questions. *Genes Dev* **26:** 203-234

Hayes CS, Aoki SK, Low DA (2010) Bacterial contact-dependent delivery systems. *Annu Rev Genet* **44:** 71-90

Hazes B, Read RJ (1997) Accumulating evidence suggests that several AB-toxins subvert the endoplasmic reticulum-associated protein degradation pathway to enter target cells. *Biochemistry* **36:** 11051-11054

Hehnly H, Sheff D, Stamnes M (2006) Shiga toxin facilitates its retrograde transport by modifying microtubule dynamics. *Mol Biol Cell* **17:** 4379-4389

Henkel JS, Baldwin MR, Barbieri JT (2010) Toxins from bacteria. *EXS* **100:** 1-29

Hill KK, Smith TJ, Helma CH, Ticknor LO, Foley BT, Svensson RT, Brown JL, Johnson EA, Smith LA, Okinaka RT, Jackson PJ, Marks JD (2007) Genetic diversity among Botulinum Neurotoxin-producing clostridial strains. *J Bacteriol* **189:** 818-832

Hinz M, Arslan SC, Scheidereit C (2012) It takes two to tango: IkappaBs, the multifunctional partners of NF-kappaB. *Immunol Rev* **246:** 59-76

Hoch DH, Romero-Mira M, Ehrlich BE, Finkelstein A, DasGupta BR, Simpson LL (1985) Channels formed by botulinum, tetanus, and diphtheria toxins in planar lipid bilayers: relevance to translocation of proteins across membranes. *Proc Natl Acad Sci U S A* **82:** 1692-1696

Holmgren J, Adamsson J, Anjuere F, Clemens J, Czerkinsky C, Eriksson K, Flach CF, George-Chandy A, Harandi AM, Lebens M, Lehner T, Lindblad M, Nygren E, Raghavan S, Sanchez J, Stanford M, Sun JB, Svennerholm AM, Tengvall S (2005) Mucosal adjuvants and anti-infection and anti-immunopathology vaccines based on cholera toxin, cholera toxin B subunit and CpG DNA. *Immunol Lett* **97:** 181-188

Holmgren J, Svennerholm AM, Lonnroth I, Fall-Persson M, Markman B, Lundbeck H (1977) Development of improved cholera vaccine based on subunit toxoid. *Nature* **269:** 602-604

Hsu LC, Park JM, Zhang K, Luo JL, Maeda S, Kaufman RJ, Eckmann L, Guiney DG, Karin M (2004) The protein kinase PKR is required for macrophage apoptosis after activation of Toll-like receptor 4. *Nature* **428:** 341-345

Hu CM, Fang RH, Luk BT, Zhang L (2013) Nanoparticle-detained toxins for safe and effective vaccination. *Nature nanotechnology* **8:** 933-938

Hu HY, Huynh PD, Murphy JR, vanderSpek JC (1998) The effects of helix breaking mutations in the diphtheria toxin transmembrane domain helix layers of the fusion toxin DAB389IL-2. *Protein Eng* **11:** 811-817

Huang B, Yang XD, Lamb A, Chen LF (2010) Posttranslational modifications of NF-kappaB: another layer of regulation for NF-kappaB signaling pathway. *Cell Signal* **22:** 1282-1290

Hunyady L, Baukal AJ, Gaborik Z, Olivares-Reyes JA, Bor M, Szaszak M, Lodge R, Catt KJ, Balla T (2002) Differential PI 3-kinase dependence of early and late phases of recycling of the internalized AT1 angiotensin receptor. *J Cell Biol* **157:** 1211-1222

Huotari J, Helenius A (2011) Endosome maturation. *EMBO J* **30:** 3481-3500

Huss M, Wieczorek H (2009) Inhibitors of V-ATPases: old and new players. *J Exp Biol* **212:** 341-346

Iacovache I, van der Goot FG, Pernot L (2008) Pore formation: an ancient yet complex form of attack. *Biochim Biophys Acta* **1778:** 1611-1623

Idziorek T, FitzGerald D, Pastan I (1990) Low pH-induced changes in *Pseudomonas* exotoxin and its domains: increased binding of Triton X-114. *Infect Immun* **58:** 1415-1420

Iglewski BH, Liu PV, Kabat D (1977) Mechanism of action of *Pseudomonas aeruginosa* exotoxin Aiadenosine diphosphate-ribosylation of mammalian elongation factor 2 in vitro and in vivo. *Infect Immun* **15:** 138-144

Itin C, Ulitzur N, Muhlbauer B, Pfeffer SR (1999) Mapmodulin, cytoplasmic dynein, and microtubules enhance the transport of mannose 6-phosphate receptors from endosomes to the trans-golgi network. *Mol Biol Cell* **10:** 2191-2197

Ivanov AI (2008) Pharmacological inhibition of endocytic pathways: is it specific enough to be useful? *Methods Mol Biol* **440:** 15-33

Izore T, Job V, Dessen A (2011) Biogenesis, regulation, and targeting of the type III secretion system. *Structure* **19:** 603-612

Jackson ME, Simpson JC, Girod A, Pepperkok R, Roberts LM, Lord JM (1999) The KDEL retrieval system is exploited by *Pseudomonas* exotoxin A, but not by Shiga-like toxin-1, during retrograde transport from the Golgi complex to the endoplasmic reticulum. *J Cell Sci* **112 (Pt 4):** 467-475

Jank T, Aktories K (2008) Structure and mode of action of clostridial glucosylating toxins: the ABCD model. *Trends Microbiol* **16:** 222-229

Jarosch E, Taxis C, Volkwein C, Bordallo J, Finley D, Wolf DH, Sommer T (2002) Protein dislocation from the ER requires polyubiquitination and the AAA-ATPase Cdc48. *Nat Cell Biol* **4:** 134-139

Jeon YJ, Han SB, Ahn KS, Kim HM (2000) Differential activation of murine macrophages by angelan and LPS. *Immunopharmacology* **49:** 275-284

Jiang JX, London E (1990) Involvement of denaturation-like changes in *Pseudomonas* exotoxin a hydrophobicity and membrane penetration determined by characterization of pH and thermal transitions. Roles of two distinct conformationally altered states. *J Biol Chem* **265:** 8636-8641

Johannes L, Decaudin D (2005) Protein toxins: intracellular trafficking for targeted therapy. *Gene Ther* **12:** 1360-1368

Johannes L, Romer W (2010) Shiga toxins--from cell biology to biomedical applications. *Nat Rev Microbiol* **8:** 105-116

Johnson LS, Dunn KW, Pytowski B, McGraw TE (1993) Endosome acidification and receptor trafficking: bafilomycin A1 slows receptor externalization by a mechanism involving the receptor's internalization motif. *Mol Biol Cell* **4:** 1251-1266

Jongeneel CV, Bouvier J, Bairoch A (1989) A unique signature identifies a family of zinc-dependent metallopeptidases. *FEBS Lett* **242:** 211-214

Jovic M, Sharma M, Rahajeng J, Caplan S (2010) The early endosome: a busy sorting station for proteins at the crossroads. *Histol Histopathol* **25:** 99-112

Just I, Selzer J, Wilm M, von Eichel-Streiber C, Mann M, Aktories K (1995) Glucosylation of Rho proteins by *Clostridium difficile* toxin B. *Nature* **375:** 500-503

Kagan BL, Finkelstein A, Colombini M (1981) Diphtheria toxin fragment forms large pores in phospholipid bilayer membranes. *Proc Natl Acad Sci U S A* **78:** 4950-4954

Kaiser E, Kroll C, Ernst K, Schwan C, Popoff M, Fischer G, Buchner J, Aktories K, Barth H (2011) Membrane translocation of binary actin-ADP-ribosylating toxins from *Clostridium difficile* and *Clostridium perfringens* is facilitated by cyclophilin A and Hsp90. *Infect Immun* **79:** 3913-3921

Kandadi MR, Frankel AE, Ren J (2012) Toll-like receptor 4 knockout protects against anthrax lethal toxin-induced cardiac contractile dysfunction: role of autophagy. *Br J Pharmacol* **167:** 612-626

Karczewski J, Zorman J, Wang S, Miezeiewski M, Xie J, Soring K, Petrescu I, Rogers I, Thiriot DS, Cook JC, Chamberlin M, Xoconostle RF, Nahas DD, Joyce JG, Bodmer JL, Heinrichs JH, Secore S (2014) Development of a recombinant toxin fragment vaccine for *Clostridium difficile* infection. *Vaccine* **32:** 2812-2818

Kelleher ZT, Matsumoto A, Stamler JS, Marshall HE (2007) NOS2 regulation of NF-kappaB by S-nitrosylation of p65. *J Biol Chem* **282:** 30667-30672

Kelly BT, McCoy AJ, Spate K, Miller SE, Evans PR, Honing S, Owen DJ (2008) A structural explanation for the binding of endocytic dileucine motifs by the AP2 complex. *Nature* **456:** 976-979

Kerfoot SM, Long EM, Hickey MJ, Andonegui G, Lapointe BM, Zanardo RC, Bonder C, James WG, Robbins SM, Kubes P (2004) TLR4 contributes to disease-inducing mechanisms resulting in central nervous system autoimmune disease. *J Immunol* **173:** 7070-7077

Kessler KR, Benecke R (1997) Botulinum toxin: from poison to remedy. *Neurotoxicology* **18:** 761-770

Khine AA, Lingwood CA (1994) Capping and receptor-mediated endocytosis of cell-bound verotoxin (Shiga-like toxin). 1: Chemical identification of an amino acid in the B subunit necessary for efficient receptor glycolipid binding and cellular internalization. *J Cell Physiol* **161:** 319-332

Kim K, Groman NB (1965) In vitro inhibition of diphtheria toxin action by ammonium salts and amines. *J Bacteriol* **90:** 1552-1556

Kirchhausen T (1999) Adaptors for clathrin-mediated traffic. *Annu Rev Cell Dev Biol* **15:** 705-732

Kirchhausen T (2000) Clathrin. *Annu Rev Biochem* **69:** 699-727

Kirchhausen T, Macia E, Pelish HE (2008) Use of dynasore, the small molecule inhibitor of dynamin, in the regulation of endocytosis. *Methods Enzymol* **438:** 77-93

Kirkham M, Parton RG (2005) Clathrin-independent endocytosis: new insights into caveolae and non-caveolar lipid raft carriers. *Biochim Biophys Acta* **1746:** 349-363

Kitchin NR (2011) Review of diphtheria, tetanus and pertussis vaccines in clinical development. *Expert review of vaccines* **10:** 605-615

Klausner RD, Ashwell G, van Renswoude J, Harford JB, Bridges KR (1983a) Binding of apotransferrin to K562 cells: explanation of the transferrin cycle. *Proc Natl Acad Sci U S A* **80:** 2263-2266

Klausner RD, Van Renswoude J, Ashwell G, Kempf C, Schechter AN, Dean A, Bridges KR (1983b) Receptor-mediated endocytosis of transferrin in K562 cells. *J Biol Chem* **258:** 4715-4724

Klimpel KR, Molloy SS, Thomas G, Leppla SH (1992) Anthrax toxin protective antigen is activated by a cell surface protease with the sequence specificity and catalytic properties of furin. *Proc Natl Acad Sci U S A* **89:** 10277-10281

Knight ZA, Chiang GG, Alaimo PJ, Kenski DM, Ho CB, Coan K, Abraham RT, Shokat KM (2004) Isoform-specific phosphoinositide 3-kinase inhibitors from an arylmorpholine scaffold. *Bioorganic & medicinal chemistry* **12:** 4749-4759

Knust Z, Blumenthal B, Aktories K, Schmidt G (2009) Cleavage of *Escherichia coli* cytotoxic necrotizing factor 1 is required for full biologic activity. *Infect Immun* **77:** 1835-1841

Kochi SK, Collier RJ (1993) DNA Fragmentation and Cytolysis in U937 Cells Treated with Diphtheria Toxin or Other Inhibitors of Protein Synthesis. *Experimental Cell Research* **208:** 296-302

Kochi SK, Martin I, Schiavo G, Mock M, Cabiaux V (1994) The effects of pH on the interaction of anthrax toxin lethal and edema factors with phospholipid vesicles. *Biochemistry* **33:** 2604-2609

Kong HJ, Moon JH, Moon JY, Kim JM, Nam BH, Kim YO, Kim WJ, Lee SJ (2011) Cloning and functional characterization of the p65 subunit of NF-kappaB from olive flounder (Paralichthys olivaceus). *Fish Shellfish Immunol* **30:** 406-411

Koopmann JO, Albring J, Huter E, Bulbuc N, Spee P, Neefjes J, Hammerling GJ, Momburg F (2000) Export of antigenic peptides from the endoplasmic reticulum intersects with retrograde protein translocation through the Sec61p channel. *Immunity* **13:** 117-127

Kothe M, Ye Y, Wagner JS, De Luca HE, Kern E, Rapoport TA, Lencer WI (2005) Role of p97 AAA-ATPase in the retrotranslocation of the cholera toxin A1 chain, a non-ubiquitinated substrate. *J Biol Chem* **280:** 28127-28132

Kounnas MZ, Morris RE, Thompson MR, FitzGerald DJ, Strickland DK, Saelinger CB (1992) The alpha 2-macroglobulin receptor/low density lipoprotein receptor-related protein binds and internalizes *Pseudomonas* exotoxin A. *J Biol Chem* **267:** 12420-12423

Kovbasnjuk O, Mourtazina R, Baibakov B, Wang T, Elowsky C, Choti MA, Kane A, Donowitz M (2005) The glycosphingolipid globotriaosylceramide in the metastatic transformation of colon cancer. *Proc Natl Acad Sci U S A* **102:** 19087-19092

Krantz BA, Finkelstein A, Collier RJ (2006) Protein translocation through the anthrax toxin transmembrane pore is driven by a proton gradient. *J Mol Biol* **355:** 968-979

Krantz BA, Melnyk RA, Zhang S, Juris SJ, Lacy DB, Wu Z, Finkelstein A, Collier RJ (2005) A phenylalanine clamp catalyzes protein translocation through the anthrax toxin pore. *Science* **309:** 777-781

Kreitman RJ (1999) Immunotoxins in cancer therapy. *Curr Opin Immunol* **11:** 570-578

Kreitman RJ (2006) Immunotoxins for targeted cancer therapy. *The AAPS journal* **8:** E532-551

Kreitman RJ (2009) Recombinant immunotoxins for the treatment of chemoresistant hematologic malignancies. *Curr Pharm Des* **15:** 2652-2664

Kreitman RJ, Pastan I (1995) Importance of the glutamate residue of KDEL in increasing the cytotoxicity of *Pseudomonas* exotoxin derivatives and for increased binding to the KDEL receptor. *Biochem J* **307 (Pt 1):** 29-37

Krieglstein KG, Henschen AH, Weller U, Habermann E (1991) Limited proteolysis of tetanus toxin. Relation to activity and identification of cleavage sites. *Eur J Biochem* **202:** 41-51

Krueger KM, Mende-Mueller LM, Barbieri JT (1991) Protease treatment of pertussis toxin identifies the preferential cleavage of the S1 subunit. *J Biol Chem* **266:** 8122-8128

Kumari S, Mg S, Mayor S (2010) Endocytosis unplugged: multiple ways to enter the cell. *Cell Res* **20:** 256-275

Kushnaryov VM, Sedmak JJ (1989) Effect of *Clostridium difficile* enterotoxin A on ultrastructure of Chinese hamster ovary cells. *Infect Immun* **57:** 3914-3921

Labruyere E, Mock M, Ladant D, Michelson S, Gilles AM, Laoide B, Barzu O (1990) Characterization of ATP and calmodulin-binding properties of a truncated form of *Bacillus anthracis* adenylate cyclase. *Biochemistry* **29:** 4922-4928

LaCasse EC, Bray MR, Patterson B, Lim WM, Perampalam S, Radvanyi LG, Keating A, Stewart AK, Buckstein R, Sandhu JS, Miller N, Banerjee D, Singh D, Belch AR, Pilarski LM, Gariepy J (1999) Shiga-like toxin-1 receptor on human breast cancer, lymphoma, and myeloma and absence from CD34(+) hematopoietic stem cells: implications for ex vivo tumor purging and autologous stem cell transplantation. *Blood* **94:** 2901-2910

LaCasse EC, Saleh MT, Patterson B, Minden MD, Gariepy J (1996) Shiga-like toxin purges human lymphoma from bone marrow of severe combined immunodeficient mice. *Blood* **88:** 1561-1567

Lacy DB, Wigelsworth DJ, Melnyk RA, Harrison SC, Collier RJ (2004) Structure of heptameric protective antigen bound to an anthrax toxin receptor: a role for receptor in pH-dependent pore formation. *Proc Natl Acad Sci U S A* **101:** 13147-13151

Ladant D, Michelson S, Sarfati R, Gilles AM, Predeleanu R, Barzu O (1989) Characterization of the calmodulin-binding and of the catalytic domains of *Bordetella pertussis* adenylate cyclase. *J Biol Chem* **264:** 4015-4020

Ladokhin AS (2013) pH-Triggered Conformational Switching along the Membrane Insertion Pathway of the Diphtheria Toxin T-Domain. *Toxins (Basel)* **5:** 1362-1380

Ladokhin AS, Legmann R, Collier RJ, White SH (2004) Reversible refolding of the diphtheria toxin T-domain on lipid membranes. *Biochemistry* **43:** 7451-7458

Laemmli UK (1970) Cleavage of structural proteins during the assembly of the head of bacteriophage T4. *Nature* **227:** 680-685

Laird MH, Rhee SH, Perkins DJ, Medvedev AE, Piao W, Fenton MJ, Vogel SN (2009) TLR4/MyD88/PI3K interactions regulate TLR4 signaling. *Journal of leukocyte biology* **85:** 966-977

Lakey JH, van der Goot FG, Pattus F (1994) All in the family: the toxic activity of pore-forming colicins. *Toxicology* **87:** 85-108

Lamaze C, Dujeancourt A, Baba T, Lo CG, Benmerah A, Dautry-Varsat A (2001) Interleukin 2 receptors and detergent-resistant membrane domains define a clathrin-independent endocytic pathway. *Mol Cell* **7:** 661-671

Lang AE, Neumeyer T, Sun J, Collier RJ, Benz R, Aktories K (2008) Amino acid residues involved in membrane insertion and pore formation of *Clostridium botulinum* C2 toxin. *Biochemistry* **47:** 8406-8413

Lang AE, Schmidt G, Schlosser A, Hey TD, Larrinua IM, Sheets JJ, Mannherz HG, Aktories K (2010) *Photorhabdus luminescens* toxins ADP-ribosylate actin and RhoA to force actin clustering. *Science* **327:** 1139-1142

Lauvrak SU, Torgersen ML, Sandvig K (2004) Efficient endosome-to-Golgi transport of Shiga toxin is dependent on dynamin and clathrin. *J Cell Sci* **117:** 2321-2331

Lauvrak SU, Walchli S, Iversen TG, Slagsvold HH, Torgersen ML, Spilsberg B, Sandvig K (2006) Shiga toxin regulates its entry in a Syk-dependent manner. *Mol Biol Cell* **17:** 1096-1109

Le Negrate G (2012) Subversion of innate immune responses by bacterial hindrance of NF-kappaB pathway. *Cell Microbiol* **14:** 155-167

Le Roy C, Wrana JL (2005) Clathrin- and non-clathrin-mediated endocytic regulation of cell signalling. *Nat Rev Mol Cell Biol* **6:** 112-126

Lee MS, Cherla RP, Tesh VL (2010) Shiga toxins: intracellular trafficking to the ER leading to activation of host cell stress responses. *Toxins (Basel)* **2:** 1515-1535

Lee RS, Tartour E, van der Bruggen P, Vantomme V, Joyeux I, Goud B, Fridman WH, Johannes L (1998) Major histocompatibility complex class I presentation of exogenous soluble tumor antigen fused to the B-fragment of Shiga toxin. *Eur J Immunol* **28:** 2726-2737

Lee SY, Lee MS, Cherla RP, Tesh VL (2008) Shiga toxin 1 induces apoptosis through the endoplasmic reticulum stress response in human monocytic cells. *Cell Microbiol* **10:** 770-780

Leka O, Vallese F, Pirazzini M, Berto P, Montecucco C, Zanotti G (2014) Diphtheria toxin conformational switching at acidic pH. *FEBS J* **281:** 2115-2122

Lemichez E, Barbieri JT (2013) General aspects and recent advances on bacterial protein toxins. *Cold Spring Harb Perspect Med* **3:** a013573

Lemichez E, Bomsel M, Devilliers G, vanderSpek J, Murphy JR, Lukianov EV, Olsnes S, Boquet P (1997) Membrane translocation of diphtheria toxin fragment A exploits early to late endosome trafficking machinery. *Mol Microbiol* **23:** 445-457

Lemonnier M, Landraud L, Lemichez E (2007) Rho GTPase-activating bacterial toxins: from bacterial virulence regulation to eukaryotic cell biology. *FEMS Microbiol Rev* **31:** 515-534

Lencer WI, Constable C, Moe S, Jobling MG, Webb HM, Ruston S, Madara JL, Hirst TR, Holmes RK (1995) Targeting of cholera toxin and *Escherichia coli* heat labile toxin in polarized epithelia: role of COOH-terminal KDEL. *J Cell Biol* **131:** 951-962

Lencer WI, Constable C, Moe S, Rufo PA, Wolf A, Jobling MG, Ruston SP, Madara JL, Holmes RK, Hirst TR (1997) Proteolytic activation of cholera toxin and *Escherichia coli* labile toxin by entry into host epithelial cells. Signal transduction by a protease-resistant toxin variant. *J Biol Chem* **272:** 15562-15568

Lencer WI, Saslowsky D (2005) Raft trafficking of AB5 subunit bacterial toxins. *Biochim Biophys Acta* **1746:** 314-321

Leppla S, Dorland RB, Middlebrook JL (1980) Inhibition of diphtheria toxin degradation and cytotoxic action by chloroquine. *J Biol Chem* **255:** 2247-2250

Leppla SH (1982) Anthrax toxin edema factor: a bacterial adenylate cyclase that increases cyclic AMP concentrations of eukaryotic cells. *Proc Natl Acad Sci U S A* **79:** 3162-3166

Li MF, Shi YL (2006) Toosendanin interferes with pore formation of botulinum toxin type A in PC12 cell membrane. *Acta Pharmacol Sin* **27:** 66-70

Li Q, Verma IM (2002) NF-kappaB regulation in the immune system. *Nat Rev Immunol* **2:** 725-734

Li YM, Vallera DA, Hall WA (2013) Diphtheria toxin-based targeted toxin therapy for brain tumors. *J Neurooncol* **114:** 155-164

Liang MC, Bardhan S, Pace EA, Rosman D, Beutler JA, Porco JA, Jr., Gilmore TD (2006) Inhibition of transcription factor NF-kappaB signaling proteins IKKbeta and p65 through specific cysteine residues by epoxyquinone A monomer: correlation with its anti-cancer cell growth activity. *Biochem Pharmacol* **71:** 634-645

Lieu ZZ, Gleeson PA (2010) Identification of different itineraries and retromer components for endosome-to-Golgi transport of TGN38 and Shiga toxin. *Eur J Cell Biol* **89:** 379-393

Lindmo K, Stenmark H (2006) Regulation of membrane traffic by phosphoinositide 3-kinases. *J Cell Sci* **119:** 605-614

Lingwood CA (1999) Glycolipid receptors for verotoxin and *Helicobacter pylori*: role in pathology. *Biochim Biophys Acta* **1455:** 375-386

Lingwood CA, Binnington B, Manis A, Branch DR (2010) Globotriaosyl ceramide receptor function - where membrane structure and pathology intersect. *FEBS Lett* **584:** 1879-1886

Lingwood CA, Khine AA, Arab S (1998) Globotriaosyl ceramide (Gb3) expression in human tumour cells: intracellular trafficking defines a new retrograde transport pathway from the cell surface to the nucleus, which correlates with sensitivity to verotoxin. *Acta Biochim Pol* **45:** 351-359

Liu ZG, Hsu H, Goeddel DV, Karin M (1996) Dissection of TNF receptor 1 effector functions: JNK activation is not linked to apoptosis while NF-kappaB activation prevents cell death. *Cell* **87:** 565-576

Lopez-Doriga MV, Barnes AC, dos Santos NM, Ellis AE (2000) Invasion of fish epithelial cells by *Photobacterium damselae* subsp. *piscicida*: evidence for receptor specificity, and effect of capsule and serum. *Microbiology* **146 (Pt 1):** 21-30

Lord JM, Deeks E, Marsden CJ, Moore K, Pateman C, Smith DC, Spooner RA, Watson P, Roberts LM (2003) Retrograde transport of toxins across the endoplasmic reticulum membrane. *Biochem Soc Trans* **31:** 1260-1262

Loregian A, Papini E, Satin B, Marsden HS, Hirst TR, Palu G (1999) Intranuclear delivery of an antiviral peptide mediated by the B subunit of *Escherichia coli* heat-labile enterotoxin. *Proc Natl Acad Sci U S A* **96:** 5221-5226

Lottenberg R, Minning-Wenz D, Boyle MD (1994) Capturing host plasmin(ogen): a common mechanism for invasive pathogens? *Trends Microbiol* **2:** 20-24

Macia E, Ehrlich M, Massol R, Boucrot E, Brunner C, Kirchhausen T (2006) Dynasore, a cell-permeable inhibitor of dynamin. *Dev Cell* **10:** 839-850

Madshus IH (1994) The N-terminal alpha-helix of fragment B of diphtheria toxin promotes translocation of fragment A into the cytoplasm of eukaryotic cells. *J Biol Chem* **269:** 17723-17729

Madshus IH, Wiedlocha A, Sandvig K (1994) Intermediates in translocation of diphtheria toxin across the plasma membrane. *J Biol Chem* **269:** 4648-4652

Magariños B, Bonet R, Romalde JL, Martinez MJ, Congregado F, Toranzo AE (1996a) Influence of the capsular layer on the virulence of *Pasteurella piscicida* for fish. *Microb Pathog* **21:** 289-297

Magariños B, Romalde JL, Bandin I, Fouz B, Toranzo AE (1992a) Phenotypic, antigenic, and molecular characterization of *Pasteurella piscicida* strains isolated from fish. *Appl Environ Microbiol* **58:** 3316-3322

Magariños B, Romalde JL, Lemos ML, Barja JL, Toranzo AE (1994) Iron uptake by *Pasteurella piscicida* and its role in pathogenicity for fish. *Appl Environ Microbiol* **60:** 2990-2998

Magariños B, Romalde JL, Noya M, Barja JL, Toranzo AE (1996b) Adherence and invasive capacities of the fish pathogen *Pasteurella piscicida*. *FEMS Microbiol Lett* **138:** 29-34

Magariños B, Santos Y, Romalde JL, Rivas C, Barja JL, Toranzo AE (1992b) Pathogenic activities of live cells and extracellular products of the fish pathogen *Pasteurella piscicida*. *J Gen Microbiol* **138:** 2491-2498

Magariños B, Toranzo AE, Romalde JL (1996c) Phenotypic and pathobiological characteristics of *Pasteurella piscicida*. *Annual Review of Fish Diseases* **6:** 41-64

Magnani E, Bettini E (2000) Resazurin detection of energy metabolism changes in serum-starved PC12 cells and of neuroprotective agent effect. *Brain Res Brain Res Protoc* **5:** 266-272

Mallard F, Antony C, Tenza D, Salamero J, Goud B, Johannes L (1998) Direct pathway from early/recycling endosomes to the Golgi apparatus revealed through the study of shiga toxin B-fragment transport. *J Cell Biol* **143:** 973-990

Mallet WG, Maxfield FR (1999) Chimeric forms of furin and TGN38 are transported with the plasma membrane in the trans-Golgi network via distinct endosomal pathways. *J Cell Biol* **146:** 345-359

Marcello A, Loregian A, Cross A, Marsden H, Hirst TR, Palu G (1994) Specific inhibition of herpes virus replication by receptor-mediated entry of an antiviral peptide linked to *Escherichia coli* enterotoxin B subunit. *Proc Natl Acad Sci U S A* **91:** 8994-8998

Marcil A, Gadoury C, Ash J, Zhang J, Nantel A, Whiteway M (2008) Analysis of PRA1 and its relationship to *Candida albicans*- macrophage interactions. *Infect Immun* **76:** 4345-4358

Marlovits TC, Stebbins CE (2010) Type III secretion systems shape up as they ship out. *Curr Opin Microbiol* **13:** 47-52

Massey S, Burress H, Taylor M, Nemec KN, Ray S, Haslam DB, Teter K (2011) Structural and functional interactions between the cholera toxin A1 subunit and ERdj3/HEDJ, a chaperone of the endoplasmic reticulum. *Infect Immun* **79:** 4739-4747

Massol RH, Larsen JE, Fujinaga Y, Lencer WI, Kirchhausen T (2004) Cholera toxin toxicity does not require functional Arf6- and dynamin-dependent endocytic pathways. *Mol Biol Cell* **15:** 3631-3641

Maxfield FR, McGraw TE (2004) Endocytic recycling. *Nat Rev Mol Cell Biol* **5:** 121-132

May KL, Yan Q, Tumer NE (2013) Targeting ricin to the ribosome. *Toxicon* **69:** 143-151

Mayle KM, Le AM, Kamei DT (2012) The intracellular trafficking pathway of transferrin. *Biochim Biophys Acta* **1820:** 264-281

Mayor S, Pagano RE (2007) Pathways of clathrin-independent endocytosis. *Nat Rev Mol Cell Biol* **8:** 603-612

McCormick JK, Yarwood JM, Schlievert PM (2001) Toxic shock syndrome and bacterial superantigens: an update. *Annu Rev Microbiol* **55:** 77-104

McIntosh D, Timar J, Davies AJ (1990) The intracellular movement and cycling of ricin. *Eur J Cell Biol* **52:** 77-86

McIntosh DP, Edwards DC, Davies AJ (1984) Transfer of ricin toxicity by spleen cells. *Toxicon* **22:** 293-299

McKee ML, FitzGerald DJ (1999) Reduction of furin-nicked *Pseudomonas* exotoxin A: an unfolding story. *Biochemistry* **38:** 16507-16513

McKenzie J, Johannes L, Taguchi T, Sheff D (2009) Passage through the Golgi is necessary for Shiga toxin B subunit to reach the endoplasmic reticulum. *FEBS J* **276:** 1581-1595

McKenzie JE, Raisley B, Zhou X, Naslavsky N, Taguchi T, Caplan S, Sheff D (2012) Retromer guides STxB and CD8-M6PR from early to recycling endosomes, EHD1 guides STxB from recycling endosome to Golgi. *Traffic* **13:** 1140-1159

McMahon HT, Boucrot E (2011) Molecular mechanism and physiological functions of clathrin-mediated endocytosis. *Nat Rev Mol Cell Biol* **12:** 517-533

Mellits KH, Hay RT, Goodbourn S (1993) Proteolytic degradation of MAD3 (I kappa B alpha) and enhanced processing of the NF-kappa B precursor p105 are obligatory steps in the activation of NF-kappa B. *Nucleic Acids Res* **21:** 5059-5066

Mellman I (1996) Endocytosis and molecular sorting. *Annu Rev Cell Dev Biol* **12:** 575-625

Menard A, Altendorf K, Breves D, Mock M, Montecucco C (1996) The vacuolar ATPase proton pump is required for the cytotoxicity of *Bacillus anthracis* lethal toxin. *FEBS Lett* **386:** 161-164

Mercurio F, DiDonato JA, Rosette C, Karin M (1993) p105 and p98 precursor proteins play an active role in NF-kappa B-mediated signal transduction. *Genes Dev* **7:** 705-718

Mere J, Morlon-Guyot J, Bonhoure A, Chiche L, Beaumelle B (2005) Acid-triggered membrane insertion of *Pseudomonas* exotoxin A involves an original mechanism based on pH-regulated tryptophan exposure. *J Biol Chem* **280:** 21194-21201

Merritt EA, Hol WG (1995) AB5 toxins. *Curr Opin Struct Biol* **5:** 165-171

Meyer E, Aglyamova GV, Wang S, Buchanan-Carter J, Abrego D, Colbourne JK, Willis BL, Matz MV (2009) Sequencing and de novo analysis of a coral larval transcriptome using 454 GSFlx. *BMC Genomics* **10:** 219

Middlebrook JL, Dorland RB, Leppla SH (1978) Association of diphtheria toxin with Vero cells. Demonstration of a receptor. *J Biol Chem* **253:** 7325-7330

Milne JC, Collier RJ (1993) pH-dependent permeabilization of the plasma membrane of mammalian cells by anthrax protective antigen. *Mol Microbiol* **10:** 647-653

Mindell JA, Silverman JA, Collier RJ, Finkelstein A (1994) Structure function relationships in diphtheria toxin channels: II. A residue responsible for the channel's dependence on trans pH. *J Membr Biol* **137:** 29-44

Mogridge J, Cunningham K, Lacy DB, Mourez M, Collier RJ (2002) The lethal and edema factors of anthrax toxin bind only to oligomeric forms of the protective antigen. *Proc Natl Acad Sci U S A* **99:** 7045-7048

Moisenovich M, Tonevitsky A, Maljuchenko N, Kozlovskaya N, Agapov I, Volknandt W, Bereiter-Hahn J (2004) Endosomal ricin transport: involvement of Rab4- and Rab5-positive compartments. *Histochem Cell Biol* **121:** 429-439

Molloy SS, Thomas L, VanSlyke JK, Stenberg PE, Thomas G (1994) Intracellular trafficking and activation of the furin proprotein convertase: localization to the TGN and recycling from the cell surface. *EMBO J* **13:** 18-33

Montecucco C (1998) Protein toxins and membrane transport. *Curr Opin Cell Biol* **10:** 530-536

Montecucco C, Papini E (1995) Cell penetration of bacterial protein toxins. *Trends Microbiol* **3:** 165-167; discussion 167-168

Montecucco C, Papini E, Schiavo G (1994) Bacterial protein toxins penetrate cells via a four-step mechanism. *FEBS Lett* **346:** 92-98

Montecucco C, Schiavo G, Tomasi M (1985) pH-dependence of the phospholipid interaction of diphtheria-toxin fragments. *Biochem J* **231:** 123-128

Moreau D, Kumar P, Wang SC, Chaumet A, Chew SY, Chevalley H, Bard F (2011) Genome-wide RNAi screens identify genes required for Ricin and PE intoxications. *Dev Cell* **21:** 231-244

Morlon-Guyot J, Mere J, Bonhoure A, Beaumelle B (2009) Processing of *Pseudomonas aeruginosa* exotoxin A is dispensable for cell intoxication. *Infect Immun* **77:** 3090-3099

Morris RE, Saelinger CB (1983) Diphtheria toxin does not enter resistant cells by receptor-mediated endocytosis. *Infect Immun* **42:** 812-817

Morris RE, Saelinger CB (1986) Reduced temperature alters *Pseudomonas* exotoxin A entry into the mouse LM cell. *Infect Immun* **52:** 445-453

Mortimer EA, Jr. (1978) Immunization against infectious disease. *Science* **200:** 902-907

Moskaug JO, Sandvig K, Olsnes S (1988) Low pH-induced release of diphtheria toxin A-fragment in Vero cells. Biochemical evidence for transfer to the cytosol. *J Biol Chem* **263:** 2518-2525

Moya M, Dautry-Varsat A, Goud B, Louvard D, Boquet P (1985) Inhibition of coated pit formation in Hep2 cells blocks the cytotoxicity of diphtheria toxin but not that of ricin toxin. *J Cell Biol* **101:** 548-559

Muhlen S, Ruchaud-Sparagano MH, Kenny B (2011) Proteasome-independent degradation of canonical NFkappaB complex components by the NleC protein of pathogenic *Escherichia coli*. *J Biol Chem* **286:** 5100-5107

Mukherjee S, Ghosh RN, Maxfield FR (1997) Endocytosis. *Physiol Rev* **77:** 759-803

Muller-Alouf H, Carnoy C, Simonet M, Alouf JE (2001) Superantigen bacterial toxins: state of the art. *Toxicon* **39:** 1691-1701

Murk JL, Humbel BM, Ziese U, Griffith JM, Posthuma G, Slot JW, Koster AJ, Verkleij AJ, Geuze HJ, Kleijmeer MJ (2003) Endosomal compartmentalization in three dimensions: implications for membrane fusion. *Proc Natl Acad Sci U S A* **100:** 13332-13337

Murphy JR (2011) Mechanism of Diphtheria Toxin Catalytic Domain Delivery to the Eukaryotic Cell Cytosol and the Cellular Factors that Directly Participate in the Process. *Toxins (Basel)* **3:** 294-308

Murray LJ, Habeshaw JA, Wiels J, Greaves MF (1985) Expression of Burkitt lymphoma-associated antigen (defined by the monoclonal antibody 38.13) on both normal and malignant germinal-centre B cells. *Int J Cancer* **36:** 561-565

Murshid A, Presley JF (2004) ER-to-Golgi transport and cytoskeletal interactions in animal cells. *Cell Mol Life Sci* **61:** 133-145

Na YJ, Han SB, Kang JS, Yoon YD, Park SK, Kim HM, Yang KH, Joe CO (2004) Lactoferrin works as a new LPS-binding protein in inflammatory activation of macrophages. *Int Immunopharmacol* **4:** 1187-1199

Nabi IR, Le PU (2003) Caveolae/raft-dependent endocytosis. *J Cell Biol* **161:** 673-677

Naglich JG, Metherall JE, Russell DW, Eidels L (1992) Expression cloning of a diphtheria toxin receptor: identity with a heparin-binding EGF-like growth factor precursor. *Cell* **69:** 1051-1061

Nascimento DS, do Vale A, Tomas AM, Zou J, Secombes CJ, dos Santos NM (2007a) Cloning, promoter analysis and expression in response to bacterial exposure of sea bass (Dicentrarchus labrax L.) interleukin-12 p40 and p35 subunits. *Mol Immunol* **44:** 2277-2291

Nascimento DS, Pereira PJ, Reis MI, do Vale A, Zou J, Silva MT, Secombes CJ, dos Santos NM (2007b) Molecular cloning and expression analysis of sea bass (*Dicentrarchus labrax* L.) tumor necrosis factor-alpha (TNF-alpha). *Fish Shellfish Immunol* **23:** 701-710

Nassi S, Collier RJ, Finkelstein A (2002) PA63 channel of anthrax toxin: an extended beta-barrel. *Biochemistry* **41:** 1445-1450

Natoli G, Costanzo A, Guido F, Moretti F, Levrero M (1998) Apoptotic, non-apoptotic, and anti-apoptotic pathways of tumor necrosis factor signalling. *Biochem Pharmacol* **56:** 915-920

Naughtin MJ, Sheffield DA, Rahman P, Hughes WE, Gurung R, Stow JL, Nandurkar HH, Dyson JM, Mitchell CA (2010) The myotubularin phosphatase MTMR4 regulates sorting from early endosomes. *J Cell Sci* **123:** 3071-3083

Neish AS, Naumann M (2011) Microbial-induced immunomodulation by targeting the NF-kappaB system. *Trends Microbiol* **19:** 596-605

Nery FC, Armata IA, Farley JE, Cho JA, Yaqub U, Chen P, da Hora CC, Wang Q, Tagaya M, Klein C, Tannous B, Caldwell KA, Caldwell GA, Lencer WI, Ye Y, Breakefield XO (2011) TorsinA participates in endoplasmic reticulum-associated degradation. *Nat Commun* **2:** 393

Nichols B (2003) Caveosomes and endocytosis of lipid rafts. *J Cell Sci* **116:** 4707-4714

Nichols BJ, Kenworthy AK, Polishchuk RS, Lodge R, Roberts TH, Hirschberg K, Phair RD, Lippincott-Schwartz J (2001) Rapid cycling of lipid raft markers between the cell surface and Golgi complex. *J Cell Biol* **153:** 529-541

Nichols BJ, Lippincott-Schwartz J (2001) Endocytosis without clathrin coats. *Trends Cell Biol* **11:** 406-412

Nishikawa S, Brodsky JL, Nakatsukasa K (2005) Roles of molecular chaperones in endoplasmic reticulum (ER) quality control and ER-associated degradation (ERAD). *J Biochem* **137:** 551-555

Noya M, Lamas J (1997) Response of eosinophilic granule cells of gilthead seabream (*Sparus aurata, Teleostei*) to bacteria and bacterial products. *Cell Tissue Res* **287:** 223-230

Noya M, Magariños B, Lamas J (1995a) Interactions between peritoneal exudate cells (PECs) of gilthead seabream (*Sparus aurata*) and *Pasteurella piscicida*. A morphological study. *Aquaculture* **131:** 11-21

Noya M, Magariños B, Toranzo AE, Lamas J (1995b) Sequential pathology of experimental pasteurellosis in gilthead seabream *Sparus aurata*. A light- and electron-microscopic study. *Dis Aquat Org* **21:** 177-186

O'Keefe DO, Cabiaux V, Choe S, Eisenberg D, Collier RJ (1992) pH-dependent insertion of proteins into membranes: B-chain mutation of diphtheria toxin that inhibits membrane translocation, Glu-349----Lys. *Proc Natl Acad Sci U S A* **89:** 6202-6206

Oberoi TK, Dogan T, Hocking JC, Scholz RP, Mooz J, Anderson CL, Karreman C, Meyer zu Heringdorf D, Schmidt G, Ruonala M, Namikawa K, Harms GS, Carpy A, Macek B, Koster RW, Rajalingam K (2012) IAPs regulate the plasticity of cell migration by directly targeting Rac1 for degradation. *EMBO J* **31:** 14-28

Odumosu O, Nicholas D, Yano H, Langridge W (2010) AB toxins: a paradigm switch from deadly to desirable. *Toxins (Basel)* **2:** 1612-1645

Oeckinghaus A, Ghosh S (2009) The NF-kappaB family of transcription factors and its regulation. *Cold Spring Harb Perspect Biol* **1:** a000034

Ogata M, Chaudhary VK, Pastan I, FitzGerald DJ (1990) Processing of *Pseudomonas* exotoxin by a cellular protease results in the generation of a 37,000-Da toxin fragment that is translocated to the cytosol. *J Biol Chem* **265:** 20678-20685

Ogata M, Fryling CM, Pastan I, FitzGerald DJ (1992) Cell-mediated cleavage of *Pseudomonas* exotoxin between Arg279 and Gly280 generates the enzymatically active fragment which translocates to the cytosol. *J Biol Chem* **267:** 25396-25401

Oh KJ, Senzel L, Collier RJ, Finkelstein A (1999) Translocation of the catalytic domain of diphtheria toxin across planar phospholipid bilayers by its own T domain. *Proc Natl Acad Sci U S A* **96:** 8467-8470

Ohkuma S, Poole B (1978) Fluorescence probe measurement of the intralysosomal pH in living cells and the perturbation of pH by various agents. *Proc Natl Acad Sci U S A* **75:** 3327-3331

Ohmori H, Toyama S (1992) Direct proof that the primary site of action of cytochalasin on cell motility processes is actin. *J Cell Biol* **116:** 933-941

Olsnes S, Moskaug JO, Stenmark H, Sandvig K (1990) Translocation of diphtheria toxin to the cytosol and formation of cation selective channels. *J Physiol (Paris)* **84:** 191-196

Olsnes S, Sandvig K (1988) How protein toxins enter and kill cells. *Cancer Treat Res* **37:** 39-73

Orlandi PA, Fishman PH (1998) Filipin-dependent inhibition of cholera toxin: evidence for toxin internalization and activation through caveolae-like domains. *J Cell Biol* **141:** 905-915

Orth JD, McNiven MA (2006) Get off my back! Rapid receptor internalization through circular dorsal ruffles. *Cancer Res* **66:** 11094-11096

Orth K (2002) Function of the Yersinia effector YopJ. *Curr Opin Microbiol* **5:** 38-43

Overholtzer M, Mailleux AA, Mouneimne G, Normand G, Schnitt SJ, King RW, Cibas ES, Brugge JS (2007) A nonapoptotic cell death process, entosis, that occurs by cell-in-cell invasion. *Cell* **131:** 966-979

Pace CN, Vajdos F, Fee L, Grimsley G, Gray T (1995) How to measure and predict the molar absorption coefficient of a protein. *Protein Sci* **4:** 2411-2423

Panchuk-Voloshina N, Haugland RP, Bishop-Stewart J, Bhalgat MK, Millard PJ, Mao F, Leung WY, Haugland RP (1999) Alexa dyes, a series of new fluorescent dyes that yield exceptionally bright, photostable conjugates. *The journal of histochemistry and cytochemistry : official journal of the Histochemistry Society* **47:** 1179-1188

Papatheodorou P, Zamboglou C, Genisyuerek S, Guttenberg G, Aktories K (2010) Clostridial glucosylating toxins enter cells via clathrin-mediated endocytosis. *PLoS One* **5:** e10673

Papini E, Rappuoli R, Murgia M, Montecucco C (1993) Cell penetration of diphtheria toxin. Reduction of the interchain disulfide bridge is the rate-limiting step of translocation in the cytosol. *J Biol Chem* **268:** 1567-1574

Papini E, Sandona D, Rappuoli R, Montecucco C (1988) On the membrane translocation of diphtheria toxin: at low pH the toxin induces ion channels on cells. *EMBO J* **7:** 3353-3359

Park JM, Ng VH, Maeda S, Rest RF, Karin M (2004) Anthrolysin O and other gram-positive cytolysins are toll-like receptor 4 agonists. *J Exp Med* **200:** 1647-1655

Parton RG, Joggerst B, Simons K (1994) Regulated internalization of caveolae. *J Cell Biol* **127:** 1199-1215

Parton RG, Simons K (2007) The multiple faces of caveolae. *Nat Rev Mol Cell Biol* **8:** 185-194

Pastan I, Chaudhary V, FitzGerald DJ (1992) Recombinant toxins as novel therapeutic agents. *Annu Rev Biochem* **61:** 331-354

Pastan I, Hassan R, Fitzgerald DJ, Kreitman RJ (2006) Immunotoxin therapy of cancer. *Nat Rev Cancer* **6:** 559-565

Pastan I, Hassan R, FitzGerald DJ, Kreitman RJ (2007) Immunotoxin treatment of cancer. *Annu Rev Med* **58:** 221-237

Pelkmans L, Helenius A (2002) Endocytosis via caveolae. *Traffic* **3:** 311-320

Pelkmans L, Kartenbeck J, Helenius A (2001) Caveolar endocytosis of simian virus 40 reveals a new two-step vesicular-transport pathway to the ER. *Nat Cell Biol* **3:** 473-483

Pelkmans L, Puntener D, Helenius A (2002) Local actin polymerization and dynamin recruitment in SV40-induced internalization of caveolae. *Science* **296:** 535-539

Perkins ND (2012) The diverse and complex roles of NF-kappaB subunits in cancer. *Nat Rev Cancer* 12: 121-132

Petosa C, Collier RJ, Klimpel KR, Leppla SH, Liddington RC (1997) Crystal structure of the anthrax toxin protective antigen. *Nature* **385:** 833-838

Pilon M, Schekman R, Romisch K (1997) Sec61p mediates export of a misfolded secretory protein from the endoplasmic reticulum to the cytosol for degradation. *EMBO J* **16:** 4540-4548

Pimental RA, Christensen KA, Krantz BA, Collier RJ (2004) Anthrax toxin complexes: heptameric protective antigen can bind lethal factor and edema factor simultaneously. *Biochem Biophys Res Commun* **322:** 258-262

Pinto RD, da Silva DV, Pereira PJ, dos Santos NM (2012) Molecular cloning and characterization of sea bass (*Dicentrarchus labrax, L.*) Tapasin. *Fish Shellfish Immunol* **32:** 110-120

Pirazzini M, Rossetto O, Bolognese P, Shone CC, Montecucco C (2011) Double anchorage to the membrane and intact inter-chain disulfide bond are required for the low pH induced entry of tetanus and botulinum neurotoxins into neurons. *Cell Microbiol* **13:** 1731-1743

Popoff MR (2005) Bacterial exotoxins. *Contrib Microbiol* **12:** 28-54

Popoff V, Mardones GA, Tenza D, Rojas R, Lamaze C, Bonifacino JS, Raposo G, Johannes L (2007) The retromer complex and clathrin define an early endosomal retrograde exit site. *J Cell Sci* **120:** 2022-2031

Porgador A, Staats HF, Itoh Y, Kelsall BL (1998) Intranasal immunization with cytotoxic T-lymphocyte epitope peptide and mucosal adjuvant cholera toxin: selective augmentation of peptide-presenting dendritic cells in nasal mucosa-associated lymphoid tissue. *Infect Immun* **66:** 5876-5881

Potala S, Sahoo SK, Verma RS (2008) Targeted therapy of cancer using diphtheria toxin-derived immunotoxins. *Drug Discov Today* **13:** 807-815

Poulos C, Bakopoulos V, Zolota V, Dimitriadis GJ (2004) Histopathological findings after sea bass (*Dicentrarhus labrax L.*) exposure to extracellular products of Photobacterium damsela subsp. piscicida produced in vivo. *Aquaculture Research* **35:** 931-936

Praefcke GJ, McMahon HT (2004) The dynamin superfamily: universal membrane tubulation and fission molecules? *Nat Rev Mol Cell Biol* **5:** 133-147

Pruitt RN, Lacy DB (2012) Toward a structural understanding of *Clostridium difficile* toxins A and B. *Front Cell Infect Microbiol* **2:** 28

Pucadyil TJ, Schmid SL (2008) Real-time visualization of dynamin-catalyzed membrane fission and vesicle release. *Cell* **135:** 1263-1275

Puhar A, Johnson EA, Rossetto O, Montecucco C (2004) Comparison of the pH-induced conformational change of different clostridial neurotoxins. *Biochem Biophys Res Commun* **319:** 66-71

Puhar A, Montecucco C (2007) Where and how do anthrax toxins exit endosomes to intoxicate host cells? *Trends Microbiol* **15:** 477-482

Qa'Dan M, Spyres LM, Ballard JD (2000) pH-induced conformational changes in *Clostridium difficile* toxin B. *Infect Immun* **68:** 2470-2474

Quinn CP, Singh Y, Klimpel KR, Leppla SH (1991) Functional mapping of anthrax toxin lethal factor by in-frame insertion mutagenesis. *J Biol Chem* **266:** 20124-20130

Rahman MM, McFadden G (2011) Modulation of NF-kappaB signalling by microbial pathogens. *Nat Rev Microbiol* **9:** 291-306

Raiborg C, Schink KO, Stenmark H (2013) Class III phosphatidylinositol 3-kinase and its catalytic product PtdIns3P in regulation of endocytic membrane traffic. *FEBS J* **280:** 2730-2742

Rainey GJ, Wigelsworth DJ, Ryan PL, Scobie HM, Collier RJ, Young JA (2005) Receptor-specific requirements for anthrax toxin delivery into cells. *Proc Natl Acad Sci U S A* **102:** 13278-13283

Rao K, van Renswoude J, Kempf C, Klausner RD (1983) Separation of Fe+3 from transferrin in endocytosis. Role of the acidic endosome. *FEBS Lett* **160:** 213-216

Ratts R, Trujillo C, Bharti A, vanderSpek J, Harrison R, Murphy JR (2005) A conserved motif in transmembrane helix 1 of diphtheria toxin mediates catalytic domain delivery to the cytosol. *Proc Natl Acad Sci U S A* **102:** 15635-15640

Ratts R, Zeng H, Berg EA, Blue C, McComb ME, Costello CE, vanderSpek JC, Murphy JR (2003) The cytosolic entry of diphtheria toxin catalytic domain requires a host cell cytosolic translocation factor complex. *J Cell Biol* **160:** 1139-1150

Ren J, Kachel K, Kim H, Malenbaum SE, Collier RJ, London E (1999) Interaction of diphtheria toxin T domain with molten globule-like proteins and its implications for translocation. *Science* **284:** 955-957

Ren Y, Savill J (1998) Apoptosis: the importance of being eaten. *Cell Death Differ* **5:** 563-568

Robbins AR, Oliver C, Bateman JL, Krag SS, Galloway CJ, Mellman I (1984) A single mutation in Chinese hamster ovary cells impairs both Golgi and endosomal functions. *J Cell Biol* **99:** 1296-1308

Rodal SK, Skretting G, Garred O, Vilhardt F, van Deurs B, Sandvig K (1999) Extraction of cholesterol with methyl-beta-cyclodextrin perturbs formation of clathrin-coated endocytic vesicles. *Mol Biol Cell* **10:** 961-974

Rodighiero C, Tsai B, Rapoport TA, Lencer WI (2002) Role of ubiquitination in retro-translocation of cholera toxin and escape of cytosolic degradation. *EMBO Rep* **3:** 1222-1227

Romalde JL (2002) *Photobacterium damselae* subsp. *piscicida*: an integrated view of a bacterial fish pathogen. *Int Microbiol* **5:** 3-9

Rombout JH, Huttenhuis HB, Picchietti S, Scapigliati G (2005) Phylogeny and ontogeny of fish leucocytes. *Fish Shellfish Immunol* **19:** 441-455

Romer W, Berland L, Chambon V, Gaus K, Windschiegl B, Tenza D, Aly MR, Fraisier V, Florent JC, Perrais D, Lamaze C, Raposo G, Steinem C, Sens P, Bassereau P, Johannes L (2007) Shiga toxin induces tubular membrane invaginations for its uptake into cells. *Nature* **450:** 670-675

Rosado CJ, Kondos S, Bull TE, Kuiper MJ, Law RH, Buckle AM, Voskoboinik I, Bird PI, Trapani JA, Whisstock JC, Dunstone MA (2008) The MACPF/CDC family of pore-forming toxins. *Cell Microbiol* **10:** 1765-1774

Rossetto O, de Bernard M, Pellizzari R, Vitale G, Caccin P, Schiavo G, Montecucco C (2000) Bacterial toxins with intracellular protease activity. *Clin Chim Acta* **291:** 189-199

Rossjohn J, Polekhina G, Feil SC, Morton CJ, Tweten RK, Parker MW (2007) Structures of perfringolysin O suggest a pathway for activation of cholesterol-dependent cytolysins. *J Mol Biol* **367:** 1227-1236

Roth TF, Porter KR (1964) Yolk Protein Uptake in the Oocyte of the Mosquito Aedes Aegypti. L. *J Cell Biol* **20:** 313-332

Rothberg KG, Heuser JE, Donzell WC, Ying YS, Glenney JR, Anderson RG (1992) Caveolin, a protein component of caveolae membrane coats. *Cell* **68:** 673-682

Rothberg KG, Ying YS, Kamen BA, Anderson RG (1990) Cholesterol controls the clustering of the glycophospholipid-anchored membrane receptor for 5-methyltetrahydrofolate. *J Cell Biol* **111:** 2931-2938

Roux A, Antonny B (2008) The long and short of membrane fission. *Cell* **135:** 1163-1165

Roux E, Yersin A (1888) Contribution à l´étude de la diphthérie. *Ann Inst Pasteur* **2:** 629-661

Ruckdeschel K, Mannel O, Richter K, Jacobi CA, Trulzsch K, Rouot B, Heesemann J (2001) *Yersinia* outer protein P of *Yersinia enterocolitic*a simultaneously blocks the nuclear factor-kappa B pathway and exploits lipopolysaccharide signaling to trigger apoptosis in macrophages. *J Immunol* **166:** 1823-1831

Rupnik M, Pabst S, von Eichel-Streiber C, Urlaub H, Soling HD (2005) Characterization of the cleavage site and function of resulting cleavage fragments after limited proteolysis of *Clostridium difficile* toxin B (TcdB) by host cells. *Microbiology* **151:** 199-208

Sachdev GP, Brownstein AD, Fruton JS (1973) N-methyl-2-anilinonaphthalene-6-sulfonyl peptides as fluorescent probes for pepsin-substrate interaction. *J Biol Chem* **248:** 6292-6299

Saint-Pol A, Yelamos B, Amessou M, Mills IG, Dugast M, Tenza D, Schu P, Antony C, McMahon HT, Lamaze C, Johannes L (2004) Clathrin adaptor epsinR is required for retrograde sorting on early endosomal membranes. *Dev Cell* **6:** 525-538

Sampath P, Pollard TD (1991) Effects of cytochalasin, phalloidin, and pH on the elongation of actin filaments. *Biochemistry* **30:** 1973-1980

Sandur SK, Ichikawa H, Sethi G, Ahn KS, Aggarwal BB (2006) Plumbagin (5-hydroxy-2-methyl-1,4-naphthoquinone) suppresses NF-kappaB activation and NF-kappaB-regulated gene products through modulation of p65 and IkappaBalpha kinase activation, leading to potentiation of apoptosis induced by cytokine and chemotherapeutic agents. *J Biol Chem* **281:** 17023-17033

Sandvig K, Bergan J, Dyve AB, Skotland T, Torgersen ML (2009) Endocytosis and retrograde transport of Shiga toxin. *Toxicon*

Sandvig K, Garred O, Holm PK, van Deurs B (1993) Endocytosis and intracellular transport of protein toxins. *Biochem Soc Trans* **21 (Pt 3):** 707-711

Sandvig K, Garred O, Prydz K, Kozlov JV, Hansen SH, van Deurs B (1992) Retrograde transport of endocytosed Shiga toxin to the endoplasmic reticulum. *Nature* **358:** 510-512

Sandvig K, Garred O, van Deurs B (1996) Thapsigargin-induced transport of cholera toxin to the endoplasmic reticulum. *Proc Natl Acad Sci U S A* **93:** 12339-12343

Sandvig K, Grimmer S, Lauvrak SU, Torgersen ML, Skretting G, van Deurs B, Iversen TG (2002) Pathways followed by ricin and Shiga toxin into cells. *Histochem Cell Biol* **117:** 131-141

Sandvig K, Moskaug JO (1987) *Pseudomonas* toxin binds triton X-114 at low pH. *Biochem J* **245:** 899-901

Sandvig K, Olsnes S (1979) Effect of temperature on the uptake, excretion and degradation of abrin and ricin by HeLa cells. *Exp Cell Res* **121:** 15-25

Sandvig K, Olsnes S (1980) Diphtheria toxin entry into cells is facilitated by low pH. *J Cell Biol* **87:** 828-832

Sandvig K, Olsnes S (1981) Rapid entry of nicked diphtheria toxin into cells at low pH. Characterization of the entry process and effects of low pH on the toxin molecule. *J Biol Chem* **256:** 9068-9076

Sandvig K, Olsnes S (1982) Entry of the toxic proteins abrin, modeccin, ricin, and diphtheria toxin into cells. II. Effect of pH, metabolic inhibitors, and ionophores and evidence for toxin penetration from endocytotic vesicles. *J Biol Chem* **257:** 7504-7513

Sandvig K, Olsnes S (1988) Diphtheria toxin-induced channels in Vero cells selective for monovalent cations. *J Biol Chem* **263:** 12352-12359

Sandvig K, Olsnes S, Brown JE, Petersen OW, van Deurs B (1989) Endocytosis from coated pits of Shiga toxin: a glycolipid-binding protein from *Shigella dysenteriae* 1. *J Cell Biol* **108:** 1331-1343

Sandvig K, Olsnes S, Petersen OW, van Deurs B (1987) Acidification of the cytosol inhibits endocytosis from coated pits. *J Cell Biol* **105:** 679-689

Sandvig K, Pust S, Skotland T, van Deurs B (2011) Clathrin-independent endocytosis: mechanisms and function. *Curr Opin Cell Biol* **23:** 413-420

Sandvig K, Ryd M, Garred O, Schweda E, Holm PK, van Deurs B (1994) Retrograde transport from the Golgi complex to the ER of both Shiga toxin and the nontoxic Shiga B-fragment is regulated by butyric acid and cAMP. *J Cell Biol* **126:** 53-64

Sandvig K, Skotland T, van Deurs B, Klokk TI (2013) Retrograde transport of protein toxins through the Golgi apparatus. *Histochem Cell Biol* **140:** 317-326

Sandvig K, Spilsberg B, Lauvrak SU, Torgersen ML, Iversen TG, van Deurs B (2004) Pathways followed by protein toxins into cells. *Int J Med Microbiol* **293:** 483-490

Sandvig K, Sundan A, Olsnes S (1984) Evidence that diphtheria toxin and modeccin enter the cytosol from different vesicular compartments. *J Cell Biol* **98:** 963-970

Sandvig K, Torgersen ML, Engedal N, Skotland T, Iversen TG (2010) Protein toxins from plants and bacteria: probes for intracellular transport and tools in medicine. *FEBS Lett* **584:** 2626-2634

Sandvig K, Torgersen ML, Raa HA, van Deurs B (2008) Clathrin-independent endocytosis: from nonexisting to an extreme degree of complexity. *Histochem Cell Biol* **129:** 267-276

Sandvig K, van Deurs B (1990) Selective modulation of the endocytic uptake of ricin and fluid phase markers without alteration in transferrin endocytosis. *J Biol Chem* **265:** 6382-6388

Sandvig K, van Deurs B (1996) Endocytosis, intracellular transport, and cytotoxic action of Shiga toxin and ricin. *Physiol Rev* **76:** 949-966

Sandvig K, van Deurs B (1999) Endocytosis and intracellular transport of ricin: recent discoveries. *FEBS Lett* **452:** 67-70

Sandvig K, van Deurs B (2000) Entry of ricin and Shiga toxin into cells: molecular mechanisms and medical perspectives. *EMBO J* **19:** 5943-5950

Sandvig K, van Deurs B (2002a) Membrane traffic exploited by protein toxins. *Annu Rev Cell Dev Biol* **18:** 1-24

Sandvig K, van Deurs B (2002b) Transport of protein toxins into cells: pathways used by ricin, cholera toxin and Shiga toxin. *FEBS Lett* **529:** 49-53

Sandvig K, van Deurs B (2005) Delivery into cells: lessons learned from plant and bacterial toxins. *Gene Ther* **12:** 865-872

Saslowsky DE, Cho JA, Chinnapen H, Massol RH, Chinnapen DJ, Wagner JS, De Luca HE, Kam W, Paw BH, Lencer WI (2010) Intoxication of zebrafish and mammalian cells by cholera toxin depends on the flotillin/reggie proteins but not Derlin-1 or -2. *J Clin Invest* **120:** 4399-4409

Scapigliati G, Romano N, Buonocore F, Picchietti S, Baldassini MR, Prugnoli D, Galice A, Meloni S, Secombes CJ, Mazzini M, Abelli L (2002) The immune system of sea bass, *Dicentrarchus labrax*, reared in aquaculture. *Developmental and comparative immunology* **26:** 151-160

Schiavo G, Papini E, Genna G, Montecucco C (1990) An intact interchain disulfide bond is required for the neurotoxicity of tetanus toxin. *Infect Immun* **58:** 4136-4141

Schiff PB, Fant J, Horwitz SB (1979) Promotion of microtubule assembly in vitro by taxol. *Nature* **277:** 665-667

Schindelin J, Arganda-Carreras I, Frise E, Kaynig V, Longair M, Pietzsch T, Preibisch S, Rueden C, Saalfeld S, Schmid B, Tinevez JY, White DJ, Hartenstein V, Eliceiri K, Tomancak P, Cardona A (2012) Fiji: an open-source platform for biological-image analysis. *Nat Methods* **9:** 676-682

Schlezinger JJ, Blickarz CE, Mann KK, Doerre S, Stegeman JJ (2000) Identification of NF-kappaB in the marine fish *Stenotomus chrysops* and examination of its activation by aryl hydrocarbon receptor agonists. *Chem Biol Interact* **126:** 137-157

Schmid A, Benz R, Just I, Aktories K (1994) Interaction of *Clostridium botulinum* C2 toxin with lipid bilayer membranes. Formation of cation-selective channels and inhibition of channel function by chloroquine. *J Biol Chem* **269:** 16706-16711

Schmid EM, Ford MG, Burtey A, Praefcke GJ, Peak-Chew SY, Mills IG, Benmerah A, McMahon HT (2006) Role of the AP2 beta-appendage hub in recruiting partners for clathrin-coated vesicle assembly. *PLoS Biol* **4:** e262

Schmid EM, McMahon HT (2007) Integrating molecular and network biology to decode endocytosis. *Nature* **448:** 883-888

Schmid SL, McNiven MA, De Camilli P (1998) Dynamin and its partners: a progress report. *Curr Opin Cell Biol* **10:** 504-512

Schmitz A, Herrgen H, Winkeler A, Herzog V (2000) Cholera toxin is exported from microsomes by the Sec61p complex. *J Cell Biol* **148:** 1203-1212

Scobie HM, Young JA (2005) Interactions between anthrax toxin receptors and protective antigen. *Curr Opin Microbiol* **8:** 106-112

Seetharam S, Chaudhary VK, FitzGerald D, Pastan I (1991) Increased cytotoxic activity of Pseudomonas exotoxin and two chimeric toxins ending in KDEL. *J Biol Chem* **266:** 17376-17381

Sen N, Paul BD, Gadalla MM, Mustafa AK, Sen T, Xu R, Kim S, Snyder SH (2012) Hydrogen sulfide-linked sulfhydration of NF-kappaB mediates its antiapoptotic actions. *Mol Cell* **45:** 13-24

Sen R, Baltimore D (1986) Multiple nuclear factors interact with the immunoglobulin enhancer sequences. *Cell* **46:** 705-716

Sever S, Damke H, Schmid SL (2000) Dynamin:GTP controls the formation of constricted coated pits, the rate limiting step in clathrin-mediated endocytosis. *J Cell Biol* **150:** 1137-1148

Shapira A, Benhar I (2010) Toxin-based therapeutic approaches. *Toxins (Basel)* **2:** 2519-2583

Sheff D, Pelletier L, O'Connell CB, Warren G, Mellman I (2002) Transferrin receptor recycling in the absence of perinuclear recycling endosomes. *J Cell Biol* **156:** 797-804

Shen A (2010) Autoproteolytic activation of bacterial toxins. *Toxins (Basel)* **2:** 963-977

Shen Y, Hendershot LM (2005) ERdj3, a stress-inducible endoplasmic reticulum DnaJ homologue, serves as a cofactor for BiP's interactions with unfolded substrates. *Mol Biol Cell* **16:** 40-50

Shinzato C, Shoguchi E, Kawashima T, Hamada M, Hisata K, Tanaka M, Fujie M, Fujiwara M, Koyanagi R, Ikuta T, Fujiyama A, Miller DJ, Satoh N (2011) Using the *Acropora digitifera* genome to understand coral responses to environmental change. *Nature* **476:** 320-323

Shone CC, Hambleton P, Melling J (1987) A 50-kDa fragment from the NH2-terminus of the heavy subunit of *Clostridium botulinum* type A neurotoxin forms channels in lipid vesicles. *Eur J Biochem* **167:** 175-180

Silva DS, Pereira LM, Moreira AR, Ferreira-da-Silva F, Brito RM, Faria TQ, Zornetta I, Montecucco C, Oliveira P, Azevedo JE, Pereira PJ, Macedo-Ribeiro S, do Vale A, dos Santos NM (2013) The apoptogenic toxin AIP56 is a metalloprotease A-B toxin that cleaves NF-kappab P65. *PLoS Pathog* **9:** e1003128

Silva MT, A. do Vale, and N.M. dos Santos (2010) AIP56: a novel bacterial apoptogenic toxin. *Toxins, Review* **2:** 905-918

Silva MT, do Vale A, dos Santos NM (2008) Secondary necrosis in multicellular animals: an outcome of apoptosis with pathogenic implications. *Apoptosis* **13:** 463-482

Silverman JA, Mindell JA, Finkelstein A, Shen WH, Collier RJ (1994a) Mutational analysis of the helical hairpin region of diphtheria toxin transmembrane domain. *J Biol Chem* **269:** 22524-22532

Silverman JA, Mindell JA, Zhan H, Finkelstein A, Collier RJ (1994b) Structure-function relationships in diphtheria toxin channels: I. Determining a minimal channel-forming domain. *J Membr Biol* **137:** 17-28

Simpson JC, Smith DC, Roberts LM, Lord JM (1998) Expression of mutant dynamin protects cells against diphtheria toxin but not against ricin. *Exp Cell Res* **239:** 293-300

Singh Y, Chaudhary VK, Leppla SH (1989) A deleted variant of *Bacillus anthracis* protective antigen is non-toxic and blocks anthrax toxin action in vivo. *J Biol Chem* **264:** 19103-19107

Sixma TK, Kalk KH, van Zanten BA, Dauter Z, Kingma J, Witholt B, Hol WG (1993a) Refined structure of *Escherichia coli* heat-labile enterotoxin, a close relative of cholera toxin. *J Mol Biol* **230:** 890-918

Sixma TK, Stein PE, Hol WG, Read RJ (1993b) Comparison of the B-pentamers of heat-labile enterotoxin and verotoxin-1: two structures with remarkable similarity and dissimilarity. *Biochemistry* **32:** 191-198

Skretting G, Torgersen ML, van Deurs B, Sandvig K (1999) Endocytic mechanisms responsible for uptake of GPI-linked diphtheria toxin receptor. *J Cell Sci* **112 (Pt 22):** 3899-3909

Smale ST (2012) Dimer-specific regulatory mechanisms within the NF-kappaB family of transcription factors. *Immunol Rev* **246:** 193-204

Smith DC, Lord JM, Roberts LM, Tartour E, Johannes L (2002) 1st class ticket to class I: protein toxins as pathfinders for antigen presentation. *Traffic* **3:** 697-704

Smith DC, Spooner RA, Watson PD, Murray JL, Hodge TW, Amessou M, Johannes L, Lord JM, Roberts LM (2006) Internalized *Pseudomonas* exotoxin A can exploit multiple pathways to reach the endoplasmic reticulum. *Traffic* **7:** 379-393

Sokolowska I, Walchli S, Wegrzyn G, Sandvig K, Slominska-Wojewodzka M (2011) A single point mutation in ricin A-chain increases toxin degradation and inhibits EDEM1-dependent ER retrotranslocation. *Biochem J* **436:** 371-385

Solan NJ, Miyoshi H, Carmona EM, Bren GD, Paya CV (2002) RelB cellular regulation and transcriptional activity are regulated by p100. *J Biol Chem* **277:** 1405-1418

Song J, Gao X, Galan JE (2013) Structure and function of the *Salmonella Typhi* chimaeric A(2)B(5) typhoid toxin. *Nature* **499:** 350-354

Songer JG (1997) Bacterial phospholipases and their role in virulence. *Trends Microbiol* **5:** 156-161

Sonnichsen B, De Renzis S, Nielsen E, Rietdorf J, Zerial M (2000) Distinct membrane domains on endosomes in the recycling pathway visualized by multicolor imaging of Rab4, Rab5, and Rab11. *J Cell Biol* **149:** 901-914

Spangler BD (1992) Structure and function of cholera toxin and the related *Escherichia coli* heat-labile enterotoxin. *Microbiol Rev* **56:** 622-647

Spiro DJ, Boll W, Kirchhausen T, Wessling-Resnick M (1996) Wortmannin alters the transferrin receptor endocytic pathway in vivo and in vitro. *Mol Biol Cell* **7:** 355-367

Spooner RA, Hart PJ, Cook JP, Pietroni P, Rogon C, Hohfeld J, Roberts LM, Lord JM (2008) Cytosolic chaperones influence the fate of a toxin dislocated from the endoplasmic reticulum. *Proc Natl Acad Sci U S A* **105:** 17408-17413

Spooner RA, Lord JM (2012) How ricin and Shiga toxin reach the cytosol of target cells: retrotranslocation from the endoplasmic reticulum. *Curr Top Microbiol Immunol* **357:** 19-40

Spooner RA, Watson PD, Marsden CJ, Smith DC, Moore KA, Cook JP, Lord JM, Roberts LM (2004) Protein disulphide-isomerase reduces ricin to its A and B chains in the endoplasmic reticulum. *Biochem J* **383:** 285-293

Springer JE, Azbill RD, Carlson SL (1998) A rapid and sensitive assay for measuring mitochondrial metabolic activity in isolated neural tissue. *Brain Res Brain Res Protoc* **2:** 259-263

Stan RV (2002) Structure and function of endothelial caveolae. *Microsc Res Tech* **57:** 350-364

Stanley AC, Wong CX, Micaroni M, Venturato J, Khromykh T, Stow JL, Lacy P (2014) The Rho GTPase Rac1 is required for recycling endosome-mediated secretion of TNF in macrophages. *Immunol Cell Biol* **92:** 275-286

Jianjun Sun (2012) Roles of Cellular Redox Factors in Pathogen and Toxin Entry in the Endocytic Pathways, Molecular Regulation of Endocytosis, Dr. Brian Ceresa (Ed.), ISBN: 978-953-51-0662-3, InTech, DOI: 10.5772/50087

Sun JB, Holmgren J, Czerkinsky C (1994) Cholera toxin B subunit: an efficient transmucosal carrier-delivery system for induction of peripheral immunological tolerance. *Proc Natl Acad Sci U S A* **91:** 10795-10799

Sun JB, Xiao BG, Lindblad M, Li BL, Link H, Czerkinsky C, Holmgren J (2000) Oral administration of cholera toxin B subunit conjugated to myelin basic protein protects against experimental autoimmune encephalomyelitis by inducing transforming growth factor-beta-secreting cells and suppressing chemokine expression. *Int Immunol* **12:** 1449-1457

Sun SC (2011) Non-canonical NF-kappaB signaling pathway. *Cell Res* **21:** 71-85

Sun SC (2012b) The noncanonical NF-kappaB pathway. *Immunol Rev* **246:** 125-140

Tacchi L, Casadei E, Bickerdike R, Secombes CJ, Martin SA (2011) Cloning and expression analysis of the mitochondrial ubiquitin ligase activator of NF-kappaB (MULAN) in Atlantic salmon (*Salmo salar*). *Mol Immunol* **49:** 558-565

Taga S, Mangeney M, Tursz T, Wiels J (1995) Differential regulation of glycosphingolipid biosynthesis in phenotypically distinct Burkitt's lymphoma cell lines. *Int J Cancer* **61:** 261-267

Tak PP, Firestein GS (2001) NF-kappaB: a key role in inflammatory diseases. *J Clin Invest* 107: 7-11

Tamayo AG, Bharti A, Trujillo C, Harrison R, Murphy JR (2008) COPI coatomer complex proteins facilitate the translocation of anthrax lethal factor across vesicular membranes in vitro. *Proc Natl Acad Sci U S A* **105:** 5254-5259

Tana LR, Ho M, Wilson BA (2013) Determinants of pH-dependent modulation of translocation in dermonecrotic G-protein-deamidating toxins. *Toxins (Basel)* **5:** 1167-1179

Taupiac MP, Alami M, Beaumelle B (1996) Translocation of full-length *Pseudomonas* exotoxin from endosomes is driven by ATP hydrolysis but requires prior exposure to acidic pH. *J Biol Chem* **271:** 26170-26173

Taylor M, Navarro-Garcia F, Huerta J, Burress H, Massey S, Ireton K, Teter K (2010) Hsp90 is required for transfer of the cholera toxin A1 subunit from the endoplasmic reticulum to the cytosol. *J Biol Chem* **285:** 31261-31267

Tcatchoff L, Andersson S, Utskarpen A, Klokk TI, Skanland SS, Pust S, Gerke V, Sandvig K (2012) Annexin A1 and A2: roles in retrograde trafficking of Shiga toxin. *PLoS One* **7:** e40429

Tesh VL (2010) Induction of apoptosis by Shiga toxins. *Future Microbiol* **5:** 431-453

Teter K, Jobling MG, Sentz D, Holmes RK (2006) The cholera toxin A1(3) subdomain is essential for interaction with ADP-ribosylation factor 6 and full toxic activity but is not required for translocation from the endoplasmic reticulum to the cytosol. *Infect Immun* **74:** 2259-2267

Theuer CP, Buchner J, FitzGerald D, Pastan I (1993) The N-terminal region of the 37-kDa translocated fragment of *Pseudomonas* exotoxin A aborts translocation by promoting its own export after microsomal membrane insertion. *Proc Natl Acad Sci U S A* **90:** 7774-7778

Thoren KL, Krantz BA (2011) The unfolding story of anthrax toxin translocation. *Mol Microbiol* **80:** 588-595

Thune RL, Stanley LA, Cooper RK (1993) Pathogenesis of gram-negative bacterial infections in warmwater fish. *Annual Review of Fish Diseases* **3:** 37-68

Todhunter DA, Hall WA, Rustamzadeh E, Shu Y, Doumbia SO, Vallera DA (2004) A bispecific immunotoxin (DTAT13) targeting human IL-13 receptor (IL-13R) and urokinase-type plasminogen activator receptor (uPAR) in a mouse xenograft model. *Protein engineering, design & selection : PEDS* **17:** 157-164

Toei M, Saum R, Forgac M (2010) Regulation and isoform function of the V-ATPases. *Biochemistry* **49:** 4715-4723

Tonello F, Naletto L, Romanello V, Dal Molin F, Montecucco C (2004) Tyrosine-728 and glutamic acid-735 are essential for the metalloproteolytic activity of the lethal factor of *Bacillus anthracis. Biochem Biophys Res Commun* **313:** 496-502

Toranzo AE, Barreiro Sn, Casal JF, Figueras A, Magariños B, Barja JL (1991) Pasteurellosis in cultured gilthead seabream (*Sparus aurata*): first report in Spain. *Aquaculture* **99:** 1-15

Torgersen ML, Engedal N, Pedersen AM, Husebye H, Espevik T, Sandvig K (2010) Toll-like receptor 4 facilitates binding of Shiga toxin to colon carcinoma and primary umbilical vein endothelial cells. *FEMS Immunol Med Microbiol* **61:** 63-75

Torgersen ML, Skretting G, van Deurs B, Sandvig K (2001) Internalization of cholera toxin by different endocytic mechanisms. *J Cell Sci* **114:** 3737-3747

Torgersen ML, Walchli S, Grimmer S, Skanland SS, Sandvig K (2007) Protein kinase Cdelta is activated by Shiga toxin and regulates its transport. *J Biol Chem* **282:** 16317-16328

Torrino S, Visvikis O, Doye A, Boyer L, Stefani C, Munro P, Bertoglio J, Gacon G, Mettouchi A, Lemichez E (2011) The E3 ubiquitin-ligase HACE1 catalyzes the ubiquitylation of active Rac1. *Dev Cell* **21:** 959-965

Trujillo C, Taylor-Parker J, Harrison R, Murphy JR (2010) Essential lysine residues within transmembrane helix 1 of diphtheria toxin facilitate COPI binding and catalytic domain entry. *Mol Microbiol* **76:** 1010-1019

Trůper HG, De'clari L (1997) Taxonomic Note: Necessary Correction of Specific Epithets Formed as Substantives (Nouns) “in Apposition”. *Int J Syst Bacteriol* **47:** 908–909

Tsai B, Rapoport TA (2002) Unfolded cholera toxin is transferred to the ER membrane and released from protein disulfide isomerase upon oxidation by Ero1. *J Cell Biol* **159:** 207-216

Tsai B, Rodighiero C, Lencer WI, Rapoport TA (2001) Protein disulfide isomerase acts as a redox-dependent chaperone to unfold cholera toxin. *Cell* **104:** 937-948

Tse SM, Furuya W, Gold E, Schreiber AD, Sandvig K, Inman RD, Grinstein S (2003) Differential role of actin, clathrin, and dynamin in Fc gamma receptor-mediated endocytosis and phagocytosis. *J Biol Chem* **278:** 3331-3338

Tsuneoka M, Nakayama K, Hatsuzawa K, Komada M, Kitamura N, Mekada E (1993) Evidence for involvement of furin in cleavage and activation of diphtheria toxin. *J Biol Chem* **268:** 26461-26465

Turton K, Chaddock JA, Acharya KR (2002) Botulinum and tetanus neurotoxins: structure, function and therapeutic utility. *Trends Biochem Sci* **27:** 552-558

Umata T, Moriyama Y, Futai M, Mekada E (1990) The cytotoxic action of diphtheria toxin and its degradation in intact Vero cells are inhibited by bafilomycin A1, a specific inhibitor of vacuolar-type H(+)-ATPase. *J Biol Chem* **265:** 21940-21945

Utskarpen A, Massol R, van Deurs B, Lauvrak SU, Kirchhausen T, Sandvig K (2010) Shiga toxin increases formation of clathrin-coated pits through Syk kinase. *PLoS One* **5:** e10944

Vallabhapurapu S, Karin M (2009) Regulation and function of NF-kappaB transcription factors in the immune system. *Annu Rev Immunol* **27:** 693-733

van Dam EM, Stoorvogel W (2002) Dynamin-dependent transferrin receptor recycling by endosome-derived clathrin-coated vesicles. *Mol Biol Cell* **13:** 169-182

van Dam EM, Ten Broeke T, Jansen K, Spijkers P, Stoorvogel W (2002) Endocytosed transferrin receptors recycle via distinct dynamin and phosphatidylinositol 3-kinase-dependent pathways. *J Biol Chem* **277:** 48876-48883

van den Akker F, Sarfaty S, Twiddy EM, Connell TD, Holmes RK, Hol WG (1996) Crystal structure of a new heat-labile enterotoxin, LT-IIb. *Structure* **4:** 665-678

van der Goot FG, Gruenberg J (2006) Intra-endosomal membrane traffic. *Trends Cell Biol* **16:** 514-521

van der Goot G, Young JA (2009) Receptors of anthrax toxin and cell entry. *Mol Aspects Med* **30:** 406-412

van Deurs B, Tonnessen TI, Petersen OW, Sandvig K, Olsnes S (1986) Routing of internalized ricin and ricin conjugates to the Golgi complex. *J Cell Biol* **102:** 37-47

van Weert AW, Dunn KW, Geuze HJ, Maxfield FR, Stoorvogel W (1995) Transport from late endosomes to lysosomes, but not sorting of integral membrane proteins in endosomes, depends on the vacuolar proton pump. *J Cell Biol* **130:** 821-834

vanderSpek JC, Howland K, Friedman T, Murphy JR (1994) Maintenance of the hydrophobic face of the diphtheria toxin amphipathic transmembrane helix 1 is essential for the efficient delivery of the catalytic domain to the cytosol of target cells. *Protein Eng* **7:** 985-989

Vanhaesebroeck B, Guillermet-Guibert J, Graupera M, Bilanges B (2010) The emerging mechanisms of isoform-specific PI3K signalling. *Nat Rev Mol Cell Biol* **11:** 329-341

Vasquez RJ, Howell B, Yvon AM, Wadsworth P, Cassimeris L (1997) Nanomolar concentrations of nocodazole alter microtubule dynamic instability in vivo and in vitro. *Mol Biol Cell* **8:** 973-985

Visvikis O, Maddugoda MP, Lemichez E (2010) Direct modifications of Rho proteins: deconstructing GTPase regulation. *Biol Cell* **102:** 377-389

Vlahos CJ, Matter WF, Hui KY, Brown RF (1994) A specific inhibitor of phosphatidylinositol 3-kinase, 2-(4-morpholinyl)-8-phenyl-4H-1-benzopyran-4-one (LY294002). *J Biol Chem* **269:** 5241-5248

Wainszelbaum MJ, Proctor BM, Pontow SE, Stahl PD, Barbieri MA (2006) IL4/PGE2 induction of an enlarged early endosomal compartment in mouse macrophages is Rab5-dependent. *Exp Cell Res* **312:** 2238-2251

Walchli S, Aasheim HC, Skanland SS, Spilsberg B, Torgersen ML, Rosendal KR, Sandvig K (2009) Characterization of clathrin and Syk interaction upon Shiga toxin binding. *Cell Signal* **21:** 1161-1168

Walchli S, Skanland SS, Gregers TF, Lauvrak SU, Torgersen ML, Ying M, Kuroda S, Maturana A, Sandvig K (2008) The Mitogen-activated protein kinase p38 links Shiga Toxin-dependent signaling and trafficking. *Mol Biol Cell* **19:** 95-104

Wang CY, Mayo MW, Baldwin AS, Jr. (1996a) TNF- and cancer therapy-induced apoptosis: potentiation by inhibition of NF-kappaB. *Science* **274:** 784-787

Wang L, Zhou ZC, Guo CJ, Rao XY, Xiao J, Weng SP, Yin ZX, Yu XQ, He JG (2009) The alpha inhibitor of NF-kappaB (IkappaBalpha) from the mandarin fish binds with p65 NF-kappaB. *Fish Shellfish Immunol* **26:** 473-482

Wang LH, Rothberg KG, Anderson RG (1993) Mis-assembly of clathrin lattices on endosomes reveals a regulatory switch for coated pit formation. *J Cell Biol* **123:** 1107-1117

Wang XM, Mock M, Ruysschaert JM, Cabiaux V (1996b) Secondary structure of anthrax lethal toxin proteins and their interaction with large unilamellar vesicles: a fourier-transform infrared spectroscopy approach. *Biochemistry* **35:** 14939-14946

Wang XM, Wattiez R, Mock M, Falmagne P, Ruysschaert JM, Cabiaux V (1997) Structure and interaction of PA63 and EF (edema toxin) of *Bacillus anthracis* with lipid membrane. *Biochemistry* **36:** 14906-14913

Wang XW, Tan NS, Ho B, Ding JL (2006) Evidence for the ancient origin of the NF-kappaB/IkappaB cascade: its archaic role in pathogen infection and immunity. *Proc Natl Acad Sci U S A* **103:** 4204-4209

Watanabe M, Nakashima M, Togano T, Higashihara M, Watanabe T, Umezawa K, Horie R (2008) Identification of the RelA domain responsible for action of a new NF-kappaB inhibitor DHMEQ. *Biochem Biophys Res Commun* **376:** 310-314

Watson P, Spooner RA (2006) Toxin entry and trafficking in mammalian cells. *Adv Drug Deliv Rev* **58:** 1581-1596

Wedekind JE, Trame CB, Dorywalska M, Koehl P, Raschke TM, McKee M, FitzGerald D, Collier RJ, McKay DB (2001) Refined crystallographic structure of *Pseudomonas aeruginosa* exotoxin A and its implications for the molecular mechanism of toxicity. *J Mol Biol* **314:** 823-837

Wei W, Lu Q, Chaudry GJ, Leppla SH, Cohen SN (2006) The LDL receptor-related protein LRP6 mediates internalization and lethality of anthrax toxin. *Cell* **124:** 1141-1154

Weldon JE, Pastan I (2011) A guide to taming a toxin--recombinant immunotoxins constructed from Pseudomonas exotoxin A for the treatment of cancer. *FEBS J* **278:** 4683-4700

Weller U, Dauzenroth ME, Meyer zu Heringdorf D, Habermann E (1989) Chains and fragments of tetanus toxin. Separation, reassociation and pharmacological properties. *Eur J Biochem* **182:** 649-656

Wernick NL, Chinnapen DJ, Cho JA, Lencer WI (2010) Cholera toxin: an intracellular journey into the cytosol by way of the endoplasmic reticulum. *Toxins (Basel)* **2:** 310-325

Wheeler AH (1997) Therapeutic uses of botulinum toxin. *Am Fam Physician* **55:** 541-545, 548

White J, Johannes L, Mallard F, Girod A, Grill S, Reinsch S, Keller P, Tzschaschel B, Echard A, Goud B, Stelzer EH (1999) Rab6 coordinates a novel Golgi to ER retrograde transport pathway in live cells. *J Cell Biol* **147:** 743-760

White MJ, DiCaprio MJ, Greenberg DA (1996) Assessment of neuronal viability with Alamar blue in cortical and granule cell cultures. *J Neurosci Methods* **70:** 195-200

Wiertz EJ, Tortorella D, Bogyo M, Yu J, Mothes W, Jones TR, Rapoport TA, Ploegh HL (1996) Sec61-mediated transfer of a membrane protein from the endoplasmic reticulum to the proteasome for destruction. *Nature* **384:** 432-438

Wigelsworth DJ, Krantz BA, Christensen KA, Lacy DB, Juris SJ, Collier RJ (2004) Binding stoichiometry and kinetics of the interaction of a human anthrax toxin receptor, CMG2, with protective antigen. *J Biol Chem* **279:** 23349-23356

Williamson LC, Neale EA (1994) Bafilomycin A1 inhibits the action of tetanus toxin in spinal cord neurons in cell culture. *J Neurochem* **63:** 2342-2345

Windschiegl B, Orth A, Romer W, Berland L, Stechmann B, Bassereau P, Johannes L, Steinem C (2009) Lipid reorganization induced by Shiga toxin clustering on planar membranes. *PLoS One* **4:** e6238

Winkeler A, Godderz D, Herzog V, Schmitz A (2003) BiP-dependent export of cholera toxin from endoplasmic reticulum-derived microsomes. *FEBS Lett* **554:** 439-442

Wolenski FS, Bradham CA, Finnerty JR, Gilmore TD (2013) NF-kappaB is required for cnidocyte development in the sea anemone *Nematostella vectensis*. *Dev Biol* **373:** 205-215

Wolf AA, Fujinaga Y, Lencer WI (2002) Uncoupling of the cholera toxin-G(M1) ganglioside receptor complex from endocytosis, retrograde Golgi trafficking, and downstream signal transduction by depletion of membrane cholesterol. *J Biol Chem* **277:** 16249-16256

Wolf P, Elsasser-Beile U (2009) *Pseudomonas* exotoxin A: from virulence factor to anti-cancer agent. *Int J Med Microbiol* **299:** 161-176

Wong BY, Gregory SA, Dang NH (2007) Denileukin diftitox as novel targeted therapy for lymphoid malignancies. *Cancer Invest* **25:** 495-501

Wong ET, Tergaonkar V (2009) Roles of NF-kappaB in health and disease: mechanisms and therapeutic potential. *Clin Sci (Lond)* **116:** 451-465

Worrall LJ, Lameignere E, Strynadka NCJ (2011) Structural overview of the bacterial injectisome. *Current Opinion in Microbiology* **14:** 3-8

Xiao G, Harhaj EW, Sun SC (2001) NF-kappaB-inducing kinase regulates the processing of NF-kappaB2 p100. *Mol Cell* **7:** 401-409

Xiao W (2004) Advances in NF-kappaB signaling transduction and transcription. *Cell Mol Immunol* **1:** 425-435

Yamaizumi M, Mekada E, Uchida T, Okada Y (1978) One molecule of diphtheria toxin fragment A introduced into a cell can kill the cell. *Cell* **15:** 245-250

Yamamoto Y, Gaynor RB (2001) Therapeutic potential of inhibition of the NF-kappaB pathway in the treatment of inflammation and cancer. *J Clin Invest* 107: 135-142

Yang H, Ganguly A, Cabral F (2010) Inhibition of cell migration and cell division correlates with distinct effects of microtubule inhibiting drugs. *J Biol Chem* **285:** 32242-32250

Ye Y, Meyer HH, Rapoport TA (2001) The AAA ATPase Cdc48/p97 and its partners transport proteins from the ER into the cytosol. *Nature* **414:** 652-656

Yen H, Ooka T, Iguchi A, Hayashi T, Sugimoto N, Tobe T (2010) NleC, a type III secretion protease, compromises NF-kappaB activation by targeting p65/RelA. *PLoS Pathog* **6:** e1001231

Yoshino A, Setty SR, Poynton C, Whiteman EL, Saint-Pol A, Burd CG, Johannes L, Holzbaur EL, Koval M, McCaffery JM, Marks MS (2005) tGolgin-1 (p230, golgin-245) modulates Shiga-toxin transport to the Golgi and Golgi motility towards the microtubule-organizing centre. *J Cell Sci* **118:** 2279-2293

Yoshino K, Abe J, Murata H, Takao T, Kohsaka T, Shimonishi Y, Takeda T (1994) Purification and characterization of a novel superantigen produced by a clinical isolate of Yersinia pseudotuberculosis. *FEBS Lett* **356:** 141-144

Young JA, Collier RJ (2007) Anthrax toxin: receptor binding, internalization, pore formation, and translocation. *Annu Rev Biochem* **76:** 243-265

Yu M, Haslam DB (2005) Shiga toxin is transported from the endoplasmic reticulum following interaction with the luminal chaperone HEDJ/ERdj3. *Infect Immun* **73:** 2524-2532

Zelenin AV (1993) *Acridine orange as a probe for molecular and cell biology.*, Mason, W T, Fluorescent and Luminescent Probes for Biologycal activity. A Pratical Guide for Quantitative Real-Time Analysis. edn. London: Academic Press.

Zhang Y, Bliska JB (2003) Role of Toll-like receptor signaling in the apoptotic response of macrophages to Yersinia infection. *Infect Immun* **71:** 1513-1519

Zheng C, Yin Q, Wu H (2011a) Structural studies of NF-kappaB signaling. *Cell Res* **21:** 183-195

Zheng Y, Lilo S, Brodsky IE, Zhang Y, Medzhitov R, Marcu KB, Bliska JB (2011b) A Yersinia effector with enhanced inhibitory activity on the NF-kappaB pathway activates the NLRP3/ASC/caspase-1 inflammasome in macrophages. *PLoS Pathog* **7:** e1002026

Zornetta I, Brandi L, Janowiak B, Dal Molin F, Tonello F, Collier RJ, Montecucco C (2010) Imaging the cell entry of the anthrax oedema and lethal toxins with fluorescent protein chimeras. *Cell Microbiol* **12:** 1435-1445